ON THE MOLECULAR MECHANISMS CONTROLLING OOCYTE MEIOTIC MATURATION IN CAENORHABDITIS ELEGANS

By

J.Amaranath Govindan

Dissertation

Submitted to the Faculty of the

Graduate School of Vanderbilt University

in partial fulfillment of the requirements

for the degree of

DOCTOR OF PHILOSOPHY

in

Cell and Developmental Biology

May, 2008

Nashville, Tennessee

Approved:

David Miller

David Greenstein

Chris Wright

Richard Breyer

Maureen Gannon

CELL AND DEVELOPMENTAL BIOLOGY

ON THE MOLECULAR MECHANISMS CONTROLLING OOCYTE MEIOTIC MATURATION IN CAENORHABDITIS ELEGANS

J. AMARANATH GOVINDAN

Dissertation under the direction of Professor David I. Greenstein

A conserved biological feature of sexual reproduction in animals is that oocytes arrest in meiotic prophase and resume meiosis in response to extra-ovarian signals. While meiotic maturation signals activate highly conserved pathways (e.g. MAP kinase and CDK/cyclin B), the receptor signaling mechanisms involved are less well defined. In *C. elegans*, sperm trigger meiotic resumption using the Major Sperm Protein (MSP) signal. MSP signaling involves two parallel genetic pathways, defined by *vab-1*, which encodes an MSP/Eph receptor protein-tyrosine kinase, and *ceh-18*, which encodes a POU-homeoprotein expressed in gonadal sheath cells. *vab-1* and *ceh-18* negatively regulate MAP kinase (MAPK) activation, and MSP relieves this inhibition to promote meiotic maturation. MSP directly binds VAB-1 on oocytes, but as *vab-1* null mutants respond normally to MSP, signaling must also involve the function of unidentified receptors. *ceh-18* functions in the gonadal sheath cells, indicating that sheath-oocyte communication may be important in maintaining meiotic arrest. Thus, additional components of the *vab-1* and *ceh-18* pathways function

to negatively regulate MAPK activation and meiotic maturation in the absence of MSP.

Using a genome-wide RNAi screen in a female-sterile genetic background, I identified seventeen conserved genes that maintain meiotic arrest in the absence of the MSP signal. Four conserved proteins, including a disabled protein (DAB-1), a vav family GEF (VAV-1), a protein kinase C (PKC-1), and a STAM homolog (PQN-19), function with the VAB-1 Eph/MSP receptor in oocytes. I show that antagonistic $G\alpha_s$ and $G\alpha_{o/i}$ signaling pathways function in the soma to regulate meiotic maturation in parallel to the VAB-1 pathway. $G\alpha_s$ activity is necessary and sufficient to promote meiotic maturation, which it does in part by antagonizing inhibitory sheath/oocyte gap-junctional communication.
Further evidence shows that MSP signaling reorganizes oocyte microtubules through a signaling network involving antagonistic $G\alpha_s$ and $G\alpha_{o/i}$ pathways and gap-junctional communication with somatic cells of the gonad. I propose that MSP-dependent microtubule reorganization promotes meiotic spindle assembly by facilitating the search and capture of microtubules by meiotic chromatin following NEBD. My findings show that oocyte Eph receptor and somatic cell G protein signaling pathways control meiotic diapause in *C. elegans*, highlighting contrasts and parallels between MSP signaling in *C. elegans* and luteinizing hormone signaling in mammals.

Approved: David Greenstein

To my beloved wife Priah

ACKNOWLEDGMENTS

I count myself as being very fortunate to have David Greenstein as my mentor. His expertise, leadership, support and hard work have been extremely helpful throughout my academic program. His passion for science has been a constant source of inspiration to me. His guidance has been invaluable to the development of my scientific creativity and writing. I would also like to thank my committee members, David Miller, Chris Wright, Rich Breyer and Maureen Gannon for their valuable suggestions and assistance at all levels of the research project. I want like acknowledge the Program in Developmental Biology for providing a wide and informative research experience at the annual retreats.

The worm community at Minneapolis provided a vibrant environment for my continued development as a critical thinker and scientist. Many thanks to Robert Herman, Jocelyn Shaw, Ann Rougvie, David Zarkower and Lihsia Chen for their helpful suggestions and comments during the worm group meetings. Special thanks to John Yochem and Leslie Bell for their helpful comments and general interest. My thanks also go to Theresa Stiernagle of Caenorhabditis Genetics Center (CGC) and Shohei Mitani of National Bioresource Project of Japan for providing strains.

There are several collaborators that I need to thank. I thank my mentor David Greenstein, who conducted the genetic mosaic analysis for *gsa-1*. I thank Hua Cheng for help in analyzing the role of *dab-1* in oocyte maturation. I thank Robert Berscheid, Aaron Timinski, Katie Steckelberg, and Carrie Lee for their

help in Snip-SNP mapping of *sgd* mutants. I thank Carrie Lee again for help in sequencing of *dab-1*, *inx-22*, and *ceh-18* alleles.

I thank several of my lab members, past and present, Mary Kosinski, Ikuko Yamamoto, Elena Matafonova, Klaudyna Borewicz, and Caroline Spike for sharing fun and scientific thoughts. Special thanks to Todd Starich for the discussion about innexins.

I have several friends whom I would like to thank, Carrie Lee, Xuelin Wang, Seongseop Kim, Jason Tennessen and Joseph Watson for making my graduate school career fun and interesting. Special thanks to Aric Daul for his help with computer. His untiring efforts to save my thesis from destruction are duly acknowledged. A special thanks to all my seniors including Vinod, Chandra, Bala, and Latchu for their cooperation and help.

This thesis is dedicated to my wife, Priah, for her love, support and understanding that enabled me to accomplish my goals. Priah is also my colleague and bench mate, with whom I live 24 -7, but we still enjoy each other's company. We've been through a lot together and she has been an incredible support ever since I met her. I would also thank my parents, who allowed me to come to US for my PhD. I would also like to thank my brother Ravi and his wife, Leena, for their support. Finally, I would like to thank my high school friends Ezhil, Shankar and Murugan who has always been with me.

TABLE OF CONTENTS

Page

LIST OF TABLES

LIST OF FIGURES

LIST OF ABBREVIATIONS

AC adenylate cyclase

Cdk1 cyclin dependent kinase 1

cAMP cyclic adenosine monophosphate

DAG diacylglycerol

dbcAMP dibutyril cyclic AMP

IP3 inositol triphosphate

LH luteinizing hormone

MAPK mitogen activated protein kinase

MPF M-phase promoting factor / maturation promoting factor

PKA/PKC protein kinase A/ protein kinase C

CHAPTER I

INTRODUCTION

Meiosis is an ancient and highly conserved process required for sexual reproduction. The low fidelity of female meiosis represents a major barrier to human reproduction and is the chief cause of birth defects (Hassold and Hunt, 2001). Because cell signaling and cell cycle control mechanisms are evolutionarily conserved, studies in genetic model systems will contribute significantly to our understanding of the mechanisms regulating meiotic maturation and fertilization in humans. The studies presented in this dissertation identify highly conserved pathways and mechanisms regulating meiotic maturation in *C. elegans*. Specifically, my studies show that somatic cells of the gonad control oocyte meiotic progression via an ancient and highly conserved mechanism: G-protein signaling. In addition, I show that the soma has both maturation-promoting and inhibiting functions. These studies complement a wide body of work showing that similar/analogous mechanisms appear to function in mammals. Thus, extensions of the work presented here will likely uncover major mechanistic pathways underlying human reproduction. To introduce these studies, I will describe the conserved process of oocyte meiotic maturation, placing it in the context of the entire meiotic process. Studies of meiotic maturation have a long history, involving biochemical and cell biological

studies in multiple systems. A synthesis of these studies is presented to place the *C.elegans* work in context. The biology and genetics of *C. elegans* is presented to highlight the approaches possible in this system and to provide clarity to the experiments. Highly conserved biochemical pathways that figure prominently in this analysis are described in detail.

Part I: Oocyte Meiotic Maturation: A Conserved Biological Process

1.1. Meiosis

In sexually reproducing organisms, meiosis generates haploid gametes (1n), which reunite during fertilization to generate a diploid embryo (2n) (reviewed by Champion and Hawley, 2002). This is achieved by two successive nuclear divisions following one round of DNA replication. Thus, meiosis gives rise to four haploid cells (1n) from a single diploid cell (2n). Each diploid cell contains two copies of a chromosome, paternal and maternal (called homologous chromosomes) (Fig. 1A). During meiosis I, DNA replication generates two copies of each chromosome that are held together by sister chromatid cohesion involving the cohesin complex (Lee and Orr-Weaver, 2001). Following DNA replication, homologous chromosomes find each other and pairing occurs. Homologous pairing occurs only in meiosis but not in mitosis. Following pairing, synaptemal complex, which is a proteinaceous structure, is formed in between the homologous chromosomes (reviewed by Colaiácovo, 2006). Pairing allows the homologous chromosomes to be brought in close proximity, permitting crossing over to occur resulting in bivalent formation (Fig.

Figure 1. Stages in Meiosis.

(A) During meiosis I, pairing of duplicated homologous chromosomes occur. Following pairing, the chromosomes undergo genetic recombination. At the end of anaphase, the homologs are separated but the sister chromatids are held together. Meiosis II is essentially similar to mitosis in which the sister chromatids are separated resulting in four haploid gametes. Unlike mitosis, meiosis II occurs in the absence of DNA replication. Adapted from Molecular Biology of the Cell, Garland Publishing, NY 1994.

(B) Stages of prophase I of meiosis. Adapted from Modern Genetic Analysis, Freeman, San Francisco 1999.

A

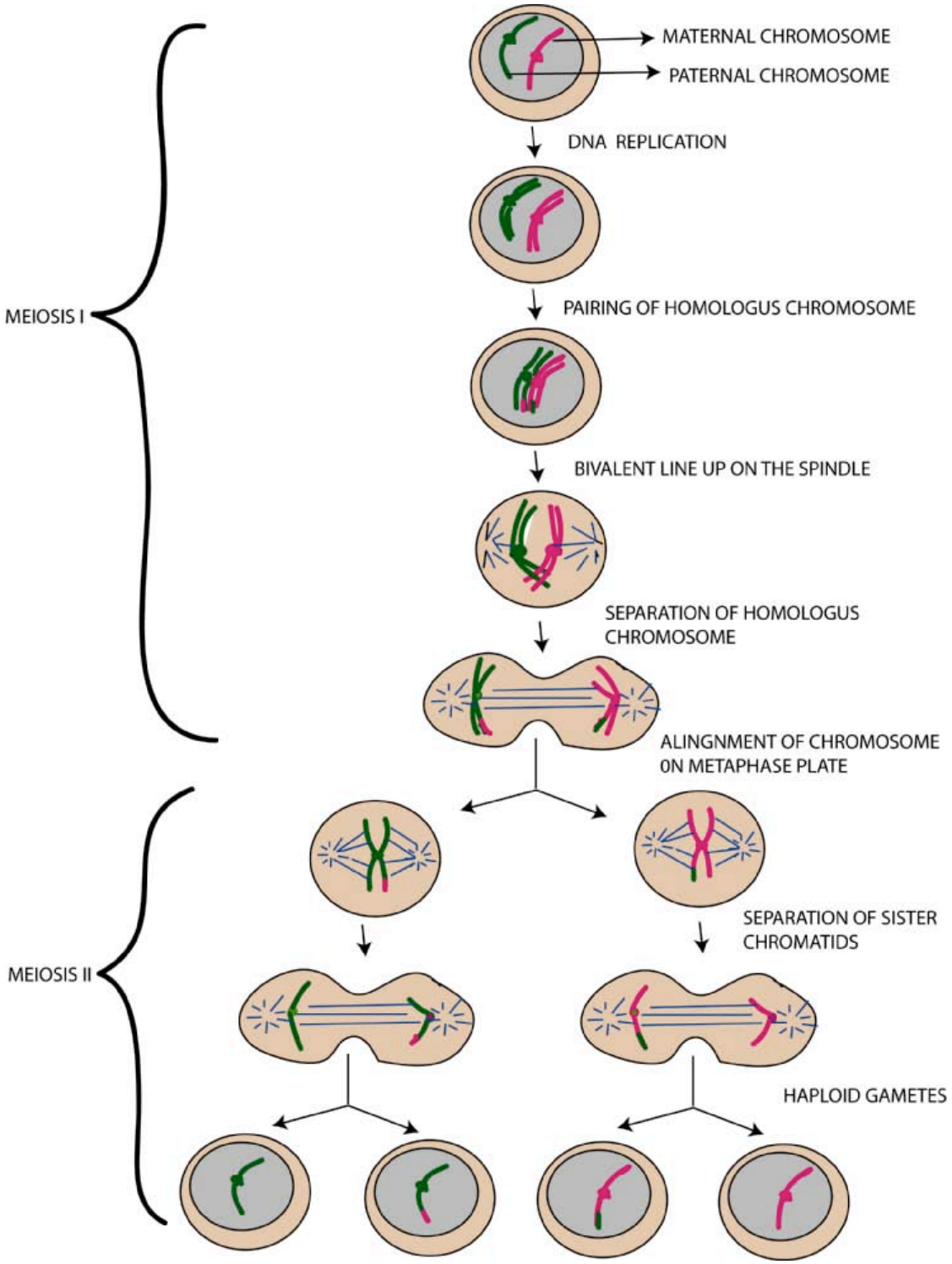
MATERNAL CHROMOSOME
PATERNAL CHROMOSOME
DNA REPLICATION
PAIRING OF HOMOLOGUS CHROMOSOME
BIVALENT LINE UP ON THE SPINDLE
SEPARATION OF HOMOLOGUS CHROMOSOME
ALINGNMENT OF CHROMOSOME ON METAPHASE PLATE
SEPARATION OF SISTER CHROMATIDS
HAPLOID GAMETES
MEIOSIS I
MEIOSIS II

B

Leptotene
Chromosomes are unpaired
Fine threads consisting of two tightly bound sister chromatids
Crossing-over is initiated

Zygotene
Maternal and paternal homologs pair together to form bivalents
Crossing-over occurs

Pachytene
Chromosomes thicken
Crossing-over and repair completed

Diplotene
Homologs separate
but are held together by chaismata

Diakinesis
Bivalents are compacted

1A). Crossing over is a characteristic feature of meiosis in which a portion of the maternal chromosome is exchanged with the homologous paternal chromosome (Fig. 1A). Crossing over results in the formation of “chaismata”, which is the point of exchange of the chromosome segment. Chiasmata are necessary for biorientation of homologous chromosomes and their faithful segregation at the end of first meiotic division. At the end of meiosis I, the chromosomes are divided into two daughter cells, each containing one homologous chromosome with 2n DNA content (Fig. 1A). The second meiotic division is essentially like mitosis but occurs without DNA synthesis resulting in the formation of haploid germ cells with 1n DNA content.

1.1.1. Stages in meiosis

Meiosis is conventionally divided into two phases: meiosis I and II (Fig. 1A). Meiosis I consists of prophase, metaphase, anaphase and telophase. Prophase of meiosis I is the longest stage and it consists of five sequential steps: leptotene, zygotene, pachytene, diplotene and diakinesis (Fig. 1B). The leptotene step begins at the end of pre-meiotic DNA replication. During leptotene, the chromosomes condense from their interphase conformation to produce fine discrete thread-like structures (Fig. 1B). Zygotene begins as soon as the pairing of homologous chromosomes or synapsis is initiated (Fig. 1B). Synapsis of homologs is complete at pachytene. Homologous chromatids are held together by the synaptonemal complexes, and crossing occurs between the paternal and maternal homologous chromosomes (Fig. 1B). During diplotene, disassembly of synaptonemal complex occurs while the homologous

chromosomes remain attached by chiasmata. The diakinesis step is similar to the prometaphase stage of mitosis. In this step, the chromosomes undergo further condensation and the tetrads are clearly visible. Toward the end of diakinesis, the nuclear envelope starts to break down and meiotic spindle assembly occurs. During the metaphase stage of meiosis I, the homologous chromosomes align along an equatorial plane with their centromeres oriented toward the opposite cell poles (Fig. 1B).

In anaphase I, homologous chromosomes separate and move to the opposite poles while the sister chromatids remain together (Fig. 1B). During telophase I, the homologous chromosomes continue to move to the spindle pole (Fig. 1B). Once they reach the opposite poles, the nuclear envelope reforms and cytokinesis begins. Meiosis II is essentially same as mitosis but is not preceded by DNA replication.

1.1.2. Sexual dimorphism in meiosis

The formation of both spermatozoa and oocytes occurs via meiosis. However, meiosis in males and females proceeds in distinct spatial and temporal fashion giving rise to morphologically different gametes (Fig. 2). For example, in most mammals including human, spermatogenesis begins after puberty. The germline stem cells called spermatogonia undergo mitotic divisions followed by meiosis to generate mature spermatozoa (Fig. 2). All the steps during spermatogenesis proceed in an uninterrupted fashion resulting in the production of four sperm from single spermatogonia, each with equal ability to fertilize. During each division, the spermatogonia generate stem cell-like

Figure 2. Comparison of male and female meiosis.

Oogenesis and spermatogenesis are shown. Differences in male and female meiosis are described in the text.

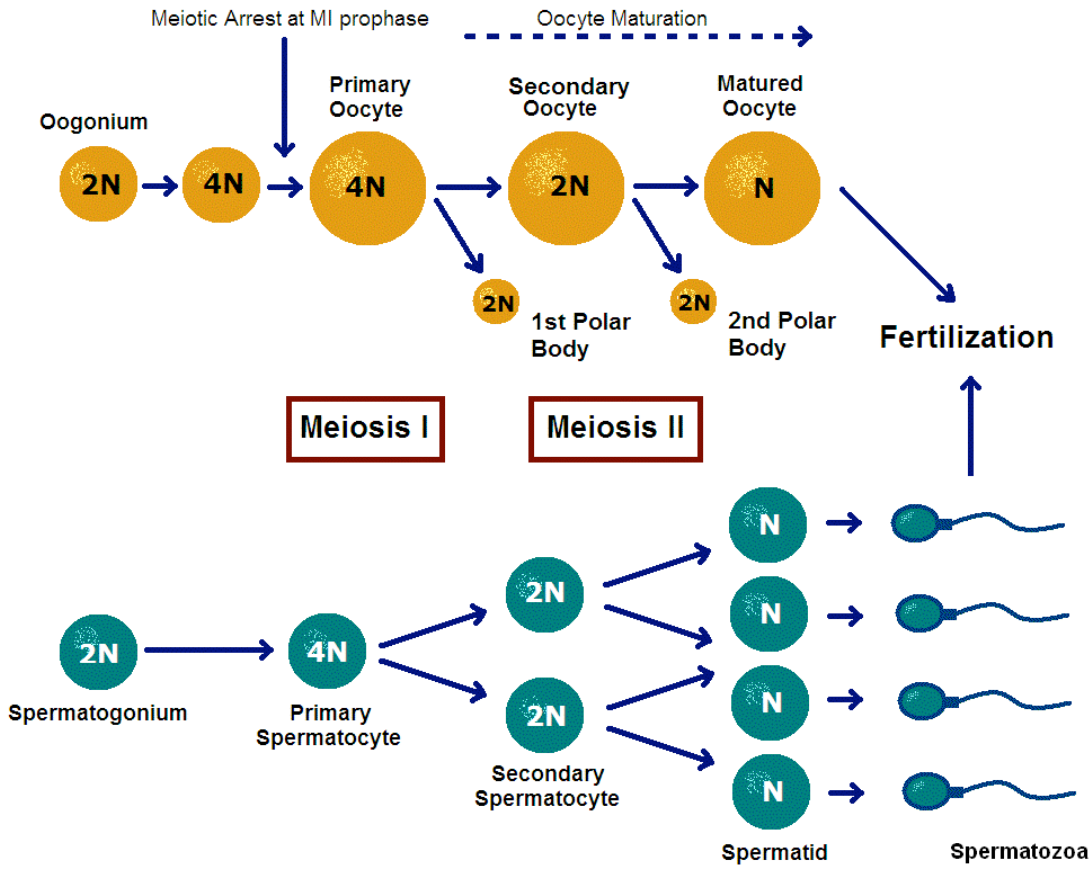
Meiotic Arrest at MI prophase
Oocyte Maturation
Oogonium
Primary Oocyte
Secondary Oocyte
Matured Oocyte
2N
4N
4N
2N
N
2N
1st Polar Body
2N
2nd Polar Body
Fertilization
Meiosis I
Meiosis II
2N
Spermatogonium
4N
Primary Spermatocyte
2N
2N
Secondary Spermatocyte
N
N
N
N
Spermatid
Spermatozoa

spermatogonia and maturing spermatogonia which undergo meiosis to generate sperm (Fig. 2). Thus, males are able to generate sperm continuously throughout their lifetime. By contrast, in most mammals including humans, oogenesis begins during embryogenesis. Female germline stem cells called oogonium divide mitotically to form primary oocytes (4N). By birth, all oogonia complete their cell divisions and enter meiosis. Thus, it was widely accepted that the mammalian oocytes are formed during prenatal development and the adult ovaries are endowed with a finite number of oocytes (Zuckerman 1951; Gosden et al., 1983). In recent years, there has been a wide spread debate about the existence of postnatal oogenesis in adult female mice (Johnson et al., 2005; Johnson et al., 2004; Tilly and Johnson, 2007). Further, bone marrow was suggested as a source for germline stem cells in the adult mouse ovary (Johnson et al., 2005). However, these findings were unable to be replicated by other groups (Eggan et al., 2006; Liu et al., 2007; Veitia et al., 2007).

A characteristic feature in female meiosis is that oocytes initiate but do not complete meiotic cell divisions in the prenatal ovaries. In the postnatal ovary, oocytes remain arrested at prophase of meiosis I until summoned upon by hormones to undergo meiotic maturation. The ultimate product of meiosis in female is a single oocyte and three small polar bodies.

1.2 Meiotic arrest in different species

In many organisms, oocytes arrest twice during meiosis. The primary arrest occurs in most species, including sponges, during the diplotene or diakinesis of prophase I (Fig. 3) (Masui, 2001; Masui and Clarke, 1979). By

contrast, in *Cerebratulus spp* (nemertean worm), *Chaetopterus spp* (annelid), and molluscs, the primary arrest occurs at metaphase of meiosis I. Oocytes resume meiosis in response to hormonal signaling. However, proximate signal, which cause meiotic resumption are quite different in each species. Fertilization triggers resumption of meiosis in *Urechis* (echiuran worm), clams and nemertean worms. Ions such as magnesium in sea water are thought to signal for meiotic maturation in the shrimp *Sicyonia spp* (Lindsay *et al*., 1992). In fishes (including zebrafish) and *Xenopus spp*, steroid hormone derivatives are thought to signal meiotic resumption (Thomas et al., 2002; Ferrell, 1999a; Ferrell, 1999b). In humans, pituitary gonadotrophins (LH and FSH) are thought to signal meiotic maturation indirectly. In other organisms, such as *Drosophila* and sea urchins, the proximate signals that trigger resumption of meiosis are not known (Page and Orr-Weaver, 1997).

Following hormonal signaling, the oocytes complete meiosis I and initiate meiosis II. Depending on the species, the oocytes arrest again at meiosis II. The stage of meiosis II at which the secondary arrest occurs differs from species to species. In vertebrates, secondary arrest occurs at metaphase of meiosis II (Tunquist and Maller, 2003). By contrast, in certain molluscs and ascidians, secondary arrest occurs at metaphase of meiosis I. Secondary arrest at the pronuclear stage has also been documented in certain Echinoderms and Coelenterates. In almost all species, fertilization triggers resumption of meiosis in a process known as egg activation. Egg activation triggers release of free calcium in the oocytes resulting in cortical granule exocytosis, which is required

Figure 3. Meiotic progression in different species.

Stages at which the meiotic arrest occurs in different species are indicated. The signal for resumption of meiosis is given in parenthesis. PB denotes polar body.

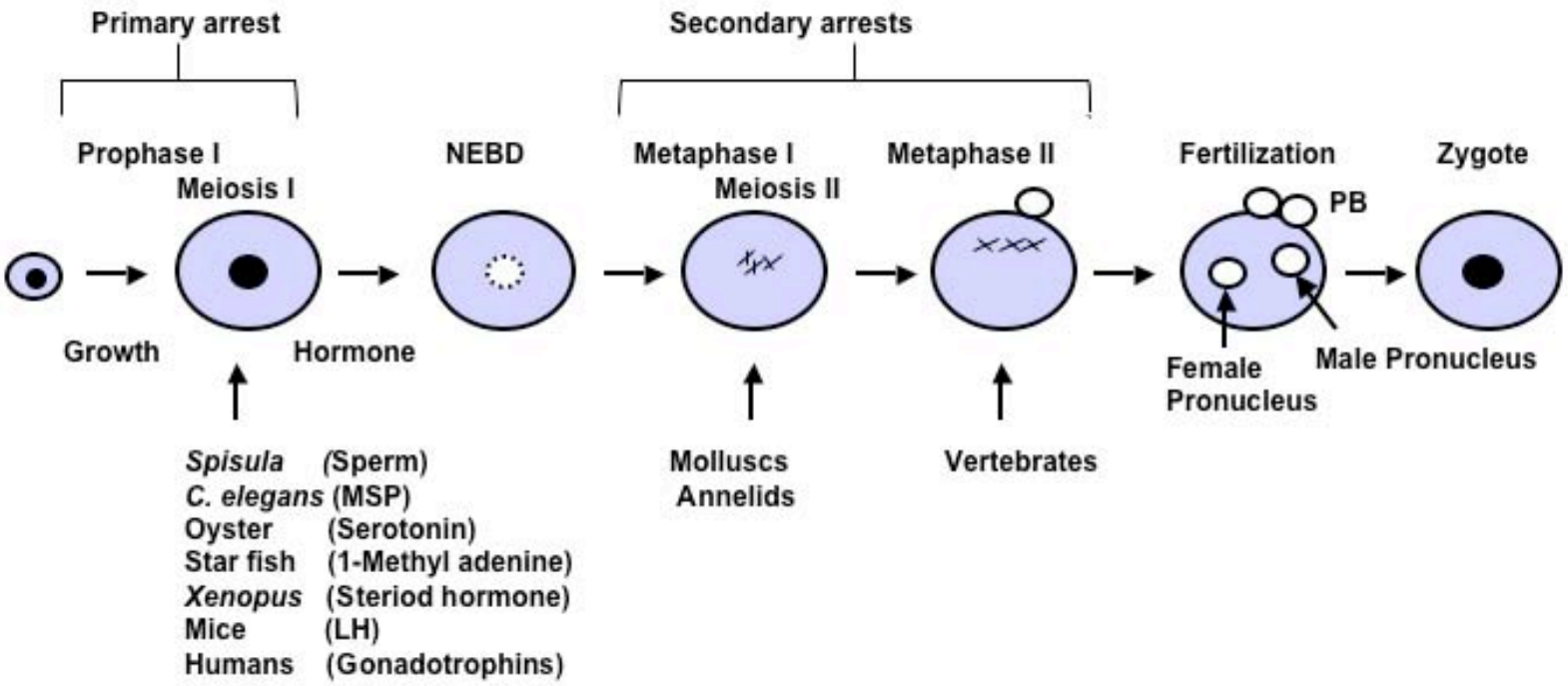
Primary arrest
Secondary arrests
Prophase I
Meiosis I
NEBD
Metaphase I
Meiosis II
Metaphase II
Fertilization
Zygote
PB
Growth
Hormone
Female Pronucleus
Male Pronucleus
Spisula (Sperm)
C. elegans (MSP)
Oyster (Serotonin)
Star fish (1-Methyl adenine)
Xenopus (Steriod hormone)
Mice (LH)
Humans (Gonadotrophins)
Molluscs
Annelids
Vertebrates

for preventing polyspermy. Following egg activation, oocytes complete meiosis, extrude polar body and form maternal pronuclei.

1.3 Humans and errors in meiosis

Studying the mechanism(s) controlling meosis is essential as errors in this process lead to birth defects and infertility. Meiosis in human females is notoriously error-prone (Hunt and Hassold, 2002; Hunt and LeMaire-Adkins, 1998). A conservative estimate is that ~ 5% of all human conceptions are aneuploid in nature, and chromosome segregation defects during female meiosis I are the most common reason for human aneuploidy (Fig. 4A) (Hassold and Hunt, 2001). Most of the aneuploid embryos result in spontaneous miscarriages; however, some of the aneuploidy results in congenital birth defects, such as the trisomies involving chromosome 21 (Down syndrome), chromosome 18 (Edward syndrome), chromosome 13 (Patau syndrome), chromosome X (Klinefelter's syndrome) and Turner's syndrome (X0) (Hassold and Hunt, 2001; Hassold et al., 1993; Hassold et al., 1995; Warren and Gorringe, 2006). Most of the chromosome segregation defects originate from errors during meiosis I. The underlying reasons for the low fidelity of human female meiosis is unknown, but the frequency of meiotic errors increases with maternal age. The amount of time that the human oocytes spend in meiotic prophase could be a major factor. Human oocytes initiate meiosis in the fetal ovaries but arrest during prophase I. This arrest lasts until oocytes are recruited for ovulation after puberty. The cyclical recruitment of oocytes for ovulation continues until menopause. Thus, the human oocytes spend between

Figure 4. Maternal age effect and aneuploidy in humans

(A) Comparison of chromosome segregation during meiosis I and II. Homologous chromosome segregates to opposite poles (Top panel). Non-disjunction results in homologous chromosomes segregating to the same pole (Bottom panel). Adapted from Hassold and Hunt, 2001.
(B) Graph depicting the relationship between non-disjunction and maternal age. Reprinted from Hassold and Hunt, 2001.

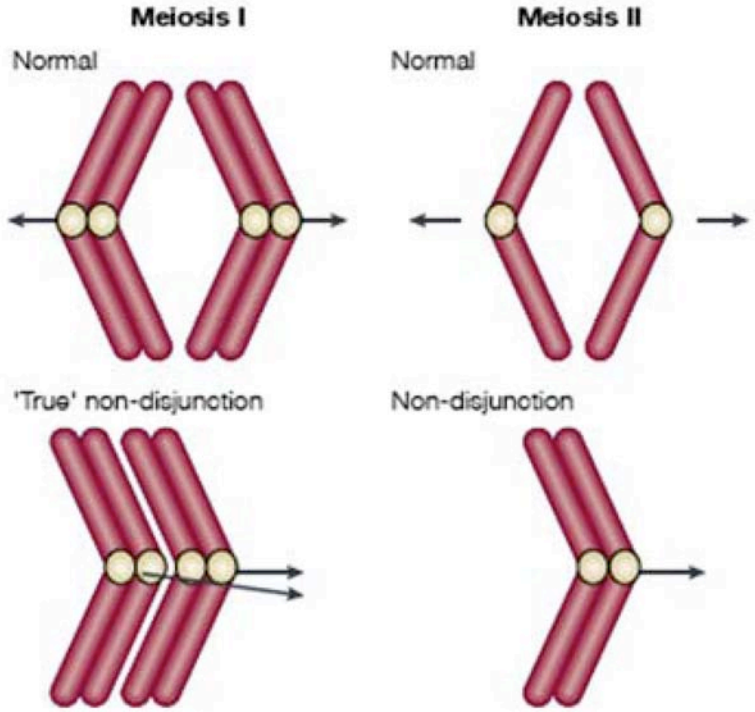
Meiosis I
Meiosis II
Normal
Normal
'True' non-disjunction
Non-disjunction

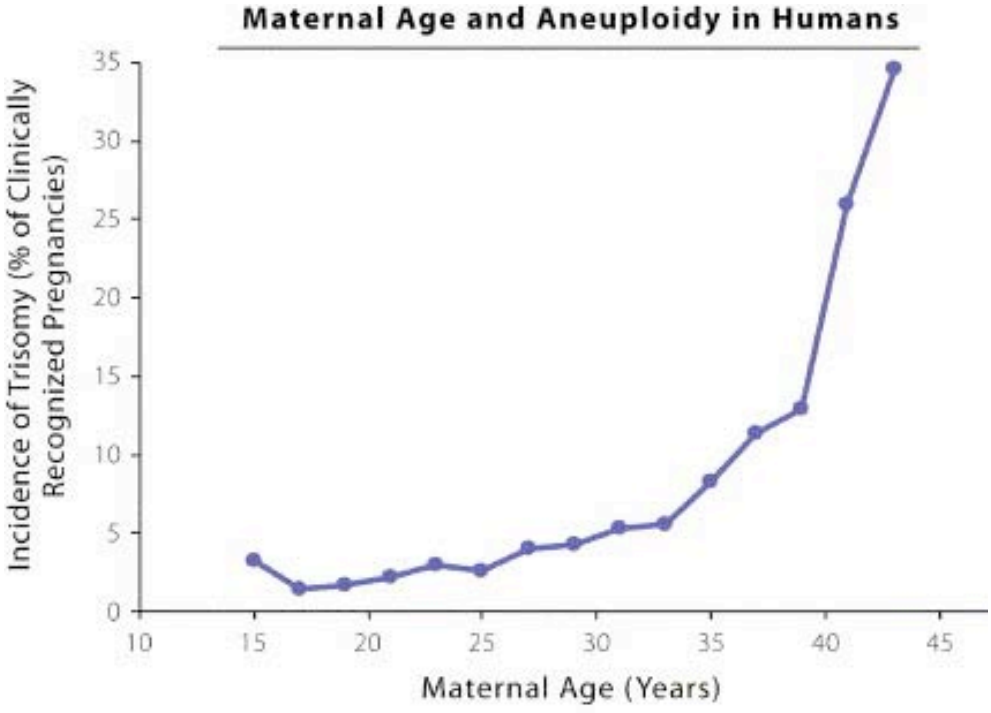
Maternal Age and Aneuploidy in Humans
Incidence of Trisomy (% of Clinically Recognized Pregnancies)
0
5
10
15
20
25
30
35
10
15
20
25
30
35
40
45
Maternal Age (Years)

15–45 years in meiotic prophase I. Interestingly, maternal age is a significant factor in the incidence of aneuploidy irrespective of race or socioeconomic factors. As the age of the mother increases, the incidence of aneuploidy also increases. This positive correlation is known as the maternal age effect (Fig. 4B). The risk of a woman having an aneuploid oocyte increases several fold after the age of thirty. Thus, a woman in her early forties has more than 35% chance of having a trisomic fetus; in comparison, there is less than 5% chance in a woman in her early twenties (Fig. 4B). Based on studies of meiotic chromosome behavior in flies and cytological studies in humans, a 'two-hit' model has been proposed for the origin of aneuploidy in humans (Hassold and Sherman, 2000). According to this model, the "first hit" occurs due to formation of susceptible meiotic configuration during the primary oocyte stage in the fetal ovaries (Hassold and Sherman, 2000). A "second hit" occurs later as the age of mother increases, and is likely due to the failure of cohesion and/or spindle checkpoint defects (Hassold and Sherman, 2000; Warren and Gorringe, 2006). Recently, it was shown that Smc1β/cohesin subunit knockout mice display an age-dependent increase in meiotic nondisjunction similar to that of human females (reviewed by Gilliland and Hawley, 2005; Hodges et al., 2005; Warren and Gorringe, 2006). Meiotic cohesins are proteins that are required for maintaining sister chromatid cohesion (Warren and Gorringe, 2006). The sister chromatid cohesion provides the force that holds the homologs together because of the chiasmata. Thus, meiotic recombination converts sister chromatid cohesion to homolog cohesion. In an aging ovarian environment, loss

of cohesin function could result in missegregation of chromosomes during meiosis. However, it is not known whether genetic variations or age-dependent loss of cohesin proteins occur in humans. Environmental factors are also thought to be part of the cause for high levels of meiotic errors in humans. Female mice fed with Bisphenol A (BPA), an estrogenic compound, display meiotic spindle defects, high levels of meiotic failure and aneuploid embryos (Hunt et al., 2003; Susiarjo et al., 2007). Since, BPA is a constituent of polycarbonate plastics and low levels of BPA have been reported in humans, it is thought that BPA may play a role in increasing meiotic errors in humans (Hunt et al., 2003). However, a direct role for BPA in human meiotic errors is still lacking. Recent studies in humans and mice show that hormonal imbalances during folliculogenesis can result in meiotic spindle assembly defects (Hodges et al., 2002). These studies suggest that hormonal disturbances may be a significant risk factor for meiotic errors in humans (Hodges et al., 2002). In the ageing ovarian environment, defective hormonal signaling responses may be a factor underlying the high rate of aneuploidy. Thus, in this dissertation work, I have focused on understanding the signaling pathways that regulate meiosis in oocytes.

1.4 Intracellular signaling pathways involved in oocyte meiotic maturation

Studies from various model organisms have shown the downstream cell cycle mechanisms underlying meiotic maturation, but comparatively less about the upstream signaling mechanisms. In this section, I will describe briefly the conserved intracellular pathways involved in oocyte meiotic maturation.

1.4.1 Role of maturation promoting factor (MPF) in oocyte meiotic maturation

Seminal studies by Yoshio Masui and colleagues on oocyte meiotic arrest in frogs lead to the discovery of MPF (Masui, 2001; Masui and Markert, 1971; Tunquist and Maller, 2003). MPF was initially characterized as an activity present in mature frog oocytes that induced maturation when injected into arrested oocytes. Serial transfer of cytoplasm from a maturing oocyte into an arrested oocyte results in meiotic maturation suggesting that MPF has autocatalytic property (Masui, 2001). Elegant biochemical and genetic studies showed that MPF is a universal regulator of G2/M transition in both meiosis and mitosis (Gautier et al., 1990; Gautier et al., 1988; Lohka et al., 1988; Maller et al., 1989; Masui, 1996; Nurse, 1990). MPF has been shown to be required for oocyte meiotic maturation in many species (Maller et al., 1989; Masui, 2001; Schmitt and Nebreda, 2002). MPF is heterodimer comprised of Cdc2/CDK1 and cyclin B (Doree and Hunt, 2002; Masui, 2001). During cell cycle progression, MPF activity is regulated by phosphorylation events (Coleman and Dunphy, 1994; Masui, 2001). In the growing oocyte, Cdc2/CDK1 complex is kept inactive by inhibitory phosporylation on Thr14 and Tyr15 catalyzed by the Myt1 kinase. During meiotic maturation, Cdc25 dual-specificity phosphatase activates MPF by removing the inhibitory phosphorylation (Masui, 2001). Maturation signals may also inhibit Myt1 activity in parallel for MPF activation. MPF is thought to promote meiotic maturation by phosphorylation of target proteins, which are involved in chromosome condensation, nuclear envelope breakdown, and meiotic spindle assembly (Abrieu et al., 2001).

1.4.2 Role of Mitogen-Activated Protein Kinases (MAPK) in oocyte meiotic maturation

MAPK or extracellular-regulated kinases (ERK) are key mediators of cell growth, proliferation, and differentiation in many organisms (Marshall, 1994; Treisman, 1996). MAP kinases are serine/threonine kinases that require dual phosphorylation on threonine and tyrosine residues to become fully activated (Anderson et al., 1990; Posada and Cooper, 1992). MAPKs are phosphorylated by MAPK kinase (MAPKK), otherwise known as MEK (*M*AP or *E*RK *k*inase) (Adams and Parker, 1992; Crews et al., 1992). MEKs themselves are activated by MAPKK kinases (MAPKKK) such as MOS and RAF (Matten et al., 1996; Resing et al., 1995; Verlhac et al., 1996).

Studies in *Xenopus* demonstrated for the first time that MAPK pathways are involved in oocyte meiotic maturation. Later, MAPK activation was shown to be important for meiotic progression in several species including mammals (Abrieu et al., 2001; Ferrell, 1999a; Ferrell, 1999b; Nebreda and Ferby, 2000; Sun et al., 1999; Lee et al., 2007). In many species, MAPK activation during meiotic maturation requires *Mos*, which encodes a MAP kinase kinase kinase (Fan and Sun, 2004; Sun et al., 1999; Verlhac et al., 2000). How hormonal signaling triggers Mos activation is not known. However, it is well known that MOS protein level in oocytes is regulated by translation. In arrested oocytes, translation of *Mos* mRNA is inhibited. In response to hormonal signaling, polyadenylation and translation of Mos mRNA occurs. MOS is necessary and sufficient for meiotic maturation in *Xenopus* (Sagata, 1998; Sagata et al., 1989; Sagata et al., 1988). By contrast, in other species *Drosophila* and mammals

(Hashimoto et al., 1994; Colledge et al., 1994; Ivanovska et al., 2004), MOS is dispensable for meiotic maturation suggesting that additional pathways are involved. However, Mos is required for MAPK activation and is involved in microtubule organization during meiotic maturation in the mouse (Verlhac et al., 1996). The exact mechanism by which MAPK signaling promotes oocyte meiotic maturation is not known. However, MAPK activation is likely to be involved in MPF activation during maturation in some species (Fan and Sun, 2004; Liang et al., 2007). Some studies have suggested that MAPK pathway is important for microtubule reorganization during oocyte meiotic maturation (Fan and Sun, 2004; Sun et al., 1999; Verlhac et al., 1993). In mouse and *Xenopus*, MAPK activation is necessary for proper meiotic spindle assembly.

1.5 Role of the somatic gonad in oocyte meiotic maturation

In sexually reproducing animals, meiosis generates haploid gametes from diploid parental cells. Proper regulation of meiosis is critical for production of fully functional gametes that can be fertilized to make viable progeny. The somatic cells of the gonad are associated with the oocyte beginning from the formation of primordial follicles at embryogenesis until the implantation of the fertilized oocyte (Fig. 5). Somatic cells play important structural, functional, and regulatory roles during oocyte development (Gilchrist et al., 2004). An important feature of the soma-oocyte communication is that it is bidirectional in nature (Sutton et al., 2003).

Figure 5. Bidirectional soma-germline communication

(A) Structure of a mammalian follicle. Diagrammatic representation of a preovulatory mammalian follicle showing the somatic cell types and their arrangement within the follicle. Adapted from Voronina and Wessel, (2003)

(B) Soma-oocyte interaction. The somatic cells associate with the oocyte very early during the primordial follicle formation. They remain associated with the oocytes throughout development and even after ovulation. The role of somatic cells in fertilization, block to polyspermy, and implantation are not shown. Adapted from Eppig, (1991)

(C) Different molecules involved in the bidirectional soma-germline communication are shown. Adapted from Sutton et al., (2003)

A

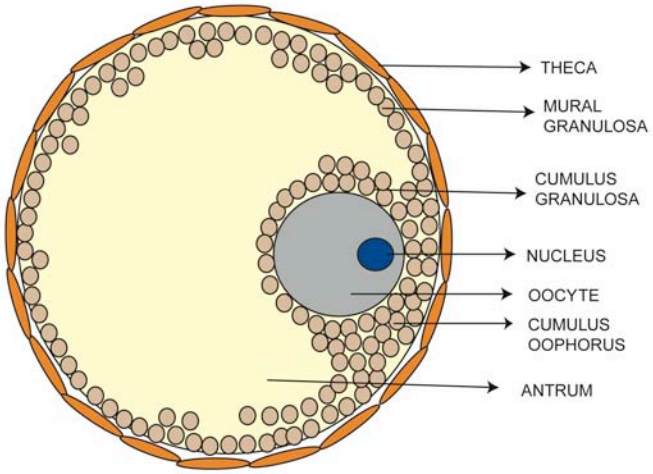

B

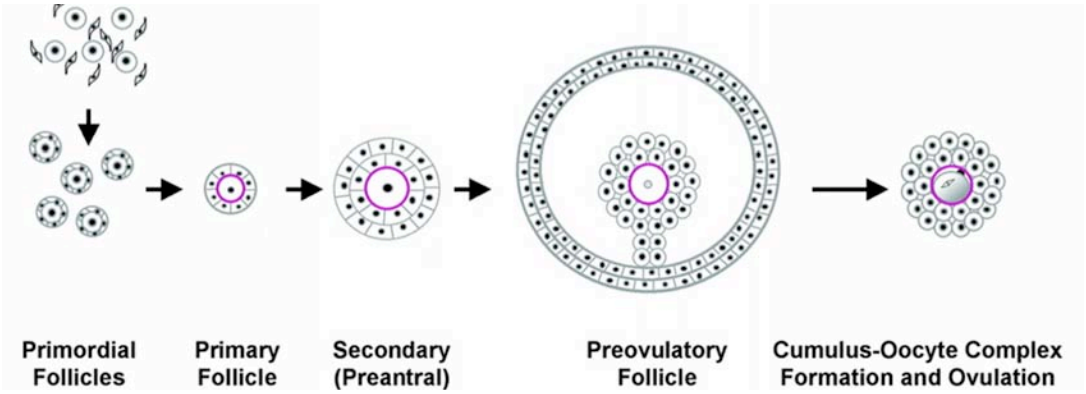

C

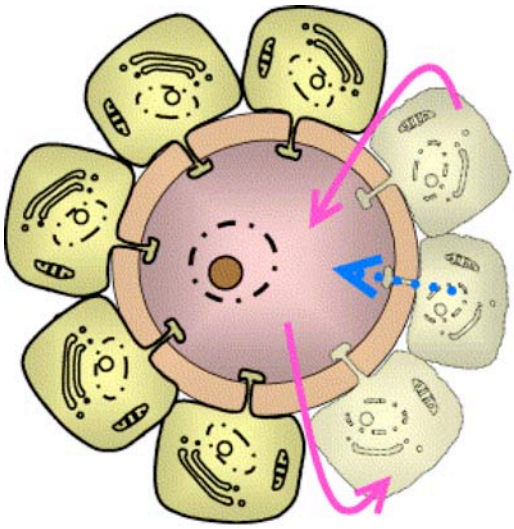

Cumulus to oocyte
- Kit-ligand
- FF-MAS
- EGF-like peptides

Gap junctional transfer
- cAMP
- Purines/pyrimidines
- Metabolites
- Amino acids

Oocyte to cumulus
- Oocyte-secreted factors
  - e.g.GDF-9
  - BMP-15
  - BMP-6
  - Activins?

While somatic cells of the follicle regulate oocyte growth, meiotic arrest and maturation, the oocyte controls follicle formation, differentiation and ovulation via paracrine signaling (Fig. 5) (Gilchrist et al., 2004; Thomas and Vanderhyden, 2006). Mammalian follicles are complex structures consisting of several layers of somatic cells surrounding a single oocyte (Fig. 5A). The outermost thecal and middle mural granulosa cells generate steroids such as estrogen. By contrast, the inner cumulus cells (Fig. 5A) provide nutrients and metabolites to the oocyte via gap junctions (Eppig, 1991; Simon et al., 1997).

Early studies on meiotic maturation demonstrated that oocytes undergo spontaneous meiotic resumption when removed from antral follicles (Edwards, 1965; Pincus and Enzmann, 1935). These studies suggested “follicle-derived factors” maintain meiotic arrest in the oocytes. Later studies suggested cAMP as a “follicle-derived factor” that maintain oocyte arrest (Conti et al., 2002). Since the oocyte forms gap junctions with the cumulus cells, gap junctional transfer of cAMP from the follicle cells to the oocyte was hypothesized to maintain meiotic arrest (Carabatsos et al., 2000; Conti et al., 2002). Somatic cells of the follicle are also important for the resumption of meiosis following hormonal signaling. After ovulation, the oocyte is shed from the follicle with a few layers of cumulus cells surrounding called the cumulus oophorus (Fig. 5A). This structure is necessary to make the oocyte competent for fertilization and may aid in block to polyspermy (Runft et al., 2002).

1.6 Intercellular signaling pathways involved in oocyte meiotic maturation

In many organisms G-protein signaling is involved in the control of oocyte meiotic maturation. In this thesis work, I investigated the role of G-protein signaling during oocyte meiotic maturation in *C. elegans*. My study shows that antagonistic G-protein signaling pathways in the somatic gonad regulate oocyte meiotic maturation in *C. elegans*. In this section, I will provide an overview of G-protein signaling pathway(s) to aid the readers.

1.6.1 G-protein signaling: An overview

The G-protein signaling is a widely conserved mechanism by which eukaryotic cells respond to various extracellular ligands (Gilman, 1987; Hamm, 1998; Neves et al., 2002). G-proteins are involved in several processes including sensing food, odor, taste, and sex hormones in the environment (Fig. 6). During development, they are involved in controlling cell proliferation, differentiation, and migration (Wettschureck and Offermanns, 2005). In humans, mutations in G-proteins have been linked to a variety of diseases ranging from endocrine disorders to cancer (Farfel et al., 1999; Spiegel, 1996). Thus, G-proteins are excellent targets for development of drugs for therapeutic use. In fact, about 30-50% of all currently used drugs target G-protein signaling (Flower, 1999; Robas et al., 2003). In summary, molecular dissection of G-protein signaling is vital for understanding human physiology as well as the pathophysiology behind various diseases.

G-proteins are heteromeric in nature, with a $G\alpha$, $G\beta$, and $G\gamma$ subunit (Neves et al., 2002). In their inactive state, G-proteins exist as a trimeric

complex at the cell membrane. In the inactive state, Gα subunit is bound to GDP. Following activation of a G-protein coupled receptor (GPCR), a conformational change in Gα induces a change of affinity for GTP instead of GDP. This induces dissociation of Gα from the Gβγ subunit and activation of downstream effectors. Gβ and Gγ exist as a Gβγ dimer even after the dissociation of the Gα subunit. In some systems, Gβγ subunits have been shown to function in downstream signaling.

G-protein coupled receptors (GPCR) are seven-transmembrane proteins that bind to extracellular ligands (Strader et al., 1994). Most GPCRs do not share sequence similarity, but they have a common membrane topology. Each GPCR has seven alpha helices spanning the membrane with an extracellular amino terminus and intracellular carboxy terminus. Mammals have more than 1,000 GPCRs that are activated by a wide variety of ligands, including hormones, light, neurotransmitters, and odorants (Pierce et al., 2002; Vassilatis et al., 2003). However, several GPCRs are “orphan receptors” because their endogenous ligands are not known (Wise et al., 2004).

Given the versatile functions of G-protein signaling, it is perhaps not surprising that there are several subtypes of G-proteins. In mammals, there are twenty Gα, five Gβ, and twelve Gγ encoding genes (Hildebrandt, 1997; Hurowitz et al., 2000; Strathmann et al., 1989; Strathmann and Simon, 1991).

Figure 6. Role of G-protein signaling pathways during development.

G-protein signaling pathways are involved in diverse biological functions. Key pathways required for the biological functions are shown. In addition, ligands known to promote these biological functions via G-protein signaling are also shown. Reprint from Neves et al., 2004

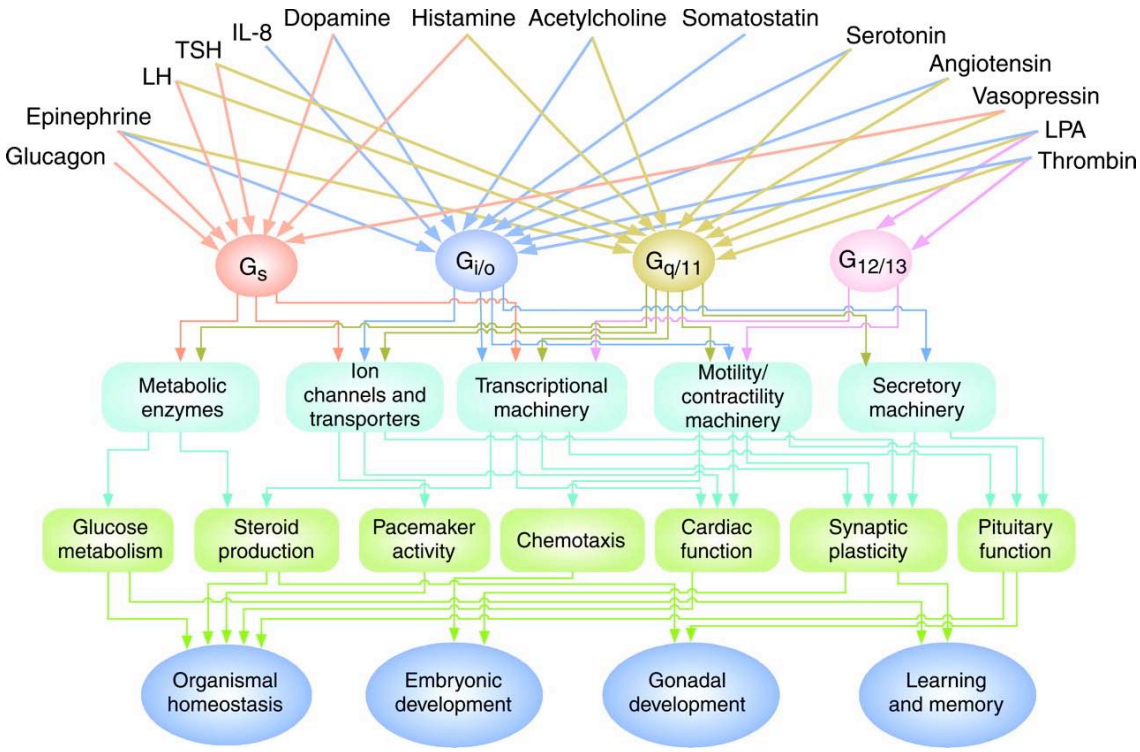
Dopamine
Histamine
Acetylcholine
Somatostatin
IL-8
TSH
LH
Epinephrine
Glucagon
Serotonin
Angiotensin
Vasopressin
LPA
Thrombin
G_s
$G_{i/o}$
$G_{q/11}$
$G_{12/13}$
Metabolic enzymes
Ion channels and transporters
Transcriptional machinery
Motility/ contractility machinery
Secretory machinery
Glucose metabolism
Steroid production
Pacemaker activity
Chemotaxis
Cardiac function
Synaptic plasticity
Pituitary function
Organismal homeostasis
Embryonic development
Gonadal development
Learning and memory

$G\alpha$ subunits are classified into four classes, $G\alpha_s$, $G\alpha_{i/o}$, $G\alpha_q$, and $G\alpha_{12/13}$ based on sequence similarities (Radhika and Dhanasekaran, 2001). The $G\alpha_s$ subunit functions by stimulating adenylate cyclase, resulting in the production of the second messenger cAMP. By contrast, activation of $G\alpha_i$ inhibits adenylate cyclases. $G\alpha_q$ subunit activates phospholipase C pathway and stimulates release of intracellular calcium. $G\alpha_{12/13}$ is thought to activate small G-proteins (Hart et al., 1998; Kozasa et al., 1998).

Attenuation of G-protein signaling involves the G-protein coupled Receptor Kinase (GRK)-arrestin pathway and Regulator of G-protein Signaling (RGS) (De Vries et al., 2000; Premont and Gainetdinov, 2007). Agonist binding to its cognate GPCR results in activation of a specific $G\alpha$ subunit, which stimulates downstream signaling cascade. Agonist-bound GPCR also causes activation of a specific GRK. Active GRK phosphorylates specific sites on intracellular loops of GPCR. Phosphorylated GPCRs are then recognized by β-arrestins, which target them for receptor-mediated endocytosis. Thus, the GRK-arrestin pathway is important for “turning-off” ligand-initiated G-protein signaling (DeWire et al., 2007; Premont and Gainetdinov, 2007).

The RGS pathway is another major mechanism by which the activity of G-protein signaling is regulated. RGS proteins contain an RGS domain that promotes the intrinsic GTPase activity of $G\alpha$. This results in GTP-hydrolysis and subsequent inactivation of $G\alpha$ subunit. In addition, RGS proteins can regulate G-protein signaling by inhibiting the interaction of G-proteins with their downstream effectors (De Vries et al., 2000; Ross and Wilkie, 2000).

1.6.2 Role of G-protein signaling in starfish oocyte meiotic maturation

In starfish, 1-methyladenine (1-MA) acts as a hormone for resumption of meiosis (Kanatani et al., 1969). 1-MA induces activation of MAPK and cyclinB/CDK1 pathways in oocytes (Tachibana et al., 2000). Induction of meiotic maturation by 1-MA is thought to occur via a $G\alpha_i$-coupled G-protein signaling pathway (Chiba et al., 1992; Kalinowski et al., 2003; Shilling et al., 1990; Tadenuma et al., 1992). In this pathway, $G\beta\gamma$ subunits regulate phosphatidylinositol 3-kinase (PI 3-kinase) and Akt kinase (Chiba et al., 1993; Jaffe et al., 1993; Nakano et al., 1999; Okumura et al., 2002; Sadler and Ruderman, 1998). However, the molecular mechanism(s) involved are not fully known. Although cAMP has been shown to be involved in meiotic arrest, the exact molecular pathways involved are not known (Meijer et al., 1989).

1.6.3 Role of G-protein signaling in Xenopus oocyte meiotic maturation

In *Xenopus*, progesterone signals oocyte meiotic resumption (Ferrell, 1999a; Ferrell, 1999b). Progesterone signaling inhibits cAMP-dependent PKA pathways (Maller and Krebs, 1977; Eyers et al., 2005; Ferrell, 1999b) suggesting that a constitutively active $G\alpha_s$ pathway maintains meiotic arrest. Consistent with this hypothesis, inhibition of $G\alpha_s$ activity results in progesterone-independent meiotic maturation (Gallo et al., 1995). Further, overexpression of $G\alpha_s$ resulted in inhibition of progesterone-dependent oocyte maturation (Romo et al., 2002). Thus, it is thought that progesterone promotes maturation by binding to and inhibiting a constitutively active $G\alpha_s$-coupled receptor (Eyers et al., 2005; Zhu et al., 2003a; Zhu et al., 2003b).

Figure 7. LH induced oocyte meiotic maturation in mammals

Structure of a mammalian follicle.
(A) The somatic cells involved and their organization within the follicle is shown.
(B) Gap junctional disassembly following LH signaling.
(C) A model for LH action based on the current literature is shown. See text for futher details. Adapted from Mehlmann, (2005b).

A

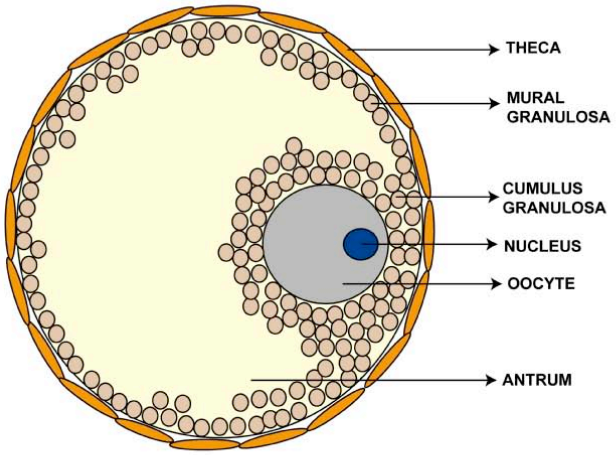
THECA
MURAL GRANULOSA
CUMULUS GRANULOSA
NUCLEUS
OOCYTE
ANTRUM

B

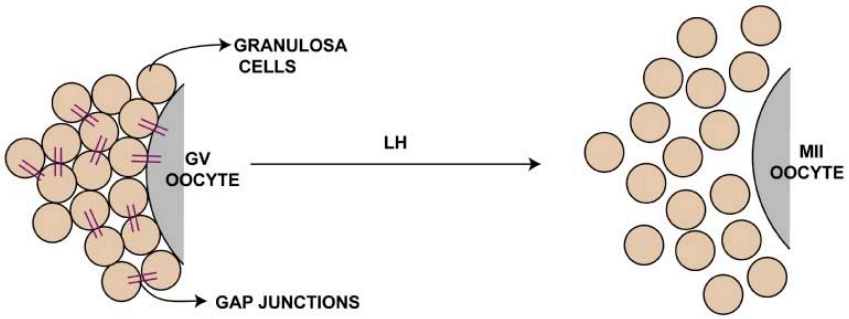
GRANULOSA CELLS
GV OOCYTE
LH
MII OOCYTE
GAP JUNCTIONS

C

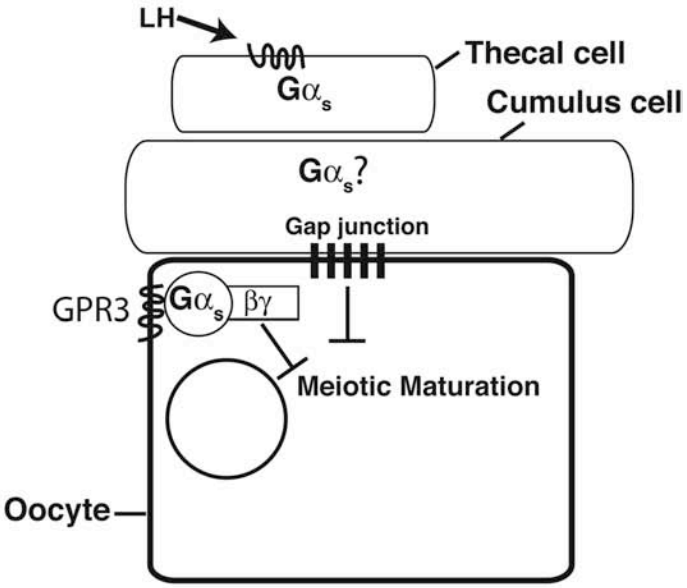
LH
Thecal cell
Gαs
Cumulus cell
Gαs?
Gap junction
GPR3
Gαs βγ
Meiotic Maturation
Oocyte

1.6.4 Role of G-protein signaling in mammalian oocyte meiotic maturation

In mammals, luteinizing hormone (LH) signals oocyte maturation by binding to LH receptor expressed in the mural granulosa cells (Fig. 7A). Interestingly, LH receptor (A $G\alpha_s$-linked GPCR) is not expressed in the cumulus cells or in oocytes suggesting that the mechanism by which LH stimulates maturation is indirect. However, the mechanism by which LH promotes oocyte maturation is not known. One model is that LH signaling promotes maturation by destabilizing gap junctions between the cumulus cells and oocyte (Fig. 7B). In this model, LH signaling causes phosphorylation and uncoupling of gap junctions, which in turn leads to low levels of cAMP within the oocyte (Edry et al., 2006; Sela-Abramovich et al., 2006). This model is in accordance with a long standing hypothesis that gap junctional transfer of cAMP produced by follicle cells maintains meiotic arrest in mammalian oocytes (Fig. 7C).
LH signaling promotes meiotic resumption likely by attenuating gap junctional transfer of cAMP. However, the signaling mechanism that generates cAMP in the cumulus cells is not known. It is thought a $G\alpha_s$ signaling pathway within the cumulus may generate cAMP via adenylate cyclase (Fig. 7C). By contrast, GPR3, a $G\alpha_s$ linked G-Protein-Coupled Receptor (GPCR), was shown to maintain meiotic prophase arrest in mouse oocytes (Mehlmann et al., 2004; Mehlmann et al., 2005b). This suggests that oocytes themselves can generate enough cAMP to maintain meiotic arrest. This study conflicts with the idea that gap junctional transfer of cAMP produced by cumulus cells is required to maintain meiotic arrest. Thus in mammals, there are at least three Gs-signaling

pathways that act in the granulosa cells, cumulus cells and within the oocyte to regulate meiotic maturation. Also, LH induces release of EGF-like ligands, which are thought to bind to EGF receptors on the cumulus cells and stimulate oocyte maturation (Park et al., 2004). How this pathway interacts and intersects with G-protein signaling is not known.

In summary, the mechanisms that regulate oocyte meiotic arrest in mammals are complex, at least in part due to the involvement of multiple cell types. Though intracellular pathways (MPF and MAPK) have been studied in detail, the intercellular pathways involved are poorly understood. Model organisms may permit the use of genetics to understand the intercellular pathways involved in meiotic arrest and maturation relevant under physiological conditions.

1.7 G-protein signaling in *C. elegans*

In *C. elegans*, there are twenty-one Gα, two Gβ and two Gγ genes (Jansen et al., 1999). Each of the four mammalian Gα classes is represented by one ortholog in *C. elegans*: *gsa-1* encodes Gαs, *goa-1* encodes $G\alpha_{i/o}$, *egl-30* or *gqa-1* encodes $G\alpha_q$, and *gpa-12* encodes $G\alpha_{12/13}$ (Brundage et al., 1996; Jansen et al., 1999; Korswagen et al., 1997; Park et al., 1997; Segalat et al., 1995). The other 17 Gα genes (*gpa-1* to *gpa-11*, *gpa-13* to *gpa-17* and *odr-3*) cannot be assigned to any of the mammalian Gα classes due to lack of sufficient homology. Many of the Gα's are widely expressed in many tissues and play pleiotropic roles. GSA-1 is expressed in many tissues and is required for viability (Korswagen et al., 1997). In addition, *gsa-1* is involved in the

regulation of egg-laying, locomotion and neuronal cell death (Berger et al., 1998; Korswagen et al., 1997; Korswagen et al., 1998). Extensive genetic analyses have demonstrated that GOA-1 and EGL-30 function in an antagonistic fashion to regulate several developmental processes including locomotion, male mating, egg-laying and feeding (Brundage et al., 1996; Dong et al., 2000; Hajdu-Cronin et al., 1999; Mendel et al., 1995; Segalat et al., 1995; van der Linden et al., 2001). Furthermore, GOA-1 is involved in cell cycle progression, embryonic viability, fertility, and regulation of spindle orientation (Afshar et al., 2004; Colombo et al., 2003; Fraser et al., 2000; Gotta and Ahringer, 2001; Miller and Rand, 2000; Simmer et al., 2003; Srinivasan et al., 2003; Tsou et al., 2003).

Two genes encoding Gβ subunits, *gpb-1* and *gpb-2* are present in *C. elegans*. *gpb-1* encodes a Gβ subunit that mediates signaling via all the Gα subunits. GPB-1 is required for viability because *gpb-1(null)* mutants are embryonic lethal. *gpb-2* encodes a Gβ subunit homologous to mammalian Gβ5, which is involved in regulation of GOA-1 and EGL-30 signaling.

In *C. elegans*, two Gγ subunits *gpc-1* and *gpc-2* are present. *gpc-1(null)* mutants are viable with no obvious phenotypes. Reduction of *gpc-2* activity resembles *gpb-1(null)* mutants suggesting that they may function in a common pathway.

Part II: *C. elegans* as a model for studying oocyte meiotic maturation

2.1 Introduction to *C. elegans* Biology

A simple organism such as *C. elegans* is a good genetic model system for studying conserved mechanisms involved in oocyte meiotic maturation (Greenstein, 2005; Hubbard and Greenstein, 2000). Within a period of three days, an egg develops into an adult hermaphrodite or male. Each hermaphrodite lays about 250-300 eggs in a period of five days and lives for approximately 20 days. The adult hermaphrodite contains 959 somatic cells that form tissues and organs such as the cuticle, pharynx, gut, nervous system and the germline. The complete embryonic as well as post-embryonic cell-lineage which is largely invariant has been determined (Sulston and Horvitz, 1977; Sulston et al., 1983). Further, the postembryonic cell lineages of the hermaphrodite gonad have been described (Kimble and Hirsh, 1979).
The short generation time, small size, and self-fertilization offers a rapid, inexpensive, and high-throughput forward and reverse genetic screens. In addition, various genomic, biochemical, and cell biological tools are available for further dissection of molecular pathways. More importantly, the transparent body allows us to directly observe oogenesis, meiotic maturation, and ovulation processes by time-lapse microscopy in an intact animal (McCarter et al., 1999).

2.2 *C. elegans* germline development

C. elegans consists of two sexes– hermaphrodites (five pairs of autosomes + one pair of sex chromosome) and males (five pairs of autosome and a single sex chromosome). Males are generated by the non-disjunction of

Figure 8. *C. elegans* germline development

(A) Overview of germline development. The L1 larva has four precursor cells: Z1, Z2, Z3, and Z4. Z1 and Z4 give rise to the somatic gonad. Z2 and Z3 give rise to the germline (Reprinted from Wormatlas).
(B) Z1 and Z4 cell lineages. DTC denotes distal tip cell. SS is sheath spermathecal cell lineage. DU is dorsal uterine cell lineage. VU denotes ventral uterine cell lineage. AC denotes anchor cell (Reprinted from Wormatlas).
(C) SS cell lineage. Each SS cell contributes to the formation of nine spermathecal and five gonadal sheath cells (Reprinted from Wormatlas).
(D) Structure of an adult germline. The U-shaped gonad arm is shown. dg and pg denotes distal gonad and proximal gonad respectively. Structure and arrangement of the sheath cells are shown (Reprinted from Wormatlas).

A

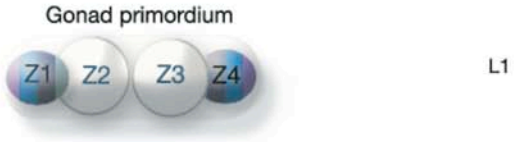
Gonad primordium
Z1
Z2
Z3
Z4
L1

B

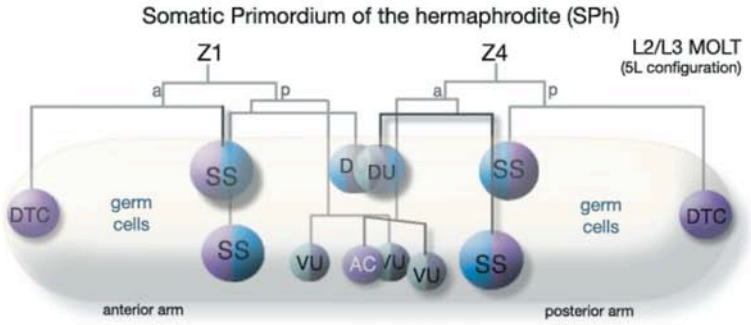
Somatic Primordium of the hermaphrodite (SPh)
Z1
Z4
L2/L3 MOLT
(5L configuration)
a
p
a
p
SS
D
DU
SS
DTC
germ cells
germ cells
DTC
SS
VU
AC
VU
VU
SS
anterior arm
posterior arm

C

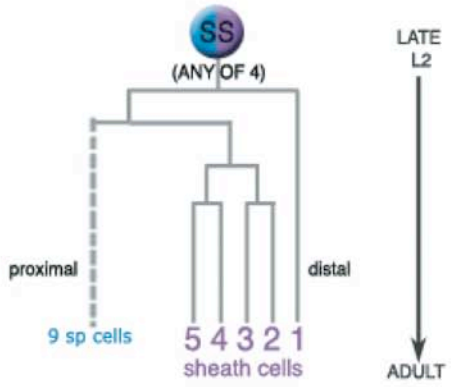
SS
(ANY OF 4)
LATE
L2
proximal
distal
9 sp cells
5 4 3 2 1
sheath cells
ADULT

D

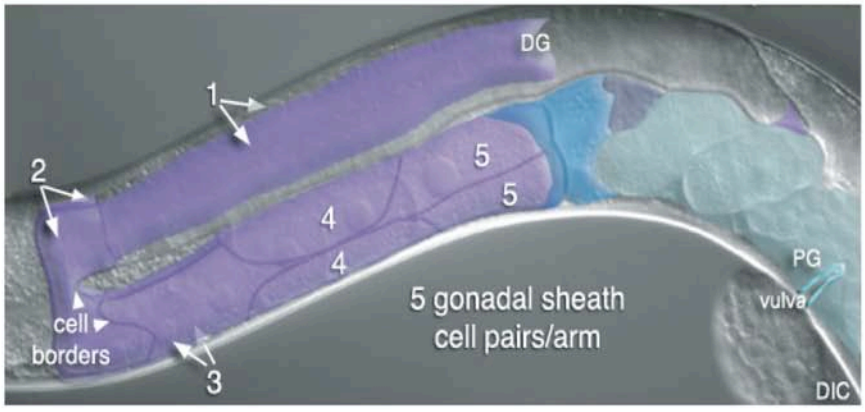
DG
1
2
5
5
4
4
PG
vulva
5 gonadal sheath
cell pairs/arm
cell
borders
3
DIC

sex chromosomes, which occurs at a rate of about 0.05%. The hermaphrodites reproduce by self-fertilization or by mating to males. When mated to males, hermaphrodites produce ~50% male cross-progeny because male sperm is preferentially utilized because of sperm competition. The hermaphrodites are basically females that produce about 300 sperm during the L4 larval stage and switch to producing oocytes as adults. At fertilization, the oocyte and sperm unite to produce a zygote (P0). The zygote (P0) divides into a large somatic (AB) and a smaller germline P1 blastomeres. The P1 germline blastomere divides asymmetrically resulting in a somatic EMS and germline P2 blastomeres. The EMS and P2 blastomeres undergo asymmetric cell divisions to generate four somatic (E, MS, C and D) and primordial germ cell P4 blastomeres (Kimble and Hirsh, 1979; Sulston and Horvitz, 1977; Sulston et al., 1983).

The single P4 cell gives rise to the entire germ line. The P4 cell divides symmetrically at about the 100-cell stage to form two germline precursor cells, Z2 and Z3 (Kimble and Hirsh, 1979; Sulston et al., 1983). The MS blastomere undergoes cell divisions to generate two somatic gonadal precursor cells (Z1 and Z4). By the end of embryogenesis, Z1 and Z4 cells migrate and join Z2 and Z3 to form the gonad primoridum, which is separated from the soma by a gonadal basal lamina (Fig. 8A). During the L1/L2 molt, Z1 and Z4 divide to produce distal tip cells (DTC's), anchor cell and somatic precursor cells. The somatic precursor cells include four sheath-spermathecal (SS), two dorsal uterine (DU), and three ventral uterine (VU) cells (Fig. 8B). By late L2, somatic

Figure 9. Structure and arrangement of gonadal sheath cells. Reprinted from Greenstein., (2005)

(A) Diagrammatic representation of an adult hermaphrodite. The position and arrangement of the ten gonadal sheath cells within a gonad arm is shown.
(B) DAPI stained gonad from wild-type hermaphrodite showing mitiotic and meiotic germ cells. Bars, 10 μm.
(C) Myoepithelial structure of the gonadal sheath cells. Dissected gonad stained with MHCA (red) and MHCB (green) to show the sheath myofilament structure.
(D) TEM section showing gap junction (gj) between oocyte and proximal sheath cell.
(E) Freeze-fracture replica showing gap junction (gj) and sheath pores.

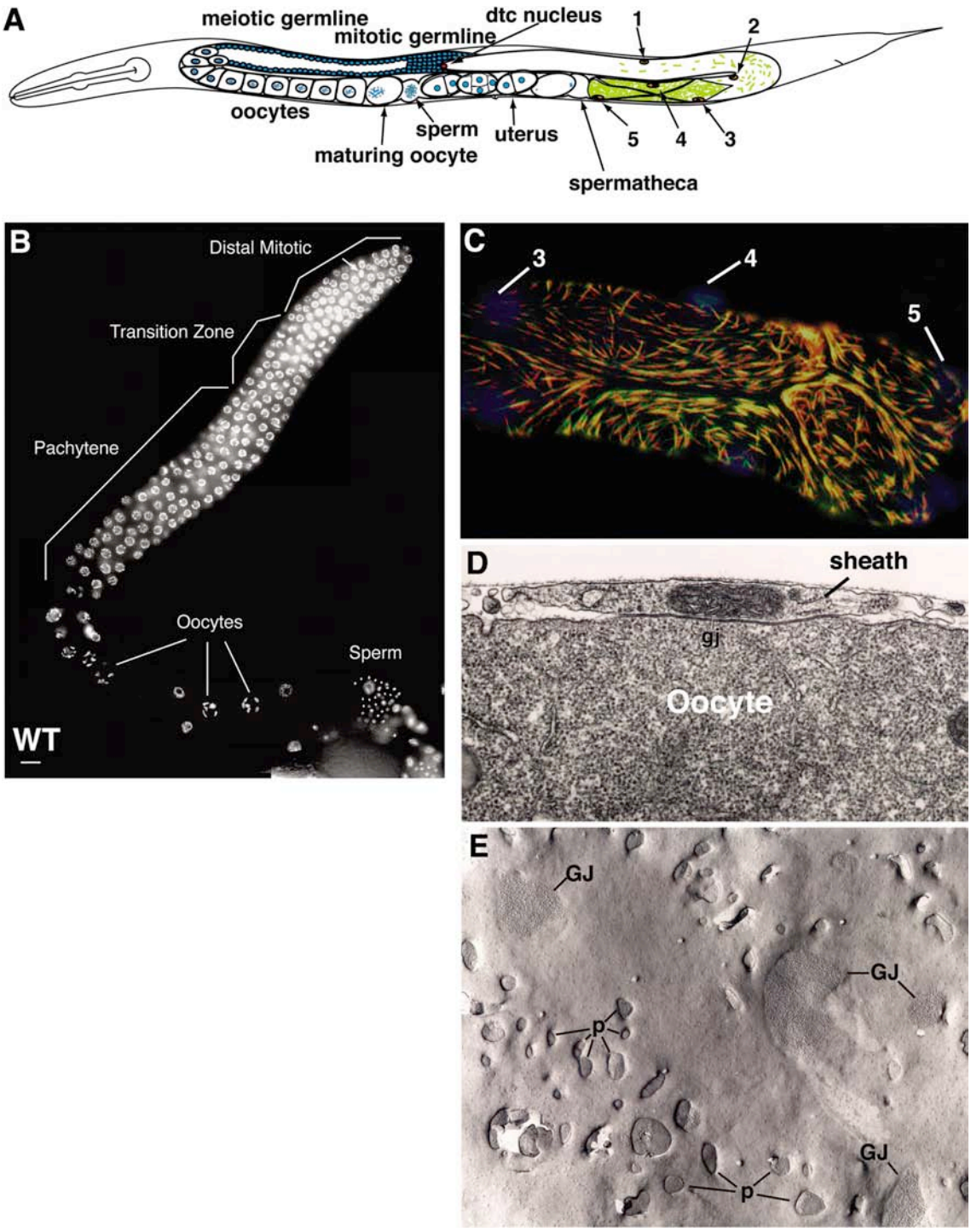
A
meiotic germline
mitotic germline
dtc nucleus
1
2
oocytes
sperm
uterus
5
4
3
maturing oocyte
spermatheca
B
Distal Mitotic
Transition Zone
Pachytene
Oocytes
Sperm
WT
C
3
4
5
D
sheath
gj
Oocyte
E
GJ
GJ
p
GJ
p

Figure 10. Schematic representation of gonadal sheath cell-oocyte interactions. Reprinted from Hall et al.,(1999).

(A) Cross section at the transition zone of the distal gonad. The syncytial germ cells are arranged around a central region called the rachis. The proximal sheath pair 1 covers the distal gonad arm only partially. Also, the sheath cell inserts in between the germ cells to form a honey-comb like structure.
(B) The position of the distal tip cell in relation to the sheath cell pair 1 is shown. A bare region formed by the gap between the distal tip cell and sheath cell is shown. Also, filopodial extensions made by sheath pair I is shown.
(C) Cross section at the proximal end of the gonad. The sheath cell pairs 4 and 5 completely enclose oocytes.
(D) Sheath-oocyte interactions in the proximal gonad. gj indicates gap junction between the oocyte and sheath cell as well as sheath-sheath gap junctions. hj are hemi-adherens junctions between the sheath cell and the basal lamina (bl). The sheath actomyosin filaments (f) are anchored at the hemi-adherens junctions. p indicates sheath pores.

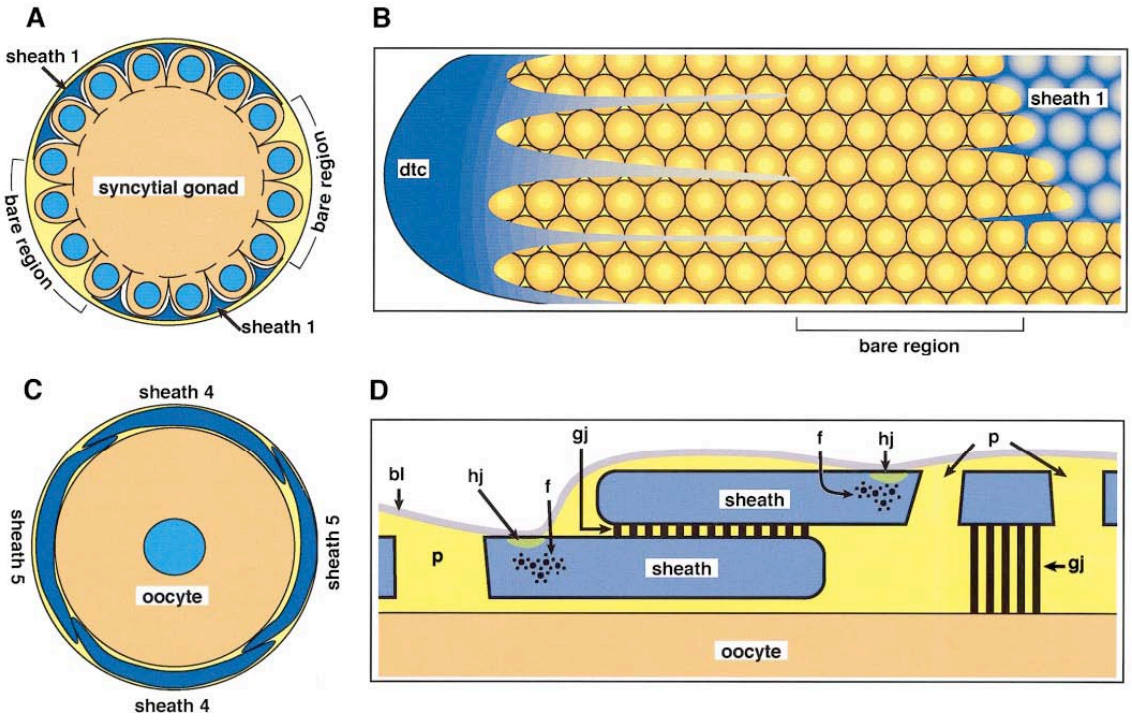
A
sheath 1
syncytial gonad
bare region
bare region
sheath 1
B
dtc
sheath 1
bare region
C
sheath 4
sheath 5
oocyte
sheath 5
sheath 4
D
bl
hj
f
gj
f
hj
p
sheath
p
sheath
gj
oocyte

precursor cells and the AC migrate to the center of the primordium resulting in segregation of germ cells into anterior and posterior gonad arms. The two distal tip cells start to migrate in anterior and posterior directions, respectively resulting in elongation of the arms. During late L3 larval stages, the SS cells divide to generate the gonadal sheath and spermatheca. (Fig. 8C and D) Meanwhile, the two dorsal uterine precursor cells (DU) and three VU cells forms dorsal and ventral uterus, respectively.

During L2 and L3 larval stages, the germ line precursor cells also undergo proliferation and give rise to ~30 germ cells (Kimble and White, 1981). During the L4 stage, germ cells undergo extensive proliferation and some of the cells enter meiosis. The mitotic germ cells occupy the distal zone of the gonad arm whereas oocytes move progressively towards the proximal end of the gonad arm. Initially, the meiotic cells divide to generate ~300 spermatids. Then, the germline switches to oogenesis and starts producing oocytes as adults.

2.3 Structure of adult hermaphrodite gonad

An adult hermaphrodite gonad consists of two U-shaped gonad arms called anterior and posterior gonad arms, which are joined together with a common uterus and vulva (Fig. 9). The somatic gonad consists of distal tip cells, gonadal sheath cells, spermatheca, uterus and vulva (Hubbard and Greenstein, 2000; McCarter et al., 1997). The somatic gonad encloses the germline, which undergoes continuous proliferation during the adult stage. The entire volume of the gonad is doubled every 6.5 hours (Fig. 9B) (Hirsh et al., 1976).

2.3.1 The gonadal sheath cells

Each gonad arm has five pairs of gonadal sheath cells (Hirsh et al., 1976; Kimble and Hirsh, 1979; McCarter et al., 1997; Rose et al., 1997). The distal sheath cells (pair 1 and 2) are morphologically very distinct from the proximal sheath cells (pair 3, 4, and 5). The sheath cell pair 1 does not cover the germ cells completely and forms finger-like projections that insert into the gaps between the germ cells forming a honeycomb like structure (Fig. 10 A&B) (Hall et al., 1999). By contrast, the distal sheath pair 2 encloses the germ cells completely (Hall et al., 1999). The proximal sheath cell pairs are positioned along the long axis of the gonad in an interdigitating pattern and are in close apposition to the oocytes (Fig. 10 C&D) (Hall et al., 1999). Ultrastructural studies show that the proximal sheath cells contain thin and thick filaments. Anti-actin or phalloidin staining shows that actin forms a non-striated filamentous network that runs in parallel as well as circumferential to the direction of the sheath cells (McCarter et al., 1997; Strome, 1986). In addition, structural proteins such as LEV-11/tropomyosin, UNC-87/calponin-like protein and PAT-10/ troponin C localizes to the thin filaments. The UNC-54/myosin heavy chain B and MYO-3/ myosin heavy chain A are principal constituents of the thick filaments (Fig. 9C). In addition, UNC-15/paramyosin and UNC-89 (a protein associated with M-line) were also found to localize to the thick filaments. The proximal sheath cell pair 5 is directly connected to spermatheca and plays an important role during ovulation (Hall et al., 1999). The proximal sheath cells form gap junctions with one another as well as with oocytes (Fig. 9 D&E, 10D).

The proximal sheath cells contain pores, which facilitates the transport of yolk from intestine to oocytes by endocytosis (Hall et al., 1999).

2.3.2 Role of gonadal sheath cells in germline development

The somatic cells of the gonad control several aspects of germline development including germ cell proliferation, stem cell maintenance, and differentiation. In the first larval stage, proliferation of the germline precursor cells, Z2 and Z3, is dependent on the somatic gonad precursor cells, Z1 and Z4. When Z1 and Z4 are ablated using laser, Z2 and Z3 do not divide and eventually undergo cell death suggesting that the somatic cells regulate germline proliferation (Kimble and White, 1981). Later in development, the somatic cells called the distal tip cells (DTC) control germline proliferation. During larval stages and in adults, germ cells divide mitotically at the distal end of the gonad and enter meiosis as they move proximally (Fig. 9A-B). Laser ablation of DTCs causes the germ cells to exit mitosis and enter meiosis prematurely (Kimble and White, 1981). Elegant studies by Judith Kimble and colleagues showed that the GLP-1/Notch signaling pathway controls germline proliferation (Austin and Kimble, 1987). In this pathway, DTCs express LAG-2/ Delta/Serrate ligand while the germ cells express the GLP-1/Notch receptor. Loss-of-function in LAG-2 or GLP-1 result in premature entry into meiosis. By contrast, GLP-1 gain-of-function results in germline tumors due to continued mitosis (Berry et al., 1997; Pepper et al., 2003). Ablation of sheath/spermathecal precursor cells results in reduced proliferation suggesting that they play an important role during germline proliferation. During later

Figure 11. A timeline showing various developmental events during later stages of oogenesis.

Adapted from McCarter et al (1999)

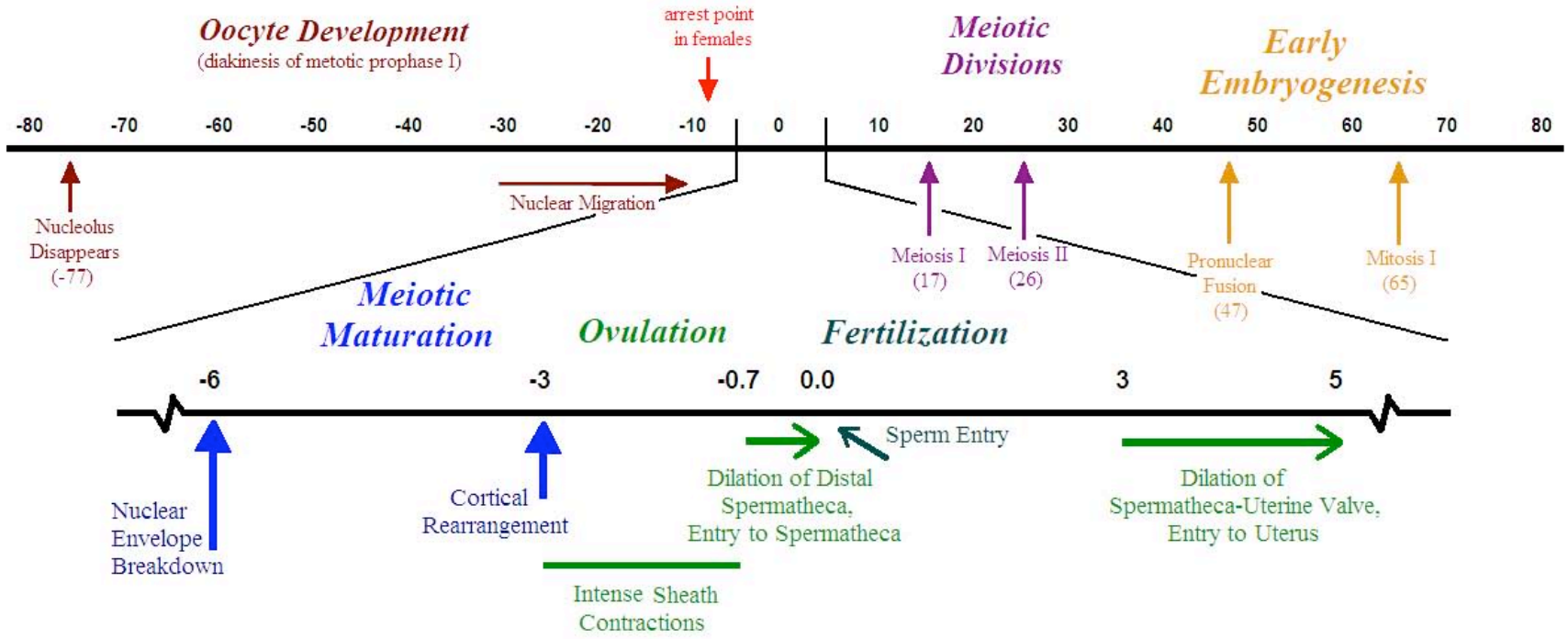
Oocyte Development
(diakinesis of metotic prophase I)
arrest point
in females
Meiotic
Divisions
Early
Embryogenesis
-80 -70 -60 -50 -40 -30 -20 -10 0 10 20 30 40 50 60 70 80
Nucleolus
Disappears
(-77)
Nuclear Migration
Meiosis I
(17)
Meiosis II
(26)
Pronuclear
Fusion
(47)
Mitosis I
(65)
Meiotic
Maturation
Ovulation
Fertilization
-6 -3 -0.7 0.0 3 5
Sperm Entry
Nuclear
Envelope
Breakdown
Cortical
Rearrangement
Dilation of Distal
Spermatheca,
Entry to Spermatheca
Dilation of
Spermatheca-Uterine Valve,
Entry to Uterus
Intense Sheath
Contractions

stages of germline development, the somatic gonad is necessary for pachytene exit and ovulation. Ablation of the two sheath/spermathecal cells at L2/L3 larval stages results in pachytene exit defect. In adult hermaphrodites, the gonadal sheath cells play important structural and regulatory roles. In *C. elegans*, germline ablation does not affect somatic gonadal development; however the germ line has been shown to systemically influence lifespan independent of its reproductive roles (Arantes-Oliveira et al., 2002; Hsin and Kenyon, 1999).

2.3.3 The germline

Germline proliferation occurs in a spatial order with the distal-most germ cells undergoing mitotic proliferation, followed by a transition zone and proximal meiotic zone (Fig. 9B). The germ cells in the distal-most zone (~20 cell diameters from the DTC) contain ~ 250 germ cells that undergo continuous mitotic proliferation. Germline stem cells are thought to reside in this zone, but their identity is not known. As the germ cells move proximally, they exit mitosis to enter meiotic prophase. This region is referred to as the transition zone. In the transition zone, the germ cells are in leptotene/zygotene stage of meiosis. A recent study determined that in hermaphrodites, a germ cell spend 54-60 hours in the meiotic prophase while in the males, the meiotic prophase lasts 20-24 hours (Jaramillo-Lambert et al., 2007). As the oocytes approach the loop region of the gonad arm, they are in the pachytene stage of meiosis I. In the distal gonad arm, the germ cells are syncytial in nature. The germ cells are incompletely cellularized and linked through cytoplasmic bridges forming an anucleate cytoplasmic core called the rachis. The rachis supplies cytoplasmic

contents to the proximal developing oocytes (Gibert et al., 1984). In the loop region of the gonad, ~ 300 germ cells undergo apoptosis (Gumienny et al., 1999). Recently, it was shown that germ cells containing unsynapsed meiotic chromosomes selectively undergo apoptosis (Bhalla and Dernburg, 2005). In addition, these germ cells may also serve as nurse cells by supplying mRNAs and proteins to the developing oocytes (Gumienny et al., 1999). As the oocytes exit from pachytene, they start to grow in size by taking cytoplasmic contents from the rachis. Most of the oocyte growth occurs in the absence of transcription. Oocyte growth involves an increase in both cytoplasmic and nuclear volume (McCarter et al., 1999). The transcriptionally active germ cells supply the mRNA and protein through the rachis by an actin-dependent and microtubule-independent cytoplasmic streaming mechanism (Wolke et al., 2007). An outline of the events occurring in oocyte development is depicted in Fig. 11. Around 80 minutes prior to maturation, the nucleolus disappears. This coincides with transcriptional quiescence of the oocytes. Around 30 minutes prior to ovulation, the oocyte nucleus begins to move to the posterior surface of the oocyte. The reason for distal nuclear migration is not known but this may be a preparatory step for the asymmetric meiotic cell divisions. In the absence of sperm, the oocytes arrest at diakinesis.

2.4 *C. elegans* oocyte meiotic maturation

In the presence of sperm, the most proximal oocyte undergoes oocyte meiotic maturation and ovulation (McCarter et al., 1999; Miller et al., 2001). Oocyte maturation is a complex process during which the oocyte progresses

from diakinesis stage to metaphase stage of meiosis I. In *C. elegans*, meiotic maturation occurs every ~20 minutes in the presence of sperm. When hermaphrodites are depleted of sperm, oocytes arrest at prophase of meiosis I. Also, in mutants with a feminized germ line (for e.g. *fog-2*) oocytes arrest at meiosis I. Meiotic maturation resumes when sperm is introduced by mating with males (McCarter et al., 1999). Thus, the sperm-sensing mechanism enables the worm to conserve metabolically costly oocytes when sperm are unavailable for fertilization. The first visible sign of meiotic maturation is nuclear membrane break down which occurs ~5 minutes prior to ovulation (Fig. 11) (McCarter et al., 1999). The nucleus disappears entirely in two minutes after ovulation and does not reappear until telophase I (Fig. 11). Approximately, two minutes prior to ovulation, the oocytes undergo a characteristic irreversible morphologic change called the cortical cytoskeletal rearrangement (McCarter et al., 1999). The cortical rearrangement converts the “cylindrical”-shaped oocyte into an “ovoid”-shaped oocyte and it is thought to be an actin-dependent process (McCarter et al., 1999). During maturation, the gonadal sheath cells contract intensely, which may contribute to the cortical rearrangement (McCarter et al., 1999; Miller et al., 2001; Rose et al., 1997). The nuclear changes during oocyte maturation include condensation of diakinetic chromosomes and their alignment at the metaphase plate (McCarter et al., 1999). Following meiotic maturation, the oocyte signals its own ovulation by modulating the intensity of sheath contraction and inducing spermathecal dilation.

During ovulation, the distal spermathecal valve dilates and pulls over the matured oocyte resulting in entry into the spermatheca where fertilization occurs (McCarter et al., 1999; Miller et al., 2001; Rose et al., 1997). Following fertilization, the oocyte enters the uterus by dilation of the spermathecal-uterine valve. Thus, in *C. elegans*, meiotic maturation, ovulation, and fertilization are coupled together. In *spe-9* mutant, sperm are defective in fertilization (Singson et al., 1998), but they can signal meiotic maturation. In this mutant, the oocytes undergo maturation and ovulation, but they are not fertilized. The ovulated oocytes complete anaphase I but do not extrude polar bodies or assemble meiosis II spindles (McNally and McNally, 2005) suggesting that fertilization triggers completion of meiosis and results in formation of maternal pronuclei. The ovulated oocytes that are not fertilized undergo endomitosis (Ward and Carrel, 1979) characterized by successive rounds of DNA synthesis and mitosis without cytokinesis, resulting in polyploid oocytes. Also, in mutants where the ovulation is impaired, the oocytes undergo endomitosis (Iwasaki et al., 1996).

2.4.1 The major sperm protein is a signal for oocyte meiotic maturation

In *C. elegans*, sperm provide a signal for oocyte meiotic maturation as the oocytes are arrested at meiosis I in the absence of sperm (McCarter et al., 1999; Miller et al., 2001). Fertilization *per se* is not required because fertilization-defective sperm can still signal meiotic maturation (McCarter et al., 1999). Major Sperm Protein (MSP) signals oocyte meiotic maturation, MAPK activation and ovulation (Miller et al., 2001). To signal oocyte meiotic maturation, MSP is released from sperm via a vesicle budding mechanism.

Figure 12. A MSP vesicle budding mechanism

A. Low magnification EM view showing vesicles (arrows) outside of sperm (S) in the extracellular space. Bar equals 500 nm.
B. High magnification view of a single MSP vesicle. The outer and inner membranes are visible. Bar equals 100 nm.
C. High magnification view of a vesicle immuno-stained for MSP. MSP is seen within the outer ring of the vesicle. Bar equals 100 nm.
D. Immuno-EM view showing a single stalk (arrows) containing MSP from the surface of sperm. Bar equals 100 nm.
E. A vesicle budding mechanism model for MSP release. Reprinted from Kosinski et al., (2005) and Yamamoto et al., (2005).

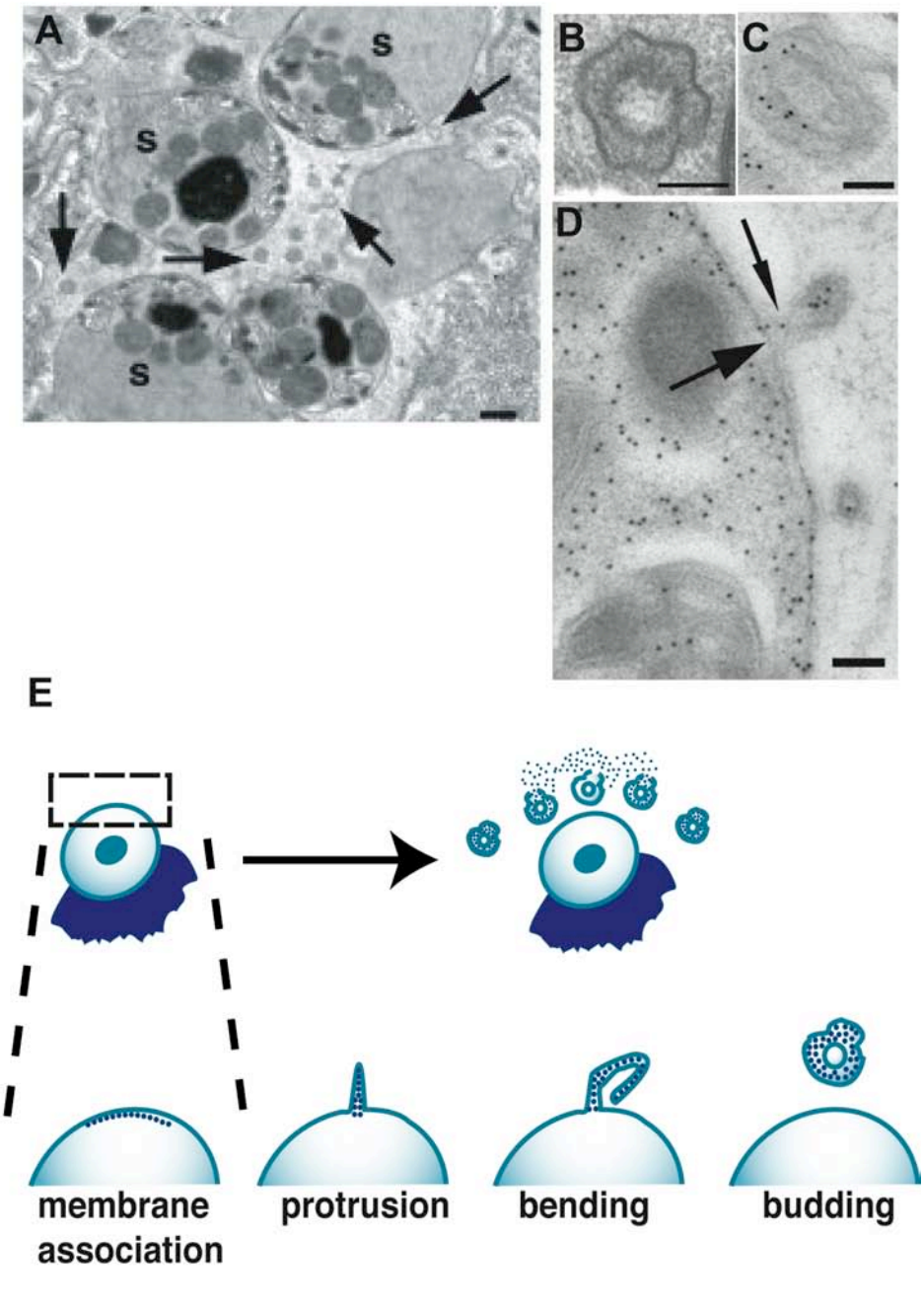
A
S
S
S
B
C
D
E
membrane association
protrusion
bending
budding

MSP is one of the most abundant proteins in nematode sperm accounting for about 15% of the total sperm protein (Klass et al., 1984; Ward et al., 1988; Ward et al., 1986). MSP is a multigene family protein encoded by more than 40 genes including many pseudogenes (Klass et al., 1984; Ward et al., 1988). The finding of MSP as a signal for maturation in *C. elegans* was surprising because previous studies showed that MSP is necessary for sperm motility. In sperm, MSP localizes to the pseudopods where they polymerize into filaments required for amoeboid motility of nematode sperm (Italiano et al., 2001; Roberts and Stewart, 2000). How is MSP released from the sperm to signal meiotic maturation? Kosinski et al. (2005) proposed that MSP is released from sperm via a vesicle budding mechanism (Fig. 12E). Ultrastructural studies using high pressure freezing technique showed the existence of a new class of vesicles that contain MSP near the spermatheca and uterus of adult hermaphrodites (Fig. 12A-D) (Kosinski et al., 2005). These unstable vesicles provide extracellular MSP for signaling (Fig. 12E) (Kosinski et al., 2005). However, the molecular mechanism involved in the formation and release of MSP vesicles are not known.

Proteins with MSP-like domains are widespread, suggesting that related signaling functions might exist. In *Drosophila*, MSP-domain containing protein DVAP-33A was shown to be involved in bouton formation at the neuromuscular junction (Pennetta et al., 2002). Mutations in the MSP domain of the vesicle-trafficking protein VAPB causes motor neural disorders in humans (Nishimura et al., 2005).

Figure 13. Schematic representation of Eph receptor signaling

Various domains in Eph and Ephrins discussed in the text are shown. Reprinted from Kullander and Klein. (2002)

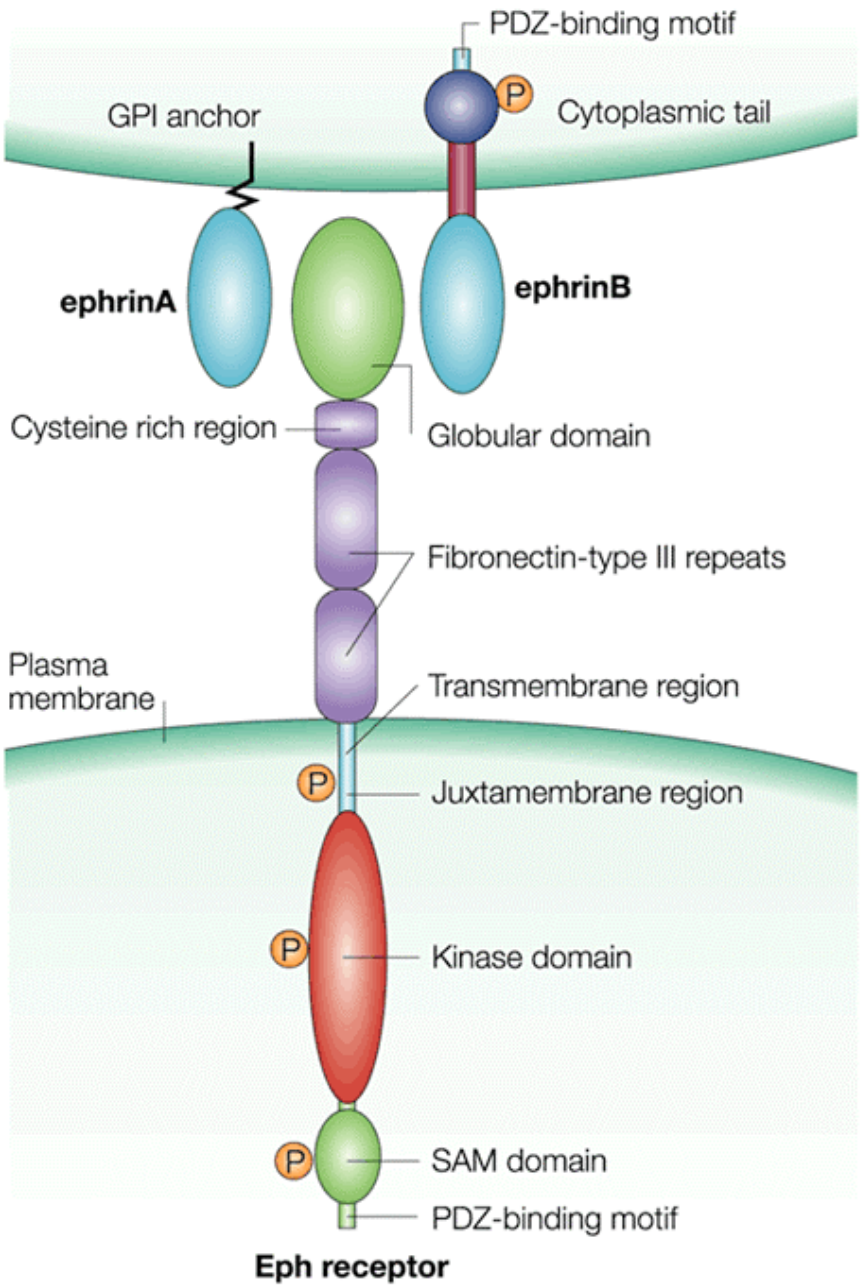
PDZ-binding motif
P
Cytoplasmic tail
GPI anchor
ephrinA
ephrinB
Cysteine rich region
Globular domain
Fibronectin-type III repeats
Plasma membrane
Transmembrane region
P
Juxtamembrane region
P
Kinase domain
P
SAM domain
PDZ-binding motif
Eph receptor

Also disruption of *Mospd*, a gene that contains two MSP domains results in right ventricle defects and neonatal lethality in mice (Pall et al., 2004). Although the function of MSP-domain containing proteins is unknown, studying MSP signaling in *C. elegans* may provide insight on the role of MSP-domain containing proteins in other systems.

2.4.2 Role of VAB-1 in C. elegans oocyte meiotic maturation

Ephrin/Eph receptor signaling is an ancient and highly conserved pathway that regulates diverse processes, including axon guidance, tissue-border formation, synaptic plasticity and neural crest cell migration (Holmberg and Frisen, 2002; Kullander and Klein, 2002; Murai and Pasquale, 2003). Ephrins are classified into two classes: those that are membrane anchored by a glycosylphosphatidylinositol (GPI) anchor (ephrin-A) or those that are transmembrane proteins (ephrin-B) (Kullander and Klein, 2002). The Eph receptors are classified as EphA or EphB based on the class of ephrins they bind and sequence homology. Most of the ephrin-A ligands bind to EphA type receptor while ephrin-B ligands bind to EphB type receptors. One notable exception to this rule is EphA4, which can bind to both ephrin-A and ephrin-B ligands (Kullander and Klein, 2002). Mammals and other vertebrates have 8 ephrins and 13 Eph receptors and many of them play redundant roles during development (Palmer and Klein, 2003).

The canonical Eph receptor consists of an extracellular region, the transmembrane region, and an intracellular part with multiple protein-protein interaction domains (Fig. 12). The extracellular part consists of a globular

domain, cysteine rich region and two fibronectin-type III repeats. The globular domain is likely to be required for ligand binding, while the role of the other domains is not well understood. The cytoplasmic part consists of a kinase domain, a sterile alpha motif (SAM) and a PDZ binding motif. The SAM and PDZ binding motif are thought to play roles in protein-protein interaction as well as dimerization of the receptor. The kinase domain of the Eph receptor is the most well characterized domain of Eph receptors. Several proteins including Nck kinases, PI3K, Ephexins, Abl/Arg and RasGAP have been shown to bind to the intracellular domain of activated Eph receptors, but the functional relevance of these interactions are not clear. It is thought that these interactions relay the signal to its downstream effectors and target proteins. The downstream effectors of Eph signaling are not well characterized but ERK/MAPK and Rho/Cdc42/Rac GTPases are thought to be mediators in some Eph-mediated cellular responses (Kullander and Klein, 2002).

C. elegans has a single Eph receptor, *vab-1*, which shares homology to both mammalian EphA and EphB type receptors (George et al., 1998). *vab-1* is necessary in the nervous system for epidermal morphogenesis, ventral closure of embryonic epidermis and neuronal organization (George et al., 1998). Mutations in *vab-1* result in incompletely penetrant abnormalities such as notched head, embryonic and larval lethality, and tail defects (Brenner, 1974; George et al., 1998). VAB-1 may have both kinase-dependent and independent functions because mutations in *vab-1* that eliminate kinase activity do not cause complete loss of VAB-1 function (George et al., 1998).

There are four ephrins (EFN-1 to EFN-4), which are similar in sequence to ephrin-B but are GPI- linked like the ephrin-A class (Wang et al., 1999). Genetic analyses suggest that ephrins are necessary for epidermal cell organization and mutations in EFN-1, EFN-2, and EFN-3 have defects in head morphology and ventral enclosure of embryo similar to *vab-1(null)* mutant (Chin-Sang et al., 1999; Chin-Sang et al., 2002; Wang et al., 1999). Biochemical analyses show that all the ephrins are required for activation of the VAB-1 tyrosine kinase under in vivo conditions (Wang et al., 1999). Together, all these data suggest that Eph signaling in *C. elegans* play critical roles during development. However, the signaling mechanism(s) downstream of VAB-1 is not well understood.

In *C. elegans*, VAB-1 functions to regulate oocyte meiotic maturation (Miller et al., 2003). Miller et al., 2003 identified VAB-1 as a potential receptor for MSP using microarray data for oocyte-enriched genes. They showed MSP-FITC binding to the dissected gonads is reduced in *vab-1(null)* mutants suggesting that MSP may bind to VAB-1. Furthermore, they showed that MSP-FITC binds to VAB-1 expressed in heterologous cell culture. To examine the role of *vab-1* in oocyte meiotic maturation, they examined *vab-1(null)* hermaphrodites and *vab-1(null);fog-2(q71)* unmated females. They found that *vab-1(null)* hermaphrodites did not exhibit any obvious defects in oocyte meiotic maturation suggesting that *vab-1* is not required for meiotic maturation.

Figure 14. A sperm-sensing mechanism regulates oocyte meiotic maturation

(A) Oocyte meiotic maturation rates. Wild type worms have a maturation rate of 2.25 maturations/gonad arm/hour whereas *fog-2(q71)* females have very low maturation rate. The maturation rate is elevated in *vab-1; fog-2(q71)* and *ceh-18(mg57); fog-2(q71)* worms compared to females. Unmated *ceh-18 (mg57);vab-1 (dx31); fog-2 (q71)* worms have a maturation rate similar to wild type.
(B) VAB-1 Eph receptor and sheath cell pathways negatively regulate meiotic maturation in the absence of sperm. MSP relieves this inhibition in part by binding VAB-1. Reprinted from Miller et al., 2003).

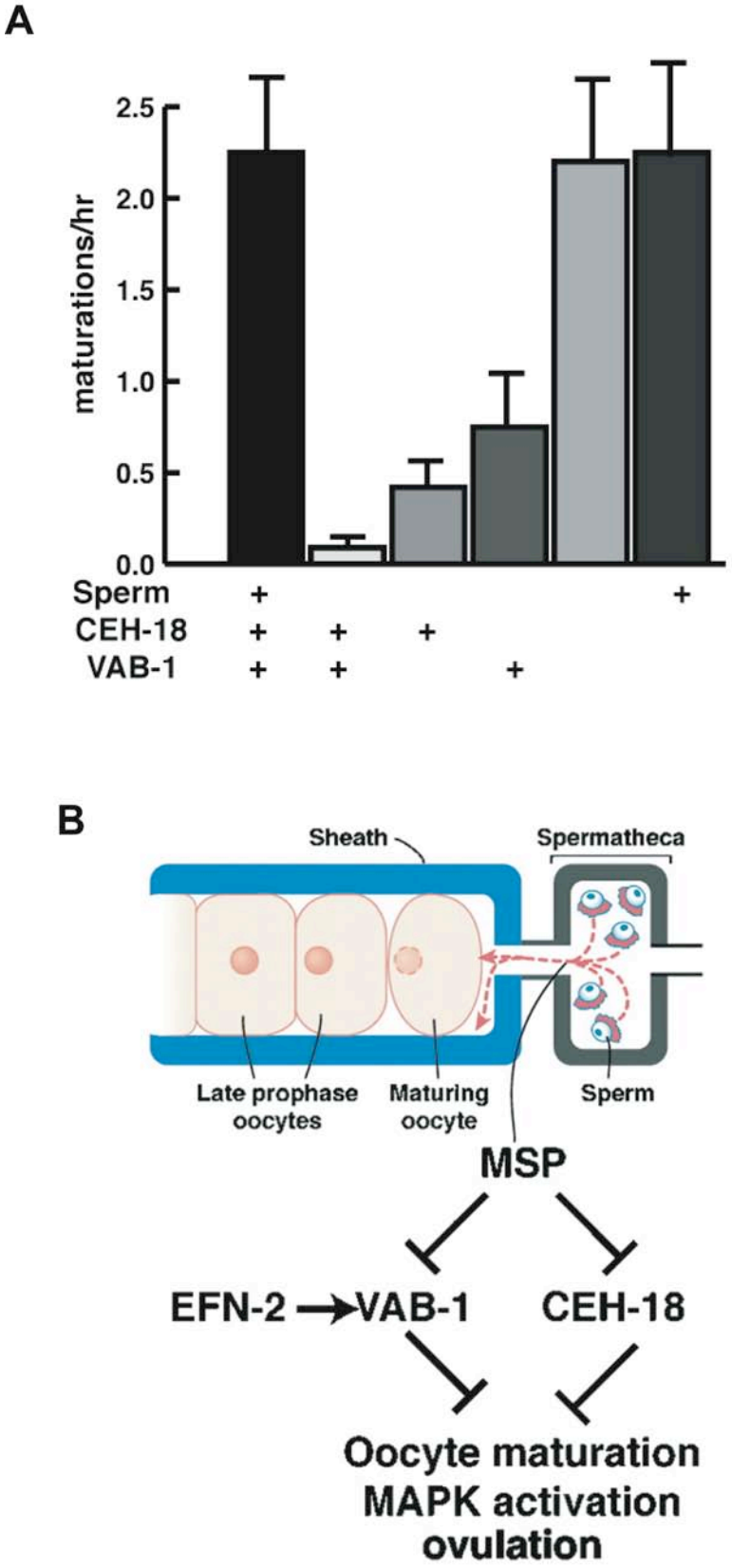
A
maturations/hr
2.5
2.0
1.5
1.0
0.5
0.0
Sperm + +
CEH-18 + + +
VAB-1 + + +
B
Sheath
Spermatheca
Late prophase oocytes
Maturing oocyte
Sperm
MSP
EFN-2
VAB-1
CEH-18
Oocyte maturation
MAPK activation
ovulation

By contrast, *vab-1(null);fog-2(q71)* unmated females showed an elevated oocyte meiotic maturation rate compared to the *fog-2(q71)* unmated females suggesting that *vab-1* is required to inhibit meiotic maturation in the absence of sperm (Fig. 14). To determine the site of action of *vab-1* in regulating oocyte meiotic maturation, Miller et al.(2003) performed *vab-1(RNAi)* analysis in *rrf-1* mutants. *rrf-1* encodes a RNA-dependent RNA polymerase that is required in the soma for the RNAi response (Sijen et al., 2001). *rrf-1(null)* mutants are resistant to RNAi function in the soma but not in the germline. Using this mutant, Miller et al (2003) showed that VAB-1 functions within the germline to regulate oocyte meiotic maturation. Collectively, these data suggest that MSP promotes oocyte meiotic maturation by antagonizing VAB-1 activity in the oocytes. However, *vab-1(null)* mutants still respond to MSP suggesting that additional receptors may be involved. In addition, the oocyte meiotic maturation rate in unmated *vab-1(null)* females is elevated compared to unmated females but is lower than that of wild-type hermaphrodites. This observation suggested that additional receptor(s) and/or pathways might function in parallel with VAB-1 to negatively regulate oocyte meiotic maturation. Therefore, Miller et al (2003) examined whether the POU-homeoprotein CEH-18 has a role in regulating oocyte maturation. Previously, it was shown that CEH-18 is required for proper gonadal sheath cell differentiation and function (Rose et al., 1997). Furthermore, CEH-18 is expressed in somatic sheath cells, but not in oocytes and is necessary for proper meiotic maturation and ovulation (Greenstein et al., 1994; Rose et al., 1997). Miller et al (2003) found that CEH-18 is necessary in

the gonadal sheath cells to inhibit oocyte meiotic maturation in the absence of sperm (Fig. 14A). To examine the genetic interaction between *ceh-18* and *vab-1*, Miller et al (2003) measured the maturation rates in unmated *vab-1(null);ceh-18(null)* females and found that unmated *vab-1(null);ceh-18(null)* females had a maturation rate similar to the wild-type (Fig. 14A). More importantly, unmated and mated *vab-1(null);ceh-18(null)* females had similar rates suggesting that oocyte maturation is independent of MSP (Fig. 14A). Taken together, these results show that VAB-1 and CEH-18 act together to inhibit meiotic maturation in the absence of sperm signal (Fig. 14B). In the absence of MSP, VAB-1/Eph receptor functions within the germline to negatively regulate oocyte maturation and MAPK activation (Fig. 14B). However, neither the signaling components downstream of VAB-1 nor the mechanism by which VAB-1 regulates oocyte meiotic maturation are known. Recently, ITR-1/IP3 receptor, UNC-43/CaMKII kinase, and NMR-1/NMDA receptor were implicated in control of oocyte meiotic maturation (Corrigan et al., 2005).

2.4.3 Role of MAPK in C. elegans oocyte meiotic maturation

In *C. elegans*, the MAPK signaling cascade plays an important role in vulval development, male spicule development, larval viability, maintenance of axon position and immunological defense mechanism (Sundaram, 2006). All the members of the conserved MAPK signaling including LET-60/RAS, LIN-45/RAF, MEK-2/MEK and MPK-1/ERK are conserved in *C. elegans* (Moghal and Sternberg, 2003; Sundaram, 2006).

In hermaphrodites, MPK-1 pathway plays several essential roles including pachytene germ cell exit during meiotic prophase, oocyte growth and meiotic maturation (Church et al., 1995). Reduction of *mpk-1* activity disrupts pachytene cellular organization accompanied by inability of germ cells to progress beyond pachytene stage of meiosis (Church et al., 1995). This suggests that MPK-1 activation is required for pachytene to diplotene transition stage of meiosis. Consistent with this conclusion, active diphosphorylated MPK-1 is detected in the pachytene region (Lee et al., 2007). In the inactive state, MPK-1 exists in the unphosphorylated form. MEK-2 phosphorylates MPK-1 resulting in MAPK activation. Following pachytene exit, the oocytes start to grow in size by accumulating nutrients and metabolites from the rachis. As oocytes grow in size they continue to move proximally. MPK-1 also appears to play a role in oocyte growth as partial depletion of *mpk-1* activity results in oocytes that are abnormally large in size (Lee et al., 2007). MPK-1 functions likely in the canonical pathway for the “large–oocyte” phenotype because partial reduction of *let-60* activity also results in the same phenotype (Lee et al., 2007). By contrast, gain-of-function in *let-60* activity results in a “small oocyte phenotype” suggesting that MPK-1 levels regulate oocyte growth (Lee et al., 2007). MPK-1 is also necessary for proper oocyte meiotic maturation because partial depletion of *mpk-1* activity by RNAi or loss-of-function mutations results in low meiotic maturation rate and defects in oocyte nuclear migration (Lee et al., 2007).

This study is consistent with previous observations that sperm–dependent MAPK activation occurs in the most proximal oocytes (Miller et al., 2001; Miller et al., 2003; Page et al., 2001). The oocyte MAPK activation is sperm-dependent because unmated females and hermaphrodites purged of sperm do not have activated MAPK. MSP signals MAPK activation in the proximal oocytes (Miller et al., 2001; Miller et al., 2003). In the absence of sperm, VAB-1 and CEH-18 act redundantly to inhibit MAPK activity in proximal oocytes because unmated *vab-1(null); ceh-18(null)* females have activated MAPK in the proximal oocytes. MSP signaling promotes MAPK activation by inhibiting VAB-1 and CEH-18 pathways (Fig.14B). Interestingly, *vab-1(null)* hermaphrodites have MAPK activation which extended to more distal (-1 to -5) oocytes suggesting that VAB-1 is a negative regulator of MAPK activation (Miller et al., 2003).

2.4.4 Positive regulators of oocyte meiotic maturation

In *C. elegans*, CDK-1/cyclin-dependent kinase is necessary for proper meiotic progression (Boxem et al., 1999). Reduction of CDK-1 activity results in delayed nuclear envelope breakdown and failure of meiotic I divisions. The oocyte eventually matures and is fertilized, but the embryos arrest at the one-cell stage (Boxem et al., 1999). In other systems, CDK-1 activity is regulated by WEE-1/Myt1 kinase, which keeps CDK-1 inactive by phosphorylation. By contrast, CDC-25 phosphatase activates CDK-1 by dephosphorylation. In addition, CDK-1 activity is also regulated by degradation of cyclin B. In *C. elegans*, WEE-1.3/ Myt1 kinase is necessary for proper meiotic maturation (Burrows et al., 2006). The *cdk-1* maturation defect can be

suppressed by WEE-1.3/ Myt1 kinase (Burrows et al., 2006) suggesting that CDK-1 is a major target of WEE-1.3 kinase. However, it is not known whether MSP promotes MPF activation by inhibiting WEE-1.3 activity and/or by promoting CDC-25. Recently, CDK-1 was shown to be required along with other kinases to promote phosphorylation and subsequent destruction of meiotic regulators for proper oocyte-to-embryo transition (Greenstein and Lee, 2006). PLK-1/polo kinase is also necessary for NEBD and meiotic progression in oocytes (Chase et al., 2000).

Two TIS11 zinc finger-containing proteins OMA-1 and OMA-2 are redundantly required for oocyte meiotic maturation (Detwiler et al., 2001). Both OMA-1 and OMA-2 are expressed only in the germline (Detwiler et al., 2001). *oma-1(null);oma-2(null)* double mutants are sterile because they fail to undergo oocyte meiotic maturation despite the presence of sperm (Detwiler et al., 2001). *oma-1(null);oma-2(null)* double mutant initiates but fails to complete meiotic maturation (Detwiler et al., 2001). Reduction of *wee-1.3* activity by RNAi can suppress the *oma-1(null);oma-2(null)* double mutant maturation defect (Detwiler et al., 2001) suggesting that OMA-1 and OMA-2 function upstream of MPF activation. OMA-1 and OMA-2 contain TIS11 zinc finger domains, which are thought to function by regulating mRNA translation. Therefore it is possible that OMA-1 and OMA-2 might also act as regulators of mRNA translation during or prior to oocyte meiotic maturation. However, it is not known whether meiotic maturation in *C. elegans* requires protein translation.

2.5 Nuclear changes during oocyte meiotic maturation

Meiotic maturation is accompanied by extensive changes to the nucleus. This includes distal nuclear migration, localization of AIR-2 to the chromosomes, NEBD, congression of bivalents to the metaphase plate, and spindle assembly. Prior to meiotic maturation, the nucleus migrates to the distal end of the oocyte. Recently, activated MPK-1/MAPK was shown to be required for distal nuclear migration (Lee et al., 2007). During meiotic maturation, the oocyte nuclear membrane breaks down. It is characterized by a decrease in the margins of nuclear membrane under the Nomarski optics. The mechanisms involved in NEBD are not known; however, it may involve CDK-1 activation because in *cdk-1(RNAi)*–treated NEBD is delayed (Boxem et al., 1999).

2.5.1 Localization of AIR-2 to meiotic chromosomes

air-2 encodes an aurora kinase that is required for polar body extrusion and cytokinesis in the embryos (Kaitna et al., 2002; Rogers et al., 2002; Schumacher et al., 1998; Severson et al., 2000). AIR-2 is a member of a family of “chromosomal passenger proteins” that localize to the chromatin during mitosis and meiosis (Adams et al., 2001). AIR-2 is necessary for histone H3 phosphorylation during mitosis as well as meiosis (Hsu et al., 2000). In wild-type hermaphrodites, AIR-2 localizes to chromosomes of the most proximal (–1) oocyte prior to NEBD (Schumacher et al., 1998). Localization of AIR-2 is dependent on the presence of sperm because when sperm is absent, AIR-2 localizes to the cytoplasm of –1 oocyte (Schumacher et al., 1998). The localization of AIR-2 to the chromatin occurs prior to NEBD. In mitosis as well

as in meiosis, localization of AIR-2 to the chromatin is dependent upon at least three proteins, BIR-1/Survivin, ICP-1/Incenp, and CSC-1/ novel protein (Kaitna et al., 2000; Romano et al., 2003; Speliotes et al., 2000). Interestingly, ICP-1 and BIR-1 localize to the chromatin of –1 oocyte in a sperm-dependent fashion (Burrows et al., 2006; Speliotes et al., 2000). However, whether AIR-2 requires ICP-1/BIR-1/CSC-1 for localization to the chromatin of the maturing oocyte is not known. Also, the functional significance of AIR-2 localization is not understood because meiotic maturation and ovulation proceeds normally in *air-2(RNAi)*–treated hermaphrodites (Schumacher et al., 1998).

2.5.2 Meiotic spindle assembly

In *C. elegans*, meiotic maturation triggers spindle assembly in the proximal oocyte after NEBD. Meiotic spindle assembly in females is unusual because it occurs in the absence of centrosomes (Schatten, 1994). In many species including humans, centrosomes are eliminated during oogenesis. Unlike in mitosis, meiotic spindle assembly is acentrosomal and anastral in nature. Acentriolar spindle assembly in the oocytes is dependent on microtubules (Schatten, 1994). In wild-type oocytes, microtubules form an interphase like cytoplasmic meshwork. Following NEBD, microtubules gain access to the chromosomes to set-up the bipolar spindle. The meiotic spindle assembly is dependent on two genes, *mei-1* and *mei-2*, which encode catalytic and regulatory subunit of katanin respectively (Clark-Maguire and Mains, 1994a; Clark-Maguire and Mains, 1994b; McNally and McNally, 2005; McNally et al., 2002; Srayko et al., 2000). Katanin is a microtubule-severing AAA

(ATPase associated with various cellular activities) protein (McNally and Vale, 1993; Patel and Latterich, 1998). The catalytic subunit is an ATPase that has ATP-dependent microtubule-severing activity (Hartman and Vale, 1999). The regulatory subunit controls the ATPase activity of catalytic subunit. Loss of *mei-1* and *mei-2* activity results in meiotic spindle assembly defects but no apparent defects in mitotic spindle assembly (Clandinin and Mains, 1993; Clark-Maguire and Mains, 1994a; Mains et al., 1990) suggesting that katanin is required for meiotic spindle assembly.

Meiotic spindle assembly is also dependent on microtubule motors such as *klp-15*/*klp-16/klp-18* (kinesins) and *dhc-1*(dynein heavy chain) (Segbert et al., 2003; Yang et al., 2005; Yang et al., 2003). MEI-1 is also required for translocation and reorientation of meiotic spindles to the oocyte cortex. Meiotic spindle transloction is essential for formation of a large oocyte and small polar body at the end of meiosis. MEI-1 and MEI-2 activity must be downregulated at the end of meiosis because improper inclusion of MEI-1 into mitotic spindle will results in defects in mitotic spindle assembly. At the end of meiosis, M-phase regulator, CDK-1, promotes phosphorylation of MEI-1 by MBK-2. This results in CUL-3/MEL-26 E3 ubiquitin ligase complex mediated MEI-1 degradation (Furukawa et al., 2003; Pang et al., 2004; Pellettieri and Seydoux, 2002; Pintard et al., 2003; Quintin et al., 2003; Shirayama et al., 2006; Stitzel et al., 2006).

2.5.3 Control of oocyte transcription

In many species, oocytes are transcriptionally inactive during meiotic arrest and resume transcription during early stages of embryogenesis. Prior to

the diakinesis stage, *C. elegans* oocytes actively transcribe and produce mRNAs which are translated immediately or stored for later use (Schisa et al., 2001). Once the oocytes enter diakinesis, they become transcriptionally silent until early stages of embryogenesis (Batchelder et al., 1999; Tenenhaus et al., 2001). In embryos, the primordial germ cells resume transcription after the onset of gastrulation in the embryos (Seydoux et al., 1996; Tenenhaus et al., 1998; Tenenhaus et al., 2001; Seydoux and Dunn, 1997).

2.6 Cytoplasmic changes during oocyte meiotic maturation

Meiotic maturation is accompanied by extensive changes in the oocyte cytoplasm that are collectively referred to as cytoplasmic maturation (Voronina and Wessel, 2003). This includes remodeling of the oocyte cytoskeleton, expression of ligands for ovulation and reorganization of cortical granules (Voronina and Wessel, 2003; Harris et al., 2006; Bembenek et al., 2007). These changes are important for fertilization and subsequent embryogenesis. However, the cytoplasmic changes associated with meiotic maturation are not well understood when compared to the nuclear events. Ultrastructural studies show that the arrested oocytes in females have highly organized and clustered cytoplasmic organelles near the cortex compared to the hermaphrodites (Kosinski, M. and Greenstein, D. unpublished data).

Figure 15. Cortical granule exocytosis in *C. elegans*

Cortical granules form in the growing oocytes and accumulate in the cytoplasm. In the -1 oocyte, cortical granules start to aggregate and form discrete filaments that are located in the cortex. Following fertilization, cortical granules undergo exocytosis and contribute to the formation of eggshell. Adapted from Bembenek et al (2007).

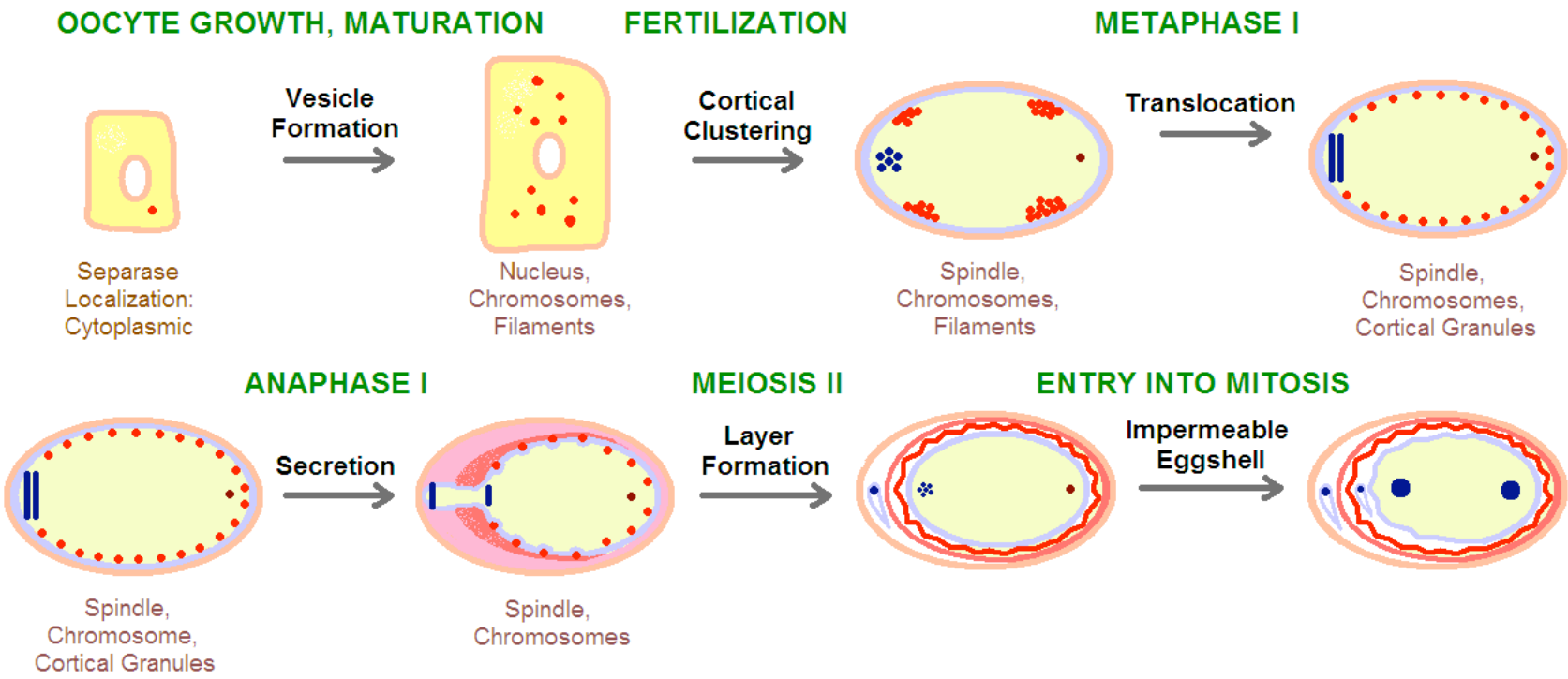
OOCYTE GROWTH, MATURATION
FERTILIZATION
METAPHASE I
Vesicle Formation
Cortical Clustering
Translocation
Separase Localization: Cytoplasmic
Nucleus, Chromosomes, Filaments
Spindle, Chromosomes, Filaments
Spindle, Chromosomes, Cortical Granules
ANAPHASE I
MEIOSIS II
ENTRY INTO MITOSIS
Secretion
Layer Formation
Impermeable Eggshell
Spindle, Chromosome, Cortical Granules
Spindle, Chromosomes

The biological function of these organized cytoplasmic organelles is not known but they may play a role in meiotic arrest. In addition, arrested oocytes in females have large cytoplasmic foci consisting of ribinucleoproteins (RNPs) (Schisa et al., 2001). MSP triggers dissociation of these cytoplasmic foci (Michael, J. and Schisa, J. unpublished data) suggesting that these foci may contain proteins and mRNA required for oocyte meiotic maturation.

2.6.1 Cortical cytoskeletal rearrangement

During meiotic maturation, oocytes undergo cortical cytoskeletal rearrangement resulting in oocyte shape change (McCarter et al., 1999). Initially, oocytes are cylindrical in shape; following cortical reorganization, oocytes are ovoid in shape. Cortical rearrangement is an intrinsically driven process that appears to function in the absence of gonadal sheath cells (McCarter et al., 1999). Though the molecular basis of cortical reorganization process is not known, it is likely to be an actin dependent process. This process is largely uncharacterized genetically because no mutations have been isolated that can uncouple maturation and cortical rearrangement.

2.6.2 Cortical granule exocytosis

Cortical granules are large secretory vesicles that are present near the cortex of oocytes (Voronina and Wessel, 2003; Wessel et al., 2001). These vesicles contain proteoglycans, structural proteins, and enzymes such as proteases and glycosidases (Wessel et al., 2001).

In many species, fertilization triggers cortical granule exocytosis and modifies the cell membrane of the oocyte. Cortical granule exocytosis contributes to the formation of an impermeable egg-shell and physical block to polyspermy (Runft et al., 2002). In *C. elegans*, cortical granules are formed in the proximal oocytes and are exocytosed following fertilization (Bembenek et al., 2007; Sato et al., 2006). Prior to meiotic maturation, the cortical granules are localized in the cytoplasm. Following meiotic maturation, cortical granules undergo clustering to form discrete filaments (Fig. 15) (Bembenek et al., 2007). After fertilization, they are redistributed in the cortex and undergo exocytosis at anaphase I of meiosis. SEP-1/separase is necessary for cortical granule exocytosis because depletion of *sep-1* activity results in significant reduction of cortical granule exocytosis (Bembenek et al., 2007). This is surprising because separase has been well documented for its role in cleavage of cohesins during metaphase-to-anaphase transition. Interestingly, the role of SEP-1/separase in cortical granule exocytosis is genetically separable from its role during metaphase-to-anaphase transition (Bembenek et al., 2007). However, the mechanism by which separase regulates exocytosis is a key question that needs to be addressed in future.

2.7. Control of ovulation

Ovulation in *C. elegans* is dependent on the conserved LIN-3(EGF)/LET-23 (EGF-receptor) signal transduction pathways (Bui and Sternberg, 2002; Clandinin et al., 1998; Kariya et al., 2004; Moghal and Sternberg, 2003). Reduction-of-function mutations in *lin-3* or *let-23* result in sterility due to failure

of spermathecal dilation during ovulation (Clandinin et al., 1998). The maturing oocyte is thought to produce LIN-3(EGF) which binds to the LET-23 receptor expressed on the distal spermatheca to promote dilation of spermatheca via a downstream IP3-mediated pathway (Clandinin et al., 1998). Binding of IP3 to ITR-1/IP3 receptor (IP3R) promotes calcium release from the endoplasmic reticulum, which in turn induce ovulation (Bui and Sternberg, 2002; Clandinin et al., 1998). Proper regulation of IP3 level is important because mutation in *ipp-5*, which encodes IP3 phosphatase, results in hyperdilation of the spermatheca and two oocytes are ovulated per cycle (Bui and Sternberg, 2002). Interestingly, ITR-1 is also a negative regulator of oocyte meiotic maturation which acts downstream of VAB-1/Eph signaling (Corrigan et al., 2005). Recently, VAV-1, a Rho/Rac-family GEF homologous to the mammalian Vav proto-oncogene, was shown to function downstream of LIN-3/LET-23 pathway for ovulation in *C. elegans* (Norman et al., 2005). However, the mechanism by which VAV-1 regulates ovulation is not known.

2.8. Fertilization and egg activation

In hermaphrodites, ~300 spermatids are generated during larval stages (Singson, 2001; Singson et al., 1999). Thus, an adult hermaphrodite generates ~300 progeny. However, when mated to males, hermaphrodites can make more than a thousand progeny (Singson et al., 1999). Sperm are stored in the spermatheca, which is the site of fertilization. Proper fertilization is essential for completion of oocyte meiosis (McNally and McNally, 2005). Fertilization is a cell-cell fusion event in which the entire sperm merges with the oocyte.

Fertilization triggers egg activation, whereby the oocyte completes meiotic divisions, establishes the block to polyspermy, and initiates the embryonic program (Runft et al., 2002). How the block to polyspermy is set up is an interesting question because each oocyte is fertilized by only one sperm. A potent mechanism must exist to prevent polyspermy because *C. elegans* oocytes do not contain an egg coat as mammalian oocytes and fertilization occurs very rapidly even before the oocyte enters the spermatheca completely. Fertilization triggers egg-shell formation, oocyte-embryo transition and anterior-posterior (A/P) polarity establishment (Goldstein and Hird, 1996; Greenstein and Lee, 2006; McNally and McNally, 2005; Yamamoto et al., 2006). In *C. elegans*, the site of sperm entry specifies the future posterior end of the embryo (Goldstein and Hird, 1996; McNally and McNally, 2005). The signal(s) from sperm that initiate A/P polarity are not known; however, centrioles play an important role in this process (Cowan and Hyman, 2004). The establishment of anterior-posterior (A/P) polarity is important for asymmetric cell division and embryonic cell fate specification.

2.9. Molecular mechanisms involved in oocyte meiotic maturation: An overview of new findings

In *C. elegans*, the major sperm protein (MSP) promotes oocyte meiotic maturation, MAPK activation, and ovulation. Prior studies have established that two genetic pathways defined by the germline VAB-1/Eph receptor and a somatic gonadal pathway defined by the POU-homeobox transcription factor, CEH-18 regulates oocyte meiotic maturation. I reasoned that many additional components of the VAB-1 and CEH-18 pathways were likely to function as

negative regulators, and I sought to identify them using a genome-wide RNAi screen. I performed this screen using a *fog-2(q71)* female sterile strain in which oocytes arrest at prophase of meiosis I and are retained in the gonad arm due to the absence of MSP. I screened for rare RNAi clones that cause meiotic maturation and ovulation to occur at elevated rates and unfertilized oocytes to be laid onto the bacterial lawn in increased numbers despite the absence of MSP. The fact that *ceh-18* was identified provides validation for the rationale and effectiveness of the screen. In this screen, I identified seventeen negative regulators of MSP signaling, including innexins and components of $G\alpha_{o/i}$ and $G\alpha_s$ signaling pathways. Further, I provide evidence that germline and somatic pathways regulate meiotic maturation. A somatic $G\alpha_{o/i}$ signaling pathway is necessary and sufficient to repress oocyte MAPK activation and meiotic maturation. By contrast, a somatic $G\alpha_s$ pathway is necessary and sufficient to promote meiotic maturation. Further, I show that *inx-14* and *inx-22*, which encode innexin/pannexin components of gap junctions, function as negative regulators of oocyte meiotic maturation and are potential targets of $G\alpha_s$ signaling. In addition, the somatic G-protein signaling pathways influence reorganization of microtubule cytoskeleton prior to fertilization. Together, my study provides key insights into the role of the somatic gonad in the control of oocyte maturation, and highlights interesting similarities and contrasts between the control of meiotic arrest in *C. elegans* and mammals.

CHAPTER II

IDENTIFICATION OF NEGATIVE REGULATORS OF OOCYTE MEIOTIC MATURATION

Introduction

Oocytes of most sexually reproducing animals arrest in meiotic prophase and actively maintain their arrest for prolonged periods—up to 50 years in humans. In response to hormonal signaling, oocytes resume meiosis in the highly conserved process of meiotic maturation, which prepares the oocyte for fertilization (Greenstein, 2005; Greenstein and Lee, 2006; Voronina and Wessel, 2003; Yamamoto et al., 2006). Oocyte meiotic maturation is defined by the transition between diakinesis and metaphase of meiosis I and is accompanied by nuclear envelope breakdown, cortical cytoskeletal rearrangement, meiotic spindle assembly, and chromosome congression. Chromosome missegregation in female meiosis I represents the leading cause of human birth defects (e.g., Down syndrome). Because advanced maternal age is the most significant risk factor (Hassold and Hunt, 2001), the mechanisms that maintain meiotic diapause and preserve oocyte vitality are of intense interest.

Great strides have been made in understanding the control of cell-cycle progression during the meiotic maturation process, culminating in the discovery of the maturation promoting factor (Cdk1/cyclin B) (Masui, 2001).

Mitogen-activated protein kinase (MAPK) cascades also play an important role in controlling meiotic progression (Fan and Sun, 2004). By contrast, comparatively less information is available about the intercellular signaling pathways that regulate meiotic resumption. Unifying conclusions from studies in vertebrate and invertebrate systems are that soma-germline interactions play a crucial role and that regulation involves both positively and negatively acting pathways (Voronina and Wessel, 2003). As meiotic maturation signals have been characterized in several invertebrate systems, studies in these organisms may offer both comparative and mechanistic insights.

In *C. elegans*, sperm export the major sperm protein (MSP) by a vesicle-budding mechanism to trigger oocyte MAPK activation and meiotic maturation (Fig. 16A) (Kosinski et al., 2005; Miller et al., 2001; Miller et al., 2003). MSP is also the key cytoskeletal element required for the actin-independent amoeboid locomotion of nematode spermatozoa (Bottino et al., 2002). Since hermaphrodites produce only a fixed number of sperm, meiotic maturation rates are initially high for the first two days of adulthood but decline as sperm are used for fertilization and the MSP signal disappears (Kosinski et al., 2005; McCarter et al., 1999). Similarly, in sex-determination mutants of *C. elegans*, which fully feminize the hermaphrodite gonad (e.g., *fog-2* or *fog-3*), oocytes arrest until sperm are supplied by mating. In *C. elegans*, the vital processes of meiotic maturation and ovulation are tightly coupled to sperm availability through a complex regulatory network involving both negative and positive controls.

Parallel genetic pathways defined by *vab-1*, which encodes an ephrin receptor, and *ceh-18*, which encodes a POU-homeoprotein expressed in gonadal sheath cells but not oocytes, together compose an MSP-sensing control mechanism that inhibits meiotic maturation, MAPK activation, and ovulation when sperm are not present in the reproductive tract (Fig. 16A) (Corrigan et al., 2005; Miller et al., 2003) Negative regulators of meiotic maturation, such as *vab-1* and *ceh-18*, are identified by RNAi knockdown or loss-of-function mutations that cause females to mature oocytes in the absence of the MSP signal. In contrast, positive regulators, such as *oma-1* and *oma-2*, which encode two TIS-11 zinc finger proteins expressed in the germline (Detwiler et al., 2001), are identified by RNAi knockdown or loss-of-function mutations that reduce or block meiotic maturation in hermaphrodites in the presence of the MSP signal.

Here I employed a genome-wide RNAi screen to define new regulators of oocyte meiotic maturation in *C. elegans*. The set of regulators defined in this screen comprises 17 highly conserved proteins (Table 1), which mediate meiotic maturation signaling functions in the soma or oocytes. Many of these genes are negative regulators of MAPK activation. Further, I show that four conserved proteins, DAB-1, PQN-19, PKC-1, and VAV-1, function with the VAB-1 MSP/Eph receptor in oocytes. In addition, I show that *goa-1* functions in parallel to the VAB-1 MSP/Eph receptor pathway to regulate oocyte meiotic maturation.

Materials and methods

Nematode strains

Standard culture techniques were used at 20ºC (Brenner, 1974). Alleles used are described in WormBase (http://www.wormbase.org). The following mutations were used:

LGI: *fog-3(q443)*, *pqn-19(ok406), goa-1(sa734)*, *goa-1(n1134rf)*

LGII: *dab-1(gk291)*, *vab-1(dx31)*

LGIV: *oma-1(zu40te33)*

LGV: *oma-2(te51), pkc-1(ok563)*, *fog-2(q71)*

LGX: *kin-2(ce179rf)*, *ceh-18(mg57)*

The following rearrangements were used: *hT2(qIs48)(I,III)*, *mIn1(II)*, *DnT1(IV,V)*.

RNA Interference

Genome-wide RNAi screening was performed using a modified method of (Kamath et al., 2003). Overnight culture of HT115(DE3) bacteria were plated per well onto M9-NGM medium (42.3mM Na2HPO4, 22.1mM KH2PO4, 8.6mM NaCl, 18.7mM NH4Cl, 1 mM CaCl2, 1 mM MgSO4, 0.5% casamino acids, 2% agar, 0.2% β-lactose, 5 µg/ml cholesterol, 25 µg/ml carbenicillin) and incubated overnight at 22ºC for induction of dsRNA. *fog-2(q71)* female worms (L3 larval stage) were placed in each well and incubated at 22ºC. *unc-22* was used as positive control for RNAi efficacy and the empty vector (L4440) as a negative control for all the screening experiments. The worms were screened on the second day of adulthood for the presence of unfertilized oocytes on the

bacterial lawn or within the uteri of the adults. The positive clones obtained from the screen were classified based on the consequence for gonadal structure: class I (17 clones) had no appreciable effects, and class II (158 clones) caused defects in gonadal morphology. All class I clones were rescreened and confirmed in more than five experiments, whereas all class II clones were confirmed by rescreening at least twice. The insert DNA of class I clones was sequenced to verify gene identity. For the *oma-1(RNAi);oma-2(RNAi)* double RNAi experiments, *oma-1* and *oma-2* bacterial clones were grown separately in LB broth and equal volume were mixed together.

Phenotypic Analysis and Immunofluorescence

Oocyte meiotic maturation rates and MAPK activation were analyzed as described. Time-lapse videomicroscopy of oocyte meiotic maturation, ovulation, and sheath cell contractions were performed. Sheath cell contraction was monitored directly in live anesthetized worms (0.1% tricaine and 0.01% tetramisole in M9 buffer) using DIC high-resolution optics as described (McCarter et al., 1999; Miller et al., 2003).

The gonads were dissected, fixed, and stained for immuno-fluorescence microscopy as described. The following antibodies were used: anti-MAPK-YT (Sigma); anti-DAB-1 (Kamikura and Cooper, 2003), anti-GOA-1 (kindly provided by Michael Koelle) anti-MSP (Kosinski et al., 2005), and Cy2- or Cy3-conjugated secondary antibody (Jackson ImmunoResearch Laboratories). Wide-field fluorescence and DIC microscopy employed a Zeiss Axioskop microscope with 40x, 63x, or 100x (NA1.4) objective lenses. Images were

acquired with an ORCA ER (Hamamatsu) charge-coupled device camera with OpenLab (Improvision) software. All exposures were in the dynamic range of the detector and each individual photograph in a montage employed the same exposure time. Student's t test was used to assess statistical significance as indicated.

Results

Identification of Negative Regulators of MSP Signaling via a Genome-Wide RNAi Screen

To identify negative regulators of oocyte meiotic maturation, I performed a genome-wide RNAi screen in *fog-2(q71)* female background. *fog-2(q71)* female is sterile strain in which oocytes arrest at prophase of meiosis I and are retained in the gonad arm due to the absence of MSP. I fed L3 larval stage *fog-2(q71)* females with bacterial clones expressing dsRNA and screened for rare clones that result in MSP-independent meiotic maturation characterized by increased number of unfertilized oocytes on the bacterial lawn (Fig. 16B). I identified 175 clones that fell into two categories depending on their consequence for gonadal structure: class I (17 clones) (Table 1) had no appreciable effects, and class II (158 clones) (Table 2) caused defects in gonadal morphology. The disruption of gonadal integrity observed after RNAi of class II clones limits the ability to study their roles in MSP signaling to varying degrees. Thus, here I focus on the 17 class I positive clones (Table 1).

Figure 16. A genome-wide RNAi screen for negative regulators of oocyte meiotic maturation

(A) The VAB-1 Eph receptor and the CEH-18 sheath cell pathways negatively regulate meiotic maturation and MAPK activation in the absence of sperm. MSP promotes meiotic maturation by antagonizing these inhibitory circuits.

(B) Strategy for genome-wide RNAi screening. Each bacterial clone from the RNAi library was grown overnight and was inoculated into 6-wells plates. After overnight induction for synthesis of dsRNA, L3 stage *fog-2(q71)* female worms were placed in the wells. The plates were screened on day-two of adulthood. RNAi of most clones have no effect on meiotic diapause (bottom left), whereas in rare cases the oocytes undergo MSP-independent meiotic maturation characterized by increased number of unfertilized oocytes on the bacterial lawn. All RNAi experiments were performed at 22^{o}C.

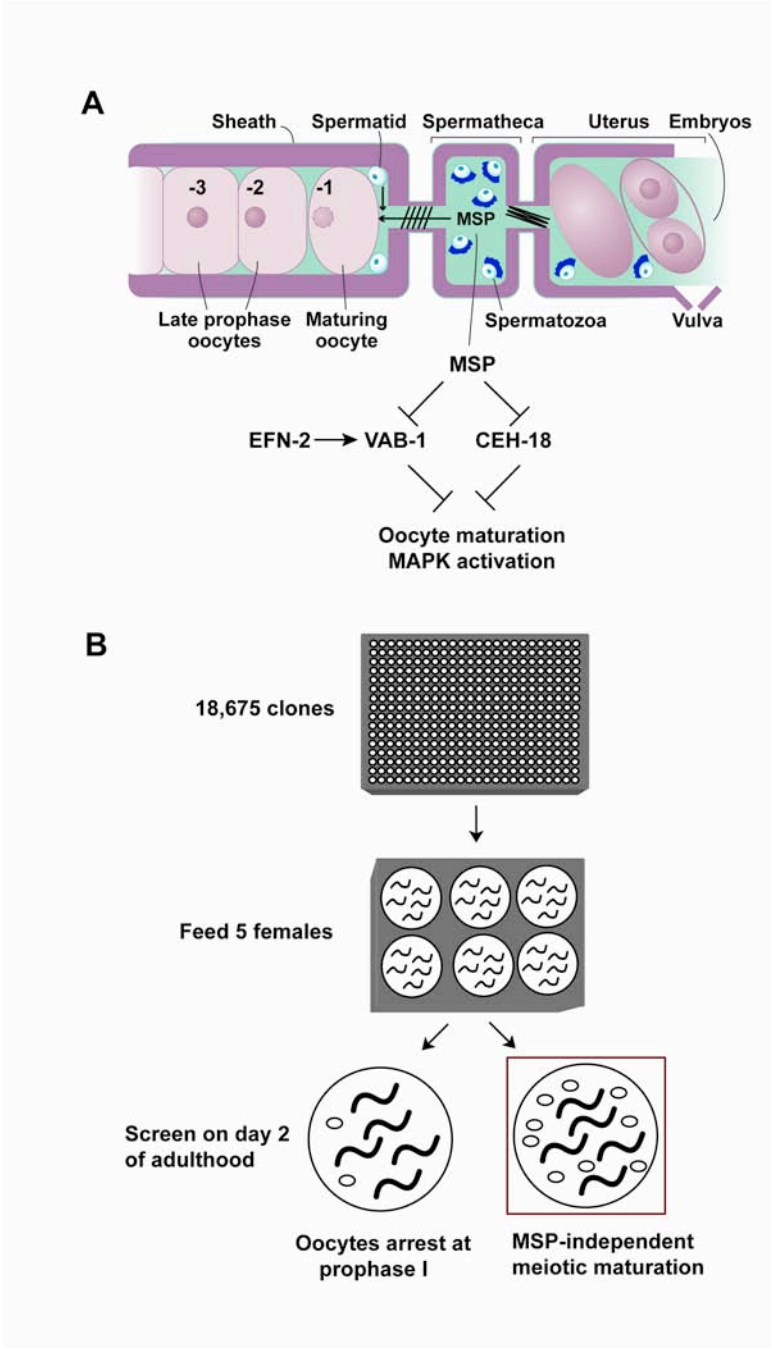
A
Sheath
Spermatid
Spermatheca
Uterus
Embryos
-3
-2
-1
MSP
Late prophase oocytes
Maturing oocyte
Spermatozoa
Vulva
MSP
EFN-2
VAB-1
CEH-18
Oocyte maturation
MAPK activation
B
18,675 clones
Feed 5 females
Screen on day 2 of adulthood
Oocytes arrest at prophase I
MSP-independent meiotic maturation

Table 1. Negative Regulators of Meiotic Maturation Identified in a Genome-Wide RNAi Screen

Gene[a]	Description	MSP[b]	Oocyte Maturation Rate in Females (hr^{-1} gonad arm^{-1})[c]	MAPK Activation[d]
Control	Wild-type hermaphrodite	+	2.50 ± 0.41 (17)	25/25 (+)
Control[e]	*fog-2(q71)* unmated female	–	0.16 ± 0.10 (17)	1/20 (–)
Control	*fog-2(q71)* mated female	+	2.42 ± 0.35 (14)	18/18 (+)
goa-1	Heterotrimeric $G_{o/i}\alpha$ protein subunit	–	1.67 ± 0.38 (36)[f]	14/15 (+)
kin-2	cAMP-dependent protein kinase (regulatory subunit)	–	1.50 ± 0.30 (9)[f]	9/13 (+)
gpb-1	Heterotrimeric G_{β} protein subunit	–	0.88 ± 0.24 (21)[f]	13/18 (+)
gsa-1	Heterotrimeric $G_s\alpha$ protein subunit	–	0.37 ± 0.18 (12)[g]	1/19 (–)
rpt-3	Component of 26S proteasome[h]	–	0.44 ± 0.15 (25)[f]	1/14 (–)
inx-14	Gap junction protein (innexin family)	–	0.99 ± 0.30 (21)[f]	17/17 (+)
inx-22	Gap junction protein (innexin family)	–	0.90 ± 0.36 (30)[f]	15/18 (+)
ran-1	Ran GTPase	–	0.72 ± 0.13 (6)[f]	0/18
ceh-18	POU-Homeo domain transcription factor	–	0.45 ± 0.18 (12)[f, i]	1/17 (+)
arf-1.1	Arf-family GTP binding protein	–	0.64 ± 0.28 (10)[f]	1/19 (–)
ptc-1	Patched receptor	–	0.60 ± 0.27 (18)[f, j]	12/15 (+)
phi-11	Splicing factor 3B, subunit 1[k]	–	0.50 ± 0.15 (10)[f]	0/15
par-5	Encodes 14-3-3 protein	–	0.49 ± 0.20 (28)[f]	0/17
pqn-19	Signal-transducing adaptor molecule (STAM)	–	0.48 ± 0.34 (12)[g]	0/17
pkc-1	Protein kinase C	–	0.44 ± 0.11 (9)[f]	1/17 (–)
vav-1	Vav-GEF proto-oncogene homolog	–	0.42 ± 0.13 (15)[f]	0/16
dab-1	Disabled homolog	–	0.38 ± 0.14 (15)[f]	0/16

[a], Shown are class I positive clones, RNAi of which does not appreciably alter gonadal morphology. The identity of the clones was verified by DNA sequencing.
[b], The absence of MSP in unmated female gonads was confirmed by staining with monoclonal anti-MSP antibodies.
[c], Oocyte maturation rates are expressed as the number of maturations per gonad arm per hour and were measured in two-day-old adult *fog-2(q71)* females (excepting the wild-type hermaphrodite control). The number of worms scored is given in the parentheses.
[d], The fraction of gonads arms showing MAPK-YT staining. MAPK activation was further classified according to whether the observed staining was strong or weak, indicated by (+) or (–), respectively.
[e], Mock RNAi using the empty vector, L4440, served as a control.
[f], $P<0.001$ compared to *control(RNAi)* in *fog-2(q71)* females.
[g], $P<0.01$ compared to *control(RNAi)* in *fog-2(q71)* females.
[h], RNAi of many 26S proteasome components resulted in gonadal defects and scored as class II positives in the screen.
[i], *ceh-18(mg57);fog-2(q71)* females have a maturation rate of 0.75 ± 0.32 .
[j], *ptc-1(ok122) unc-4(e120);fog-2(q71)* females have a maturation rate of 0.56 ± 0.26 (Miller et al., 2004).
[k], Many splicing factors were identified as class II positives.

Table 2. Class II negative regulators identified in the genome-wide RNAi screen

rpl-7	*rps-9*	R144.2	Y47H9C.7
eif-3.h	*eif-3.B*	*cyk-4*	H28O16.1
ars-1	*ubl-1*	F01F1.7	W07E6.1
crs-1	*rpl-3*	F54C8.5	*rpt-4*
pbs-4	*rps-12*	*rpn-7*	F23F1.5
noah-1	*rpn-6*	*dnc-1*	F52C6.3
Y110A7A.8	*cct-6*	F33D4.5	F52C6.2
rpl-24	*eft-1*	Y55H10A.1	F54D10.7
pqn-52	C13B9.3	*mls-1*	ZK546.14B
mtk-1	*rps-8*	C02B10.2	F10E7.6
F48C1.4	*wrs-2*	F55F10.1	B0511.6
T09B4.9	*ula-1*	H06H21.3	*eif-3.G*
rpl-19	*rpn-2*	*ima-3*	F25F2.1
rps-17	*rpl-23*	*grp-1*	T23D8.3
E03H4.8	*apt-4*	*rps-2*	
F55A12.8	*snr-3*	*cbp-1*	
F55F8.3	*prs-1*	*ndc-80*	
phi-15	*ubq-2*	K04D7.1	
snr-7	*rpl-21*	F32B6.3	
rpl-1	*rpl-9*	*nhr-67*	
Y65B4BL.2	*aco-2*	T14G10.5	
rps-20	*rpl-35*	*ssq-1*	
Y39G10AR.8	*pbs-1*	*klp-8*	
Y39G10AR.7	*rpl-20*	*pfn-2*	
apt-1	*rpn-1*	Y45F10D.10	
npp-4	*lin-3*	*far-6*	
rpl-17	*rps-5*	*uvt-3*	
imb-5	*uba-1*	*vha-11*	
pbs-5	*srs-2*	*clc-2*	
phi-6	*rpl-12*	*coh-1*	
nmy-2	*rpl-18*	*klp-13*	
nrs-1	*hsp-2*	*flp-2*	
eft-2	*act-4*	F33C8.1	
rpl-14	*mup-2*	F23A7.7	
rpl-24.2	F28C6.8	*dnj-25*	
rps-19	*nos-2*	F21D9.2	
pbs-7	M28.5	Y113G7A.3	
lin-41	F59E10.3	*nxf-2*	
rpl-15	*sel-8*	*cng-1*	
pas-5	*hsp-3*	F08H9.4	
eif-3.E	*tba-9*	F23B12.3	
prs-2	F54A3.3	*hda-1*	
rpl-33	Y39G8C.2	T08G5.2	
iff-2	*phi-10*	T01C3.3	
eiF-4	*phi-3*	F25H5.3	
cct-1	R06B10.1	*cep-1*	
rpl-26	*rrt-1*	K02B12.3	
cct-4	*asb-1*	F16D3.4	

Descriptions of these genes can be found at *www.wormbase.org*
The identity of class II positives were not verified by DNA sequencing

RNAi to class I genes had no apparent effects on germline sex determination, yet I verified the absence of MSP by immunostaining in all cases (Table 1).

RNAi of class I positives results in elevated oocyte meiotic maturation rates in a female background

To begin to analyze the role of these genes, I quantified the effects of class I positives by measuring the meiotic maturation rates (Table 1) as described (McCarter et al., 1999; Miller et al., 2003). I performed RNAi of each class I positives on L3 stage *fog-2(q71)* females and measured the meiotic maturation rates on day-two of adulthood. As a control, I used females treated with empty L4440 vector RNAi. Within class I positives, I found that the level of derepression of meiotic maturation differed between clones (Table 1). Remarkably, RNAi of *goa-1* and *kin-2* resulted in approximately 60% of the wild-type rate in the presence of sperm (Table 1).

RNAi of several class I positives results in derepression of MAPK activation in a female background

MSP is sufficient to activate MAPK in female gonads when assessed with antibodies to the diphosphorylated activated form of MPK-1/MAPK (MAPK-YT) (Miller et al., 2001; Miller et al., 2003). To determine whether the negative regulators affect MAPK activation, I performed MAPK staining on female worms treated with the class I positives. I stained dissected gonadal preparations with the monoclonal anti-MAPK-YT antibody.

Figure 17. RNAi to Several Negative Regulators Causes MSP-Independent MAPK Activation in Oocytes

Fluorescence micrographs showing MAPK-YT staining (red) in oocytes. MAPK-YT staining is observed in the most proximal oocyte of wild-type hermaphrodites (A), but not in *fog-2(q71)* females (B). By contrast, MAPK-YT staining is observed in *fog-2(q71)* females after *goa-1(RNAi)* (C), *kin-2(RNAi)* (D), *inx-14(RNAi)* (E), and *gpb-1(RNAi)* (F). *goa-1(RNAi)* or *goa-1(null)* females exhibit expanded MAPK-YT staining to distal oocytes, though the specific pattern of relative staining intensities, such as the alternating peaks of staining in (C), can be variable. *inx-22(RNAi)* and *ptc-1(RNAi)* also result in MSP-independent MAPK activation (Table 1). Scale bar equals 10 μm.

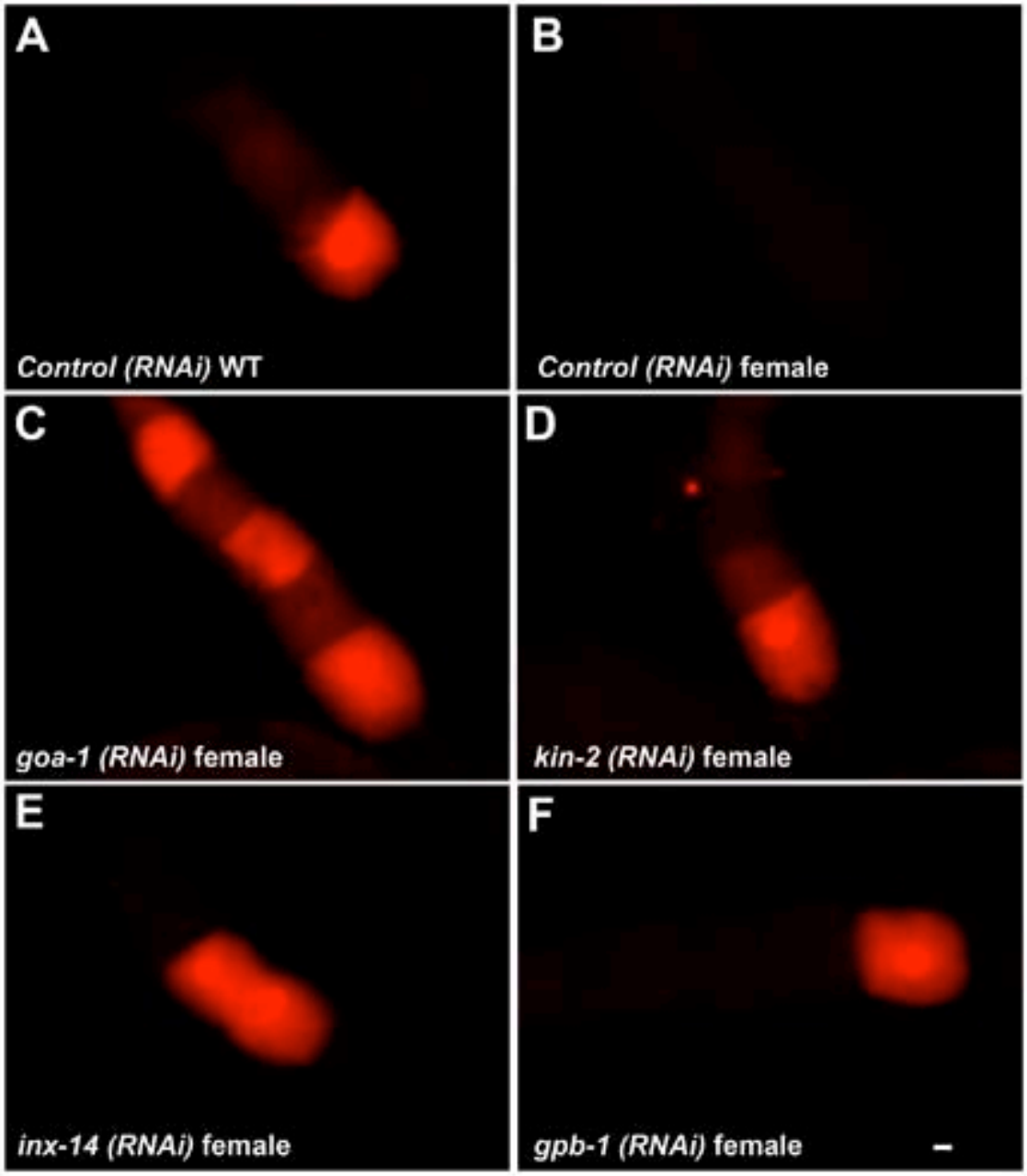
A
Control (RNAi) WT
B
Control (RNAi) female
C
goa-1 (RNAi) female
D
kin-2 (RNAi) female
E
inx-14 (RNAi) female
F
gpb-1 (RNAi) female

As a control, I used dissected gonads from females treated with empty L4440 vector RNAi. I found that RNAi to six genes (*goa-1*, *kin-2*, *gpb-1*, *inx-14*, *inx-22*, and *ptc-1*) resulted in MAPK activation in the absence of MSP (Table 1 and Fig. 17).

Germline and somatic sheath cell pathways regulate oocyte meiotic maturation

To determine whether negative regulators function in the soma or the germline, I conducted RNAi analysis in an *rrf-1(null)* mutant background (Table 3). *rrf-1* encodes an RNA-dependent RNA polymerase (RdP) that is required for normal RNAi responses in many somatic cells (Sijen et al., 2001) but is dispensable for germline RNAi, which employs the EGO-1 RdP (Smardon et al., 2000). Thus, an RNAi response in an *rrf-1(null)* female background is indicative of a germline function, whereas a significantly reduced response suggests gene function in the soma. As a control, I conducted *ceh-18(RNAi)* and observed elevated meiotic maturation rates in the female background, but not in *rrf-1* females (Table 3), consistent with the idea that *ceh-18* is required for normal sheath cell differentiation and function (Rose et al., 1997). By contrast, *vab-1* functions in the germline via this test. The *rrf-1* RNAi test suggests that the function of 11 genes, including *inx-14* and *inx-22*, is needed in the germline for full repression of meiotic maturation (Table 3). By contrast, the function of four genes (*goa-1*, *kin-2*, *gpb-1*, and *rpt-3*) is predominantly somatic via this test (Table 3).

Table 3. Parsing the Function of Negative Regulators to the Germ Line or Soma.

RNAi	Oocyte Maturation Rate in Females[a] (N)	Oocyte Maturation Rate in *rrf-1(null)* Females[b] (N)
Control	0.17 ± 0.14 (15)	0.20 ± 0.10 (12)
ceh-18	0.44 ± 0.16 (11)[c]	0.21 ± 0.10 (10)[f]
goa-1	1.51 ± 0.20 (10)[d]	0.50 ± 0.20 (16)[g]
kin-2	1.45 ± 0.60 (12)[d]	0.54 ± 0.16 (15)[g]
gpb-1	1.03 ± 0.20 (12)[d]	0.44 ± 0.22 (16)[g]
gsa-1	0.37 ± 0.22 (13)[e]	0.21 ± 0.20 (10)[f]
rpt-3	0.51 ± 0.16 (12)[c]	0.30 ± 0.18 (12)[f]
inx-14	1.03 ± 0.22 (12)[e]	0.88 ± 0.34 (12)[g]
inx-22	0.84 ± 0.13 (12)[e]	1.00 ± 0.31 (16)[g]
ran-1	1.00 ± 0.30 (6)[e]	1.39 ± 0.32 (5)[g]
arf-1.1	0.53 ± 0.20 (9)[e]	0.45 ± 0.28 (12)[h]
ptc-1	0.63 ± 0.13 (12)[e]	0.74 ± 0.17 (14)[g]
phi-11	0.50 ± 0.20 (12)[e]	0.58 ± 0.30 (11)[g]
par-5	0.80 ± 0.29 (11)[e]	0.71 ± 0.29 (14)[g]
pqn-19	0.46 ± 0.17 (12)[e]	0.47 ± 0.14 (13)[g]
pkc-1	0.48 ± 0.16 (12)[e]	0.40 ± 0.10 (7)[g]
vav-1	0.44 ± 0.11 (11)[e]	0.48 ± 0.20 (14)[g]
dab-1	0.39 ± 0.15 (11)[e]	0.43 ± 0.10 (8)[g]

[a], Meiotic maturation rates were measured in a *fog-3(q443)* female background.

[b], Meiotic maturation rates were measured in *rrf-1(pk1417);fog-3(q443)* double mutant females.

[c], P<0.01 compared to the rate following RNAi in the *rrf-1(null*) female background.

[d], P<0.001 compared to the rate following RNAi in the *rrf-1(null*) female background.

[e], P>0.1 compared to the rate following RNAi in the *rrf-1(null)* female background.

[f], P>0.1 compared to the rate following control RNAi in the *rrf-1(null)* female background.

[g], P<0.001 compared to the rate following control RNAi in the *rrf-1(null*) female background.

[h], P<0.01 compared to the rate following control RNAi in the *rrf-1(null*) female background.

The slight RNAi responses observed in *rrf-1(null)* females for *goa-1*, *kin-2*, *gpb-1*, and *rpt-3* might be due to residual somatic effects, as shown by the fact that under our conditions, *unc-22(RNAi)* produces overt muscle twitching and weak uncoordination in 5.3% of *rrf-1(null)* animals (n = 228). Nonetheless, I cannot exclude the possibility that these genes may also have some germline functions.

DAB-1, PKC-1, VAV-1, AND PQN-19 function in the VAB-1 pathway to regulate oocyte meiotic maturation

To identify genes that play a major role in the *vab-1* pathway, I set three stringent genetic and phenotypic criteria. First, the RNAi inactivation of a *vab-1* pathway gene should derepress meiotic maturation to a similar extent as a *vab-1(null)* mutant. Second, the RNAi inactivation of a *vab-1* pathway gene should not exhibit additive or synergistic interactions with a *vab-1(null)* mutant. Finally, the RNAi inactivation of a *vab-1* pathway gene should synergize with a *ceh-18(null)* mutant. I considered the eleven genes (*inx-14*, *inx-22*, *ran-1*, *arf-1.1*, *ptc-1*, *phi-11*, *par-5*, *pqn-19*, *pkc-1*, *vav-1*, and *dab-1*), whose activity is needed in the germ line for full repression of meiotic maturation, as candidates for functioning in the VAB-1 MSP/Eph receptor signal transduction pathway. Four of these genes meet these initial criteria, DAB-1, a disabled homolog, PKC-1, a protein kinase C homolog, PQN-19, a STAM homolog, and VAV-1, a Rho-family guanine-nucleotide exchange factor (Fig. 18A; Table 4).

Figure 18. Genetic Analysis of the VAB-1 Eph/MSP Receptor Pathway

(A) Organization of signaling domains in VAB-1 pathway proteins. PQN-19 contains VHS (VPS-27/Hrs/STAM), UIM (ubiquitin-interaction motif), and SH3 domains. PKC-1 contains C1, C2, kinase, and protein kinase C domains. DAB-1 contains a phosphotyrosine binding (PTB) domain. VAV-1 contains CH (calponin homology), C1, RhoGEF, SH2, and SH3 domains.
(B) Measurement of oocyte meiotic maturation rates after *dab-1*, *vav-1*, *pqn-19*, *pkc-1*, or control RNAi in *fog-2(q71)*, *vab-1(dx31);fog-2(q71)*, or *ceh-18(mg57);fog-2(q71)* female genetic backgrounds. Each of the four genes synergize with *ceh-18* but not *vab-1*. Error bars represent SD.
(C–H) Fluorescence micrographs showing MAPK-YT staining (red) in oocytes.
(C) In wild-type hermaphrodites, MSP-dependent MAPK-YT staining is observed in proximal oocytes (typically oocytes -1 through -3).
(D) MAPK-YT staining is extended to three to eight proximal oocytes in *vab-1(null)* hermaphrodites, consistent with the idea that *vab-1* is a negative regulator of meiotic maturation and MAPK activation in oocytes (Miller et al., 2003).
(E–H) Similarly, *dab-1(null)* (E), *pqn-19(null)* (F), *pkc-1(null)* (G), and *vav-1(RNAi)* hermaphrodites (H) exhibit an extended MAPK-YT staining pattern similar to that of *vab-1(null)* hermaphrodites (D).
(I–K) Fluorescent detection of DAB-1 in oocytes from wild-type hermaphrodites (I) and *fog-2(q71)* females (J), but not *dab-1(gk291)* hermaphrodites (K). DAB-1 is cortically enriched when sperm are present.

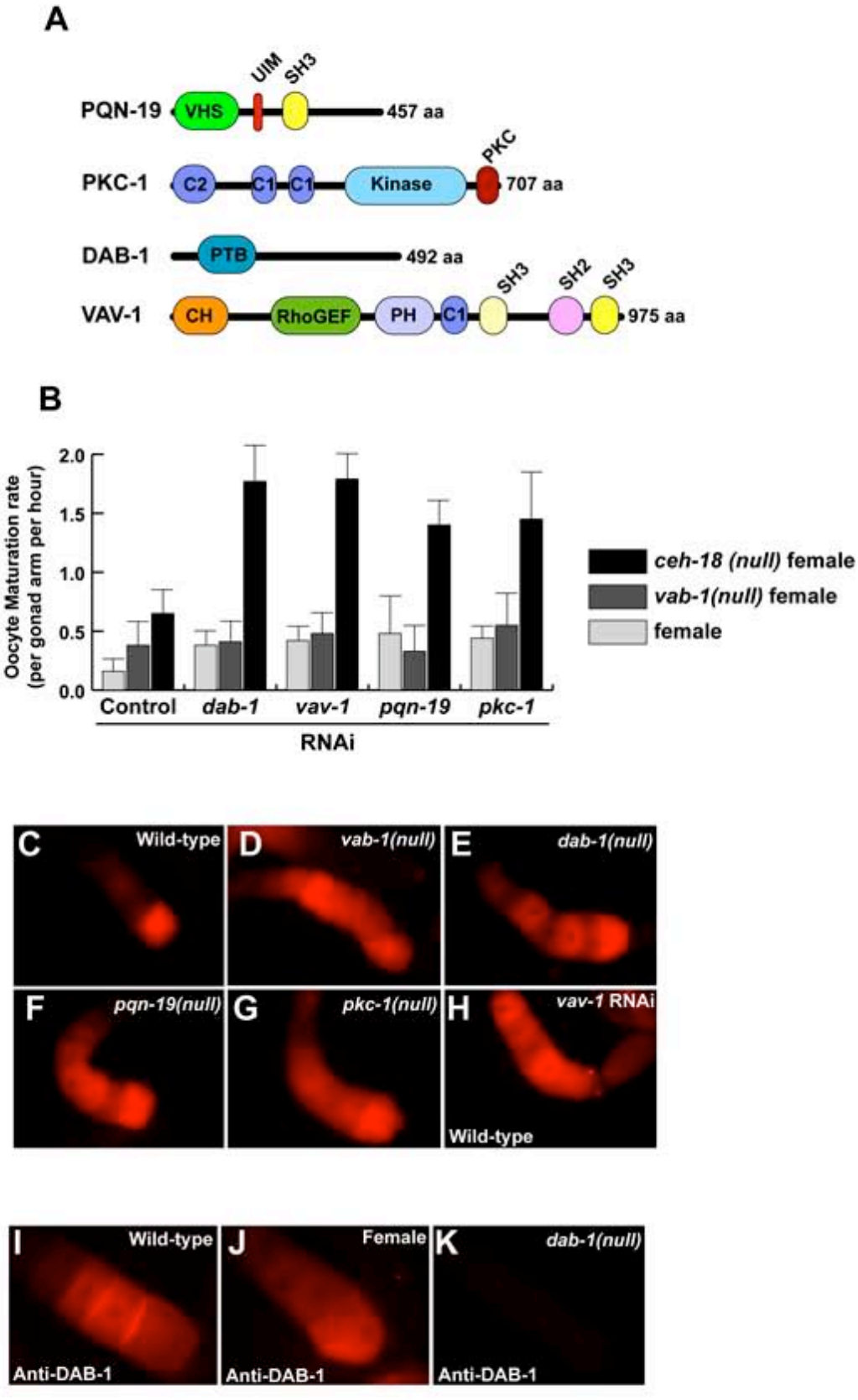
A
UIM
SH3
PQN-19
VHS
457 aa
PKC
PKC-1
C2
C1
C1
Kinase
707 aa
DAB-1
PTB
492 aa
SH3
SH2
SH3
VAV-1
CH
RhoGEF
PH
C1
975 aa
B
Oocyte Maturation rate
(per gonad arm per hour)
2.0
1.5
1.0
0.5
0.0
Control
dab-1
vav-1
pqn-19
pkc-1
RNAi
ceh-18 (null) female
vab-1(null) female
female
C
Wild-type
D
vab-1(null)
E
dab-1(null)
F
pqn-19(null)
G
pkc-1(null)
H
vav-1 RNAi
Wild-type
I
Wild-type
Anti-DAB-1
J
Female
Anti-DAB-1
K
dab-1(null)
Anti-DAB-1

Table 4. Effect of *vab-1* and *ceh-18* Mutations on Meiotic Maturation Rates following RNAi of Class I Genes in the Absence of Sperm

Gene (RNAi)	Oocyte Maturation Rate in Females[a] (N)	Oocyte Maturation Rate in *vab-1(null)* Females[b] (N)	Oocyte Maturation Rate in *ceh-18(null)* Females[c] (N)
Control[d]	0.16 ± 0.10 (17)	0.38 ± 0.25 (18)	0.65 ± 0.25 (12)
goa-1	1.67 ± 0.38 (36)	2.19 ± 0.35 (17)	0.92 ± 0.30 (19)
gpb-1	0.88 ± .24 (21)	1.63 ± 0.36 (15)	0.64 ± 0.21 (27)
inx-22	0.90 ± 0.36 (30)	1.90 ± 0.25 (10)	0.99 ± 0.30 (22)
inx-14	0.99 ± 0.30 (26)	1.94 ± 0.28 (21)	0.67 ± 0.25 (11)
par-5	0.49 ± 0.20 (28)	0.80 ± 0.25 (26)	0.82 ± 0.28 (17)
kin-2[e]	1.50 ± 0.30 (9)	1.70 ± 0.26 (15)	0.83 ± 0.47 (17)
rpt-3	0.44 ± 0.15 (25)	0.82 ± 0.19 (5)	0.45 ± 0.18 (15)
arf-1.1	0.64 ± 0.28 (10)	0.44 ± 0.14 (13)	0.73 ± 0.19 (14)
ptc-1	0.60 ± 0.27 (18)	0.75 ± 0.24 (10)	0.59 ± 0.09 (7)
gsa-1	0.37 ± 0.18 (12)	0.52 ± 0.25 (12)	0.79 ± 0.22 (9)
ran-1	0.72 ± 0.13 (6)	0.80 ± 0.19 (6)	1.30 ± 0.23 (12)
phi-11	0.50 ± 0.15 (10)	0.44 ± 0.20 (10)	0.53 ± 0.21 (12)
dab-1	0.38 ± 0.14 (15)	0.41 ± 0.24 (10)	1.77 ± 0.32 (18)
vav-1	0.42 ± 0.13 (15)	0.48 ± 0.18 (10)	1.79 ± 0.20 (10)
pkc-1	0.44 ± 0.11 (9)	0.55 ± 0.28 (13)	1.45 ± 0.40 (18)
pqn-19	0.48 ± 0.34 (12)	0.33 ± 0.20 (13)	1.40 ± 0.16 (12)

[a], Meiotic maturation rates were measured in a *fog-2(q71)* female background.
[b], Meiotic maturation rates were measured in a *vab-1(dx31);fog-2(q71)* females.
[c], Meiotic maturation rates were measured in a *ceh-18(mg57);fog-2(q71)* females. *ceh-18* mutant sheath cells respond to RNAi, as *gfp(RNAi)* could silence *lim-7::gfp* expression in a *ceh-18(mg57)* mutant background.
[d], Mock RNAi using the empty vector, L4440, served as a control.
[e], Worms fed *kin-2(RNAi)* become lethargic and bloated with unfertilized oocytes on the second day of adulthood.

Of these four genes, only *vav-1* was previously implicated in Eph receptor signaling by the finding that Rho family GEF Vav2 interacts with the EphA4 receptor and promotes ephrin-triggered endocytosis (Cowan et al., 2005). As a further test that *dab-1*, *vav-1*, *pkc-1*, and *pqn-19* function as part of the *vab-1* pathway, I examined the effect of null mutants and RNAi of these genes on oocyte MAPK activation in hermaphrodites. *vab-1(null)* hermaphrodites exhibit an expanded pattern of MAPK activation in which MAPK-YT staining extends to distal oocytes (Fig. 18D) (Miller et al., 2003). Similarly, *dab-1(gk291* or *RNAi)*, *pkc-1(ok563* or *RNAi)*, *pqn-19(ok406* or *RNAi)*, and *vav-1(RNAi)* hermaphrodites display expanded patterns of MAPK-YT staining in oocytes (Fig. 18E-H), suggesting that these genes, like *vab-1*, function as germline negative regulators of MAPK activation. I analyzed *vav-1* using RNAi only because a *vav-1(null)* mutation is lethal (Norman et al., 2005). Additionally, *vab-1* functions in parallel to *ceh-18* in the negative control of oocyte MAPK activation: *vab-1(null); ceh-18(null)* females show MAPK-YT staining in oocytes despite the absence of MSP. By these criteria, *dab-1*, *vav-1*, *pkc-1*, and *pqn-19* behave similarly to *vab-1*, as MAPK-YT staining is observed when RNAi is carried out for these genes in a *ceh-18(null)* mutant female background (Fig. 19).

Because strong conclusions regarding genetic pathways are not possible without phenotypic analysis of null mutations, I analyzed meiotic maturation phenotypes in deletions alleles of *dab-1*, *pkc-1*, and *pqn-19*, which are predicted to significantly reduce or eliminate gene function.

Figure 19. *dab-1*, *pqn-19*, *pkc-1*, and *vav-1* negatively regulate oocyte MAPK activation in parallel to *ceh-18*

Fluorescence micrographs showing MAPK-YT staining (red) in oocytes. No MAPK-YT staining is seen in oocytes in *ceh-18(mg57);fog-2(q71)* females after control RNAi (A); however, MAPK-YT staining is observed after *vav-1(RNAi)* (B), *pqn-19(RNAi)* (C), *pkc-1(RNAi)* (D), and *dab-1(RNAi)* (E) in the *ceh-18(mg57); fog-2(q71)* background (D). Scale bar equals 10 μm.

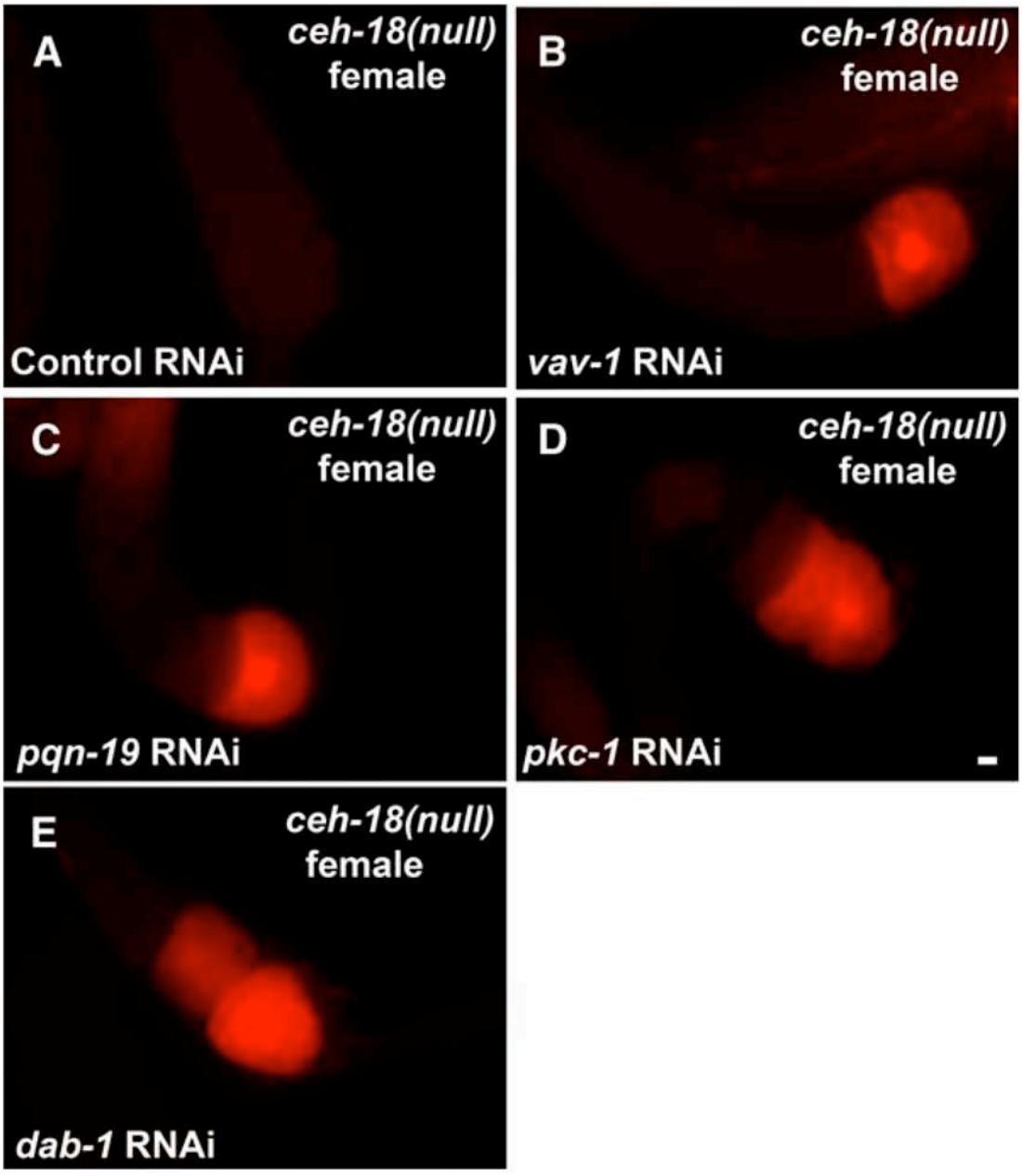
A
ceh-18(null)
female
Control RNAi
B
ceh-18(null)
female
vav-1 RNAi
C
ceh-18(null)
female
pqn-19 RNAi
D
ceh-18(null)
female
pkc-1 RNAi
E
ceh-18(null)
female
dab-1 RNAi

In collaboration with Hua Cheng, a graduate student in the lab, I explored the involvement of *dab-1* disabled in oocyte maturation. We analyzed meiotic maturation rates in females homozygous for a *dab-1* null mutation, *gk291*, which deletes exons two and three, including the phosphotyrosine-binding domain (Kamikura and Cooper, 2003; Kamikura and Cooper, 2006). We found that *dab-1(gk291)* null mutant females exhibit increased meiotic maturation rates [0.42 ± 14 (n=22)] compared to normal females [0.16 ± 0.1(n=17), P<0.001]. This derepression of meiotic maturation is similar to that observed in *vab-1(null)* mutant females [0.38 ± 0.25 (n=18)]. Further, *vab-1(null)dab-1(null)* double mutant females exhibit a meiotic maturation rate of 0.43 ± 0.19 (n=22), consistent with the idea that these two genes function in a common pathway. Strikingly, DAB-1 protein localization is altered in the absence of sperm, no longer exhibiting cortical enrichment between oocytes (Fig. 18J). Recent data indicates that DAB-1 physically interacts with the VAB-1 intracellular domain in vitro and is required for the trafficking/localization of the receptor in the absence of sperm (Cheng, H. and Greenstein, D., unpublished results).

In contrast to *dab-1*, we did not observe elevated meiotic maturation rates in *pqn-19(ok406)fog-3(q443)* females, which displayed rates (0.10 ± 0.15; n=22) similar to unmated female controls. Likewise, meiotic maturation rates in *pkc-1(ok563);fog-3(q443)* females, though slightly elevated (0.18 ± 0.20; n=24), were significantly lower than those of *vab-1* females (P<0.001). Thus, for *pqn-19* and *pkc-1*, the analysis of meiotic maturation rates in a female background led to a different conclusion from the RNAi and MAPK activation studies

described above. To reconcile this discrepancy, we analyzed oocyte meiotic maturation by time-lapse videomicroscopy and noticed that *pqn-19(ok406)* and *pkc-1(ok563)* hermaphrodites exhibited an incompletely penetrant (~33%) delay in nuclear envelope breakdown during oocyte meiotic maturation. We made the same observation in *dab-1(gk291)* hermaphrodites and similar data were published for *vav-1(null)* mutant hermaphrodites for which the lethal pharyngeal defects were transgenically rescued (Norman et al., 2005). Since this delay in nuclear envelope breakdown is not observed in *vab-1(null)* mutants, we conclude that *dab-1*, *pkc-1*, *pqn-19*, and *vav-1* may also have redundant functions as positive regulators of meiotic maturation, through *vab-1*-independent pathways.

GOA-1 is necessary and sufficient to inhibit oocyte meiotic maturation and MAPK activation in the absence of sperm

The strongest negative regulator of meiotic maturation identified in the RNAi screen is *goa-1*, which encodes a heterotrimeric $G\alpha_{o/i}$ protein. *goa-1(*RNAi*)* in a female background triggers meiotic maturation and MAPK activation in oocytes despite the absence of MSP (Table 1 and Fig. 17C). Extending these RNAi results using genetics, I found that *goa-1(sa734)* null mutant females exhibited significantly higher meiotic maturation rates than control females and they showed MSP-independent MAPK activation in oocytes (Table 5, compare lines 4 and 2, and Fig. 20C, $P<0.001$). The *goa-1(n1134)* reduction-of-function (rf) allele behaved similarly (Table 5, compare lines 6 and 2, and Fig. 20E, $P<0.001$).

Table 5. Genetic analysis of G-Protein Signaling

	Genotype[a]	Sperm (yes/no)	Oocyte Maturation Rate[b] (N)	MAPK Activation[c]
1.	Wild-type hermaphrodite	yes	2.50 ± 0.41 (16)	on
2.	*fog-3(q443)* unmated	no	0.17 ± 0.14 (15)	off
3.	*fog-3(q443)* mated	yes	2.29 ± 0.43 (20)	on
4.	*goa-1(sa734) fog-3(q443)* female	no	0.47 ± 0.17 (30)	on
5.	*goa-1(sa734)*hermaphrodite	yes	1.23 ± 0.18 (15)	on
6.	*goa-1(n1134)fog-3(q443)* female	no	1.06 ± 0.25 (16)	on
7.	*goa-1(n1134)* hermaphrodite	yes	2.55 ± 0.40 (18)	on
8.	*oma-1(RNAi);oma-2(RNAi)* hermaphrodite	yes	0.06 ± 0.07 (13)	off
9.	*oma-1(RNAi);oma-2* (RNAi); *goa-1(sa734)fog-3(q443)* female	no	0.00 ± 0.00 (13)	off
10.	*oma-1(RNAi);oma-2* (RNAi); *goa-1(sa734)* hermaphrodite	yes	0.00 ± 0.00 (17)	off
11.	*goa-1(gf)* hermaphrodite[d]	yes	0.76 ± 0.62 (19)	on

[a], Genotypes utilized null mutations unless where indicated by “d” or “rf” for dominant gain-of-function and reduction-of-function mutations, respectively. The position and morphology of sheath cell nuclei were unaffected by RNAi of *gsa-1*, *kin-2*, or *goa-1*, or in mutants of these genes.

[b], Meiotic maturation rates were measured in two-day-old adult animals. N denotes number of worms examined.

[c], MAPK activation was scored as described above, with “on” denoting strong staining in proximal oocytes and “off,” an absence of staining.

[d], The PS1493 transgenic strain that expresses constitutively-activated GOA-1($G\alpha_oQL$) under the control of *goa-1* promoter was used (Mendel et al., 1995).

Figure 20. *goa-1* is a negative regulator of oocyte MAPK activation

(A-F) Fluorescence micrographs showing MAPK-YT staining (red) in oocytes from hermaphrodites (A) and females (B-F) of the indicated genotypes. In the absence of MSP, MAPK activation is absent in females (B) whereas in *goa-1(sa734)fog-3(q443)* (C), and *goa-1(n1134)fog-3(q443)* (E) MAPK activation is seen. *oma-1(RNAi); oma-2(RNAi)* prevents MAPK activation in *goa-1(sa734))fog-3(q443)* (D), and *goa-1(n1134)fog-3(q443)* (F) genetic backgrounds.

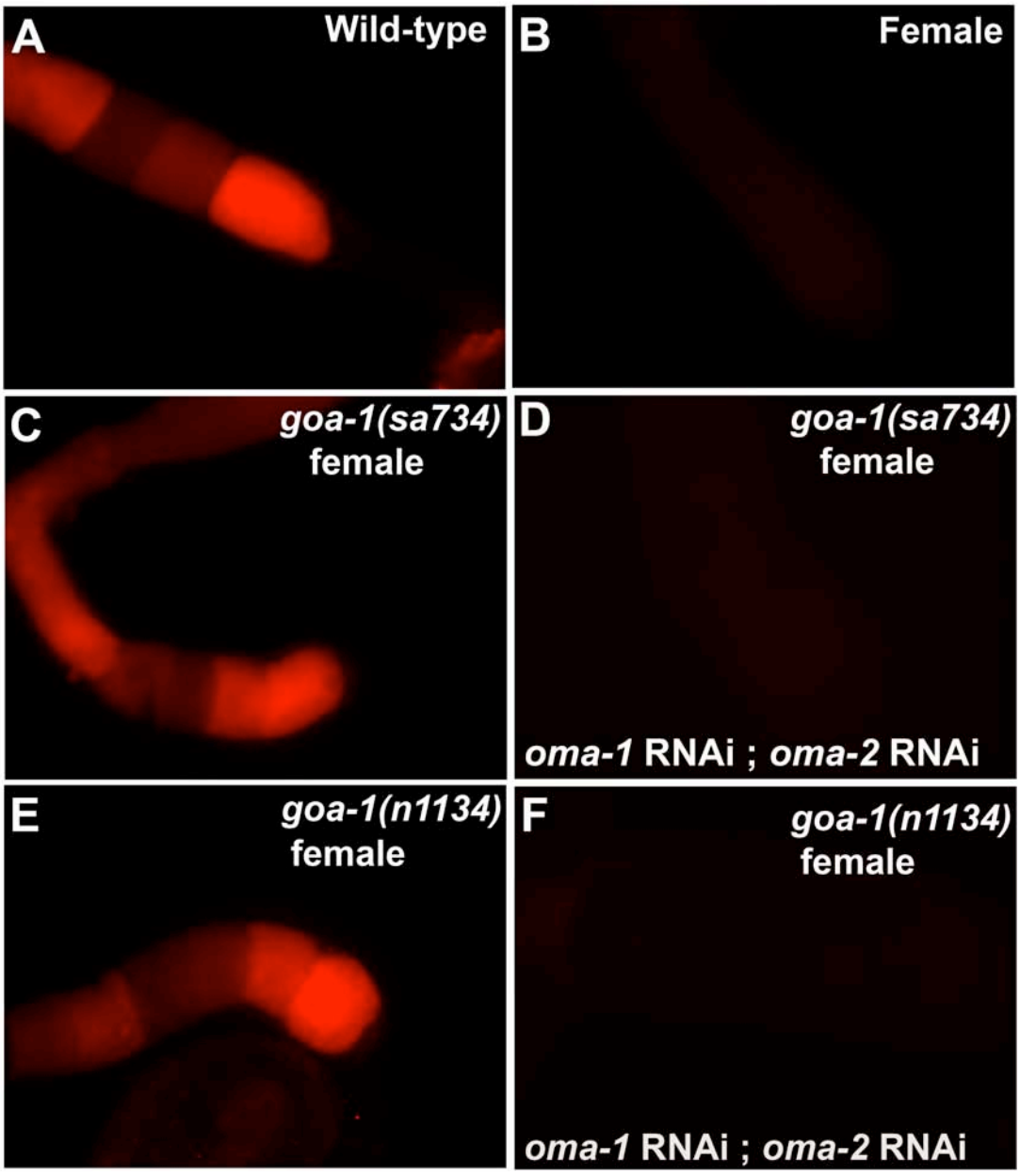
A
Wild-type
B
Female
C
goa-1(sa734)
female
D
goa-1(sa734)
female
oma-1 RNAi ; oma-2 RNAi
E
goa-1(n1134)
female
F
goa-1(n1134)
female
oma-1 RNAi ; oma-2 RNAi

Meiotic maturation rates were lower in *goa-1(sa734)* null mutant females compared to *goa-1(RNAi)* females, however, most likely because the *goa-1(sa734)* females appeared starved and produced fewer oocytes. Consistent with this interpretation, *goa-1(n1134*rf*)* females were healthier and exhibited higher meiotic maturation rates than null mutant females, and *goa-1(sa734)* hermaphrodites had lower rates than the wild type (Table 5, compare lines 1-7). Time-lapse videomicroscopy of meiotic maturation and ovulation in *goa-1(n1134)fog-3(q443)* (n=8) and *goa-1(RNAi);fog-2(q71)* (n=8) females indicated that nuclear envelope breakdown, cortical cytoskeletal rearrangement, and ovulation all occurred normally despite the absence of MSP.

MSP-dependent MAPK activation and meiotic maturation require the downstream action of OMA-1 and OMA-2, two TIS-11 zinc-finger proteins expressed in the germ line (Detwiler et al., 2001). No MAPK activation or meiotic maturation is observed in *goa-1(sa734);oma-1(RNAi);oma-2(RNAi)* or *goa-1(n1134);oma-1(RNAi);oma-2(RNAi)* hermaphrodites and females (Fig. 20D and F, Table 5, lines 8-10 and data not shown). Thus, $G\alpha_{o/i}$ likely functions upstream or in parallel with OMA-1/OMA-2 to repress meiotic maturation in the absence of the MSP signal, with the caveat that RNAi is not necessarily equivalent to null mutations in genetic epistasis experiments.

To test whether GOA-1 activity is sufficient to repress meiotic maturation, we measured meiotic maturation rates in hermaphrodites expressing constitutively-activated GOA-1(Q205L) under control of the *goa-1* promoter (Mendel et al., 1995) and observed that meiotic maturation rates were reduced

by 70% despite the presence of MSP (Table 5, line 11). These results suggest that *goa-1* activity is needed to fully repress meiotic maturation in the absence of MSP and that it is also sufficient to partially repress meiotic maturation in the presence of MSP. Since transgenes are ordinarily silenced in the germ line (Kelly et al., 1997), this finding constitutes a further line of evidence suggesting *goa-1* functions in the soma.

The analysis of *goa-1(RNAi)* in an *rrf-1* mutant female background described above suggests that *goa-1* functions in the somatic control of oocyte meiotic maturation (Table 3). Since *goa-1* is maternally required for positioning mitotic spindles in embryonic blastomeres (Gotta and Ahringer, 2001), I examined the expression of GOA-1 in dissected gonads of hermaphrodites and females using specific antibodies (Fig. 21). In hermaphrodites, I observed cytoplasmic staining in oocytes as well as staining that appeared to be in the surrounding sheath (Fig. 21A). No staining was observed in *goa-1(sa734)* null mutants or following *goa-1(RNAi)*, confirming the specificity of the antibodies (Fig. 21C and data not shown). In dissected gonads from females, I observed cortical enrichment of GOA-1 between oocytes as well as staining that appeared to be in the sheath (Fig. 21B). Since sheath cell and oocyte plasma membranes are in close apposition and the sheath cells are extremely thin (~0.2 μm) (Hall et al., 1999), I needed a way to visualize GOA-1 expression in sheath cells separately from oocytes. Thus, I reduced the expression of GOA-1 in the germ line by performing *goa-1* RNAi on *rrf-1* females and stained the dissected gonads with anti-GOA-1 antibody.

Figure 21. Expression of GOA-1 in the soma is sufficient to inhibit MAPK activation in oocytes

(A–E) Fluorescent micrographs of dissected gonads stained for GOA-1 (red) and DNA (blue). GOA-1 is expressed in sheath cells, oocytes, and spermathecal cells of wild-type hermaphrodites (A) and *fog-2(q71)* (B) and *fog-3(q443)* (not shown) females. In females, GOA-1 is cortically enriched between oocytes (B). No GOA-1 staining is observed in *goa-1(sa734)* mutants (C). GOA-1 staining in oocytes is significantly reduced after *goa-1(RNAi)* in an *rrf-1(null)fog-3(q443)* mutant female background (D). Note, GOA-1 staining between oocytes is reduced in the medial focal plane, comparing (D) and (B), yet staining in the sheath (Sh) and spermatheca (Sp) persists. GOA-1 staining also persists when viewed in superficial focal planes (E) in *goa-1(RNAi);rrf-1(null)fog-3(q443)* females with punctate staining possibly corresponding to the sheath cell processes (arrowheads). (F) Fluorescence micrograph of MAPK-YT staining after *goa-1(RNAi)* in a *rrf-1(null)fog- 3(q443)* mutant female background. MAPKYT staining is not observed, suggesting that GOA-1 expression in the soma (D and E) is sufficient to repress MAPK activation in oocytes. Scale bar represents 10 μm.

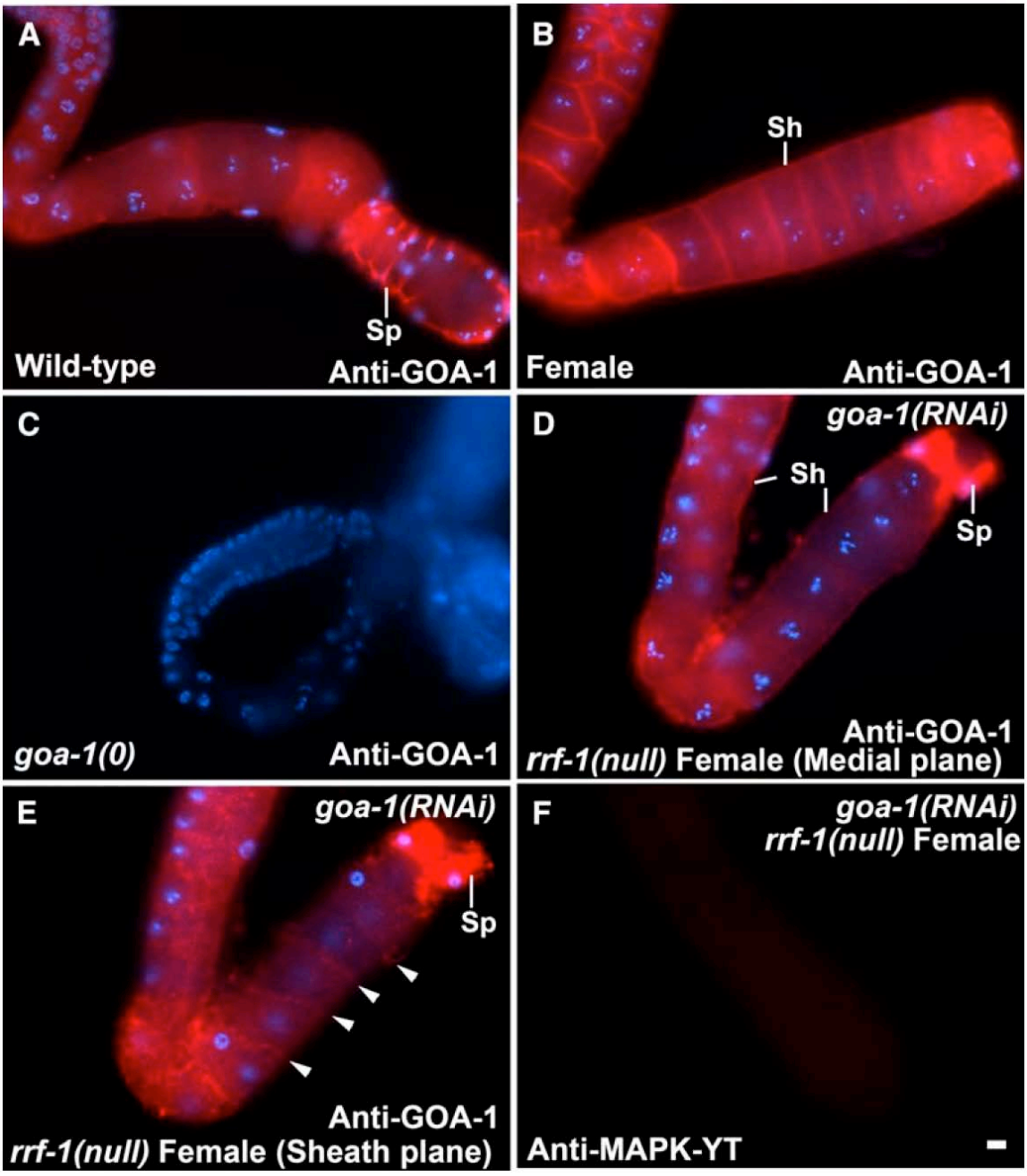
A
Sp
Wild-type
Anti-GOA-1
B
Sh
Female
Anti-GOA-1
C
goa-1(0)
Anti-GOA-1
D
goa-1(RNAi)
Sh
Sp
Anti-GOA-1
rrf-1(null) Female (Medial plane)
E
goa-1(RNAi)
Sp
Anti-GOA-1
rrf-1(null) Female (Sheath plane)
F
goa-1(RNAi)
rrf-1(null) Female
Anti-MAPK-YT

In these *goa-1(RNAi);rrf-1* female gonads, cortical GOA-1 staining between oocytes is significantly reduced through medial focal planes, yet staining persists in the thin layer surrounding oocytes, consistent with sheath cell expression (Fig. 21, D and E). The gonadal sheath cells insert finger-like projections between oocytes that can only be resolved by electron microscopy (Hall et al., 1999). In these *goa-1(RNAi);rrf-1* female gonads, punctate staining is observed between oocytes mainly in superficial focal planes, suggesting that GOA-1 may be present in the sheath cell processes (Fig. 21E). We stained dissected gonads from these *goa-1(RNAi);rrf-1* mutant females with MAPK-YT antibodies and observed an absence of MAPK activation in the proximal gonad, suggesting that *goa-1* activity might be sufficient in the soma to negatively regulate MAPK activation in oocytes (Fig. 21F).

Since the sheath cells mediate the *ceh-18*-dependent inhibition of MAPK activation and meiotic maturation, which in turn is antagonized by MSP (Miller et al., 2003), we tested whether *ceh-18* and *goa-1* genetically interact. The high meiotic maturation rate (1.67 ± 0.38) observed following *goa-1(RNAi)* in a *fog-2(q71)* background depends on *ceh-18(+)* function because *goa-1(RNAi)* in a *ceh-18(null);fog-2(q71)* background results in a lower meiotic maturation rate (0.92 ± 0.30; Table 4). This result is consistent with a model in which *goa-1* functions in the sheath cell control of meiotic maturation. A role for *goa-1* in the soma is additionally suggested by the observation that the basal sheath cell contraction rate is elevated in *goa-1(n1134)fog-3(q443)* and *goa-1(RNAi);fog-2(q71)* females (data not shown).

Discussion

MSP promotes oocyte meiotic maturation by antagonizing two parallel negative regulatory circuits: an oocyte VAB-1/Eph receptor pathway and a somatic gonadal sheath cell pathway defined by the POU-homeoprotein CEH-18 (Miller et al., 2001; Miller et al., 2003). I reasoned that additional components of the VAB-1 and CEH-18 pathways were likely to function as negative regulators, and I sought to identify them by a genome-wide RNAi screen. I performed this screen with a *fog-2(q71)* female sterile strain in which oocytes arrest at prophase of meiosis I and are retained in the gonad arm due to the absence of MSP. I screened for rare RNAi clones in which meiotic maturation and ovulation occur at elevated rates and unfertilized oocytes are laid onto the bacterial lawn in increased numbers despite the absence of MSP.

In this screen, I identified 17 new negative regulators of oocyte meiotic maturation including *ceh-18*. The fact that *ceh-18* was identified validates the rationale and effectiveness of the screen. However, this screen is not saturated because I did not identify *vab-1*, *nmr-1*, and *itr-1*, three known negative regulators of meiotic maturation (Corrigan et al., 2005). Class I genes encode several proteins with well-characterized intercellular signaling functions, such as components of multiple G protein signaling pathways (*goa-1*, *kin-2*, *gpb-1*, and *gsa-1*), protein kinase C var epsilon (*pkc-1*), a 14-3-3 protein (*par-5*), and a disabled homolog (*dab-1*).

Figure 22. A model for parallel control of meiotic maturation in *C. elegans* by G protein signaling from the soma and an oocyte MSP/Eph receptor pathway.

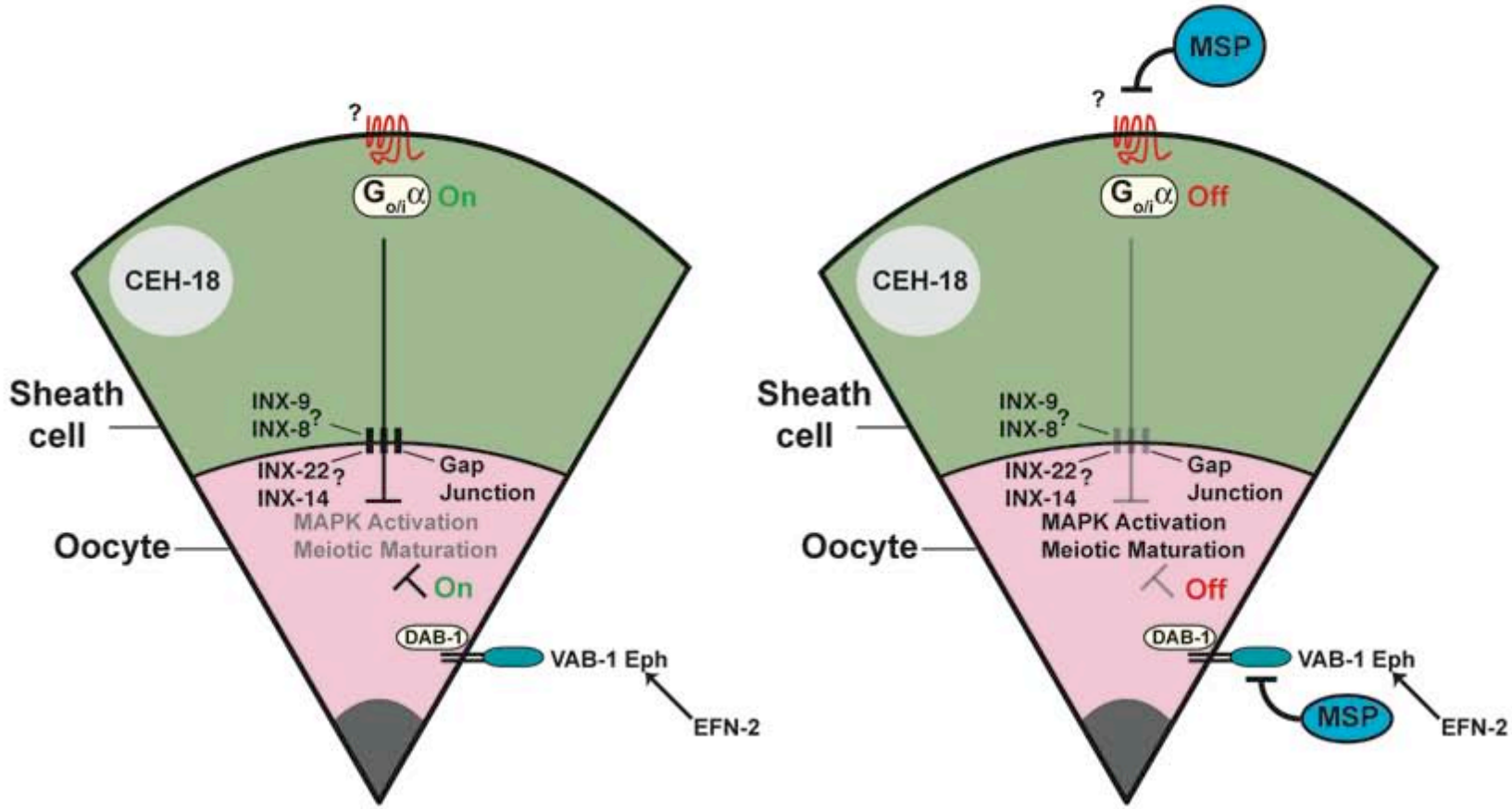
?
$G_{o/i}\alpha$ On
CEH-18
Sheath cell
INX-9
INX-8?
INX-22?
INX-14
Gap Junction
MAPK Activation
Meiotic Maturation
Oocyte
On
DAB-1
VAB-1 Eph
EFN-2
MSP
?
$G_{o/i}\alpha$ Off
CEH-18
Sheath cell
INX-9
INX-8?
INX-22?
INX-14
Gap Junction
MAPK Activation
Meiotic Maturation
Oocyte
Off
DAB-1
VAB-1 Eph
MSP
EFN-2

Previous studies demonstrated that somatic and germline regulatory pathways work in concert to control oocyte meiotic maturation (Miller et al., 2003; Yamamoto et al., 2006). The *rrf-1* RNAi analysis shows that *goa-1*, *kin-2*, *gpb-1*, and *rpt-3* function likely in the soma to regulate oocyte meiotic maturation. My hypothesis is that these genes function in the somatic sheath cells to regulate oocyte meiotic maturation. To test this idea, I performed RNAi analysis in the *vab-1(dx31*) female background. Previous studies show the *ceh-18* somatic sheath cell pathway functions in parallel to the oocyte *vab-1* pathway to regulate meiotic maturation. Consistent with this idea, I found that *goa-1*, *kin-2*, and *gpb-1* synergize with *vab-1* to regulate oocyte meiotic maturation (Table 4). Thus, it is likely that *goa-1*, *kin-2*, and *gpb-1* may function in the somatic sheath cells to negatively regulate oocyte meiotic maturation. Genetic mosaic analysis of *goa-1* and *kin-2* in a female background will be needed to test this possibility.

In the genome-wide RNAi screen, I identified *inx-14* and *inx-22* as germline negative regulators of meiotic maturation and MAPK activation in the absence of sperm (Table 1 and Table 3, Fig. 17F). Since oocytes have been observed to form gap junctions only with sheath cells (Hall et al., 1999), *inx-14* and *inx-22* likely encode oocyte components of sheath/oocyte gap junctions. *ceh-18(mg57)* mutants do not have gap junctions suggesting that ooocyte-sheath cell gap junctional communication may play a important role in oocyte meiotic maturation. *rrf-1* RNAi analysis shows that *inx-22* and *inx-14* are necessary in the germline to inhibit oocyte meiotic maturation.

In future, cell biological and ultrastructural studies are required to address the role of gap junctions in meiotic maturation.

The RNAi screen identified four genes (*dab-1*, *vav-1*, *pqn-19*, and *pkc-1*) satisfying multiple genetic criteria expected of genes functioning in the *vab-1* Eph receptor pathway (Fig. 18). *vab-1* was previously shown to be necessary for complete MSP binding to gonads via an in situ binding assay and also to be sufficient to confer specific MSP binding activity to cultured mammalian cells (Miller et al., 2003). Further, VAB-1 ectodomain can directly bind MSP (Govindan et al., 2006). Recently, it was suggested that VAB-1 may switch from a negative regulator to a redundant positive regulator of meiotic maturation upon binding MSP (Corrigan et al., 2005). Consistent with the possibility that negative regulators of meiotic maturation may also have redundant activating functions, mutations in *dab-1*, *pqn-19*, and *pkc-1* confer an incompletely penetrant delay in nuclear envelope breakdown during meiotic maturation, and a similar observation was made previously for *vav-1* (Norman et al., 2005). The maturation-promoting redundant functions of *dab-1*, *pqn-19*, *pkc-1*, and *vav-1* are likely through a *vab-1*-independent pathway because *vab-1(null)* mutations do not exhibit delays in nuclear envelope breakdown. The mechanisms by which the *vab-1* pathway represses meiotic maturation and MAPK activation in oocytes in the absence of MSP will take additional work to decipher. Nonetheless, the conserved *vab-1* pathway genes described here are likely to mediate analogous signaling functions in mammals. In fact, a recent study of Eph receptor signaling during axonal guidance in mammals found a critical role

for a homolog of VAV-1, the Rho family guanine nucleotide exchange factor Vav2 (Cowan et al., 2005).

As I mentioned in the introduction, G-protein signaling regulates meiotic maturation in a variety of species including mammals. It is interesting that several genes involved in G-protein signaling pathways (*goa-1*, *kin-2*, *gpb-1*, and *gsa-1*), were identified in the genome-wide RNAi screen. Also, of all the negative regulators identified by the RNAi screen, *goa-1* and *kin-2* exhibit the most robust maturation phenotype. *goa-1* encodes a heterotrimeric $G\alpha_{o/i}$ protein previously shown to regulate locomotion, egg-laying, and male mating behaviors (Mendel et al., 1995; Segalat et al., 1995). Using RNAi and genetic analysis, I show that *goa-1* is necessary to inhibit oocyte meiotic maturation and MAPK activation in the absence of sperm (Fig. 22). Further, I show that *goa-1* is sufficient to inhibit oocyte meiotic maturation.

To address in which cells *goa-1* is necessary to inhibit oocyte meiotic maturation, I examined the expression of GOA-1 in the germline. GOA-1 is expressed both in the oocytes as well as in the somatic sheath cells (Fig. 21). However, *goa-1* is sufficient in the soma to inhibit maturation and MAPK activation (Table 3 and Fig. 21F). A genetic mosaic analysis in the female background is needed to demonstrate that *goa-1* is required in the somatic sheath cells to inhibit maturation. We were unable to perform mosaic analysis because our attempts to rescue the *goa-1(sa734)* phenotype failed.

In the genome-wide RNAi screen, I identified *kin-2* as a negative regulator of meiotic maturation in the absence of sperm (Table 1). Genetic

analysis shows that *kin-2* is necessary and sufficient in the soma to inhibit oocyte maturation in the absence of sperm (Table 3). *kin-2* encodes the regulatory subunit of cAMP-dependent protein kinase A. The cAMP-dependent protein kinase A (PKA) is a holoenzyme that consists of catalytic subunits and regulatory subunits. In the holoenzyme form, the catalytic subunit is inactive. Binding of cAMP to the regulatory subunit releases the active catalytic subunit. Thus, it is possible that the catalytic subunit of PKA, encoded by the gene *kin-1* in *C. elegans* is a positive regulator of meiotic maturation. In addition, the involvement of of cAMP dependent PKA suggests that cAMP may be involved in maturation. In the canonical G-protein signaling pathway, activation of $G\alpha_s$ results in production of cAMP via adenylate cyclase. Paradoxically, in the genome-wide RNAi screen, I identified $G\alpha_s$ as a weak negative regulator of meiotic maturation. In chapter III, I will show that $G\alpha_s$ is a positive regulator of meiotic maturation in the presence of sperm and a weak negative regulator in the absence of sperm. In addition, my preliminary results suggest that ACY-4, which encodes adenylate cyclase is a positive regulator of meiotic maturation.

In the genome-wide RNAi screen, I identified a large number of new negative regulators. Many of these genes are predicted to participate in diverse biological functions. RNAi inactivation of most of these genes produces a robust phenotype. It is interesting that some of the negative regulators such as ARF-1.1, PAR-5, PTC-1, and PHI-11 belong to functional classes that have not been implicated in control of meiotic maturation before. Future functional and biochemical characterization of the negative regulators will provide novel

insights into how meiotic maturation is controlled in response to sperm in *C. elegans*.

CHAPTER III

A SOMATIC $G\alpha_s$ IS NECESSARY AND SUFFICIENT TO PROMOTE OOCYTE MEIOTIC MATURATION IN THE PRESENCE OF SPERM

Introduction

In most sexually reproducing organisms, the oocytes arrest at prophase I of meiosis. Following hormonal signaling, the oocytes resume meiosis and undergo oocyte meiotic maturation. In *C. elegans*, MSP signals oocyte meiotic maturation, MAPK activation and ovulation (Miller et al., 2001; Miller et al., 2003) . MSP signaling involves two parallel genetic pathways that negatively regulate meiotic maturation. *vab-1* encodes an Eph/MSP receptor tyrosine kinase that is required in the oocytes to negatively regulate meiotic maturation (Miller et al., 2003). Signaling by VAB-1 and a somatic gonadal pathway, defined by the POU-class homeobox gene *ceh-18* negatively regulates oocyte maturation. MSP promotes meiotic maturation by binding to VAB-1 and additional unidentified receptor(s). In addition, *vab-1* and *ceh-18* pathways negatively regulate MAPK activation in the absence of sperm. MSP activates MAPK by antagonizing *vab-1* and *ceh-18* pathways.

In a genome-wide RNAi screen for negative regulators of meiotic maturation (Table 1), I identified *kin-2*, which encodes a regulatory subunit of cAMP-activated protein kinase A (PKA-R), as a negative regulator of meiotic

maturation. In addition, I found that KIN-2 functions in the soma to inhibit oocyte meiotic maturation and MAPK activation.

In the canonical G-protein pathway, KIN-2 inhibits downstream signal transduction by binding to the catalytic subunit of PKA. Activation of G_s by GPCR results in production of cAMP, which binds KIN-2 thereby resulting in active PKA (Cabrera-Vera et al., 2003). Since KIN-2 is a negative regulator of meiotic maturation, I reasoned that $G\alpha_s$ and adenylate cyclase may be positive regulators of meiotic maturation. In *C. elegans*, *gsa-1* encodes a G_s-protein alpha subunit that is expressed in several tissues and is required for viability (Korswagen et al., 1997; Park et al., 1997). *pk75*, a putative null allele of *gsa-1* is larval lethal. In addition, it is involved in egg-laying, locomotion and neuronal cell death (Berger et al., 1998; Korswagen et al., 1997; Korswagen et al., 1998). Surprisingly, in the genome-wide RNAi screen, I identified *gsa-1* as a weak negative regulator of meiotic maturation in the absence of sperm (Table 1). To resolve this paradox, I reasoned that *gsa-1* might have an MSP-dependent function in promoting meiotic maturation through the canonical pathway and a weak MSP-independent function in inhibiting meiotic maturation through a noncanonical pathway. Importantly, the genome-wide RNAi screen could not reveal a positive role for *gsa-1* because it was conducted in the absence of the MSP signal.

In this chapter, using RNAi and genetic approaches, I show that $G\alpha_s$ is necessary and sufficient for oocyte meiotic maturation and MAPK activation in wildtype hermaphrodites. Further, using *rrf-1* mutant analysis, I found that $G\alpha_s$

is sufficient in the soma to promote oocyte meiotic maturation and MAPK activation.

Extending these results, I demonstrate that $G\alpha_s$ functions in the gonadal sheath-spermathecal cell lineages to promote oocyte meiotic maturation using genetic mosaic analysis. In addition, I established that $G\alpha_{i/o}$ signaling antagonizes $G\alpha_s$ signaling to inhibit oocyte meiotic maturation in the absence of sperm. Finally, I present the results of a forward genetic screen for suppressors of *gsa-1* oocyte meiotic maturation defect.

Materials and methods

Worm handling and strains

Techniques for culturing worms are described by Brenner (1974). Worms were grown at 20^{o}C unless otherwise indicated. Wild-type strain used was *C. elegans* Bristol strain N2. CB4856 strain was used for single-nucleotide polymorphism (SNP) mapping as described by (Davis et al., 2005). The following marker mutations and balancer chromosomes were used:

LGI: *fog-3(q443)*, *gsa-1(pk75)*, *gsa-1(ce81)*, *gsa-1(ce94)*, *dpy-5(e61)*, *unc-13(e51)*, *hT2(qIs48)(I,III)*

LGII: *vab-1(dx31)*, *dpy-10(e128)*, *unc-4(e120)*, *mIn1(II)*

LGIII: *unc-45(e286)*, *dpy-1(e1)*, *dpy-17(e164)*, *unc-32(e189)*, *hT2(qIs48)(I,III)*

LGIV: *oma-1(zu405te33)*, *dpy-13(e184)*, *unc-24(e138)*, *DnT1(IV,V)*.

LGV: *oma-2(te51)*, *fog-2(q71)*, *unc-46(e177)*, *dpy-11(e224)*, *unc-23(e25)*, *DnT1(IV;V)*

LGX: *dpy-6(e14)*, *unc-9(e101)*, *kin-2(ce179rf)*, *ceh-18(mg57)*

Phenotypic analysis

Oocyte meiotic maturation rates were measured as described in Miller et al. (2003). Sheath cell contraction was monitored directly in live anesthetized worms (0.1% tricaine and 0.01% tetramisole in M9 buffer) using DIC high-resolution optics as described by Miller et al. (2003). MAPK staining was performed as described in Miller et al. (2003).

RNA interference assay

RNAi feeding experiments were performed as described in Govindan et al. (2006). For all *gsa-1(RNAi)* experiments, *gsa-1* feeding bacteria was grown overnight and seeded onto modified M9-NGM medium containing 0.2% β-lactose and 25µg/ml carbenicillin. The bacteria were grown overnight at 22ºC for induction of dsRNA. All the RNAi clones were verified by sequencing.

Plasmid constructs used

Plasmid pRP1505 (containing a 13-kb *HindIII* fragment spanning entire *gsa-1*) was obtained from Ron Plasterk (Korswagen et al., 1997). Plasmid pTG96 (a gift from Jane Hubbard) consists of 7.3-kb of genomic DNA from *sur-5* locus fused to GFP from pPD95.70 vector (Yochem et al., 1998).

Germline transformation

Hermaphrodites of genotype, *gsa-1(pk75)/ hT2[bli-4(e937) let-?(q782) qIs48] (I;III)* were injected in the distal gonad arms with plasmid pRP1505 and pTG96 at a concentration of 50µg/ml (Fire, 1986; Mello et al., 1991), using a micromanipulator and an Axiovert-35 inverted microscope (Zeiss).

Injected worms were recovered in M9 buffer and transferred to NGM plates seeded with *E.coli*. Trangenic animals were identified by nuclear GFP expression and loss of pharyngeal GFP. Transgenic worms that bred true were maintained and used for mosaic analysis.

Mosaic analysis

Adult hermaphrodites were mounted on agar pads with anesthetic solution (0.1% tricaine and 0.01% tetramisole) and scored for loss of GFP expression using a Zeiss Axioscope in several landmark cells (Sulston et al., 1983; Yochem et al., 2006).

Isolation of suppressors of gsa-1(RNAi) meiotic maturation defect mutations

I mutagenized wild-type hermaphrodites with ethyl methanesulfonate (EMS) as described by Brenner (1974) with some modifications. L4 stage wildtype hermaphrodites were washed with M9 buffer (42.2 mM Na_2HPO_4, 22 mM KH_2PO_4, 85.6 mM NaCl and 1.0 mM $MgSO_4$) and incubated for four hours in a 4 ml solution of M9 buffer containing 25 mM EMS. Worms were washed three times in M9 buffer and placed on seeded plates for recovery. Three to four mutagenized L4 larvae or young adults were transferred to 35 mm plates and incubated at 20^{o}C. Thirty F_1 gravid adults per plate were picked onto a new 35 mm plate and allowed to produce F_2 progeny for about 5 hours. The adult worms were picked off the plates and the eggs were allowed to grow up to L3 larval stage. F_2 worms were transferred to six-well RNAi plates seeded with bacteria expressing *gsa-1*dsRNA.

gsa-1(RNAi) in wild-type hermaphrodites results in sterility due to the inability of the oocytes to undergo meiotic maturation despite the presence of sperm. I screened the mutagenized worms on the second day of adulthood for fertile worms. Mutants were recovered from the RNAi plates and cultured in NGM medium for subsequent analysis.

I screened ~80,000 haploid genomes using this procedure and recovered 127 strains that were resistant to *gsa-1(RNAi)* by feeding. To eliminate mutations that were resistant to general RNAi, I subjected the strains to *unc-22(RNAi)* by feeding. Any mutant that was resistant to *gsa-1(RNAi)* and *unc-22(RNAi)* by feeding were classified as RNAi-resistant mutants. Mutants that were 100% sensitive to *unc-22(RNAi)* by feeding but resistant to *gsa-1(RNAi)* were classified as "suppressors of *gsa-1(RNAi)* meiotic maturation defect". All the mutants were outcrossed at least two-times to remove background mutations.

Single nucleotide polymorphism (SNP) mapping

All mutations were mapped to a linkage group using the CB4856 Hawaiian strain for SNP mapping as described (Davis et al., 2005). The mutations were mapped by crossing CB4856 males to mutant hermaphrodites. Late L4-stage F1 progeny were plated to individual RNAi-plates seeded with bacteria expressing *gsa-1*dsRNA. Individual F_2 progeny were scored for suppression of *gsa-1(RNAi)* maturation defect. ~100 sterile and fertile F_2 progeny were analyzed by bulk segregant analysis using SNP markers as described in (Davis et al., 2005).

Genetic mapping

Standard three-factor mapping techniques were used for mapping suppressors to a genetic interval. Before performing crosses, the mapping strains were tested for any unlinked or linked *gsa-1(RNAi)* resistance.

Complementation tests

I assigned each mutation to a complementation group by crossing heterozygous mutant male with either a Dpy-marked or Unc-marked mutation. In case of *tn1339*, we crossed heterozygous *tn1339* males to *inx-22(tm1661)* females. The resultant progeny were fed with *gsa-1*dsRNA and observed for suppression of maturation defect. I expected that if a mutation failed to complement another mutation, we would observe 50% fertile cross-progeny. Complementation tests, as measured by *gsa-1(RNAi)* resistance could only be performed on recessive mutations. Thus, *ceh-18* could not be tested in this way because *ceh-18(mg57)* heterozygotes are resistant to *gsa-1(RNAi)*.

Sequencing

Candidate genes were amplified using PCR from the mutant genomic DNA. Purified PCR products were then submitted to University of Minnesota DNA Sequencing and Analysis Facility for sequencing.

Double-mutant strain construction and analysis

To construct *sgd-1(tn1237)I; tnIs6[lim-7::GFP + rol-6(su1006)]V*, I crossed *sgd-1(tn1237)/+* males into *tnIs6[lim-7::GFP + rol-6(su1006)]* hermaphrodites. *tnIs6[lim-7::GFP + rol-6(su1006)]* is a spontaneous integrant

in LGV (Yasso. C and Vallier. L., personnel communication). L4 stage F1 cross-progeny were subjected to *gsa-1(RNAi)* and the fertile F2 worms were picked to individual NGM plates. From these F2 worms, rollers with GFP expression in the gonadal sheath cells were isolated. I used the same method to construct *sgd-8(tn1283)III; tnIs5[lim-7::GFP + rol-6(su1006)]I*.

Fluorescence Microscopy

Phalloidin staining was performed as per the protocol from Strome, 1986 and McCarter et al. (1997). Young adult hermaphrodite gonads were dissected and fixed with 3% paraformaldehyde in egg salts for an hour. Following fixation, gonads were washed once in PBT (1%PBS+ 0.1% Tween 20) and post-fixed in -20^{o}C methanol for 5 min. Then, gonads were washed three times using PBT and incubated with 0.5 µM Phalloidin-TRITC (Sigma) for 30 minutes.

Results

***gsa-1* is required for oocyte meiotic maturation**

To determine whether *gsa-1* is required for oocyte meiotic maturation, I performed *gsa-1(RNAi)* on wild-type hermaphrodites. *gsa-1(RNAi)* in a wild-type hermaphrodite background results in significant reduction of oocyte meiotic maturation rate compared to control (RNAi) treated worms (Table 6, compare lines 2 and 1, $p < 0.001$). As a result, oocytes stack in the gonad arm (Fig. 23B). In cases where meiotic maturation and ovulation had occurred, worms are egg-laying defective suggesting that *gsa-1* may have a role in egg-laying.

Table 6. *gsa-1* is necessary and sufficient to promote oocyte meiotic maturation

	Genotype	Oocyte meiotic maturation rates (per gonad arm per hour)	N
1.	Control RNAi on wildtype	2.50 ± 0.41	16
2.	*gsa-1(RNAi)* on wildtype	0.30 ± 0.11	17
3.	*gsa-1(pk75)/+* hermaphrodite	1.60 ± 0.40	10
4.	*fog-3(q443)* unmated	0.17 ± 0.14	15
5.	*fog-3(q443)* mated	2.29 ± 0.43	20
6.	*gsa-1(ce81* gf*)fog-3(q443)* unmated	0.38 ± 0.14	12
7.	*gsa-1(ce94* gf*)fog-3(q443)* unmated	0.44 ± 0.13	13
8.	Control RNAi on *vab-1(dx31)*, hermaphrodites	2.44 ± 0.60	15
9.	*gsa-1(RNAi)* on *vab-1(dx31)*, hermaphrodites	0.20 ± 0.17	15
10.	Control RNAi on *ceh-18(mg57)*, hermaphrodites	1.76 ± 0.44	15
11.	*gsa-1(RNAi)* on *ceh-18(mg57)*, hermaphrodites	1.78 ± 0.36	16
12.	*oma-1(RNAi);oma-2(RNAi)* hermaphrodite	0.06 ± 0.07	13
13.	*oma-1;oma-2* (RNAi); *gsa-1(ce94* d*)* hermaphrodite	0.00 ± 0.00	10
14.	Control RNAi on *rrf-1(pk1417)*, hermaphrodites	2.39 ± 0.50	12
15.	*gsa-1(RNAi)* on *rrf-1(pk1417)*, hermaphrodites	2.06 ± 0.40	15
16.	Control RNAi on *goa-1(sa734)*, hermaphrodites	1.23 ± 0.18	15
17.	*gsa-1(RNAi)* on *goa-1(sa734)*, hermaphrodites	0.14 ± 0.10	16
18.	Control RNAi on *goa-1(n1134)*, hermaphrodites	2.55 ± 0.40	18
19.	*gsa-1(RNAi)* on *goa-1(n1134)*, hermaphrodites	0.34 ± 0.20	14

Figure 23. $G\alpha_s$ signaling is required for oocyte meiotic maturation

DIC micrographs of wildtype (A), *gsa-1(RNAi)* treated wildtype (B), *gsa-1(pk75); tnEx31[gsa-1(+)+sur-5::gfp]* (C), and *acy-4(ok1806)* hermaphrodites (D).
(A) In wildtype hermaphrodites, the proximal gonad (pg) contains oocytes that undergo meiotic maturation, ovulation and fertilization in an assembly line fashion. Fertilized embryos accumulate in the uterus (ut) until they are laid.
(B) In *gsa-1(RNAi)*-treated hermaphrodites, oocytes fail to undergo maturation and they accumulate in the proximal gonad (pg) despite the presence of sperm. No embryos are found in the uterus (ut).
(C) *gsa-1(pk75); tnEx31[gsa-1(+)+sur-5::gfp]* worm that lost *tnEx31* array in gonadal sheath/spermathecal cell lineages as determined by the loss of GFP. This mosaic phenocopies the *gsa-1(RNAi)* phenotype characterized by inability to undergo maturation despite the presence of sperm.
(D) *acy-4(ok1806)* hermaphrodites phenocopies *gsa-1(RNAi)* maturation defect characterized by stacking of oocytes in the proximal gonad (pg) and an empty uterus (ut).

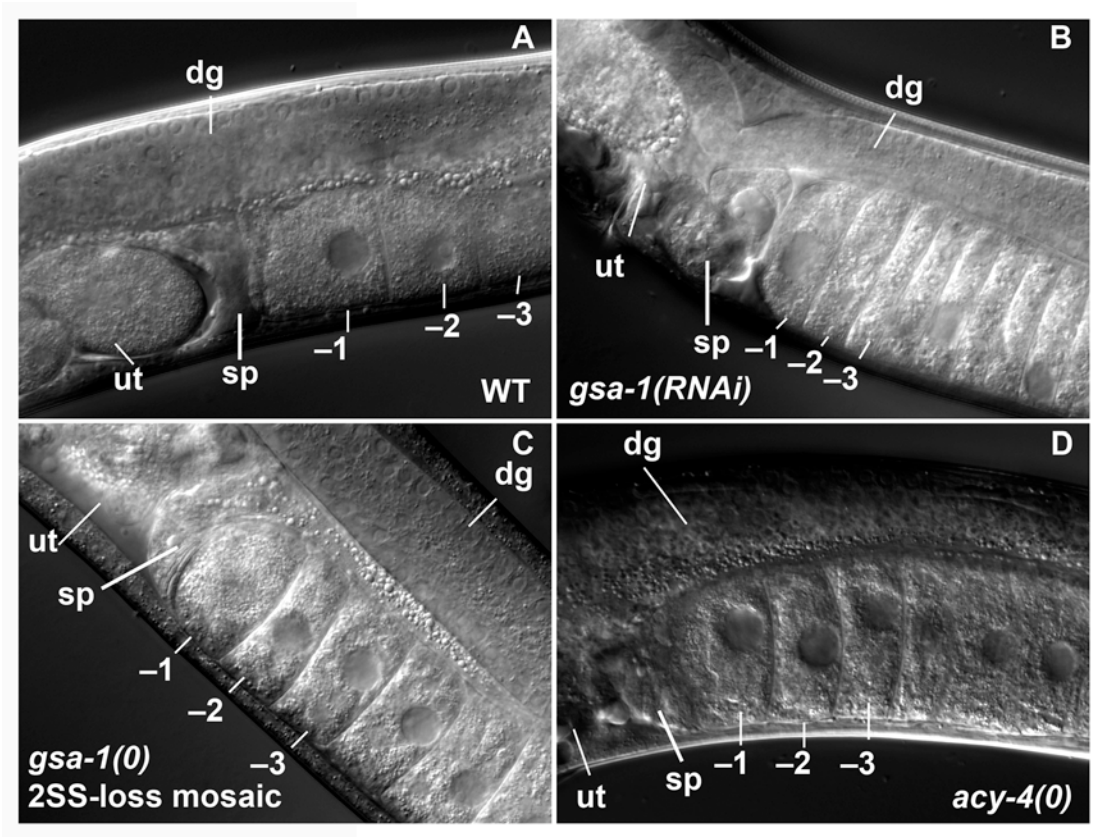
A
dg
ut
sp
–1
–2
–3
WT
B
dg
ut
sp
–1
–2
–3
gsa-1(RNAi)
C
dg
ut
sp
–1
–2
–3
gsa-1(0)
2SS-loss mosaic
D
dg
ut
sp
–1
–2
–3
acy-4(0)

Figure 24. $G\alpha_s$ signaling is necessary and sufficient for oocyte MAPK activation.

Activation of MAPK was assessed using an antibody that recognizes active phosphorylated form of MPK-1/MAP kinase. The most proximal -1 oocyte shows MAPK activation in wildtype hermaphrodites (A) whereas females do not show MAPK activation (E). By contrast, *gsa-1(RNAi)* on wildtype (B) as well as on *vab-1(dx31)* mutants (C) does not show MAPK activation. By contrast, *gsa-1(RNAi)* on *ceh-18(mg57)* hermaphrodites (D) exhibits MAPK activation.

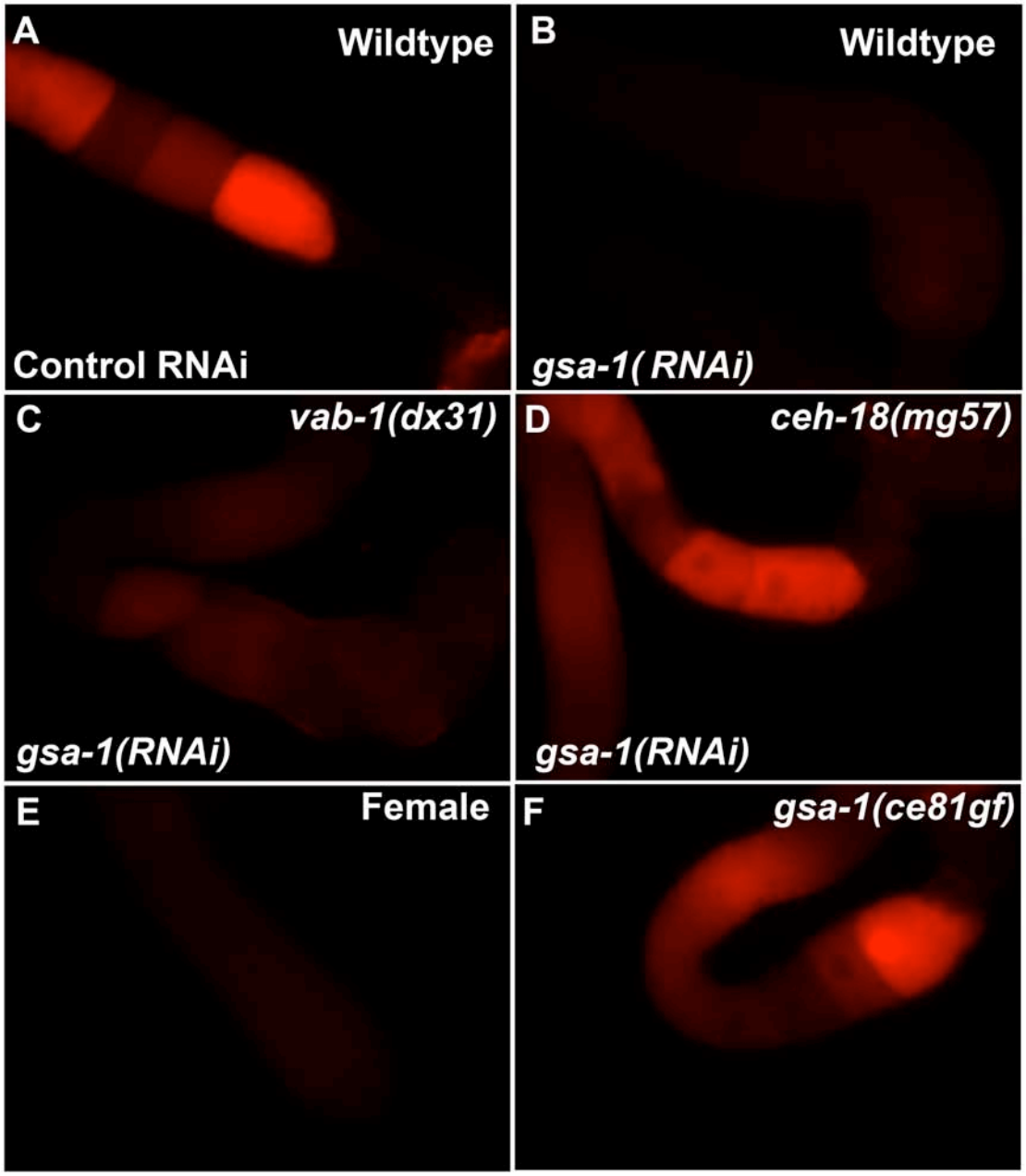
A
Wildtype
Control RNAi
B
Wildtype
gsa-1(RNAi)
C
vab-1(dx31)
gsa-1(RNAi)
D
ceh-18(mg57)
gsa-1(RNAi)
E
Female
F
gsa-1(ce81gf)

I could not examine the *gsa-1* null mutants since the *gsa-1(pk75)* mutant is larval lethal (Korswagen et al., 1997). However, I observed that *gsa-1(pk75)* heterozygous hermaphrodites exhibit a significant reduction in meiotic maturation rates (Table 6, compare lines 3 and 1, $p < 0.001$). In addition, I observed that *gsa-1(pk75)* heterozygous worms were healthy and well-fed but moved slowly and were slightly egg-laying defective. Extracellular MSP can be detected in the spermatheca and gonad arms (data not shown) of *gsa-1(RNAi)*-treated worms suggesting that the meiotic maturation defect is not due to a defect in MSP release. Furthermore, mating *gsa-1(RNAi)* treated worms with males cannot rescue the *gsa-1* maturation defect suggesting that the maturation defect is not due to defective sperm or MSP release.

In the GTP-bound state, $G\alpha_s$ activates adenylate cyclase to produce cAMP. My hypothesis is that $G\alpha_s$ activates an adenylate cyclase to promote meiotic maturation. To test this hypothesis, I examined whether any of the adenylate cyclase (ACY-1 to ACY-4) genes in *C. elegans* play a role in maturation. Loss of function alleles in ACY-1 do not exhibit any apparent defects in meiotic maturation. The role of other adenylate cyclases (ACY-2 and ACY-3) is not known because no mutations are available for these genes. Recently, two deletion alleles in *acy-4*, *ok1806* and *tm2510* became available. Hermaphrodite worms homozygous for *ok1806* as well as *tm2510* deletion are sterile. Nomarski microscopic analysis revealed that the sterility is due to a failure of the oocytes to undergo maturation despite the presence of sperm (Fig.

23D). This phenotype is similar to the *gsa-1(RNAi)* maturation defect suggesting that *acy-4* may be a downstream activator of meiotic maturation.

gsa-1 is required for MAPK activation

To determine whether *gsa-1* is required for MAPK activation, I immuno-stained control RNAi-treated and *gsa-1(RNAi)*-treated wild-type hermaphrodites with rabbit anti-MAPK antibodies. This antibody specifically recognizes the phosphorylated active form of MAPK protein (Miller et al., 2001; Miller et al., 2003). In wild-type hermaphrodites, the most proximal one to three oocytes show MAPK activation in the presence of sperm (Fig. 24A) (Miller et al., 2001; Miller et al., 2003). By contrast, *gsa-1(RNAi)* on wild-type hermaphrodites blocks MAPK activation in proximal oocytes (Fig. 24B). Further, *gsa-1(RNAi)* can block meiotic maturation and MAPK activation in the *vab-1(null)* mutant hermaphrodite background where MAPK activation is ordinarily expanded to distal oocytes (Miller et al., 2003) (Table 6, compare lines 8 and 9, $p < 0.001$; Fig. 24C). These results suggest that $G\alpha_s$ signaling is necessary for MSP-dependent MAPK activation in the oocytes. By contrast, *gsa-1(RNAi)* cannot block meiotic maturation and MAPK activation in the *ceh-18(null)* mutant hermaphrodites (Table 6, compare lines 10 and 11; Fig. 24D). This result suggests that the requirement of *gsa-1* for oocyte MAPK activation is dispensable in a *ceh-18(null)* background.

gsa-1 is sufficient for oocyte meiotic maturation and MAPK activation

To examine whether *gsa-1* is sufficient to promote meiotic maturation, I examined gain-of-function (gf) alleles in *gsa-1*. Two viable alleles, *ce94gf* and

ce81gf, carrying G45R and R182C substitutions respectively were available (Schade et al., 2005). Comparative studies predict that these substitutions in $G\alpha_s$ stabilize the GTP-bound state (Schade et al., 2005). I constructed *gsa-1(ce94gf)* and *gsa-1(ce81gf)* female strains using *fog-3(q443)*. FOG-3 is required for spermatogenesis and mutations in *fog-3* results in feminization of the germline. *fog-3(q443)* females have low meiotic maturation rates compared to mated females (Table 6, compare lines 4 and 5). By contrast, *gsa-1(ce94gf)* and *gsa-1(ce81gf)* females exhibit higher oocyte meiotic maturation rates compared to *fog-3(q443)* females (Table 6, compare lines 4, 6, and 7). In addition, I found that *gsa-1(ce94gf)* and *gsa-1(ce81gf)* females show MAPK activation in the proximal oocytes (Fig. 24F) whereas *fog-3(q443)* unmated females do not show MAPK activation (Fig. 24E). These results suggest that *gsa-1* is sufficient to promote oocyte meiotic maturation and MAPK activation in the absence of MSP.

Two zinc finger proteins, OMA-1 and OMA-2 are redundantly required for oocyte maturation and MAPK activation. Since, *gsa-1* is required for oocyte maturation, I tested whether *gsa-1* functions upstream or in parallel to *oma-1* and *oma-2* to promote meiotic maturation using gain-of-function *gsa-1* alleles. No MAPK activation or meiotic maturation was observed in *oma-1(RNAi);oma-2(RNAi);gsa-1(ce94*gf*)* or in *oma-1(RNAi);oma-2(RNAi);gsa-1(ce81*gf*)* hermaphrodites or females (Table 6, compare lines 12 and 13; data not shown), suggesting that $G\alpha_s$ is either an upstream regulator, or functions in parallel.

gsa-1 is required in the somatic sheath-spermathecal cell lineages to promote oocyte meiotic maturation

To determine the focus of action of *gsa-1*, I performed *gsa-1(RNAi)* in *rrf-1(null)* hermaphrodites. *rrf-1(null)* hermaphrodites are resistant to RNAi in the soma but sensitive to RNAi in the germline (Sijen et al., 2001). I observed that in the *rrf-1(null)* background, oocyte meiotic maturation rates and MAPK activation were similar in both control-and *gsa-1(RNAi)*-treated worms (Table 6, compare lines 14 and 15 and data not shown). This suggests that *gsa-1* function may be sufficient in the soma to promote oocyte meiotic maturation. Consistent with these data, I found that extrachromosomal arrays bearing transcriptional and translational *gsa-1::gfp* reporter constructs are expressed in the somatic sheath cells (data not shown).

To establish that $G\alpha_s$ is required in the gonadal sheath cell to promote meiotic maturation, David Greenstein and I conducted a genetic mosaic analysis. We constructed a strain that carries an extrachromosomal array *tnEx31[gsa-1(+), sur-5::gfp]* and is also homozygous for *pk75*, a putative null allele of *gsa-1*. *sur-5::gfp* was used as a cell autonomous marker (Yochem et al., 1998). This strain was constructed by coinjection of a *gsa-1(+)* cosmid and *sur-5::gfp* containing cosmid by germline transformation into a strain. Homozygous *gsa-1(pk75)* worms die at the L1 larval stages (Korswagen et al., 1997). By contrast, homozygous *gsa-1(pk75)* worms that carry the *tnEx31* extrachromosomal array are rescued for the larval lethal phenotype and are wildtype. However, the extrachromosomal arrays are mitotically unstable and are occasionally lost during embryonic cell divisions. Such mitotic loss

generates a clone of genetically mutant *gsa-1(-)* cells that can be recognized by the loss of GFP in an otherwise *gsa-1(+)* GFP background. We examined the genetic mosaics to analyze the role of *gsa-1* in oocyte maturation. In *C. elegans*, the first embryonic cell division generates AB and P1 cells (Fig. 25). Loss of the array in the AB cell lineages–AB (Fig. 25 mosaics 26-28) or ABa (Fig. 25 mosaic 29) or ABp (Fig. 25 mosaics 30-33) results in larval lethality similar to the *gsa-1(pk75)* null mutant. This suggests that the foci of lethality of *gsa-1(pk75)* exists in the AB cell lineage, which is consistent with the previous findings (Korswagen et al., 1997). Our mosaic analysis suggests that there may be a separate lethal fous early in the EMS cell lineage.

To determine whether *gsa-1* is required within the germline to promote meiotic maturation, we examined mosaics that lost the array in the germline cell lineages. The P1 cell divides to form EMS and P2 cells. The P2 divides to give rise to C and P3 cells, which subsequently forms D and P4 cells (Fig. 25). The entire germline is derived from P4 cell. Loss of the array at any point except for P1 in the P lineage P2 (Fig. 25; mosaics 1-3), P3 (Fig. 25; mosaics 11-12), or P4 (Fig. 25; mosaics 13-14) did not result in sterility. All worms that had lost *gsa-1* in the germline cell lineages were fertile; however, their progeny were dead because of the larval lethality. In addition, we found one fertile mosaic that had lost the array in P4 and C cell lineages (Fig. 25; mosaic 10). These results suggest that *gsa-1* is not required in the germ line for meiotic maturation.

To examine whether *gsa-1* is required in the somatic gonad for maturation, we examined mosaic worms for loss of array in the P1, EMS or MS

lineages because all these lineages contribute to the formation of somatic gonad. We obtained several independent mosaic animals that had lost the array in the somatic gonad lineages (Fig. 25; mosaics 9 and 15-20). *gsa-1(RNAi)* on wildtype hermaphrodites results in sterility due to the inability of the oocyte to undergo maturation (Fig. 23B). We found mosaics that lost the array in the sheath-spermathecal cell lineages exhibited the same phenotype as that of *gsa-1(RNAi)*-treated worms. MSapp contributes to the formation of the entire posterior somatic gonad while MSppp contributes to the formation of the anterior somatic gonad. We found one mosaic worm that had lost the array in the MSapp cell lineage (Fig. 25; mosaic 16). In this mosaic, the posterior gonad arm was sterile while the anterior arm was fertile. Similarly, three mosaic worms that lost the array in the MSppp cell lineage had a sterile anterior gonad arm and fertile posterior gonad arm (Fig. 25; mosaics 17-19). Furthermore, we found a sterile mosaic (Fig. 25; mosaic 20) that had lost the array in the Z1 and Z4 cell lineage that gives rise to anterior and posterior somatic gonad respectively. In addition, we found one mosaic sterile worm that had lost the array in the Z4 and MSpp cell lineage (Fig. 25; mosaic 15). In summary, mosaic analysis is consistent with RNAi and genetic analysis that *gsa-1* is required in the gonadal sheath cells for oocyte meiotic maturation. *gsa-1* function is sufficient in half of the gonadal sheath cells because, we observed that when the array is lost in a subset of sheath-spermathecal cell lineage, the mosaics were fertile (Fig. 25; mosaics 21-25). The fact that the proximal gonadal sheath cells are connected via gap junctions may explain this observation.

Figure 25. *gsa-1* is required in the sheath/spermathecal cell lineages for oocyte meiotic maturation

Partial depiction of early cell lineages of *C.elegans*. Most cell lineages after MS are shown while the cell lineages from AB, E, C, and D are not shown. Sheath/spermathecal precursor (SS) cells each generate five gonadal sheath cells and half of the spermatheca. Symbols show the points in the lineage at which the extrachromosomal array was lost: circles denote single losses and polygons denote double losses. Cases in which gonad arms affected by the loss were sterile are shown by open symbols, whereas the filled-symbols indicate the animal was fully fertile. Sad faces indicate a lethal focus (within the AB lineage). Mosaics are numbered for ease of reference in the text.

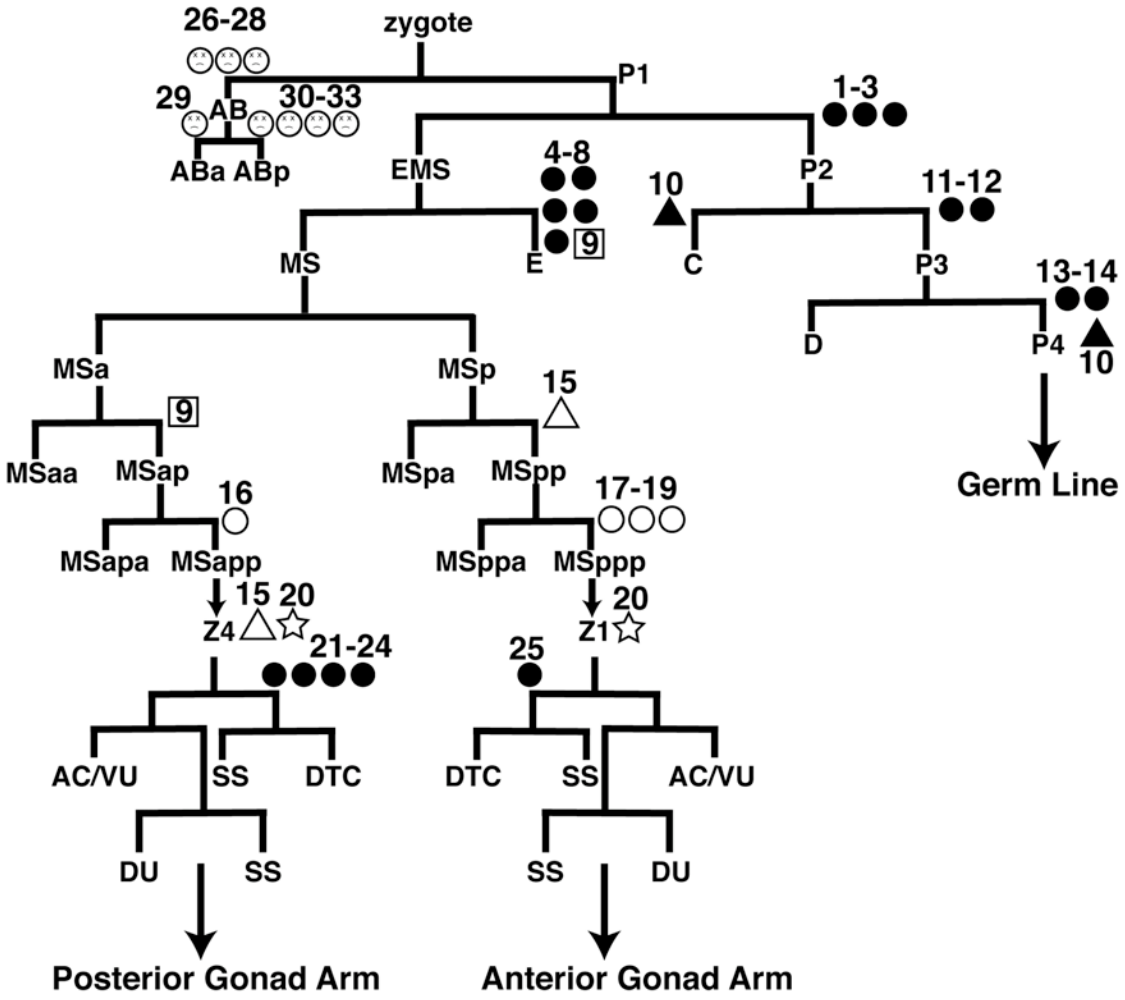
26-28
zygote
P1
29
AB
30-33
1-3
ABa ABp
EMS
4-8
P2
10
11-12
MS
E
9
C
P3
13-14
D
P4
10
MSa
MSp
15
9
MSaa
MSap
MSpa
MSpp
Germ Line
16
17-19
MSapa
MSapp
MSppa
MSppp
15 20
20
Z4
Z1
21-24
25
AC/VU
SS
DTC
DTC
SS
AC/VU
DU
SS
SS
DU
Posterior Gonad Arm
Anterior Gonad Arm

$G\alpha_{o/i}$ antagonizes $G\alpha_s$ signaling to repress meiotic maturation in the absence of MSP

Since $G\alpha_{o/i}$ activity is required for repressing meiotic maturation in the absence of MSP, and $G\alpha_s$ signaling is necessary and sufficient to promote meiotic maturation, I asked whether *goa-1* negatively regulates *gsa-1* in analogy to regulation of $G\alpha_q$ *egl-30* pathway by *goa-1* in neurons (Bastiani and Mendel. 2006). I performed *gsa-1(RNAi)* on *goa-1(sa734)* and *goa-1(n1134)* hermaphrodites and females and observed low meiotic maturation rates and an absence of MAPK activation in proximal oocytes despite the presence of MSP (Table 6, lines 16-19, data not shown). David Greenstein and I conducted a mosaic analysis of *gsa-1* in *goa-1(sa734)* null background to establish that *gsa-1* is epistatic to *goa-1* in the presence of MSP. We constructed a strain homozygous for *goa-1(sa734)* and *gsa-1(pk75)* rescued for the *gsa-1(null)* phenotype by the transgenic array, *tnEx31* (*gsa-1(+)* + *sur-5::gfp*). We looked for mosaics that lost the array in the sheath-spermathecal cell lineages in this strain. We found nine mosaics that lost the array in the somatic sheath-spermathecal cell lineages and these worms were sterile suggesting *gsa-1* is epistatic to *goa-1*.

$G\alpha_s$ signaling may promote oocyte meiotic maturation by antagonizing inhibitory sheath/oocyte gap junctional communication

A key clue of how *gsa-1* might promote meiotic maturation comes from the observation that *gsa-1(RNAi);ceh-18(null)* hermaphrodites exhibit normal meiotic maturation rates and show MAPK activation in oocytes (Table 6, compare lines 10 and 11, Fig. 24D).

How might *gsa-1*'s function to promote meiotic maturation become dispensable in the absence of *ceh-18* activity? In *ceh-18(null)* mutants, sheath cells and oocytes are not in close apposition and sheath/oocyte gap junctions are rare or absent (Hall et al., 1999; Rose et al., 1997). In the genome-wide RNAi screen, I identified *inx-14* and *inx-22* as germline negative regulators of meiotic maturation and MAPK activation in the absence of sperm (Fig. 17E and Table 1). *inx-14* and *inx-22* likely encode oocyte components of sheath/oocyte gap junctions. Since oocytes have only been observed to form gap junctions with sheath cells (Hall et al., 1999), and sheath/oocyte gap junctions must be lost when oocytes lose contact with sheath cells during ovulation, I considered the possibility that $G\alpha_s$ signaling promotes meiotic maturation in part by destabilizing inhibitory sheath/oocyte gap junctions. To test this possibility, I conducted *gsa-1(RNAi)* on *inx-22(tm1661)* hermaphrodites. *tm1661* is a likely null allele in *inx-22*. *gsa-1(RNAi)* in wild type hermaphrodites resulted in sterility due to the inability of the oocytes to undergo meiotic maturation despite the presence of sperm. This is a highly penetrant defect because 100% of the worms fed with *gsa-1(RNAi)* are sterile (n>1000). By contrast, all of the *gsa-1(RNAi)* treated worms are fertile in the *ceh-18(mg57)* (n= 100) and *inx-22(tm1661)* (n=100) hermaphrodite background. Similar suppression was observed in two partial loss-of-function alleles, *mg58* and *mg61* in *ceh-18*. My hypothesis is that $G\alpha_s$ promotes meiotic maturation by antagonizing inhibitory sheath/oocyte gap junctions.

Isolation of suppressors of *gsa-1(RNAi)* meiotic maturation defect

To test the hypothesis that $G\alpha_s$ promotes meiotic maturation by antagonizing inhibitory sheath/oocyte gap junctions, I conducted a forward genetic screen for suppressors of the *gsa-1(RNAi)* meiotic maturation defect. I mutagenized wild-type hermaphrodites using EMS mutagenesis to identify mutations that can suppress meiotic maturation defect and restore fertility in *gsa-1(RNAi)* treated wildtype hermaphrodites (Fig. 26; see materials and methods). From a screen of ~ 80,000 EMS-mutagenized haploid genomes, I obtained 127 strains, which suppressed *gsa-1(RNAi)* oocyte meiotic maturation defect and produced viable progeny. One inherent problem with the screen is that loss-of-function mutations in genes required for RNAi response will suppress the *gsa-1(RNAi)* maturation defect. To eliminate this class, I tested whether the mutants can respond to *unc-22(RNAi)*. *unc-22* encodes a "twitchin" protein that is necessary in muscle for actomyosin contractility in *C. elegans* (Benian et al., 1993). *unc-22(RNAi)* in wild-type hermaphrodites results in a distinctive uncoordinated phenotype that can be easily recognized under dissecting microscope. Of the 127 strains, sixty-five did not respond to *unc-22(RNAi)* suggesting that they have a generalized defect in RNAi response. I focused on forty-two mutations that were 100% sensitive to *unc-22(RNAi)* but resistant to *gsa-1(RNAi)*. All mutants were recessive and homozygous viable. I named these mutations as *sgd* for "suppressor of *gsa-1(RNAi)* meiotic maturation defect". I backcrossed the mutants to wild type at least twice and tested for *gsa-1(RNAi)* suppression level. 100% of wildtype worms fed with *gsa-*

1(RNAi) are sterile (Fig. 27). In most mutants 100% of *gsa-1(RNAi)* treated worms are fertile whereas in some cases it varies between 40-90% (Fig. 27).

sgd mutations define a large set of genes

Using Snip-SNP mapping method (See materials and methods), I mapped all the mutations to linkage groups. Suppressor mutations were distributed on all six chromosomes and defined 19 complementation groups (Table 7). For most of the sgd genes, Snip-SNP mapping was verified using genetic three-factor mapping analyses (Table 8).

SNP mapping data showed that the locus defined by *tn1339* is located on the left arm of linkage group I (Table 7). One previously known *sgd* loci, *inx-22*, map to the same region. To test whether *tn1339* is an allele of *inx-22*, I performed a complementation test. I found that these two mutations fail to complement for Sgd phenotype, suggesting that *tn1339* is a new allele of *inx-22*. DNA sequencing of *inx-22* gene in *tn1339* is in progress to identify the mutation.

SNP mapping data showed that one of the sgd allele, *tn1345* is located on linkage group II. Further three-factor mapping analysis showed that *tn1345* is in the *dpy-10* to *unc-4* interval (Table 8). One previously known negative regulator of meiotic maturation in this genomic region is *dab-1*. Since *tn1345* mutants exhibited phenotypes similar to *dab-1*, we performed complementation tests with the *dab-1(gk291)* allele and found that *tn1345* is an allele of *dab-1*. Sequencing of *tn1345* allele revealed a GC to CG change in *dab-1* coding sequence, which corresponds to arginine-to-valine change in amino acid 341.

Figure 26. A forward genetic screen for suppressors of *gsa-1(RNAi)* meiotic maturation defect

Wildtype hermaphrodites were mutagenized with EMS and F2 progeny were subjected to *gsa-1(RNAi)* at L3 larval stage. F2 progeny from wildtype (+/+) will be sterile whereas 25% from the rare (m/+) will be fertile.

A genetic screen for suppressors of *gsa-1* meiotic maturation defect

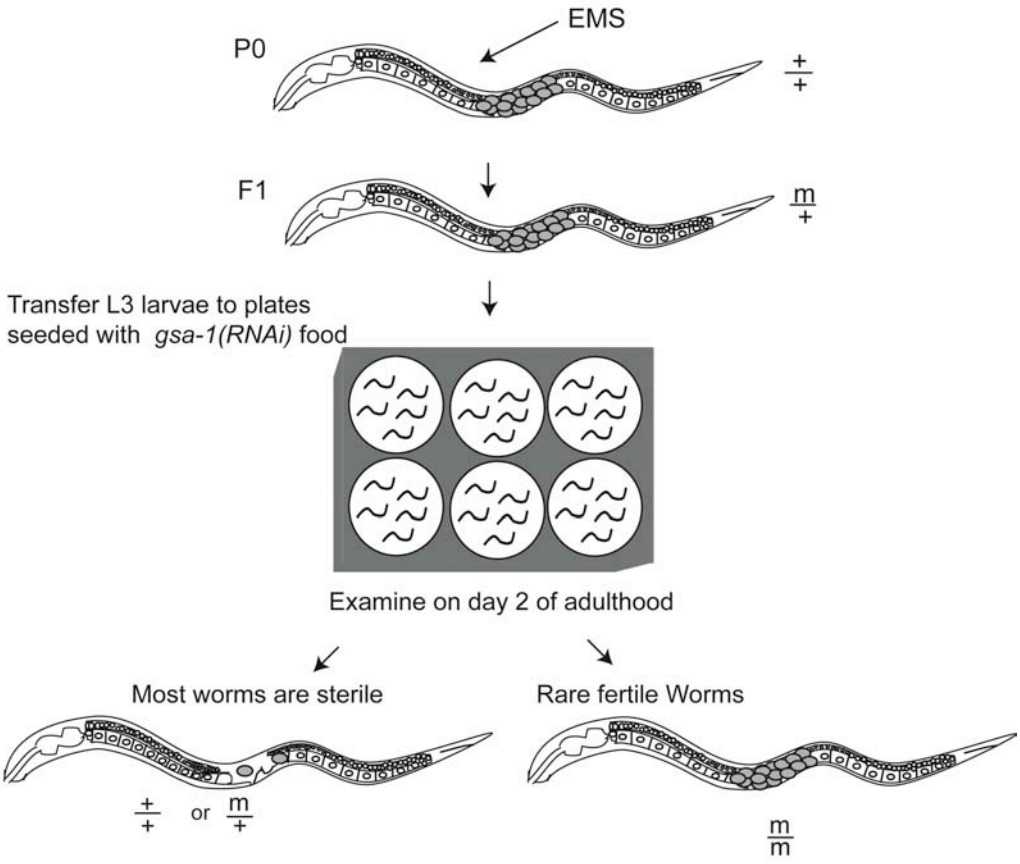

Figure 27. Suppression of *gsa-1(RNAi)* maturation defect

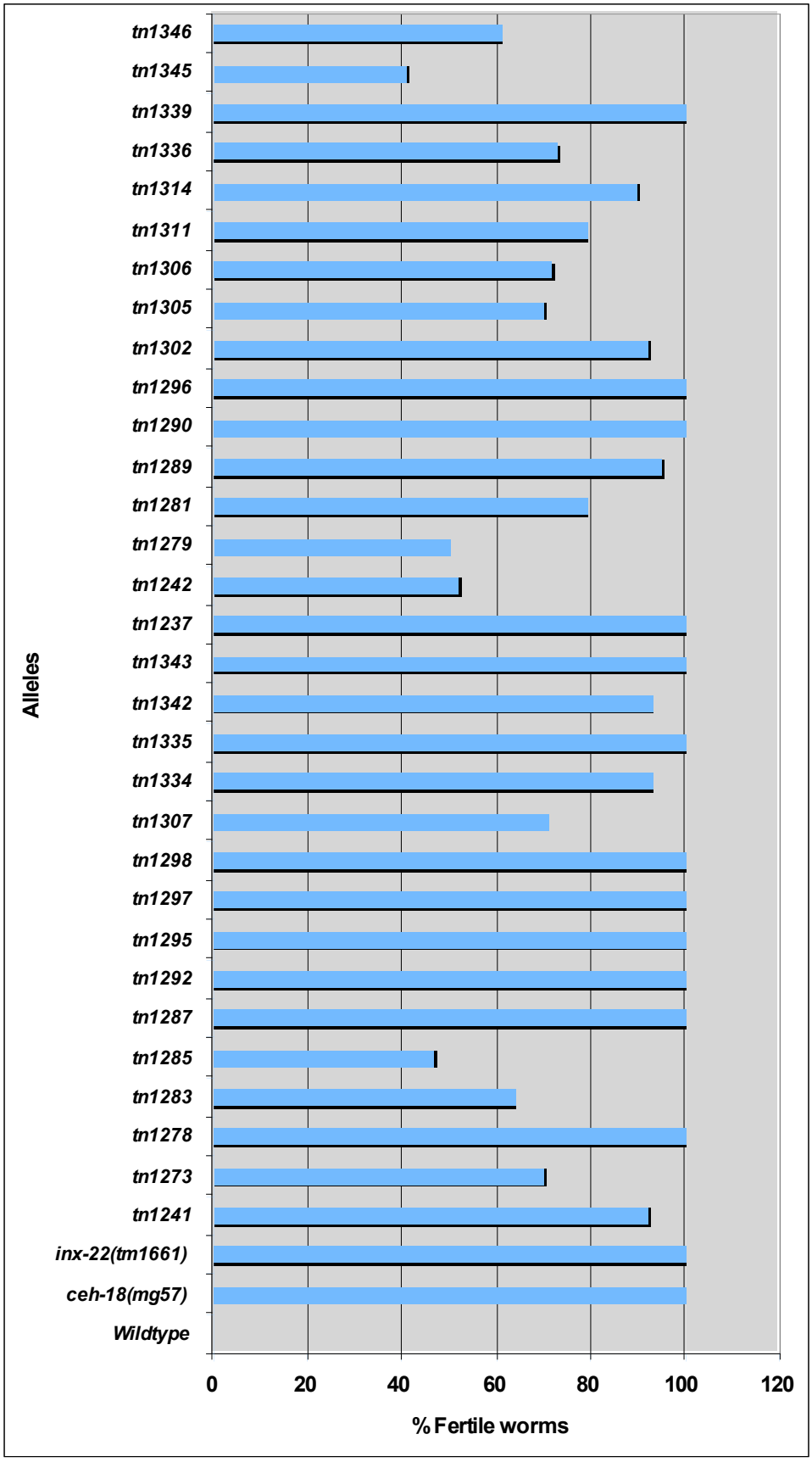
tn1346
tn1345
tn1339
tn1336
tn1314
tn1311
tn1306
tn1305
tn1302
tn1296
tn1290
tn1289
tn1281
tn1279
tn1242
tn1237
tn1343
tn1342
tn1335
tn1334
tn1307
tn1298
tn1297
tn1295
tn1292
tn1287
tn1285
tn1283
tn1278
tn1273
tn1241
inx-22(tm1661)
ceh-18(mg57)
Wildtype
Alleles
0
20
40
60
80
100
120
% Fertile worms

Table 7. *sgd* mutations define a large set of genes.

	Gene Name	Alleles
LG I	*sgd-1*	*tn1237*, *tn1242*, *tn1336*
	sgd-2	*tn1279*
	inx-22	*tn1339*, *tm1661*[a]
	sgd-3[b]	*tn1335*
	sgd-4[b]	*tn1343*, *tn1241*
	sgd-5[b]	*tn1307*
LG II	*lin-10*[c]	*n1402*
	unc-101[c]	*m1*
	dab-1	*tn1345*, *gk291*[d]
	lin-7[c]	*e1413*
	tub-1/tubby[c]	*nr2004*, *ok1972*
LG III	*sgd-6*	*tn1314*
	grk-2[c]	*gk268*
	sgd-7[b]	*tn1278*
	sgd-8[b]	*tn1283*, *tn1285*, *tn1342*, *tn1297*, *tn1334*
LG IV	*sgd-9*	*tn1306*, *tn1340*
	sgd-10[b]	*tn1273*
	sgd-11[b]	*tn1292*, *tn1287*
LG V	*sgd-12*	*tn1302*
	sgd-13	*tn1346*
	sgd-14[b]	*tn1295*, *tn1298*
LG X	*sgd-15*	*tn1290*
	ceh-18[e]	*tn1281*, *tn1296*, *tn1311*, *tn1305*, *mg57*, *mg58*, *mg61*
	sgd-16	*tn1344*
	lin-2[c]	*n1610*, *e1309*
	arr-1[c]	*ok401*
	kin-2[f]	*ce179*

Alleles with a *tn* designation were obtained from the EMS screen.

[a], An allele of *inx-22* containing a 765 bp deletion in the exon 2 and 3. In Govindan et al., (2006) we reported that depletion of *inx-22* and *inx-14* was necessary to suppress *gsa-1(RNAi)*. After additional backcrossing, we now know that *inx-22(tm1661)* by itself can suppress *gsa-1(RNAi).*

[b], Germline RNAi resistant.

[c], Mutations in *lin-2, lin-7, lin-10, tub-1, arr-1, grk-2, and unc-101* were found by a candidate gene approach.

[d], A putative null allele of *dab-1* in which the exons two and three, including the phosphotyrosine-binding domain are deleted.

[e], *mg57*, *mg58*, and *mg61* were isolated by Greenstein et al.(1994). *mg57* is a putative null allele. *mg58* lacks the POU homeodomain while *mg61* lacks the POU specific region. *tn1281*, *tn1311*, *tn1305*, *tn1296* were tentatively assigned as *ceh-18* alleles based on the genetic Snip-SNP mapping analysis. *tn1281* and *tn1296* fails to complement for the Sgd phenotype suggesting that they are alleles of the same gene. *tn1281*, *tn1305*, and *tn1311* fail to complement the germline phenotypes of *ceh-18(mg57)* allele. Since *mg57* is haploinsufficient for s*gd* phenotype, we could not perform complementation test for *gsa-1(RNAi)* sensitivity.

[f], Reduction-of-function allele.

Table 8. Three-factor analysis for *sgd* mutations

Gene (Allele)	Heterozygote genotype	Recombinant phenotype	Recombinant genotype	No. of Recombinants
sgd-1(tn1237)	*dpy-5+unc-13/+tn1237+*	Dpy	*dpy-5tn1237+*	3/7
			dpy-5++	4/7
		Unc	*+tn1237unc-13*	1/8
			++unc-13	7/8
sgd-2(tn1279)	*dpy-5+unc-13/+tn1279+*	Dpy	*dpy-5tn1279+*	6/7
			dpy-5++	1/7
		Unc	*+tn1279unc-13*	5/7
			++unc-13	2/7
sgd-3(tn1335)	*+dpy-5unc-13/tn1335++*	Dpy	*+dpy-5+*	10/10
		Unc	*tn1335+unc-13*	18/18
dab-1(tn1345)	*dpy-10+unc-4/+tn1345+*	Dpy	*dpy-10tn1345+*	3/6
			dpy-10++	3/6
		Unc	*+tn1345unc-4*	8/15
			++unc-4	7/15
sgd-6(1314)	*unc-45+dpy-1/+tn1314+*	Dpy	*+tn1314dpy-1*	0/10
			++dpy-1	10/10
		Unc	*unc-45tn1314+*	8/11
			unc-45++	3/11
sgd-8(tn1283)	*dpy-17+unc-32/+tn1283+*	Dpy	*dpy-17tn1283+*	1/4
			dpy-17++	3/4
		Unc	*+tn1283unc-32*	4/6
			++unc-32	2/6
sgd-9(tn1306)	*dpy-13+unc-24/+tn1306+*	Dpy	*dpy-13tn1306+*	2/3
			dpy-13++	1/3
		Unc	*+tn1306unc-24*	6/11
			++unc-24	5/11
sgd-11(tn1287)	*dpy-13unc-24+/++tn1287*	Dpy	*dpy-13+tn1287*	4/4
		Unc	*+unc-24+*	6/6
sgd-12(tn1302)	*+dpy-11unc-23/tn1302++*	Dpy	*+dpy-11+*	10/10
		Unc	*tn1302+unc-23*	8/8
	unc-46+dpy-11/+tn1302+	Dpy	*+tn1302dpy-11*	0/4
			++dpy-11	4/4
		Unc	*unc-46tn1302+*	5/9
			unc-46++	4/9
sgd-14(tn1298)	*unc-46dpy-11+/++tn1298*	Dpy	*+dpy-11+*	6/6
		Unc	*unc-46+tn1298*	6/6
sgd-17(tn1290)	*dpy-6+unc-9/+tn1290+*	Dpy	*dpy-6tn1290+*	NS
			dpy-6++	NS
			+tn1290unc-9	10/14
			++unc-9	4/14

Genetic mapping shows that *tn1305*, *tn1311*, *tn1281*, and *tn1296* map to the left arm of linkage group X (Table 7). These four alleles result in partial to complete suppression of *gsa-1(RNAi)* defect (Fig. 27). Hermaphrodites carrying the mutations *tn1305*, *tn1311*, *tn1281*, and *tn1296* display a range of phenotypes similar to those of *ceh-18(mg57)*. These phenotypes include endomitotic oocytes, haploid embryos, double row of oocytes in the gonad, and misshapen embryos due to defects in oocyte meiotic maturation and ovulation (Rose et al., 1997). To test whether *tn1305*, *tn1311*, and *tn1281* are alleles of *ceh-18(mg57)*, we performed complementation tests. *ceh-18(mg57)* is haploinsufficient for the Sgd phenotype (data not shown), therefore we could not perform the complementation test for *gsa-1(RNAi)* sensitivity. Therefore, we tested these alleles for the germline defects. The four alleles *tn1305, tn1311, tn1281*, and *tn1296* are recessive for the Sgd phenotype as well as the other germline phenotypes. I found that *tn1305, tn1311,* and *tn1281* cannot complement the germline defects of *ceh-18(mg57)*, which suggests that these are likely alleles of the same gene. *tn1296* fails to complement *tn1281* for the Sgd phenotype suggesting that they are alleles of the same gene. DNA sequencing of *ceh-18* gene in *tn1305, tn1311, tn1281,* and *tn1296* is in progress.

A subset of *sgd* mutants is resistant to germline RNAi

All *sgd* mutants are completely sensitive to *unc-22(RNAi)* suggesting that they are responsive to somatic RNAi. However, mutations in eight genes (sgd-3, -4, -5, -7, -8, -10, -11, and -14) are resistant to RNAi in the germ line, but

sensitive in somatic cells (Table 7) as assessed by *pos-1(RNAi)*. *pos-1* encodes a zinc-finger protein required for cell fate specification in the embryos. Depletion of *pos-1* by RNAi results in 100% embryonic lethality. In these eight *sgd* mutant (Table 7) backgrounds, *pos-1(RNAi)* does not cause embryonic lethality indicating that they are resistant to germline RNAi. This finding was surprising because *gsa-1* is required in the somatic sheath spermathecal cell lineages to promote meiotic maturation (Fig. 25). Further, known germline RNAi resistant mutants such as *ppw-1*, *pgl-1*, *mes-3*, *mes-4*, and *mes-6* are not sensitive to *gsa-1(RNAi)*. One possibility is that the gonadal sheath cells are not fully sensitive to RNAi in the germline RNAi resistant mutants. To test this possibility, I constructed *sgd-8(tn1283); tnIs5[lim-7::GFP + rol-6(su1006)]* worms. *tnIs5* is an integrated array that expresses green fluorescent protein (GFP) in the gonadal sheath cells and a few head neurons (Rose et al.,1997) (Fig. 28). I subjected *sgd-8(tn1283); tnIs5* worms to control(RNAi) and *gfp(RNAi)*. As a control, I performed *gfp(RNAi)* on *tnIs5* worms. I found that the GFP expression was completely silenced in *tnIs5* and *sgd-1(tn1283); tnIs5* worms treated with *gfp(RNAi)* but not by control(RNAi) (Fig. 28M-R). I performed the same analysis in *sgd-1(tn1237)*, *inx-22(tn1339)*, *sgd-4, -11*, and *-14* mutants (Fig. 28 G-L and data not shown). In all cases, I was able to eliminate GFP expression completely in the sheath cells suggesting that the gonadal sheath cells respond to RNAi. Currently, I am performing similar analysis for all *sgd* mutants.

Figure 28. *sgd* mutants respond fully to RNAi

(A-R) Visualization of distal sheath cells using transgenic strains that express GFP in the gonadal sheath cells.
(A, D, G, J, M, and P) Nomarski micrographs showing germline nuclei in the distal gonad arm (dg).
(B, E, H, K, N, and Q) GFP fluorescence micrographs.
(C, F, I, L, O, and R) Merged DIC and fluorescence micrographs.
(A-C) control RNAi treated transgenic worms.
(D-F) *gfp(RNAi)* treated transgenic worms.
(G-H) control RNAi treated *sgd-1(tn1237)* transgenic worms.
(J-L) *gfp(RNAi)* treated *sgd-1(tn1237)* transgenic worms.
(M-O) control RNAi treated *sgd-8(tn1283)* transgenic worms.
In all control RNAi treated worms (A-C), (G-I), and (M-O), GFP expression shows the honeycomb like pattern of distal sheath cells. In contrast, *gfp(RNAi)* treated worms (D-F), (J-L), and (P-R), GFP expression is eliminated. In E-F, K-L, and Q-R, non-specific gut autofluorescence (i) is shown as a control for equivalent fluorescence exposure.

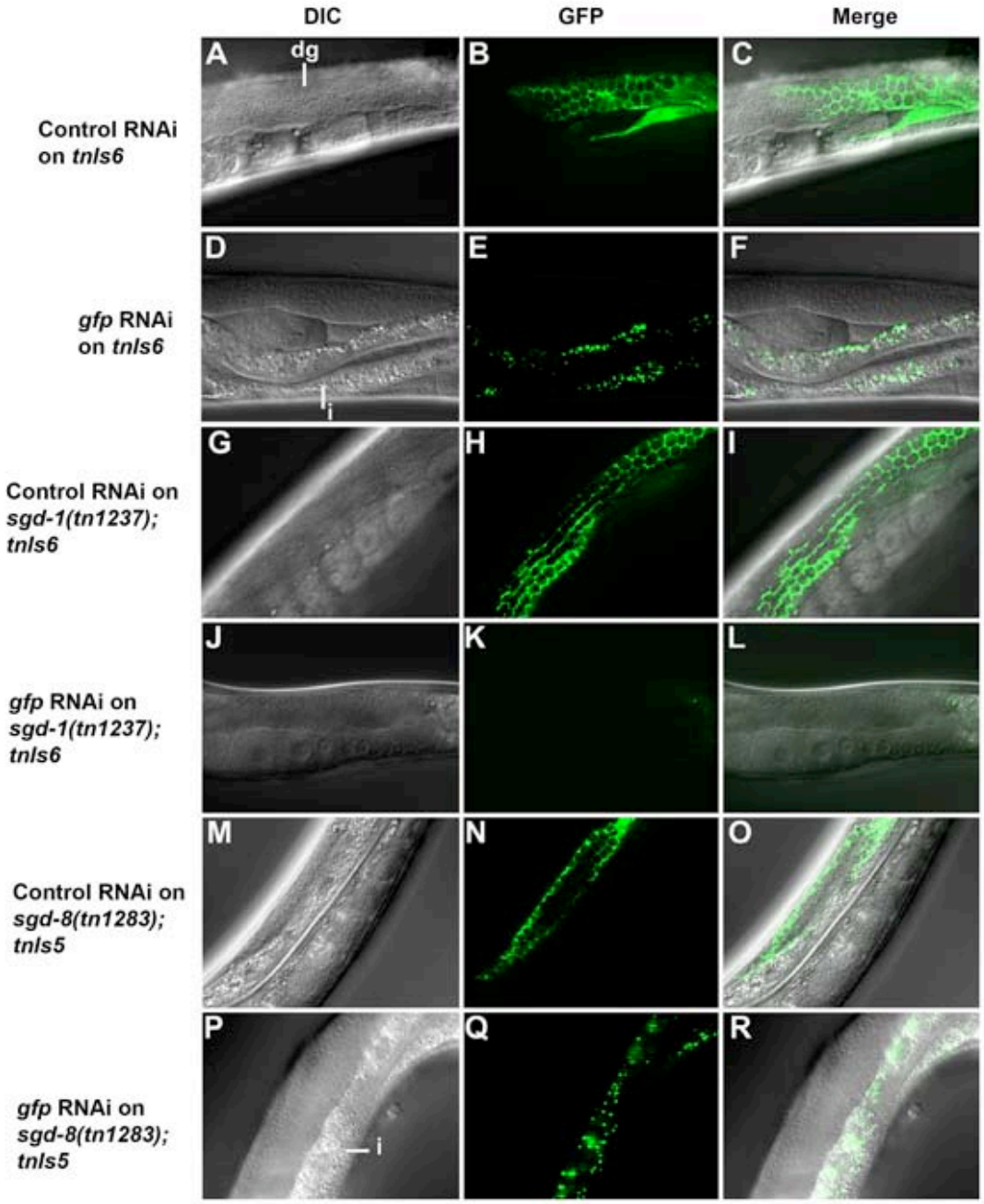
DIC
GFP
Merge
A
dg
B
C
Control RNAi on tnls6
D
i
E
F
gfp RNAi on tnls6
G
H
I
Control RNAi on sgd-1(tn1237); tnls6
J
K
L
gfp RNAi on sgd-1(tn1237); tnls6
M
N
O
Control RNAi on sgd-8(tn1283); tnls5
P
i
Q
R
gfp RNAi on sgd-8(tn1283); tnls5

Sgd mutations do not suppress *gsa-1(null)* larval lethality

To test whether *sgd* mutants can suppress *gsa-1(null)* larval lethal phenotype, I constructed *sgd;gsa-1(null)* double mutants that are rescued for *gsa-1* larval lethality with *tnEx31* array. *sgd* mutants that lost the array in the germline are larval lethal suggesting that they cannot suppress *gsa-1(null)* phenotype. This is perhaps not surprising because in a large scale screen for suppressors of *gsa-1(null)* larval lethality, no mutations were obtained (Kim, S. and Greenstein, D. unpublished results). In this *sgd;gsa-1(null) tnEx31* array containing mutants, I will conduct a mosaic analysis to address whether *sgd* mutants can suppress the sterility phenotype due to loss-of-*gsa-1* in the sheath-spermathecal cell lineages.

Some *sgd* mutants affect sheath structure and morphology

Previously, Rose et al (1997) showed that *ceh-18* is required for proper sheath cell differentiation and function. In *ceh-18 (null)* mutants, the filamentous actin network is disorganized as assessed by antibodies to proteins of the actomyosin apparatus (Rose et al., 1997). Since *ceh-18* is a suppressor of the *gsa-1(RNAi)* maturation defect, I considered the possibility that some of the *sgd* mutants may disrupt sheath structure. To determine whether *sgd* mutants affect sheath cell structure, I performed phalloidin staining for actin filaments. Staining of the sheath cells with phalloidin-TRITC reveals the filamentous network of sheath cells in wildtype hermaphrodites (Fig. 29A-C). *gsa-1(RNAi)*-treated hermaphrodites have no apparent defects in sheath cell morphology (Fig. 30B). By contrast, in *ceh-18(null)* mutants the filamentous actin network is

disorganized (Rose et al., 1997 and data not shown). INX-22 does not appear to play a role in sheath cell morphology because in *inx-22(null)* mutants, sheath cell actin network is apparently normal (Fig. 29C). Similarly, *sgd-3(tn1335)*, *sgd-4(tn1241)*, and *sgd-8(tn1283)* have apparently normal sheath cell morphology (data not shown). Currently, I am examining all *sgd* mutants using phalloidin staining to determine whether they disrupt sheath cell structure.

Some *sgd* mutants are required to inhibit chromatin localization of AIR-2 in the distal oocytes

In the presence of sperm, AIR-2/Aurora kinase localizes to chromosomes in the most proximal (–1) oocyte (Burrows et al., 2006; Detwiler et al., 2001; Schumacher et al., 1998). AIR-2 localization to chromatin is sperm-dependent because in the absence of sperm, AIR-2 is localized in the cytoplasm (Schumacher et al., 1998). In the presence of sperm, AIR-2 localization to the chromatin is restricted to the most proximal oocyte (Detwiler et al., 2001; Schumacher et al., 1998). In the distal (–2, –3 and so on) oocytes, AIR-2 is localized in the cytoplasm. In the most proximal oocyte, AIR-2 begins to accumulate in the chromatin before NEBD and reaches maximum levels when the chromosomes congress to the metaphase plate after NEBD (Lee et al., 2007). Thus, AIR-2::GFP can be used as a marker for a subset of sperm-dependent meiotic maturation events. To address whether *sgd* mutants prevent chromatin localization of AIR-2 in the distal oocytes, I examined a transgenic strain that expresses AIR-2 fused with GFP (Audhya et al., 2005). In this transgenic strain, GFP: AIR-2 was localized to the most proximal (–1) oocyte (Fig. 30A-C). GFP: AIR-2 localization to the chromatin of –1 oocyte is

Figure 29. Sheath cell morphology in *sgd* mutants

Phallodin-TRITC stained gonads from wildtype (A), *gsa-1(RNAi)*-treated (B) and *inx-22(tm1661)* hermaphrodites (C). sp indicates spermatheca. Proximal sheath cells are numbered. DAPI staining shows sheath nuclei.

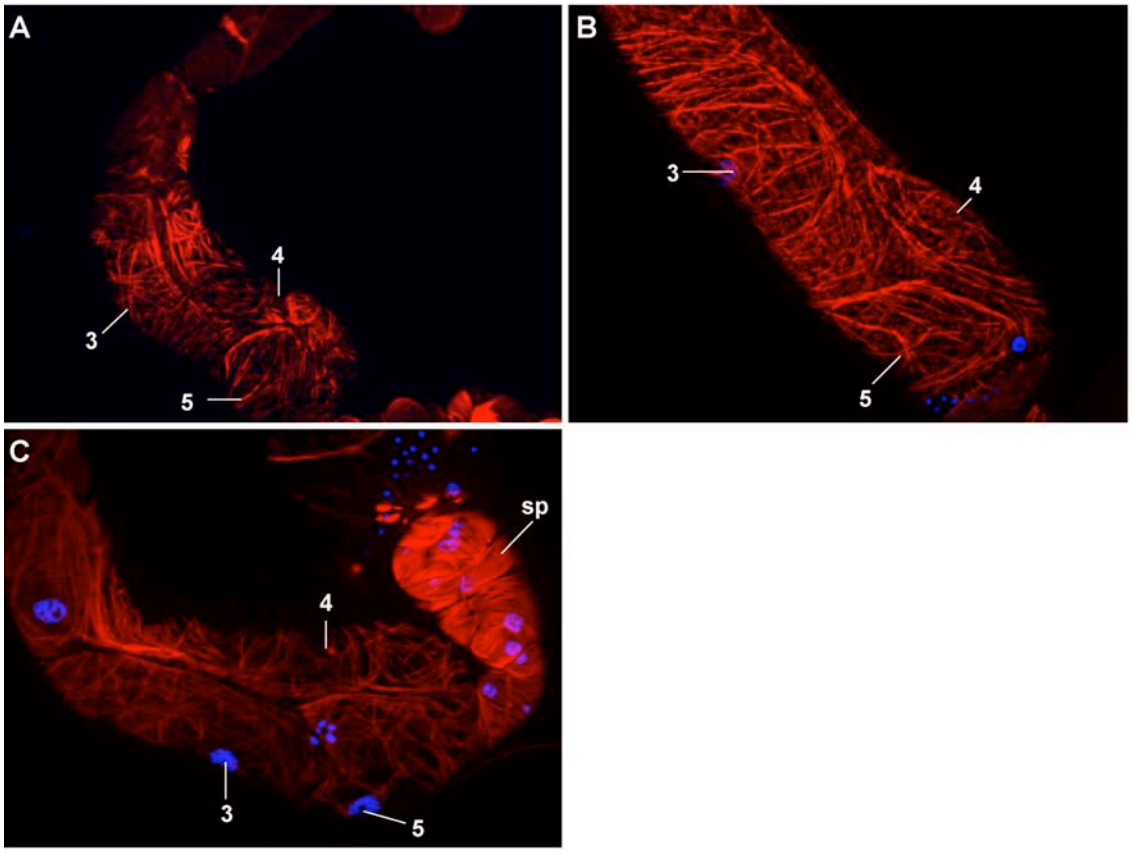
A
4
3
5
B
3
4
5
C
sp
4
3
5

Figure 30. Some *sgd* mutants inhibit chromatin localization of AIR-2 in the distal oocytes.

(A-C) Wildtype, GFP:AIR-2 is associated with the chromatin of -1 oocyte (B & C).
(D-F) *goa-1(RNAi)* treated wildtype hermaphrodites showing GFP: AIR-2 (E & F) in -1 and -2 oocytes.
(G-I) *inx-14(RNAi)* treated wildtype hermaphrodites showing GFP: AIR-2 (H & I) in -1, -2, and -3 oocytes.
(J-L) *inx-22(tm1661)* hermaphrodites showing GFP: AIR-2 (K & L) in -1 to -4 oocytes.
(M-O) *ceh-18(mg57)* hermaphrodites showing GFP: AIR-2 (N&O) in -1 to -3 oocytes.
(P-R) control RNAi on *vab-1(dx31)* hermaphrodites showing GFP: AIR-2 (Q&R) in -1 and -2 oocytes.
(S-U) *goa-1(RNAi)* on *vab-1(dx31)* hermaphrodites showing GFP: AIR-2 (T&U) in -1 to -5 oocytes.

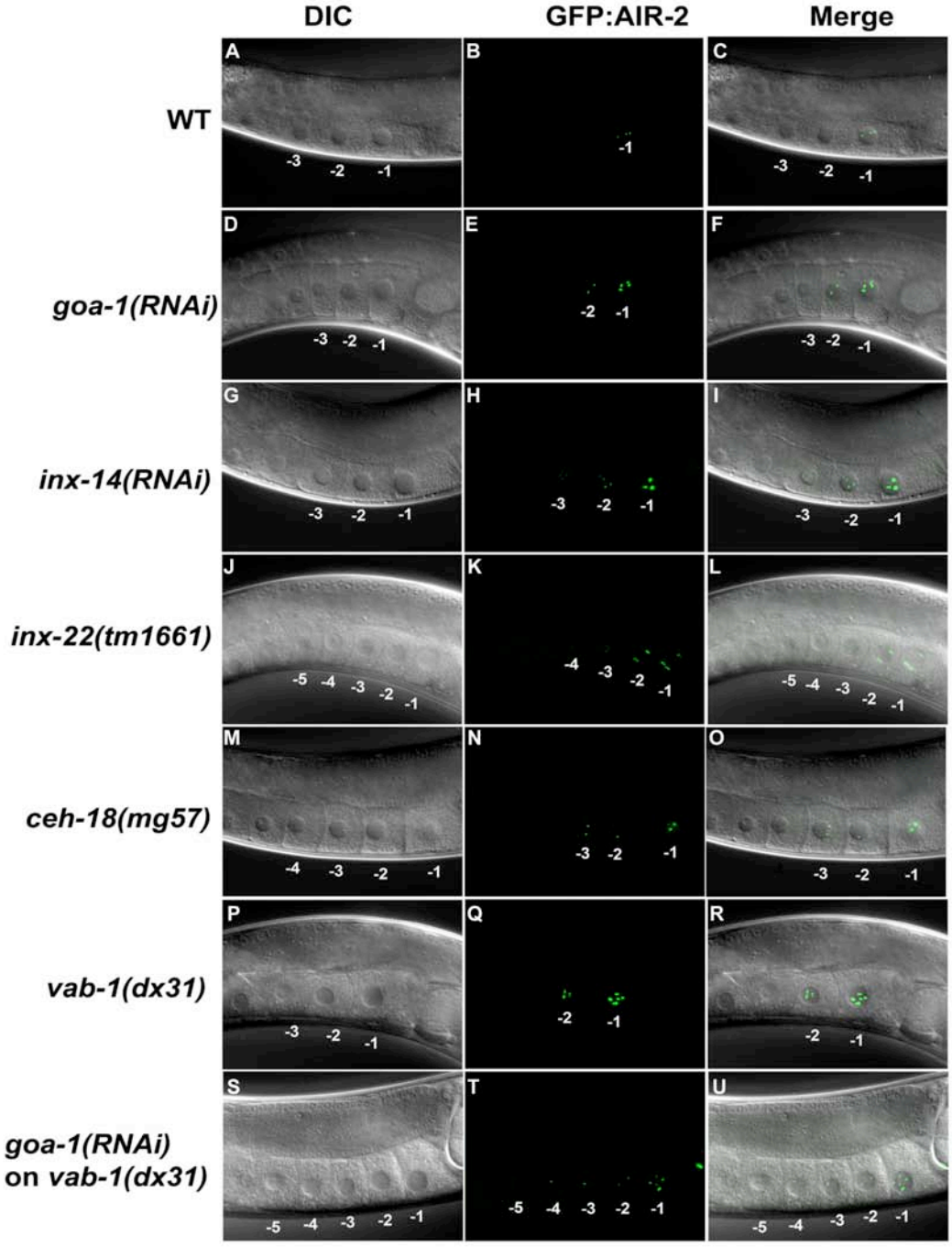
DIC
GFP:AIR-2
Merge
WT
goa-1(RNAi)
inx-14(RNAi)
inx-22(tm1661)
ceh-18(mg57)
vab-1(dx31)
goa-1(RNAi)
on vab-1(dx31)
A
B
C
D
E
F
G
H
I
J
K
L
M
N
O
P
Q
R
S
T
U

dependent on presence of sperm because in females, no GFP is detectable in the chromatin of –1 oocyte (data not shown). However, in *inx-22(tm1661)*, *ceh-18(mg57)* and *sgd-1(tn1237)* mutant backgrounds, GFP:AIR-2 chromatin localization was extended to distal (–2, –3, and so on) oocytes (Fig. 30G-O). By contrast, other negative regulators of meiotic maturation (Table 1) including *vab-1* and *goa-1* do not have ectopic GFP:AIR-2 in the chromatin of distal oocytes (Fig. 30D-F, P-R and data not shown). This suggests that some sgd mutants prevent precocious chromatin association of GFP:AIR-2 in the distal oocytes. Since AIR-2 localization to the chromatin of the –1 oocyte is a late event in meiotic maturation, it is possible that the distal oocytes in *sgd* mutants have initiated some aspects of meiotic maturation prematurely. *goa-1* is necessary to inhibit meiotic maturation in the absence of sperm (Table 1). Surprisingly, *goa-1(RNAi)* does not result in ectopic GFP:AIR-2 in the distal oocytes (Fig. 30P-R). However, *vab-1(dx31)* worms treated with *goa-1(RNAi)* show GFP:AIR-2 localized to the chromatin in the distal oocytes (Fig. 30S-U) suggesting that *vab-1* and *goa-1* function in parallel to prevent AIR-2 chromatin localization in the distal oocytes. I will examine whether *sgd* mutants exhibit chromatin localization of GFP:AIR-2 in the distal oocytes.

Discussion

In *C. elegans*, MSP signals oocyte meiotic maturation and MAP kinase activation (Miller et al., 2001; Miller et al., 2003). Two parallel genetic pathways defined by the VAB-1/Eph receptor and the CEH-18 sheath cell pathway

function together to inhibit oocyte meiotic maturation in the absence of sperm (Miller et al., 2003). In this Chapter, I showed that *gsa-1*, which encodes a $G\alpha_s$ subunit (Korswagen et al., 1997; Park et al., 1997), is necessary and sufficient to promote oocyte meiotic maturation in the presence of sperm (Fig. 31). Since a null mutation in *gsa-1* is larval lethal (Korswagen et al., 1997), I performed RNAi analysis on wild-type hermaphrodites to address the role of *gsa-1* in meiotic maturation. I found that *gsa-1* is necessary for oocyte meiotic maturation in the presence of sperm.

Further, *gsa-1* is also required for activation of MAPK in the oocytes. Using gain-of-function mutations, I showed that *gsa-1* is sufficient for oocyte meiotic maturation and MAPK activation.

Using RNAi analysis in the *rrf-1* background, I found that *gsa-1* is sufficient in the soma to promote oocyte meiotic maturation. My hypothesis is that *gsa-1* is required in the somatic sheath cells to promote meiotic maturation and MAPK activation. To address this hypothesis, I performed genetic mosaic analyses. I rescued the larval lethal phenotype of *gsa-1(null)* mutants using an extrachromosomal array that consisted of genomic *gsa-1(+)* and a cell autonomous marker sur-5::GFP. Using this transgenic strain, I examined for *gsa-1* losses in the somatic sheath cell lineages. I found several mosaics that had lost *gsa-1* in the sheath-spermathecal cell lineages were sterile suggesting that *gsa-1* is necessary in the somatic sheath cells for meiotic maturation. By contrast, germline mosaics are fertile suggesting that *gsa-1* is not necessary in the oocytes to promote maturation.

In the genome-wide RNAi screen (Table 1), I identified *goa-1* as a negative regulator of oocyte meiotic maturation and MAPK activation. Using RNAi and genetic analysis, I showed that *goa-1* is necessary and sufficient in the soma to inhibit oocyte meiotic maturation and MAPK activation in the absence of sperm. Since, *goa-1* inhibits meiotic maturation in the absence of sperm and *gsa-1* promotes meiotic maturation in the presence of sperm, I considered the hypothesis that *goa-1* inhibits *gsa-1*. To test this hypothesis, I performed *gsa-1(RNAi)* on *goa-1(null)* mutant hermaphrodites.

I found that *gsa-1(RNAi)* on *goa-1(null)* hermaphrodites result in maturation defect similar to *gsa-1(RNAi)* on wildtype hermaphrodites suggesting that *gsa-1* is epistatic to *goa-1*. To establish definitively that *gsa-1* is epistatic to *goa-1*, I performed mosaic analysis of *gsa-1* in a *goa-1(null)* background. Consistent with the RNAi analysis, I found that mosaic worms that lost *gsa-1* in the sheath-spermathecal cell lineages were sterile suggesting that $G\alpha_s$ is epistatic to $G\alpha_{o/i}$. However, I cannot rule out whether $G\alpha_s$ functions either downstream or in parallel to $G\alpha_{o/i}$ to promote oocyte meiotic maturation.

The precise mechanism(s) by which G-protein signaling in the soma regulates oocyte meiotic maturation is not known. My hypothesis is that $G\alpha_s$ promotes meiotic maturation by antagonizing inhibitory sheath/oocyte gap junctions Fig. 31). To test this hypothesis, I performed *gsa-1(RNAi)* on *ceh-18(null)* and *inx-22(tm1661)* hermaphrodites. *gsa-1(RNAi)* in wild-type hermaphrodites results in sterility due to inability of the oocytes to undergo maturation. By contrast, *gsa-1(RNAi)* in *ceh-18(null)* and *inx-22(tm1661)*

Figure 31. A model for control of meiotic maturation in *C. elegans* by somatic G protein signaling.

The somatic pathways involved in the control of meiotic maturation are depicted in two states, depending on whether the MSP signal is absent (left panel) or present (right panel). $G\alpha_{o/i}$ negatively regulates meiotic maturation and oocyte MAPK activation and antagonizes a $G\alpha_s$ pathway that promotes maturation. The $G\alpha_s$ pathway is drawn showing involvement of the regulatory subunit (KIN-2) of cyclic-AMP-dependent protein kinase A (PKA) and adenylate cyclase (ACY-4). *inx-8* and *inx-9* are possibly sheath cell- expressed innexins. Unidentified sheath cell GPCRs are proposed to receive the MSP signal in parallel to VAB-1 on the oocyte, such that GPCR's coupled to $G\alpha_{o/i}$ are antagonized by MSP, whereas $G\alpha_s$-coupled receptors are stimulated by MSP. The $G\alpha_s$ pathway is proposed to directly destabilize the inhibitory sheath/oocyte gap junctions (INX-14 and INX-22), but a parallel function is equally consistent with current genetic data. The CEH-18 POU-homoeprotein localizes to sheath cell nuclei where it functions to control sheath cell differentiation, in part, by directly or indirectly affecting the assembly of sheath/oocyte gap junctions. Figure adapted from Govindan et al., (2006).

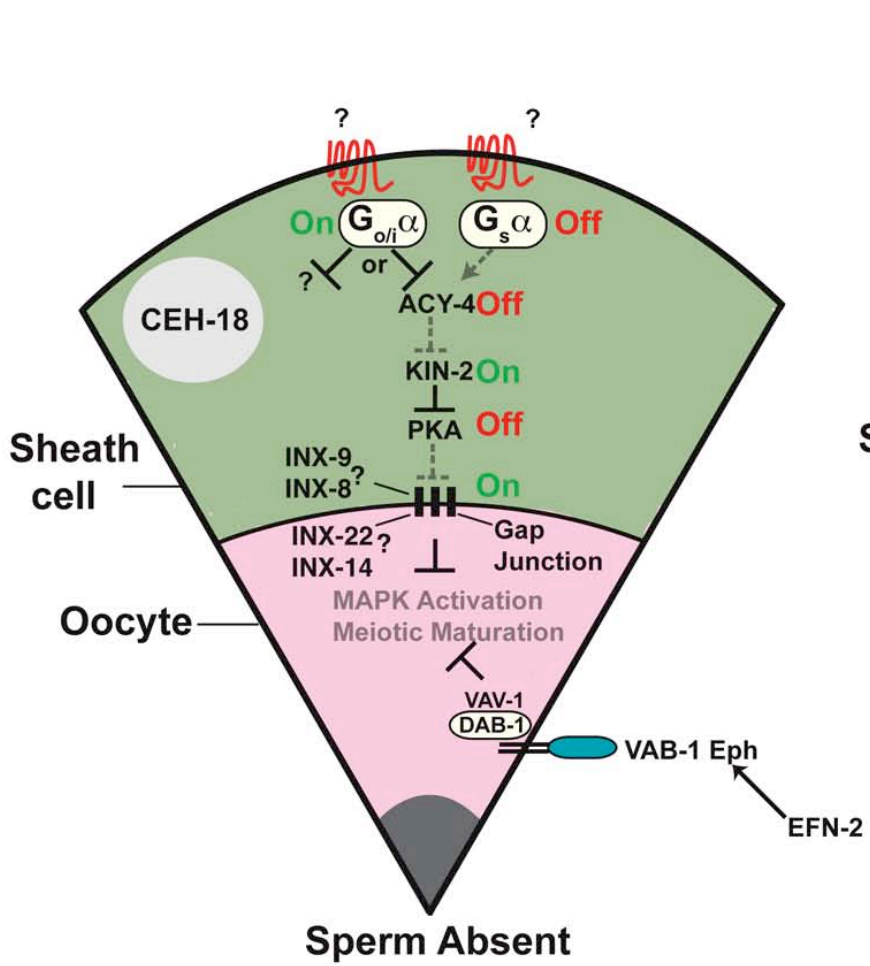
?
?
On
$G_{o/i}\alpha$
$G_s\alpha$
Off
?
or
CEH-18
ACY-4 Off
KIN-2 On
PKA Off
Sheath cell
INX-9
INX-8?
On
INX-22?
INX-14
Gap Junction
MAPK Activation
Meiotic Maturation
Oocyte
VAV-1
DAB-1
VAB-1 Eph
EFN-2
Sperm Absent

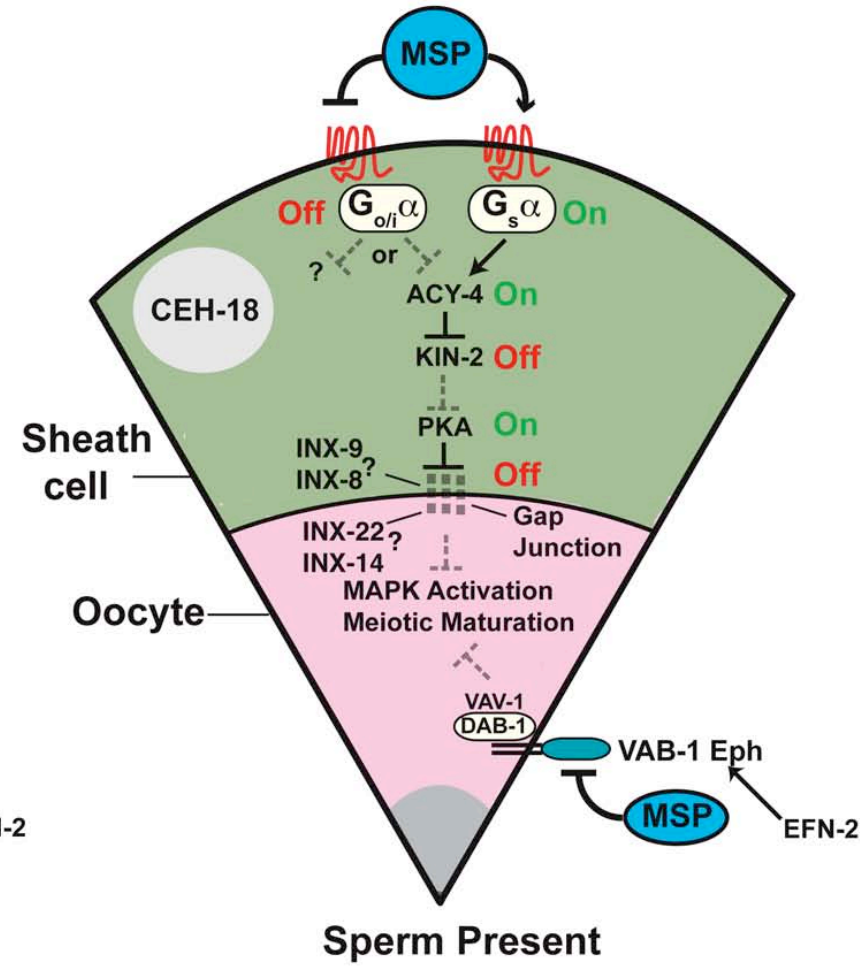
MSP
Off
$G_{o/i}\alpha$
$G_s\alpha$
On
?
or
CEH-18
ACY-4 On
KIN-2 Off
PKA On
Sheath cell
INX-9
INX-8?
Off
INX-22?
INX-14
Gap Junction
MAPK Activation
Meiotic Maturation
Oocyte
VAV-1
DAB-1
VAB-1 Eph
MSP
EFN-2
Sperm Present

hermaphrodite genetic backgrounds has no effect suggesting that the $G\alpha_s$ signaling disrupts sheath cell-oocyte gap junctional communication. However, further ultrastructural studies are needed to test this model.

To address how $G\alpha_s$ signaling in the soma regulates meiotic maturation, I conducted a forward genetic screen to identify novel loci involved in *C. elegans* oocyte meiotic maturation. The robust maturation defect produced by *gsa-1(RNAi)* on wildtype hermaphrodites can be scored easily under the dissecting scope.In *gsa-1(RNAi)* treated worms, oocytes do not undergo maturation resulting in sterility. By contrast, *inx-22* and *ceh-18* null mutants treated with *gsa-1(RNAi)* are fertile. Therefore, I reasoned that it is possible to identify mutations that can suppress the *gsa-1(RNAi)* maturation defect, a phenotype that I named as Sgd for suppressors of *gsa-1(RNAi)* maturation defect. I screened for and identified 17 new *sgd* genes that strongly suppress the meiotic maturation defect of *gsa-1(RNAi)* treated wildtype hermaphrodites. My choice of the Sgd phenotype as the basis for the screen is validated by the fact that I identified putative alleles in *ceh-18* and *inx-22*, which are previously known *sgd* genes. I propose that some or all of these genes are involved in oocyte meiotic maturation mediated by G-protein signaling. The *sgd* genes could be the downstream effectors of $G\alpha_s$ signaling or potentially unidentified genes in a redundant pathway.

The suppressor screen is not saturated because I identified only single alleles for several of the *sgd* genes. In addition, I did not identify any *kin-2* alleles in this screen. In the future, one could conduct a similar screen for more

sgd mutations to saturate the genome. None of the sgd mutants can suppress the larval lethality of *gsa-1(null)* mutant. This is perhaps not surprising because in a large scale screen for suppressors of *gsa-1(null)* larval lethality, no mutations were obtained (Kim, S. and Greenstein, D. unpublished results). This suggests that the larval lethality of $G\alpha_s$ could be a result of multiple targets of $G\alpha_s$. Therefore, a single-gene mutation may not be sufficient to suppress the *gsa-1(null)* larval lethality.

The genetic suppressor screen was specifically designed to identify homozygous viable and fertile Sgd mutants. As a result, I may have missed a category of *sgd* mutants that function in essential processes such as germline development and embryonic viability. However, some of the alleles I identified may be viable hypomorphic alleles of essential genes. All *sgd* mutations that I uncovered in the screen were recessive in nature suggesting that they may be reduction or loss-of-function alleles. Further experiments are needed to determine the nature of these mutations.

How might *sgd* mutants suppress the *gsa-1* maturation defect? I propose that some of the *sgd* mutants could affect assembly or localization of gap junctions. In a candidate gene screen, I identified mutations in *lin-2*, *lin-7*, and *lin-10* can suppress *gsa-1(RNAi)* phenotype. LIN-2/LIN-7/LIN-10 are PDZ domain-containing proteins that form a macromolecular complex required for polarized localization of some receptors including LET-23/EGFR and GLR-1/glutamate receptor (Simske et al., 1996; Hoskins et al., 1996; Rongo et al., 1998). It is possible that some of the sgd genes could be involved in assembly,

trafficking or localization of gap junction components. Two PDZ domain-containing proteins ZO-1 and discs large, were shown to interact with connexins and regulate gap-junction assembly (Laing et al., 2005; Duffy et al., 2007). Molecular identification of *sgd* mutations will provide insights on their role in meiotic maturation.

Another mechanism by which some *sgd* mutants suppress the *gsa-1* maturation defect is by regulation of GPCRs involved in meiotic maturation. In the canonical G-protein signaling pathways, ligand binding to the cognate GPCRs causes activation of G-protein coupled Receptor Kinase (GRKs) (DeWire et al., 2007). GRKs phosphorylate GPCR resulting in binding of β-arrestin to the GPCRs. β-arrestin binding results in endocytosis of GPCRs. After endocytosis, GPCRs are either recycled back to the plasma membrane or undergo degradation in the lysosomes (Moore et al., 2007; Premont and Gainetdinov, 2007). Thus, blocking endocytosis of GPCRs causes constitutive activation of receptors (Ferguson, 2001; Pitcher et al., 1998). Consistent with this idea, I found that *grk-2(null)* and *arr-1(null)* mutant can suppress the *gsa-1(RNAi)* maturation defect. *grk-2* and *arr-1* encode a G-protein coupled Receptor Kinase and β-arrestin respectively (Fukuto et al., 2004). To clarify this hypothesis, I examined mutations that affect endocytosis. I found that *unc-101(null)* mutants can suppress the *gsa-1(RNAi)* maturation defect. *unc-101* encodes the medium chain of a clathrin-associated protein involved in endocytosis (Lee et al., 1994). Thus, it is possible that in *grk-2(null)*, *arr-1(null)* and *unc-101(null)* mutants, the unknown $G\alpha_s$-linked GPCRs may be

constitutively active. Since *gsa-1(RNAi)* may not completely eliminate GSA-1 protein, a constitutively activated receptor may be sufficient to suppress *gsa-1(RNAi)* meiotic maturation defect.

dab-1 encodes an adapter protein involved in several intracellular signaling pathways (Holmes et al., 2007). I found that *dab-1(null)* and *dab-1(tn1345)* alleles can suppress the *gsa-1(RNAi)* meiotic maturation defect. This is surprising because previously I found that *dab-1* functions in the germline *vab-1* pathway to regulate oocyte meiotic maturation. *dab-1* is epistatic to *gsa-1*, suggesting that DAB-1 functions either downstream or in parallel to $G\alpha_s$ signaling to inhibit meiotic maturation. Since *dab-1* encodes an adapter protein, it is possible that it may function similar to *unc-101* (described above). It is possible that *dab-1* has roles both in the somatic gonad as well as in the germline. Within the germline DAB-1, may function downstream of the VAB-1 pathway to inhibit meiotic maturation whereas in the sheath cells, DAB-1 may be required for endocytosis of GPCRs. In the future, mosaic analysis would be required to determine whether DAB-1 is required in the soma or germ line to suppress *gsa-1(RNAi)* meiotic maturation defect.

A subset of *sgd* mutations is resistant to RNAi in the germline but fully sensitive to RNAi in the soma. Possibly, these mutations confer a subtle somatic RNAi defect, despite responding fully to *unc-22(RNAi)*. However, *sgd* mutant sheath cells respond to RNAi because they can silence an exogenously expressed GFP. One possibility is that endogenous germline RNAi pathways might regulate meiotic maturation. A recent study showed that dicer-depleted

mouse oocytes fail to undergo maturation and exhibit chromosome congression defects (Murchison et al., 2007). Dicer is required for RNAi as well as to generate siRNAs and microRNAs. To test whether dicer plays a role in meiotic maturation, we constructed *dcr-1(null)* females. We found that *dcr-1(null)* females have reduced germline proliferation and they do not make oocytes. Thus, we cannot address whether *dcr-1* is involved in meiotic maturation. It is possible that in *C. elegans*, endogenous microRNA pathways may inhibit oocyte maturation in the absence of sperm. Since RNAi pathways are involved in regulating post transcriptional gene silencing, it is possible that they control the translation of proteins required for maturation. In the absence of sperm, microRNAs could inhibit the translation of proteins required for oocyte maturation. Sperm signaling may trigger meiotic maturation by counteracting the microRNA pathways.

Future directions

My studies examine how $G\alpha_s$ signaling in the sheath cells promotes meiotic maturation. To address this, I conducted a genetic screen to identify mutations that suppress *gsa-1(RNAi)* maturation defect. I hope that genotypic and phenotypic analysis of these mutants will provide significant insights on the control of meiotic maturation in *C. elegans*. One of the most interesting questions to be addressed is whether the *sgd* mutants are negative regulators of meiotic maturation and MAPK activation. *ceh-18*, *kin-2* and *inx-22* were previously identified as negative regulators of meiotic maturation. I found that

ceh-18, *kin-2* and *inx-22* can suppress the *gsa-1(RNAi)* maturation defect, which is consistent with the idea that they are downstream negative regulators of meiotic maturation. Therefore, I expect that all *sgd* mutants should be negative regulators of meiotic maturation. To address this possibility, I constructed *sgd-1(tn1237);fog-2(q71)* female double mutants and found that they have a maturation rate of 0.42 ± 14 (n=22) maturation per gonad arm per hour compared to that in *fog-2(q71)* of 0.16 ± 0.10(n=17), suggesting that *sgd-1* is a negative regulator of meiotic maturation. Similar analysis in the *fog-2(q71)* female background has to be done for all sgd mutants to address whether they are negative regulators of meiotic maturation and MAPK activation. In *inx-22* and *sgd-1* hermaphrodites, GFP: AIR-2 localizes ectopically to chromatin in the distal oocytes (Fig. 30). A similar analysis should be done in all *sgd* mutants to address whether they are negative regulators of maturation. Another important question to be addressed is whether the germline RNAi resistant *sgd* mutants are bona fide regulators. Some *sgd* mutations are resistant to RNAi in the germline but fully sensitive to RNAi in the soma. To definitively establish that these mutations are bonafide regulators of meiotic maturation, I am testing whether *sgd* mutations can suppress the sterility phenotype due to loss of *gsa-1* in the sheath-spermathecal cell lineage. To address this, I constructed *sgd; gsa-1(null)* double mutants that carry *tnEx31* (*gsa-1(+)* + *sur-5::gfp*) array. In these mutant backgrounds, I will examine whether mosaic worms that lost *gsa-1* in the sheath-spermathecal cell lineages are fertile or sterile. Preliminary observations show that *inx-22(tm1661)* can suppress the sterility defect due to

loss of *gsa-1* in the sheath-spermathecal cell lineages. By contrast, *sgd-16(tn1344)* and *sgd-4(tn1343)* cannot suppress the sterility defect. Recently, I found that deletion in *acy-4* results in a sterility phenotype similar to loss of *gsa-1* in sheath-spermathecal cell lineages. As an additional test, I will examine whether *sgd* mutants can suppress the sterility phenotype of *acy-4(ok1806)* or *acy-4(tm2510)* mutants. If the germline RNAi resistant *sgd* mutant can suppress the *acy-4(ok1806)* sterility phenotype, then it will show that they are genuine regulators of maturation. Postional cloning of selected loci will be given priority based on the above mentioned properties.

CHAPTER IV

Somatic G-protein signaling regulates oocyte microtubule reorganization prior to fertilization

Introduction

Meiosis generates haploid gametes, which combine through fertilization to generate a diploid zygote (reviewed by Page and Hawley, 2004). The viability of the resulting embryo, and the whole species for that matter, depends critically on the faithful segregation of the genetic material during meiosis. Nondisjunction during either of the meiotic divisions gives rise to aneuploid embryos, containing too many or too few chromosomes, typically with dire consequences owing to the deleterious effects of abnormal gene dosage. In humans, nondisjunction during female meiosis I represents the leading cause of miscarriage and congenital birth defects, such as Down's syndrome (Hassold and Hunt, 2001). Previous studies in humans and mice suggest that disturbances in the hormonal regulation of folliculogenesis are associated with chromosome congression failure during meiotic spindle assembly, and may represent a significant risk factor for nondisjunction errors (Hodges et al., 2002). At present, it is not understood how signals that regulate oocyte growth and meiotic progression might influence meiotic spindle assembly and chromosome segregation.

The meiotic spindles of most animal oocytes are distinguished from mitotic spindles of somatic cells in terms of their mechanism of assembly, their function, and their modes of regulation. The female meiotic spindles of many species are both acentriolar and anastral (Albertson and Thomson, 1993; Matthies et al., 1996; Schatten, 1994; Szollosi et al., 1972). Instead of relying on centrosomes, which are eliminated during oogenesis in many species, the meiotic chromatin directs assembly of a bipolar spindle both by nucleating microtubules and organizing preexisting microtubules, which then self-organize through incompletely understood mechanisms involving microtubule motors and dynamics (Heald et al., 1996; Matthies et al., 1996; Skold et al., 2005; Walczak et al., 1998). Biochemical studies in *Xenopus* egg extracts, which provide a model for assembly of the meiosis II spindle, indicate that DNA-coated beads can drive the self-organization of microtubules into bipolar spindles (Heald et al., 1996). Cultured mammalian cells might utilize analogous mechanisms in parallel with centrosome-dependent mechanisms as bipolar spindles can assemble after laser ablation of centrosomes (Khodjakov et al., 2000). Chromatin-based microtubule assembly pathways employ Ran-GTP-dependent mechanisms (Carazo-Salas et al., 1999; Kalab et al., 1999; Ohba et al., 1999; Wilde and Zheng, 1999), as well as mechanisms utilizing the Aurora B kinase chromosomal passenger complex (Sampath et al., 2004).

Assembly of a bipolar meiotic spindle requires that the cytoplasmic microtubules gain access to the nuclear environment, which occurs upon nuclear envelope breakdown (NEBD) during the meiotic maturation process.

While there have been many biochemical and cell biological investigations of meiotic spindle assembly, few studies have examined microtubule behavior during the earliest stages before cytoplasmic microtubules become associated with chromatin upon NEBD. Studies in sea urchin oocytes have revealed that cortical microtubules undergo a dramatic structural reorganization from an extensive basket-like array to a diminishing population of shorter microtubules during meiotic maturation (Boyle and Ernst, 1989). The signaling mechanisms that bring about these major cytoplasmic changes and their potential biological significance are, however, unclear.

C. elegans is an ideal system for studying the effects of hormonal signaling on oocyte microtubules during the meiotic maturation process. These animals are transparent so that meiotic maturation can be directly observed (McCarter et al., 1999; Ward and Carrel, 1979), and recent studies have begun to elucidate the key intercellular signaling pathways that regulate this process (reviewed by Yamamoto et al., 2006). In *C. elegans*, sperm trigger oocyte meiotic maturation using the major sperm protein (MSP) as a signaling molecule (Kosinski et al., 2005; Miller et al., 2001; Miller et al., 2003). MSP is also the key cytoskeletal element required for the actin-independent amoeboid locomotion of nematode spermatozoa (Bottino et al., 2002; Italiano et al., 1996). Since hermaphrodites produce only a fixed number of sperm, meiotic maturation rates are initially high, but decline as sperm are consumed by fertilization and levels of the MSP signal decline (Kosinski et al., 2005; McCarter et al., 1999). In sex-determination mutants of *C. elegans* that feminize the

gonad (e.g., *fog-2* or *fog-3*) such that no sperm are produced, oocytes arrest at the diakinesis stage until sperm are supplied by mating (McCarter et al., 1999).

In *C. elegans*, meiotic maturation and ovulation are coupled to sperm availability through a complex regulatory network involving germline and somatic controls (Corrigan et al., 2005; Govindan et al., 2006). Parallel genetic pathways defined by *vab-1*, which encodes an MSP-binding ephrin receptor, and *ceh-18*, which encodes a POU-homeoprotein expressed in gonadal sheath cells but not oocytes, together compose an MSP-sensing control mechanism that regulates meiotic maturation (Govindan et al., 2006; Miller et al., 2003). Somatic control of meiotic maturation, likely through the *ceh-18* pathway, involves antagonistic $G\alpha_{o/i}$ and $G\alpha_s$ signaling pathways that define negatively- and positively-acting inputs, respectively (Govindan et al., 2006). $G\alpha_s$ signaling is necessary and sufficient to trigger oocyte mitogen-activated protein kinase (MAPK) activation and meiotic maturation, in part, through antagonizing inhibitory sheath/oocyte gap-junctional communication. While these studies provided initial insights into the complex signaling pathways regulating meiotic maturation in response to MSP in *C. elegans*, they raise new questions about how the *vab-1* and *ceh-18* pathways control nuclear and cytoplasmic events during maturation, as well as the division of labor among the pathways. During this thesis work, I collaborated with another graduate student in the lab, Jana Harris, to investigate the changes in the oocyte microtubule cytoskeleton during early steps of the meiotic maturation process. Jana showed that MSP signaling reorganizes the microtubule cytoskeleton of oocytes prior to NEBD.

Furthermore, she found that the VAB-1 Eph/MSP receptor pathway has no apparent role in regulating the distribution of oocyte microtubules. By contrast, *ceh-18* influences the microtubule cytoskeleton of the oocyte. During the same period, I was conducting a genome-wide RNAi screen for negative regulators of meiotic maturation. I provided the newly described key signaling genes and mutant alleles that were likely to regulate oocyte microtubule reorganization based on my observations of meiotic maturation signaling and oocyte shape. Dr. Harris collaboratively utilized this new information to conduct antibody staining experiments. This work was published in *Developmental Biology* in which I shared the distinction of being co-first authors. Our collaborative studies showed that somatic G-protein signaling pathways play antagonistic roles in oocyte microtubule reorganization depending on the availability of sperm. We propose a model in which MSP signaling alters microtubule localization and plus-end dynamics to facilitate the search and capture of microtubules by chromatin during meiotic spindle assembly.

Materials and methods

Nematode Strains, Nomenclature, and Phenotypic Analysis

Standard techniques were used for nematode culture at 20°C, except where indicated otherwise. The *C. elegans var. Bristol* strain, N2, was used as the wild-type hermaphrodite strain. *fog-2(q71)* and *fog-3(q443)* mutations, which feminize the germ line, were used to generate *XX* animals that do not produce sperm (females). In all tested cases, mutations in *fog-2* and *fog-3* gave identical

results and thus could be used interchangeably, however, for technical reasons most experiments were performed using *fog-2(q71)*, unless genetic markers on LGI were utilized. Key strains and alleles used are described in WormBase (http://www.wormbase.org), in (Govindan et al., 2006) or as follows:

LGI: *gsa-1(ce81)*, *gsa-1(ce94)*, *goa-1(sa734)*, *rrf-1(pk1417)*, *fog-3(q443)*

LGII: *vab-1(dx31), ptc-1(ok122)*

LGIII: *mpk-1(ga111*ts*), cgh-1(ok492)*

LGIV: *unc-24(e138)*, *oma-1(zu40te33)*, *fem-3(e1990)*

LGV: *oma-2(te51)*, *emo-1(oz1)*, *fog-2(q71)*

LGX: *ceh-18(mg57), kin-2(ce179)*

Rearrangements used were *hT2(qIs48)(I, III)*, *mIn1II*, *DnT1(IV, V)*. Transgenes used were: TH66 *pie-1::ebp-2::gfp* (Srayko et al., 2005*)*; and AZ244 *pie-1::gfp::tubulin* (Praitis et al., 2001).

RNA interference employed a modification of the method of (Kamath and Ahringer, 2003), which was performed as described (Govindan et al., 2006). MSP injections (200 nM MSP-142) and analysis of oocyte MAPK activation were described in Miller et al. (2001). To reduce the extent of MAPK activation, *fog-2(q71)* females were microinjected with the MEK1/2 inhibitor, U0126 (100 μM in egg salts; Sigma). cAMP-soaking experiments utilized an 8 mg/ml dibutyryl cyclic AMP (Sigma) in M9 buffer.

Fluorescence Microscopy

Preparation of dissected gonads and antibody staining

Gonads were dissected, fixed, and stained for immunofluorescence microscopy as described (Rose et al., 1997).

GFP fluorescence was analyzed in whole-mount using 0.1% tricaine/0.01% tetramisole treatment for 30 minutes as an anesthetic or in unfixed dissected gonads, which were mounted on agar pads using double-sided tape as a spacer to prevent the cover glass from smashing the gonads. Antibodies used were: YL1/2 rat monoclonal anti-α-tubulin (Kilmartin et al., 1982) (Accurate Chemical and Scientific Corporation); mouse monoclonal anti-actin (MP Biomedicals); anti-MAPK-YT (Sigma); and Cy2- or Cy3-conjugated secondary antibodies (Jackson ImmunoResearch Laboratories).

Laser-scanning confocal microscopy

Confocal images were acquired on a Zeiss LSM510 microscope with a pinhole of 1.0 Airy Units and 63X (NA 1.4) objective lens. Gain and offset were set so that all data were within the dynamic range of the PMT. Band pass filters were used to optically isolate the Cy2 and Cy3 fluorophores, and no cross-talk was observed.

Quantitation of cortical microtubule enrichment

To calculate the cortical microtubule enrichment factor (CMEF), z-stack images of dissected gonads labeled with anti-tubulin and anti-actin antibodies were obtained on the confocal microscope and analyzed using MetaMorph software (Universal Imaging). Cross-sectional images through medial focal

planes were analyzed to avoid the overlying gonadal sheath cells. For each oocyte analyzed, ten line scans, each 10 pixels thick, were drawn from either the proximal to distal cortex or from the dorsal to ventral cortex, avoiding the nucleus. For each pixel, the corresponding intensities for tubulin and actin were then exported into an Excel spreadsheet (Microsoft). The cortex was defined operationally, using an observer blind method, as the region of the micrograph in which the actin intensity was greater than one standard deviation above its mean. Use of line scans, instead of regions of interest, reduced the potential for sampling bias, however, the use of a mathematical definition of the cortex tended to reduce the magnitude of the increase in cortical enrichment in females. The CMEF was defined as the ratio of the average microtubule intensity at the cortex to the average microtubule intensity in the cytoplasm. Use of a ratio enabled comparisons between separate experiments that may have had varying overall staining levels. Because we measured pixel intensities, we could exclude the possibility that the results were due to over-sampling cortical regions of adjacent oocytes relative to the cytoplasm. In time-course analyses, CMEF values among oocytes –1 to –5 within each day examined, and among days examined within each oocyte, were tested using Fisher's protected least significant difference (*lsd*) method at p=0.01.

Results

MSP signals oocyte microtubule reorganization

Sperm dependence of microtubule reorganization

During female meiosis, dynamic microtubules assemble around chromatin instead of relying upon centrosomal microtubule-organizing centers (Varmark, 2004). Meiotic spindle assembly commences when the cytoplasmic microtubules gain access to the chromatin upon nuclear envelope breakdown (NEBD) during the oocyte meiotic maturation process. To investigate the origins of this specialized microtubule behavior during *C. elegans* oocyte meiotic maturation, we examined the organization of the dynamic microtubule cytoskeleton in oocytes prior to the onset of NEBD in the absence and presence of the MSP meiotic maturation signal. Since tyrosinated α-tubulin is associated with newly formed microtubule populations (Westermann and Weber, 2003), we used YL1/2 monoclonal antibodies to stain tyrosinated-α-tubulin in dissected and fixed gonads from unmated and mated *fog-2(q71)* females, and we analyzed the results using laser-scanning confocal microscopy (Fig. 32B,C). In unmated females, in which sperm are absent, microtubules are highly enriched at the proximal and distal cortical edges of oocytes, but are sparsely dispersed throughout the cytoplasm (Fig. 32B). By contrast, in mated females, in which sperm are present, microtubules in proximal oocytes (–1 to –4) are evenly dispersed throughout the oocyte cytoplasm in a dense net-like array (Fig. 32C). Strikingly, the cortical enrichment of microtubules observed in the absence of sperm (Fig. 32B) is not observed in presence of sperm (Fig.

32C). This result suggests that the presence of sperm in the reproductive tract influences the organization of the oocyte microtubule cytoskeleton. Moreover, these data indicate that the sperm-dependent change in microtubule organization occurs prior to both NEBD, which is spatially restricted to the most proximal (–1) oocyte, and to fertilization, which occurs as the oocyte enters the spermatheca during ovulation (Fig. 32A).

To determine whether the detection of tyrosinated α-tubulin in dissected and fixed gonads reflects the localization of bulk microtubules in living animals, we compared oocyte microtubules in unmated and mated *fog-2(q71)* females containing a β-tubulin-GFP fusion using confocal microscopy (Fig. 32D,E). Using this method, we observed a similar difference between the microtubule organization of unmated and mated females, with oocytes exhibiting an enrichment of microtubules at the proximal and distal cell cortex in the absence of sperm (Fig. 32D).

Measurement of cortical microtubule enrichment

To quantify this sperm-dependent difference in microtubule organization, we measured the average pixel intensity of cortical and cytoplasmic microtubules of the three most proximal oocytes in unmated (n=25) and mated (n=34) females, and calculated a cortical microtubule-enrichment factor (CMEF), expressed as the ratio of cortical to cytoplasmic intensities (Fig. 32F,G; see Materials and methods). In the absence of sperm, we observed a significant (p<0.0001) 1.5-fold enrichment of microtubules at the proximal and distal cortices (CMEF=1.51 ± 0.20).

Figure 32. Organization of microtubules in *C. elegans* oocytes

(A) Diagram of the hermaphrodite reproductive tract. Oocytes undergo meiotic maturation in an assembly-line fashion in response to the extracellular MSP signal (depicted in light blue), which exhibits a graded distribution from proximal to distal in mated females. MSP functions by antagonizing the VAB-1 and CEH-18 pathways to promote meiotic maturation. In all depictions and photomicrographs of the gonad, proximal is at the right, and distal is at the left. The –1 through –3 oocytes are indicated. (B-E) Single confocal images of the oocyte microtubule cytoskeleton in dissected and fixed gonads (B and C) or living animals (D and E) showing the localization of α-tubulin (B and C) or β-tubulin::GFP (D and E). (B and D) In unmated females, microtubules are cortically enriched between oocytes. (C and E) Microtubules are evenly dispersed throughout the cytoplasm in the most proximal oocytes in mated *fog-2(q71)* females. The perinuclear accumulation of microtubules observed in panel (D) and in subsequent figures is variable. (F) Single confocal image of a proximal oocyte in a dissected gonad stained for α-tubulin (red) and actin (green), illustrating the strategy for quantifying microtubule enrichment along the proximal-distal and dorsal-ventral axes with representative line scans drawn using Metamorph software. (G) Comparison of cortical microtubule enrichment factors from unmated and mated females at the proximal-distal and dorsal-ventral cortices of the -1 through -3 oocytes (in this and subsequent bar graphs the –1 oocyte is on the left). *t*-test between mated and unmated females, **p*<0.0001, †*p*<0.01, or ‡*p*<0.05, error bars represent s.d. Scale bars: 10 μm.

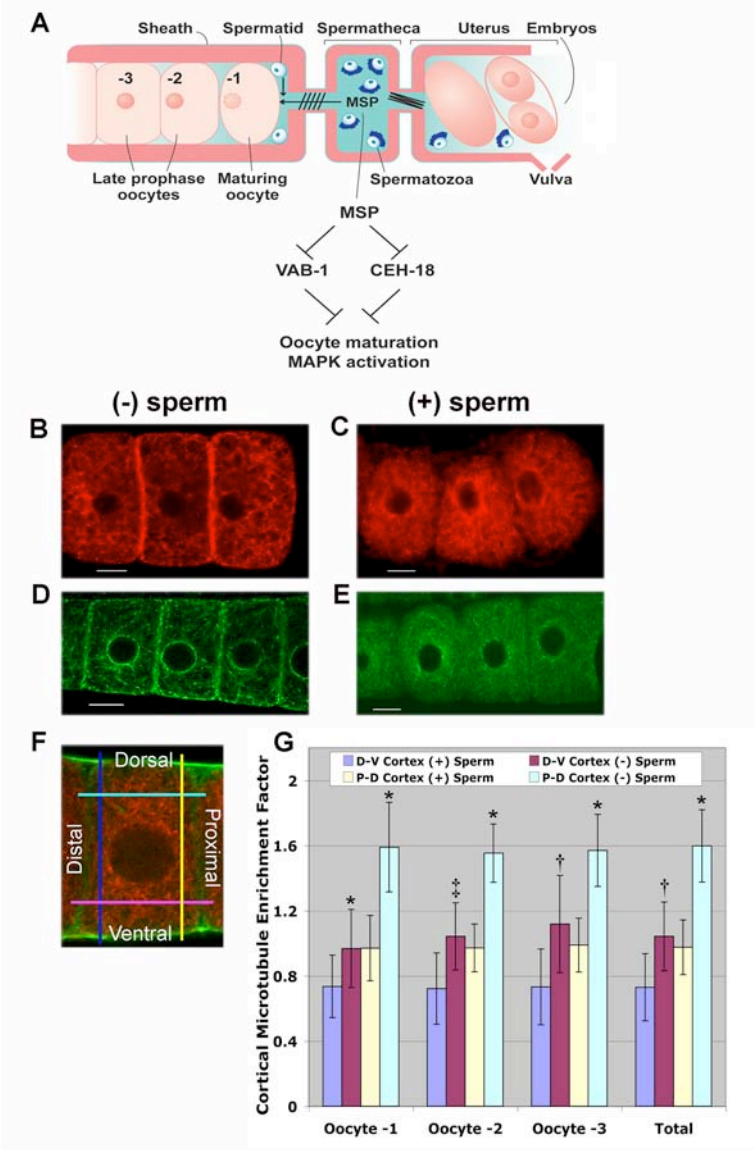
A
Sheath
Spermatid
Spermatheca
Uterus
Embryos
-3
-2
-1
MSP
Late prophase oocytes
Maturing oocyte
Spermatozoa
Vulva
MSP
VAB-1
CEH-18
Oocyte maturation
MAPK activation
(-) sperm
(+) sperm
B
C
D
E
F
Dorsal
Distal
Proximal
Ventral
G
D-V Cortex (+) Sperm
D-V Cortex (-) Sperm
P-D Cortex (+) Sperm
P-D Cortex (-) Sperm
Cortical Microtubule Enrichment Factor
0
0.4
0.8
1.2
1.6
2
Oocyte -1
Oocyte -2
Oocyte -3
Total

By contrast, microtubules were uniformly distributed throughout the cytoplasm of oocytes and were not enriched at the proximal and distal cortices of the cell in the presence of sperm (CMEF=1.02 ± 0.20) (Fig. 32G). In the absence of sperm, microtubule enrichment is limited to the proximal and distal cortical edges between oocytes as demonstrated by the lack of comparable microtubule enrichment at the dorsal and ventral cortical edges of oocytes in females (CMEF=1.04 ± 0.21, n=30) (Fig. 32G).In addition, microtubules were not highly enriched at the most proximal edge of the –1 oocyte, closest to the spermatheca, in females (CMEF=1.12 ± 0.32, n=10) compared to the distal edge adjacent to the –2 oocyte (CMEF=1.67 ± 0.29, n=10). These results define a sperm-dependent process, we term “oocyte microtubule reorganization,” referring to the global transition between cortically enriched microtubules, as observed in unmated female oocytes, and uniformly distributed microtubules, as observed in oocytes from mated females.

Spatial and temporal distribution of cortical microtubule enrichment in hermaphrodites

C. elegans hermaphrodites produce a fixed amount of sperm. Consequently, extracellular levels of MSP in the reproductive tract and meiotic maturation rates progressively decline when sperm become depleted as hermaphrodites age (Kosinski et al., 2005). To determine whether microtubule reorganization is influenced by the decline in sperm numbers that occur as hermaphrodites age, we performed a time-course analysis of microtubule organization in proximal oocytes (Fig. 33A-C). We found that CMEF values along the proximal-distal axis progressively increase over the first five days of

adulthood from 0.95 ± 0.08 at day 1 (n=76) to 1.40 ± 0.04 at day 5 (n=62) (Fig. 33B), approaching the CMEF levels seen in unmated females (Fig. 32G). To distinguish between aging and the presence of sperm as factors promoting microtubule reorganization in hermaphrodites, we mated 4-day-old hermaphrodites and analyzed their microtubules on day 5. These mated old hermaphrodites displayed reorganized microtubules characteristic of young hermaphrodites (CMEF=1.03 ± 0.23, n=73), suggesting that the presence of sperm, not age, is the key factor controlling microtubule organization in oocytes (Fig 33B). Since the CMEF measurements in this time-course analysis represent quantitative parameters describing oocyte microtubule organization, we applied the least significant difference (*lsd*) approach for performing pairwise comparisons to statistically analyze the CMEF values (see Materials and methods). This analysis indicates that microtubule reorganization is not an all-or-none phenomenon in that there is a temporally graded response with intermediate CMEF levels observed in oocytes from 2-3-day-old hermaphrodites (Fig. 33A, C). If MSP signaling were directly responsible for microtubule reorganization, we would expect to observe a spatially graded response of oocyte microtubules because sperm in the spermatheca generate an extracellular MSP gradient such that proximal oocytes are exposed to greater MSP levels than distal oocytes (Kosinski et al., 2005).

Figure 33. MSP is sufficient to reorganize oocyte microtubules.

(A) Single confocal images of hermaphrodite oocytes labeled with tubulin (red) and actin (green) during the time course. Day-4 hermaphrodites were mated with males and analyzed on day 5 (bottom panel). (B) Comparison of cortical microtubule enrichment over time (between 13-17 gonad arms were analyzed per time point). When MSP is present during the first few days of adulthood, the CMEF is low. As hermaphrodites age and MSP is depleted, the CMEF increases. The wedge depicting the MSP gradient is an estimate for illustrative purposes–see Kosinski et al. (2005) for measurements. The *lsd* method was used to compare the means of different oocytes at each time. Means with the same letter designation are not significantly different from one another within each individual day grouping (e.g., a=a, b=bc, and bc=c); whereas means with different letter designations are significantly different ($p<0.01$; eg., b ≠ c, but bc=c and bc=b). Distal oocytes exhibit higher CMEF values than proximal oocytes. (C) Comparison of cortical microtubule enrichment by oocyte. The *lsd* method was used to compare means at different time points for each individual oocyte. For each oocyte, CMEF values are lower earlier in adulthood when extracellular MSP levels are higher. (D) Effect of MSP on oocyte microtubule reorganization. Females were injected with either 200 μM purified MSP or a control buffer. Single confocal images of oocytes are labeled with tubulin (red) and actin (green). Microtubules appear cortically enriched in buffer-injected females and reorganized in MSP-injected females. (E) Quantification of oocyte microtubule reorganization in MSP-injected females, which were allowed to recover for 30 min, 1 hour, or 2 hours after injection (*t*-test between buffer injected females and each MSP injection condition, *$p<0.0001$, §$p<0.001$, †$p<0.01$, ‡$p<0.05$, error bars represent s.d.). Scale bars: 10 μm.

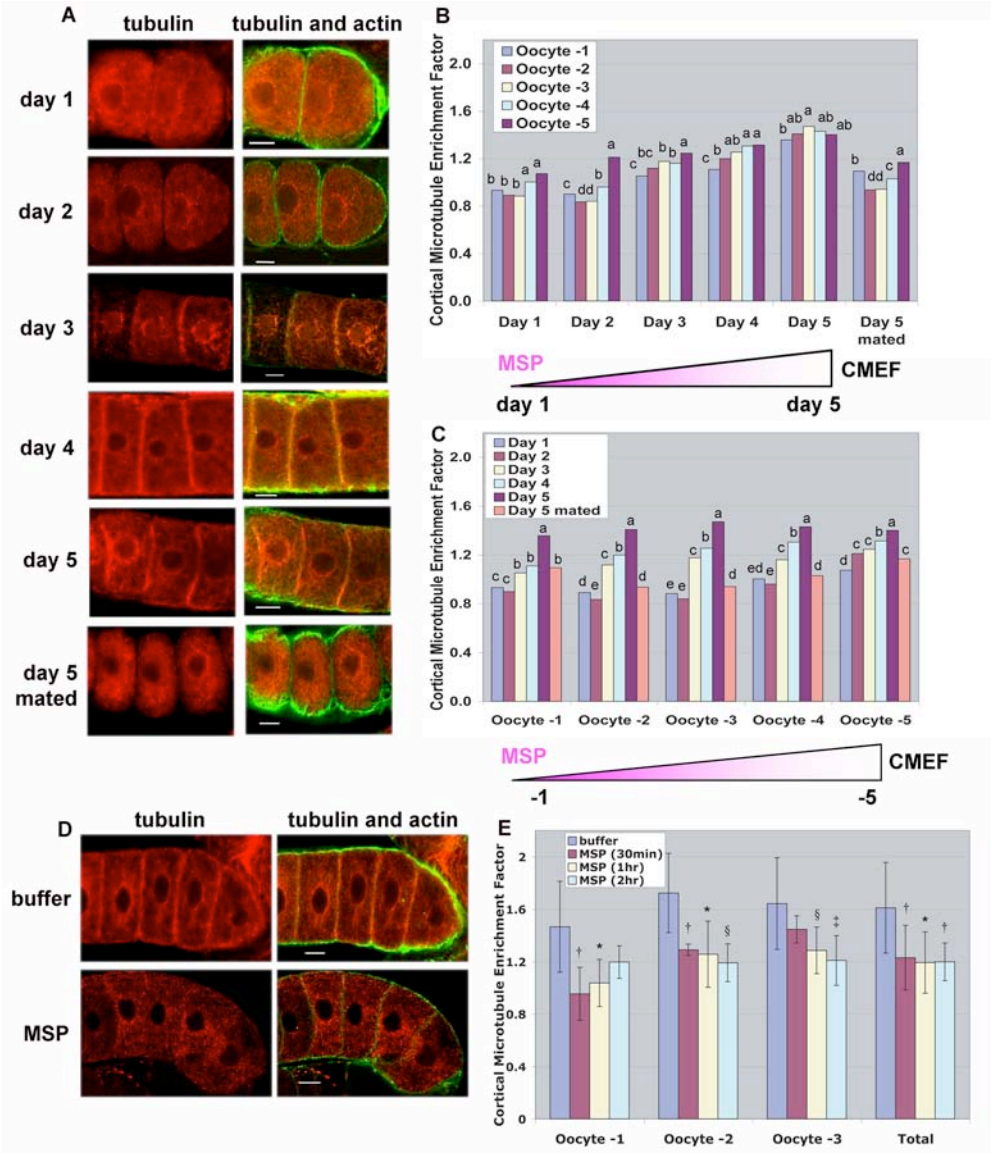
A
tubulin
tubulin and actin
day 1
day 2
day 3
day 4
day 5
day 5 mated
B
Cortical Microtubule Enrichment Factor
Oocyte -1
Oocyte -2
Oocyte -3
Oocyte -4
Oocyte -5
Day 1
Day 2
Day 3
Day 4
Day 5
Day 5 mated
MSP
CMEF
day 1
day 5
C
Day 1
Day 2
Day 3
Day 4
Day 5
Day 5 mated
Oocyte -1
Oocyte -2
Oocyte -3
Oocyte -4
Oocyte -5
MSP
CMEF
-1
-5
D
tubulin
tubulin and actin
buffer
MSP
E
buffer
MSP (30min)
MSP (1hr)
MSP (2hr)
Oocyte -1
Oocyte -2
Oocyte -3
Total

To test this possibility, we analyzed CMEF values among oocytes within a time point using *lsd* (Fig. 33B). Significantly lower CMEF values were observed in proximal (–1, –2, –3) than in distal (–4, –5) oocytes, supporting the idea that microtubule reorganization is spatially graded over the proximal gonad arm (Fig. 33A, B).

MSP is sufficient for oocyte microtubule reorganization

These time-course data are consistent with the hypothesis that MSP may be sufficient to signal microtubule reorganization. To test this possibility directly, we injected 200 nM purified MSP or a control buffer into the uterus of unmated females. After various recovery times (30, 60, or 120 min), we quantified oocyte microtubule organization (Fig. 33D, E). Females injected with MSP exhibited a decreased average CMEF value of 1.23 ± 0.30 (n=15) by 30 min following MSP injection compared to buffer injected controls, which displayed an average CMEF value of 1.61 ± 0.42 (n=60). Oocytes located more distal from the uterine injection site (e.g., oocytes –2 and –3), tended to exhibit higher CMEF values than the most proximal oocyte. These results provide evidence that the MSP signal is sufficient to reorganize microtubules in proximal oocytes. These results further suggest that as the MSP signal diminishes, oocyte microtubules become cortically enriched.

Figure 34. MSP signaling genes regulate oocyte microtubule reorganization.

(A and B) Single confocal images of *vab-1(dx31)* mated (A) and unmated (B) females labeled with tubulin (red) and actin (green). Null mutations in *vab-1* have no effect on microtubule organization. (C and D) Single confocal images of *ceh-18(mg57)* mated (C) and unmated (D) females. Unmated females (D) do not exhibit cortical microtubule enrichment. (E) CMEF measurements in *ceh-18* and *vab-1* mutants in the absence and presence of sperm (error bars represent s.d.). (F-O) Single confocal images of dissected gonads from mutants or RNAi-treated animals labeled as indicated. (F) Hermaphrodites treated with empty-vector control RNAi. (G) Hermaphrodites treated with *gsa-1* RNAi. (H) *rrf-1(pk1417)* hermaphrodites treated with *gsa-1* RNAi. (I) *gsa-1(ce81*gf*)fog-3(q443)* unmated females. (J) Unmated *fog-2* females treated with *kin-2* RNAi. (K) Unmated *fog-3(q443)rrf-1(pk1417)* females treated with *kin-2* RNAi. (L) *goa-1(sa734)fog-3(q443)* unmated females. (M) *fog-3(q443)rrf-1(pk1417)* unmated females treated with *goa-1* RNAi. (N) Unmated *fog-2* females treated with *inx-14* RNAi. (O) Unmated *fog-2* females treated with *inx-22* RNAi. (P) CMEF measurements for the indicated genotypes (between 6-18 gonad arms were analyzed; error bars represent s.d.). Scale bars: 10 μm.

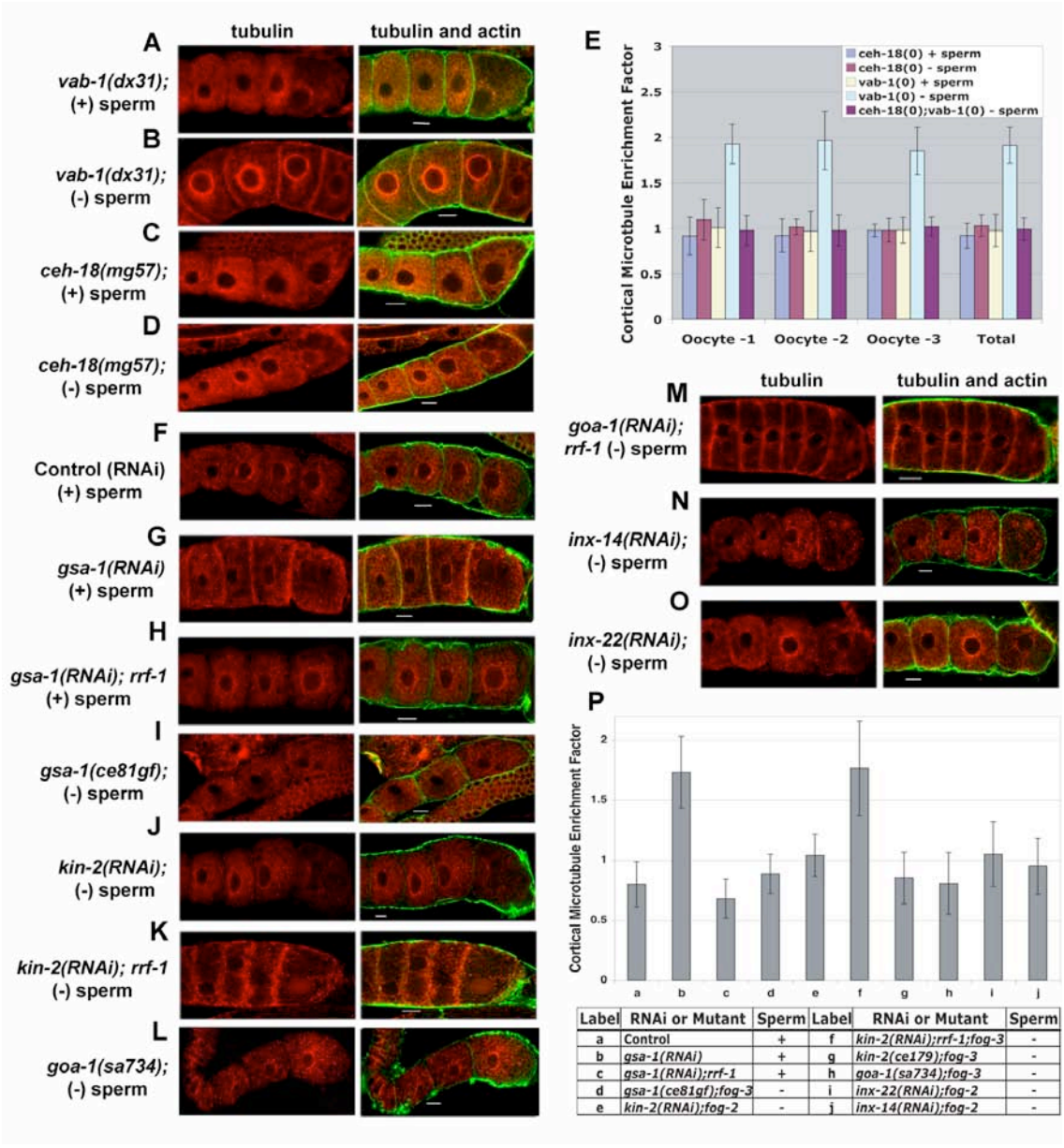

Label	RNAi or Mutant	Sperm	Label	RNAi or Mutant	Sperm
a	Control	+	f	*kin-2(RNAi);rrf-1;fog-3*	-
b	*gsa-1(RNAi)*	+	g	*kin-2(ce179);fog-3*	-
c	*gsa-1(RNAi);rrf-1*	+	h	*goa-1(sa734);fog-3*	-
d	*gsa-1(ce81gf);fog-3*	-	i	*inx-22(RNAi);fog-2*	-
e	*kin-2(RNAi);fog-2*	-	j	*inx-14(RNAi);fog-2*	-

Antagonistic $G\alpha_s$ and $G\alpha_{o/i}$ Signaling Pathways in the Soma Regulate Oocyte Microtubule Reorganization

ceh-18, but not vab-1, affects microtubule reorganization

MSP promotes oocyte meiotic maturation by antagonizing two parallel negative regulatory circuits: an oocyte VAB-1, Eph/MSP receptor, pathway and a somatic gonadal sheath cell pathway defined by the POU-homeoprotein, CEH-18 (Miller et al., 2003). To determine whether either of these pathways affects MSP-dependent oocyte microtubule reorganization, we examined oocytes from unmated and mated *vab-1(null)* and *ceh-18(null)* mutant females (Fig. 34A-E). *vab-1(dx31)* null mutants did not have an effect on microtubule reorganization either in the absence (CMEF=1.91 ± 0.20, n=15; Fig. 34B, E) or presence (CMEF=0.97 ± 0.18, n=20; Fig. 34A, E) of sperm. By contrast, *ceh-18(mg57)* null mutant females did not exhibit cortical microtubule enrichment in the absence of sperm (CMEF=1.03 ± 0.12, n=18) (Fig. 34D, E), but contained evenly dispersed microtubules throughout the cytoplasm as in mated females (CMEF=0.92 ± 0.14, n=14) (Fig. 34C, E). Likewise, oocytes in *vab-1(dx31);ceh-18(mg57)* mutant females exhibited reorganized microtubules (CMEF=0.99 ± 0.12, n=18) (Fig. 34E). These results indicate that the *ceh-18* pathway inhibits microtubule reorganization in the absence of MSP, thereby suggesting a role for the gonadal sheath cells in regulating the organization of oocyte microtubules.

$G\alpha_s$ signaling promotes oocyte microtubule reorganization

$G\alpha_s$ signaling is necessary and sufficient to promote meiotic maturation and MAPK activation in oocytes in the presence of MSP (Govindan et al., 2006). To test whether *gsa-1*, which encodes $G\alpha_s$, affects microtubule

reorganization, we analyzed microtubules following *gsa-1(RNAi)* in a hermaphrodite background (Fig. 34G). We observed that oocyte microtubules were cortically enriched at the proximal and distal edges following *gsa-1(RNAi)* in the presence of sperm (CMEF=1.73 ± 0.30, n=54) (Fig. 34G, P) compared to the empty vector RNAi control (CMEF=0.80 ± 0.19, n=33) (Fig. 34F, P), indicating that *gsa-1* is required for MSP-dependent microtubule reorganization. To determine whether *gsa-1* functions in the soma or the germ line to promote microtubule reorganization, we conducted RNAi analysis in an *rrf-1(null)* mutant background. *rrf-1* encodes an RNA-dependent RNA polymerase (RdP) that is required for the RNAi response in many somatic cells (Sijen et al., 2001), but is dispensable for germline RNAi, which employs the EGO-1 RdP (Smardon et al., 2000). Thus, an RNAi response in an *rrf-1(null)* background is indicative of a germline function, whereas an absence of a response suggests sufficiency of gene function in the soma. In these animals we observed that microtubules were not enriched at the proximal-distal cortex of oocytes following *gsa-1(RNAi)* in an *rrf-1(null)* mutant background (CMEF=0.68 ± 0.16, n=27; Fig. 34H,P), suggesting that $G\alpha_s$ signaling in the soma is sufficient to promote microtubule reorganization in oocytes in the presence of MSP.

To test whether *gsa-1* activity is sufficient to promote microtubule reorganization in the absence of MSP, we examined two gain-of-function (gf) *gsa-1* alleles, *ce94*gf and *ce81*gf, which are predicted to stabilize the GTP-bound form of $G\alpha_s$ through G45R and R182C substitutions, respectively (Schade et al., 2005). In *gsa-1(ce81*gf*)* and *gsa-1(ce94*gf*)* females, we

observed that oocyte microtubules were dispersed evenly throughout the cytoplasm (CMEF=0.88 ± 0.16, n=17; Fig. 34I, P; and data not shown), like in mated females. In canonical $G\alpha_s$ signaling, activated $G\alpha_s$ stimulates adenylate cyclase resulting in production of cAMP, which binds the regulatory subunit of cAMP-dependent PKA thereby releasing the active catalytic subunit (Cabrera-Vera et al., 2003). Thus, we tested the involvement of *kin-2*, which encodes the regulatory subunit of cAMP-activated protein kinase, in regulating oocyte microtubule reorganization. We examined oocyte microtubules in *kin-2(ce179);fog-3(q443)* females or following *kin-2(RNAi)* in a *fog-2(q71)* female background (Fig. 34J,P, and data not shown). In both cases, we observed that oocyte microtubules were reorganized despite the absence of MSP (CMEF=0.85 ± 0.22, n=15, and CMEF=1.04 ± 0.18, n=39, respectively).

To determine whether *kin-2* functions in the germ line or soma to prevent microtubule reorganization in the absence of MSP, we tested the effect of *kin-2(RNAi)* in an *rrf-1(pk1417)fog-3(q443)* female background. We observed cortically enriched microtubules (CMEF=1.76 ± 0.39, n=30) (Fig. 34K, P), indicating that *kin-2* function is sufficient in the soma to prevent oocyte microtubule reorganization when MSP is absent.

This observation is consistent with the finding that *kin-2* functions in the soma to prevent meiotic maturation in the absence of MSP (Govindan et al., 2006). The contribution of both $G\alpha_s$ and KIN-2 to microtubule reorganization in oocytes suggests that cAMP may also be involved in this regulation. To test this hypothesis, we soaked unmated *fog-2(q71)* females in an 8 mg/ml solution of

dibutyryl-cAMP for two hours. Although the effects were weak, variable, and required high levels of dibutyryl-cAMP, they were quantifiable in that the dibutyryl-cAMP-soaked females exhibited decreased CMEF values (CMEF=1.24 ± 0.21, n=33) compared to the buffer control (CMEF=1.61 ± 0.34, n=60; p<0.001; data not shown). Thus, $G\alpha_s$ signaling in the soma, likely in the gonadal sheath cells, is necessary and sufficient to promote oocyte microtubule reorganization.

$G\alpha_{o/i}$ signaling inhibits oocyte microtubule reorganization in the absence of sperm

goa-1 is necessary and sufficient to negatively regulate meiotic maturation and MAPK activation when MSP was absent. To determine whether *goa-1* is a regulator of oocyte microtubule reorganization, we examined *goa-1(sa734)fog-3(q443)* females and observed evenly dispersed microtubules (CMEF=0.81 ± 0.26, n=24) (Fig. 34L,P). By contrast, cortically enriched microtubules were observed following *goa-1(RNAi)* in an *rrf-1(null)* female background (Fig. 34M). These data suggest that *goa-1* is required in the soma to prevent oocyte microtubule reorganization in the absence of the MSP signal.

Regulation of oocyte microtubule reorganization by $G\alpha_s$, $G\alpha_{o/i}$, and gap junctions

To investigate the relationship between *goa-1* and *gsa-1* in the regulation of oocyte microtubule reorganization, we performed *gsa-1(RNAi)* on *goa-1(sa734)* hermaphrodites and examined oocyte microtubules. Microtubules were cortically enriched at the proximal and distal cortical edges of oocytes (data not shown), which is consistent with the finding that *gsa-1* is

required for oocyte microtubule reorganization in a hermaphrodite background (Fig. 34G). When we conducted *gsa-1(RNAi)* in a *goa-1(sa734)fog-3(q443)* female background, however, oocyte microtubules were reorganized (data not shown). This is interesting because *gsa-1(RNAi)* in a *goa-1(sa734)* female background results in low meiotic maturation rates and an absence of detectable MAPK activation in oocytes (Govindan et al., 2006). Thus, microtubule reorganization might represent a separable element of the meiotic maturation process requiring different thresholds of signaling. Together, these data suggest the involvement of antagonistic $G\alpha_s$ and $G\alpha_{o/i}$ signaling in sheath cells in the regulation of microtubule reorganization in oocytes.

$G\alpha_s$ signaling appears to promote meiotic maturation in part by affecting the synthesis or stability of sheath/oocyte gap junctions (Govindan et al., 2006). The existence of gap-junctional communication between sheath cells and oocytes provides a potential mechanism for coordinating their behaviors (Hall et al., 1999). To determine whether gap-junctional communication between sheath cells and oocytes regulates oocyte microtubule reorganization, we used RNAi to inactivate *inx-14* and *inx-22*, which likely encode innexin components of the sheath/oocyte gap junctions (Govindan et al., 2006). When we conducted *inx-14(RNAi)* or *inx-22(RNAi)* in a *fog-2(q71)* female background, we observed oocytes that contained evenly dispersed microtubules (CMEF=0.95 ± 0.23, (n=15) and CMEF=1.05 ± 0.27, (n=18), respectively) (Fig. 34N-P). These data suggest that gap-junctional communication between sheath cells and oocytes prevents microtubule reorganization in the absence of MSP.

Figure 35. Additional genetic mutations or RNAi treatments that affect microtubule reorganization.

(A-F) Single confocal images of animals labeled with tubulin (red) and actin (green). (A) *goa-1(sa734)fog-3(q443)* unmated females treated with *gsa-1* RNAi do not exhibit cortically enriched microtubules. (B) *oma-1(zu405te33);oma-2(te51)* hermaphrodites contain oocytes with cortically enriched microtubules. (C-E) *emo-1(oz1)* (C), *ptc-1(ok122)* (D), and *cgh-1(ok492)* (E) unmated females contain reorganized microtubules. (F and G) Unmated females treated with either *wee-1.3* RNAi (F) or *gpb-1* RNAi (G) contain reorganized microtubules. Scale bars: 10 μm.

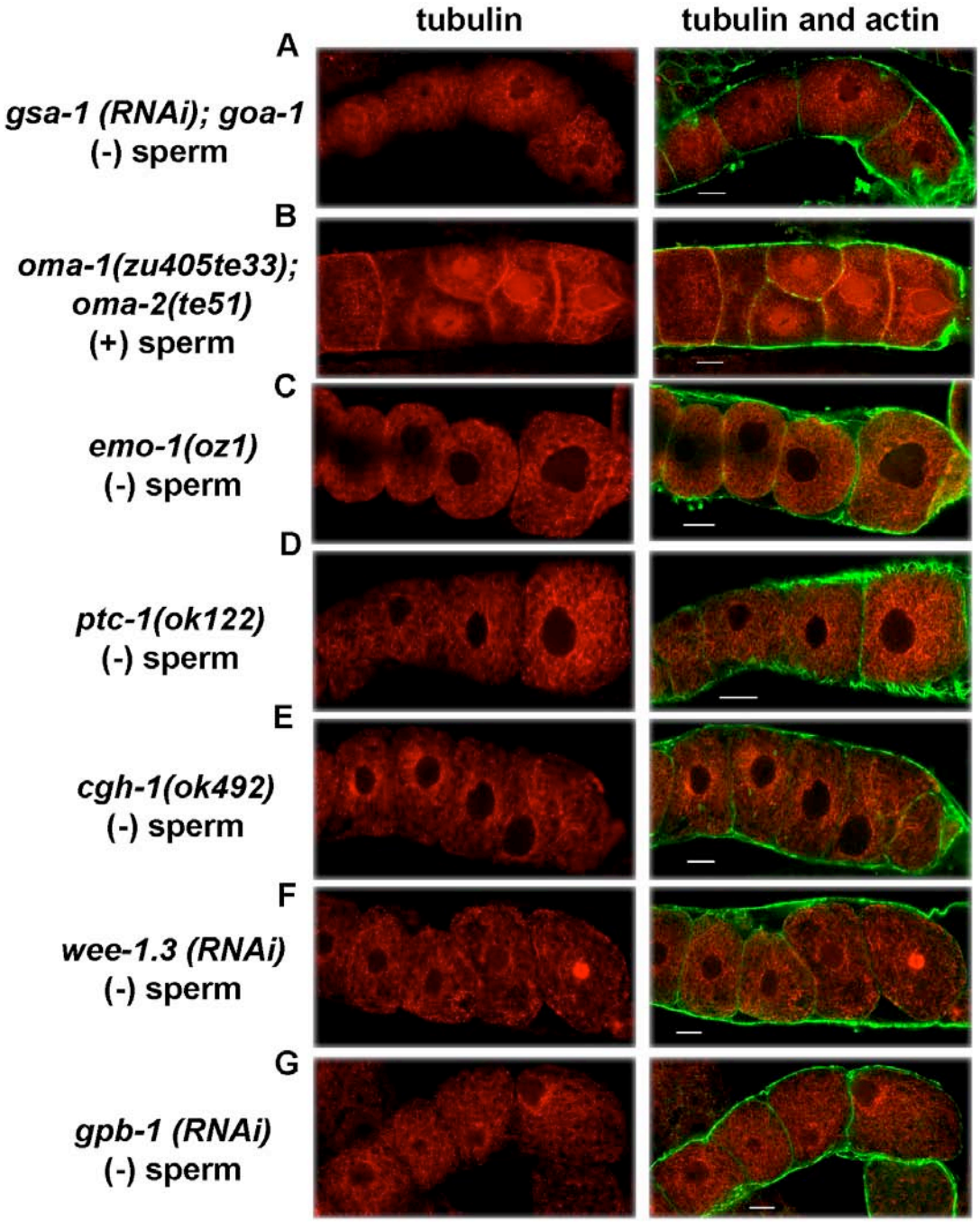
tubulin
tubulin and actin
A
gsa-1 (RNAi); goa-1
(-) sperm
B
oma-1(zu405te33);
oma-2(te51)
(+) sperm
C
emo-1(oz1)
(-) sperm
D
ptc-1(ok122)
(-) sperm
E
cgh-1(ok492)
(-) sperm
F
wee-1.3 (RNAi)
(-) sperm
G
gpb-1 (RNAi)
(-) sperm

Germline regulators of oocyte microtubule reorganization

MSP-dependent MAPK activation and meiotic maturation require the downstream action of OMA-1 and OMA-2, two TIS-11 zinc-finger proteins expressed in the germ line (Detwiler et al., 2001). When we examined microtubules in *oma-1(zu405te33);oma-2(te51)* double mutant hermaphrodites, microtubules were enriched at the proximal and distal cortex (Fig. 35B). This observation indicates that OMA-1 and OMA-2 may function to promote microtubule reorganization directly, or indirectly, as a consequence of their requirement for promoting meiotic maturation. Analysis of genetic mutants in three negative regulators of meiotic maturation and MAPK activation in oocytes, *emo-1(oz1)* (Iwasaki et al., 1996), *ptc-1(ok122)* (Govindan et al., 2006), and *cgh-1(ok492)* (Yamamoto, I. and Greenstein, D. unpublished results), indicated that these mutants exhibit reorganized oocyte microtubules in a female genetic background (Fig. 35C-E).

Recently, Burrows et al. (2006) demonstrated that the Myt1 homolog WEE-1.3 is required for the normal timing of NEBD during the meiotic maturation process in hermaphrodites and for proper meiotic spindle assembly. Consistent with the proposal that *wee-1.3* regulates oocyte microtubules (Burrows et al., 2006), we found that *wee-1.3(RNAi)* in a *fog-2(q71)* female background causes oocyte microtubule reorganization (Fig. 35F). Burrows et al. (2006) reported that *wee-1.3(RNAi)* in a female background is not sufficient to trigger maturation, however, under our RNAi conditions *wee-1.3(RNAi)* was sufficient to cause NEBD (data not shown), suggesting the microtubule effect

could be downstream of *cdk-1* activation. While *cdk-1(RNAi)* in a hermaphrodite background did not block oocyte microtubule reorganization (data not shown), it may be difficult to completely deplete CDK-1 from the germline using RNAi, as discussed previously (Boxem et al., 1999; Burrows et al., 2006).

To begin to address the mechanism of microtubule reorganization, we used RNAi to test whether known microtubule regulators, such as kinesin and dynein motors and microtubule-associated proteins, function to promote oocyte microtubule reorganization when sperm are present, or, alternatively, whether they are needed for blocking reorganization in female backgrounds.
None of the tested microtubule regulators (data not shown) affected oocyte microtubule reorganization, indicating that further work will be needed to determine the mechanism at the level of individual microtubules.

Oocyte microtubule reorganization does not require high levels of MAPK activation

MSP signaling triggers MAPK activation in oocytes (Miller et al., 2001; Miller et al., 2003) . Because there is a general correlation between MAPK activation and oocyte microtubule reorganization: negative regulators of MAPK activation (eg., *kin-2*, *inx-14*, *inx-22*, *ptc-1*, *cgh-1*, *goa-1*, *gpb-1*, *ceh-18)* block microtubule rearrangement in females whereas positive regulators (eg., *oma-1/2* and *gsa-1*) are required in hermaphrodites, we addressed the requirement for *mpk-1* MAPK (Govindan et al., 2006). Since null mutations in *mpk-1* MAPK cause a sterile phenotype in which germ cells fail to progress through pachytene, thereby disrupting oogenesis at an early stage (Church et al., 1995),

we tested the involvement of *mpk-1* MAPK using three methods that reduce but do not eliminate *mpk-1* activity: 1) the temperature-sensitive (ts) *mpk-1(ga111*ts*)* allele; 2) *mpk-1(RNAi)*; and 3) the chemical inhibitor U0126. One-day-old adult hermaphrodites were shifted to the restrictive temperature (25°C) for 12-16 hrs and their oocyte microtubules were analyzed by confocal microscopy. All gonad arms examined containing oocytes exhibited microtubule reorganization for both *mpk-1(ga111*ts*)* (n=10) and *mpk-1(RNAi)* (n=8). We also injected the gonads of young adult hermaphrodites with a 100 μM solution of the MEK1/2 inhibitor, U0126, as an additional approach for inhibiting MAPK activation. When we assessed the efficacy of the U0126 injections by staining dissected gonads with antibodies to the diphosphorylated, activated form of MPK-1 MAPK (MAPK-YT), we found that only 50% of the gonads exhibited observable MAPK-YT staining (n=40). In contrast, staining of U0126-injected gonads with anti-α-tubulin antibodies indicated that microtubules were reorganized in all proximal oocytes. Together these results suggest that MAPK activation may not be essential for MSP-dependent microtubule reorganization. This result is consistent with the observation, described above, that oocyte microtubules are reorganized following *gsa-1(RNAi)* in a *goa-1(sa734)fog-3(q443)* female background, despite the lack of observable MAPK activation in oocytes. The interpretation of these results has the major caveat that we cannot exclude the possibility that residual levels of activated MAPK may be available for promoting oocyte microtubule reorganization.

Discussion

In addition to nuclear changes presaging the final steps of meiotic chromosome segregation, the meiotic maturation process encompasses cytoplasmic alterations, collectively referred to as “cytoplasmic maturation,” which include reorganization of cytoplasmic organelles, cytoskeletal remodeling, activation of signaling for ovulation, and cellular events important for fertilization and polarity establishment (reviewed by Greenstein and Lee, 2006; reviewed by Voronina and Wessel, 2003; Yamamoto et al., 2006). The full extent of the cytoplasmic meiotic maturation program and its regulation is considerably less well understood than the control of meiotic cell cycle progression. Here, we investigated changes in the oocyte microtubule cytoskeleton during early steps of the meiotic maturation process in *C. elegans*. We provide evidence that the sperm-derived meiotic maturation signal, MSP, triggers cytoplasmic microtubule reorganization in the oocyte prior to NEBD. When MSP is absent, as in females or older hermaphrodites, microtubules are enriched at the proximal and distal cortices of oocytes. In mated females or younger hermaphrodites, microtubules are dispersed evenly in a net-like fashion throughout the cytoplasm of proximal oocytes. We used a quantitative assay for oocyte microtubule reorganization to show that purified MSP is sufficient to direct this cytoskeletal remodeling. Overall, these studies reveal that a remarkable change in the microtubule cytoskeleton occurs in response to the MSP meiotic maturation hormone and that these changes occur prior to both NEBD and fertilization.

The microtubule changes termed “oocyte microtubule reorganization,” are distinct from “oocyte cortical rearrangement,” or the rounding-up of the oocyte just prior to ovulation, described by McCarter et al (1999), in at least two significant ways. First, oocyte microtubule reorganization occurs prior to the onset of NEBD, whereas oocyte cortical rearrangement occurs after the onset of NEBD (McCarter et al., 1999). Second, oocyte cortical rearrangement is spatially restricted to the maturing –1 oocyte and occurs in the time window between the onset of NEBD and ovulation (3-5 min prior to ovulation).
By contrast, proximal oocytes that receive the MSP signal undergo microtubule reorganization. The possibility that oocyte cortical rearrangement (McCarter et al., 1999) represents an actin-based process is consistent with static images of phalloidin- or anti-actin-stained fixed gonads and embryos (Strome, 1986), but real-time analysis will be needed to address this possibility fully. MSP signaling thus induces an early reorganization of the microtubule cytoskeleton, which might be followed by later changes in the actin cytoskeleton.

Microtubules play critical roles during oogenesis by controlling cell shape, protein trafficking, RNA localization, and cell polarity. Despite these essential functions, it is incompletely understood how meiotic or follicular signals regulate microtubule organization and function in oocytes. We used quantitative confocal microscopy and genetics to analyze the regulation of oocyte microtubule reorganization. Our analyses defined two groups of regulators: the first group promotes microtubule reorganization in the presence of MSP; and the second group prevents reorganization in the absence of MSP.

A null mutation in the POU-homeobox gene *ceh-18* leads to microtubule reorganization in a female genetic background in which MSP is absent. This finding, taken together with the observation that *ceh-18* is expressed in gonadal sheath cells but not oocytes, and is required for proper sheath cell differentiation and function (Greenstein et al., 1994; Rose et al., 1997), suggests a role for the gonadal sheath cells in controlling the microtubule cytoskeleton of the oocyte. Consistent with this idea, *goa-1*, which encodes a $G\alpha_{o/i}$ protein shown to inhibit meiotic maturation through its action in the soma (Govindan et al., 2006), is a negative regulator of oocyte microtubule reorganization. Further, we used the *rrf-1* genetic background, in which somatic cells are less sensitive to RNAi, to provide evidence that *goa-1* functions in the soma to prevent oocyte microtubule reorganization in the absence of sperm. To explore how sheath cell signaling might influence the localization and dynamics of microtubules within oocytes, we tested several known germline-expressed microtubule regulators (e.g., microtubule-associated proteins and motors) for their potential involvement using RNAi, but none of the tested microtubule regulators had an effect (data not shown). While it will take further work to uncover the mechanism by which the somatic gonad controls microtubule localization and dynamics in oocytes, signaling through sheath/oocyte gap junctions is likely to play an important role, as *inx-14(RNAi)* or *inx-22(RNAi)* cause microtubule reorganization in female genetic backgrounds. These findings mesh with prior TEM studies that indicated that sheath/oocyte gap junctions were rare or absent in *ceh-18* mutants (Hall et al., 1999; Rose et al.,

1997). These observations raise the possibility that small molecules or ions transferred through these junctions might critically influence microtubule localization and dynamics.

MSP signaling stimulates the basal contraction of the proximal sheath cells (McCarter et al., 1999; Miller et al., 2001). Several observations discount the possibility that the absence or presence of external mechanical pressure from sheath cell contractions represents a major factor regulating MSP-dependent oocyte microtubule reorganization. For example, *oma-1(zu40te33); oma-2(te51)* mutant hermaphrodites exhibit substantial sheath cell contractions (5.6 ± 3.6 contractions/min; n=14; Yamamoto.I, Greenstein.D, unpubl. results), but lack oocyte microtubule reorganization, whereas *ceh-18(mg57)* females exhibit low basal sheath cell contraction rates, but have reorganized oocyte microtubules.

What is the biological significance of MSP-dependent oocyte microtubule reorganization?

To address the potential function of oocyte microtubule reorganization, we attempted to determine the consequence of blocking the process. We found two situations in which oocyte microtubule reorganization was disrupted despite the presence of MSP: (1) *oma-1(zu40te33);oma-2(te51)* hermaphrodites; and (2) *gsa-1(RNAi)* hermaphrodites. Because meiotic maturation, ovulation, and fertilization do not occur in the *oma-1;oma-2* double mutant (Detwiler et al., 2001), we were unable to discern whether there is a detrimental consequence for the embryo. In a similar vein, meiotic maturation only occurs at a low rate following *gsa-1(RNAi).* The few fertilization events that were observed following

gsa-1(RNAi), typically one per gonad arm resulted in viable hermaphrodite offspring, perhaps suggesting a nonessential or modulatory role for oocyte microtubule reorganization. Nonetheless, several considerations affect the interpretation of this result.

First, for technical reasons, we could not address whether microtubule reorganization can occur in the few maturing oocytes observed following *gsa-1(RNAi),* similar to the result seen in spontaneous meiotic maturation events in a female background. Second, we were unable to examine *gsa-1(null)* hermaphrodites owing to the fact that *gsa-1* is an essential gene (Korswagen et al., 1997), and thus the caveat that RNAi was used in this experiment should be considered. Genetic or experimental (i.e., RNAi) perturbations that specifically affect microtubule reorganization, but not other components of the meiotic maturation process, will be needed to address the question of biological significance more fully.

Although it is formally possible that MSP-dependent oocyte microtubule reorganization is nonessential, our bias is that this dramatic cytoskeletal transformation has functional importance for the worm, which we can only hypothesize. Nonetheless, here we hazard a few speculations. In the first model, we suggest that microtubule reorganization might facilitate the assembly of the meiotic spindle (Fig. 36A). Because MSP affects the localization and the directionality of movement of growing microtubule plus ends (data not shown), these changes in microtubule dynamics may promote search and capture of meiotic chromatin after NEBD (Fig. 36A). Thus, MSP may “prime” microtubule

Figure 36. Models for the biological significance of MSP-dependent oocyte microtubule reorganization.

(A) Microtubule reorganization prepares the oocyte for meiotic spindle assembly upon NEBD. Changes in microtubule localization and dynamics (indicated by plus signs) in the presence of MSP facilitate search and capture of chromatin by microtubules. (B) Microtubule reorganization repatterns the oocyte cortex to facilitate the irreversible cell-cycle transition of meiotic maturation. Cortical reorganization may affect the trafficking of membrane proteins that inhibit meiotic maturation (depicted in blue).

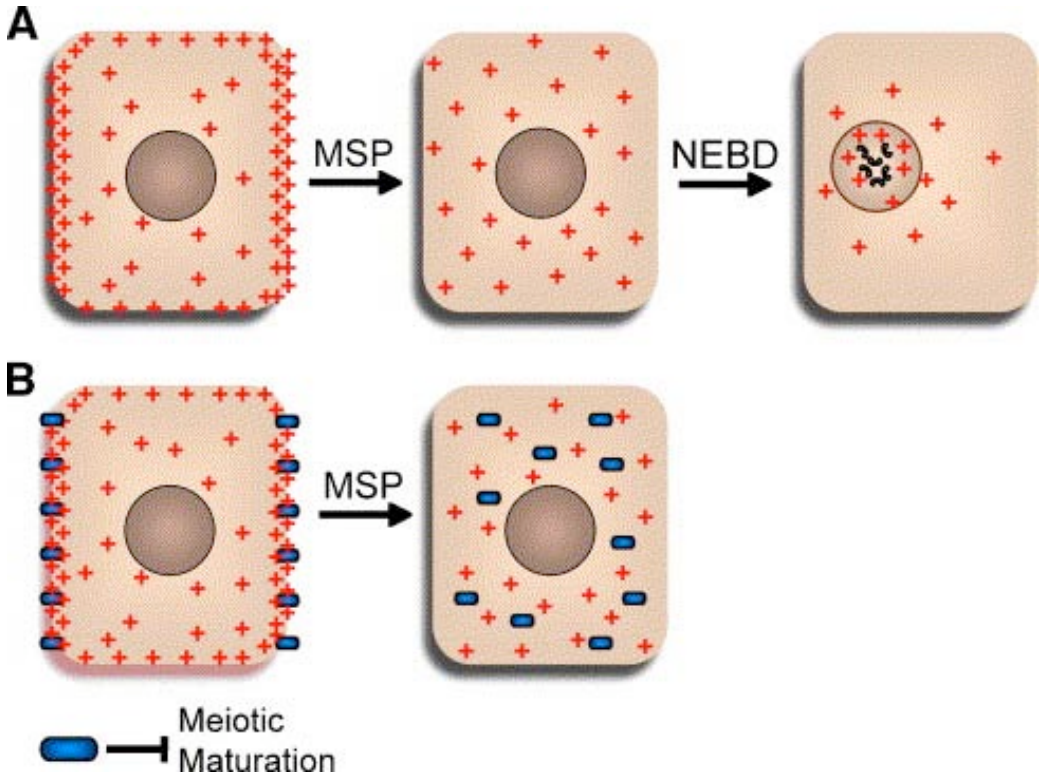
A
MSP
NEBD
B
MSP
Meiotic
Maturation

dynamics for meiotic spindle assembly early in the process, so that the spindle can form rapidly upon NEBD. However, we found that sperm availability affects the frequency of meiotic maturation (data not shown), but apparently not the timing of spindle assembly once maturation occurs. It remains a formal possibility, however, that oocyte microtubule reorganization may have a redundant role in influencing the timing of meiotic spindle assembly.

In a second, but not mutually exclusive model, cortical microtubule enrichment in the absence of MSP might facilitate trafficking of proteins needed to maintain meiotic diapause (Fig. 36B). For instance, meiotic arrest depends on the assembly of sheath/oocyte gap junctions and the function of the VAB-1 MSP/Eph receptor (Corrigan et al., 2005; Govindan et al., 2006; Miller et al., 2003). These regulators are likely depended on microtubules for trafficking to the cortex (Musch, 2004). By contrast, removal or depletion of negative regulators of meiotic maturation from the cortex upon microtubule reorganization might aid in flipping an “all or none” switch that drives the oocyte to meiotically mature once it reaches the most proximal position. Interestingly, we observed an asymmetry of cortical microtubule accumulation in the –1 oocyte in the absence of sperm in that microtubules was enriched at the distal but not the proximal cortex. Although the significance of this finding is unclear, we speculate that this asymmetry may be part of the mechanism by which this oocyte “knows” it is in the most proximal position and is thus competent to undergo meiotic maturation upon receiving the MSP signal.

Microtubule reorganization in response to MSP signaling might also play a role in refashioning the cortex or plasma membrane domains for the later developmental events of fertilization or embryogenesis.

At anaphase I, the DYRK-family kinase MBK-2 translocates from the cell cortex to intracellular puncta in a trafficking process, which depends on CDK-1 and the anaphase-promoting complex (McNally and McNally, 2005; Stitzel et al., 2006). Although prior studies have not addressed whether microtubules play a key role in promoting MBK-2 redistribution, it is interesting that microtubules in the embryo are themselves a downstream target of MBK-2. MBK-2 phosphorylates the MEI-1 subunit of katanin, a dimeric microtubule-severing AAA-ATPase (Srayko et al., 2000), which marks it for ubiquitin-mediated degradation by a CUL-3/MEL-26 E3 ubiquitin ligase (Furukawa et al., 2003; Pintard et al., 2003). MEI-1 is required for assembly of anastral barrel-shaped female meiotic spindles (Clark-Maguire and Mains, 1994a; Clark-Maguire and Mains, 1994b), and the inappropriate inclusion of MEI-1 into mitotic spindles is lethal because excessive shortening of astral microtubule arrays disrupts spindle positioning and the asymmetric partitioning of cell-fate determinants (Clandinin and Mains, 1993). Our work here defines two classes of microtubule arrangements in oocytes: one associated with diapause; and the other associated with meiotic maturation. Both modes appear to represent active states with several genes required for their maintenance, suggesting complex regulation. We anticipate that the underlying mechanisms controlling cytoplasmic microtubule

organization in this system may be relevant to the oocytes or epithelial cells of other organisms in which most microtubules are noncentrosomal.

CHAPTER V

GENERAL DISCUSSION AND FUTURE DIRECTIONS

Summary

Oocyte meiotic maturation is a conserved biological process in sexually reproducing species. Studying the molecular underpinnings involved in meiotic maturation is important because meiotic errors are associated with aneuploidy and developmental defects in humans. In *C. elegans*, MSP signals the oocyte to undergo meiotic maturation. MSP promotes meiotic maturation by antagonizing two parallel pathways defined by the VAB-1/Eph receptor and a somatic gonad sheath cell pathway. In my dissertation work, I have investigated the molecular mechanisms involved in *C. elegans* oocyte meiotic maturation. This study emphasizes a role for somatic gonad in controlling oocyte meiotic maturation. The somatic gonad plays a critical role in "sensing" the availability of sperm to regulate oocyte meiotic maturation. Furthermore, I present evidence that the somatic gonadal G-protein pathways regulate oocyte microtubule rearrangement prior to fertilization. In addition, I uncovered new genes in the VAB-1 pathway that regulate oocyte meiotic maturation. These additional genes provide insights on the mechanism by which VAB-1 may regulate oocyte meiotic maturation. In this section, I present a summary of major findings and discuss in length a model for the regulation of oocyte meiotic maturation.

Figure 37. A model for parallel control of meiotic maturation in *C. elegans* by antagonistic G protein signaling from the soma and an oocyte MSP/Eph receptor pathway.

The germline and soma meiotic maturation control network is depicted in two states, depending on whether the MSP signal is absent (left panel) or present (right panel). $G\alpha_{o/i}$ negatively regulates meiotic maturation and oocyte MAPK activation and antagonizes a $G\alpha_s$ pathway that promotes maturation. The $G\alpha_s$ pathway is drawn showing involvement of the regulatory subunit (KIN-2) of cyclic-AMP-dependent protein kinase A (PKA) and adenylate cyclase (ACY-4). *inx-8* and *inx-9* are possibly sheath cell- expressed innexins. Unidentified sheath cell GPCRs are proposed to receive the MSP signal in parallel to VAB-1 on the oocyte, such that GPCR's coupled to $G\alpha_{o/i}$ are antagonized by MSP, whereas $G\alpha_s$-coupled receptors are stimulated by MSP. The $G\alpha_s$ pathway is proposed to directly destabilize the inhibitory sheath/oocyte gap junctions, but a parallel function is equally consistent with current genetic data. The CEH-18 POU-homoeprotein localizes to sheath cell nuclei where it functions to control sheath cell differentiation, in part, by directly or indirectly affecting the assembly of sheath/oocyte gap junctions. DAB-1 and VAV-1 function in the VAB-1 MSP/Eph receptor pathway in the germ line. This figure was modified from Govindan et al. (2006)

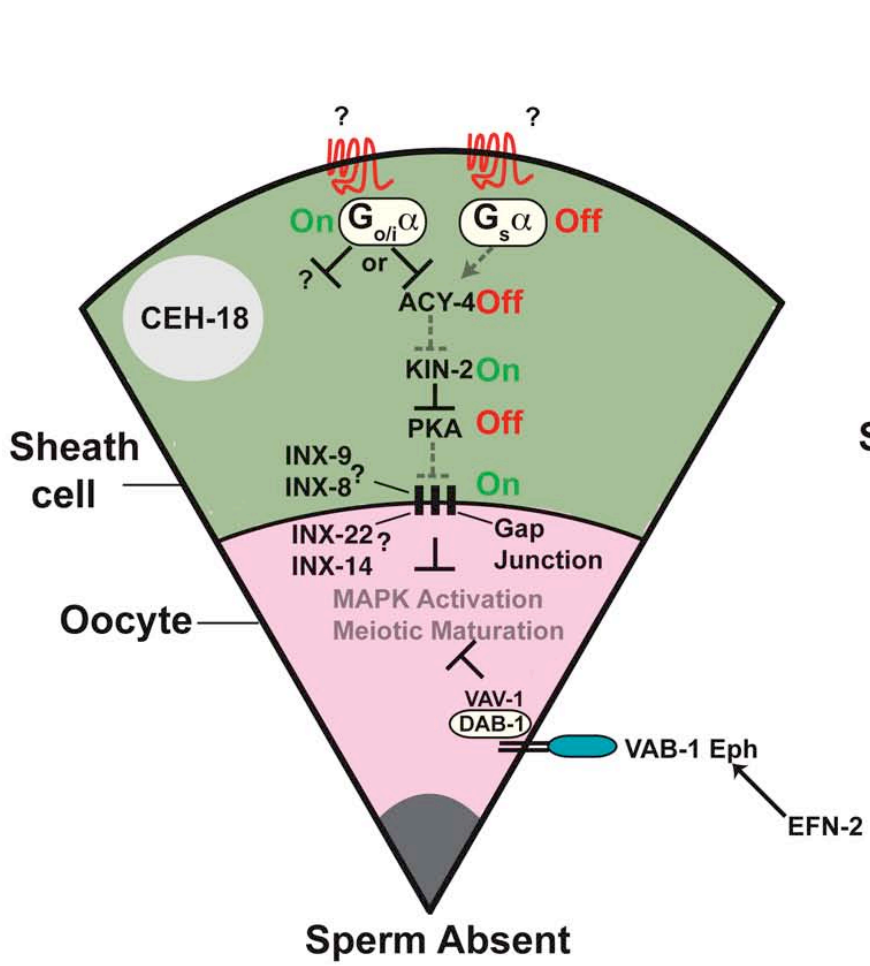
?
?
On
$G_{o/i}\alpha$
$G_s\alpha$
Off
?
or
CEH-18
ACY-4 Off
KIN-2 On
PKA Off
Sheath cell
INX-9
INX-8?
On
INX-22?
INX-14
Gap Junction
Oocyte
MAPK Activation
Meiotic Maturation
VAV-1
DAB-1
VAB-1 Eph
EFN-2
Sperm Absent

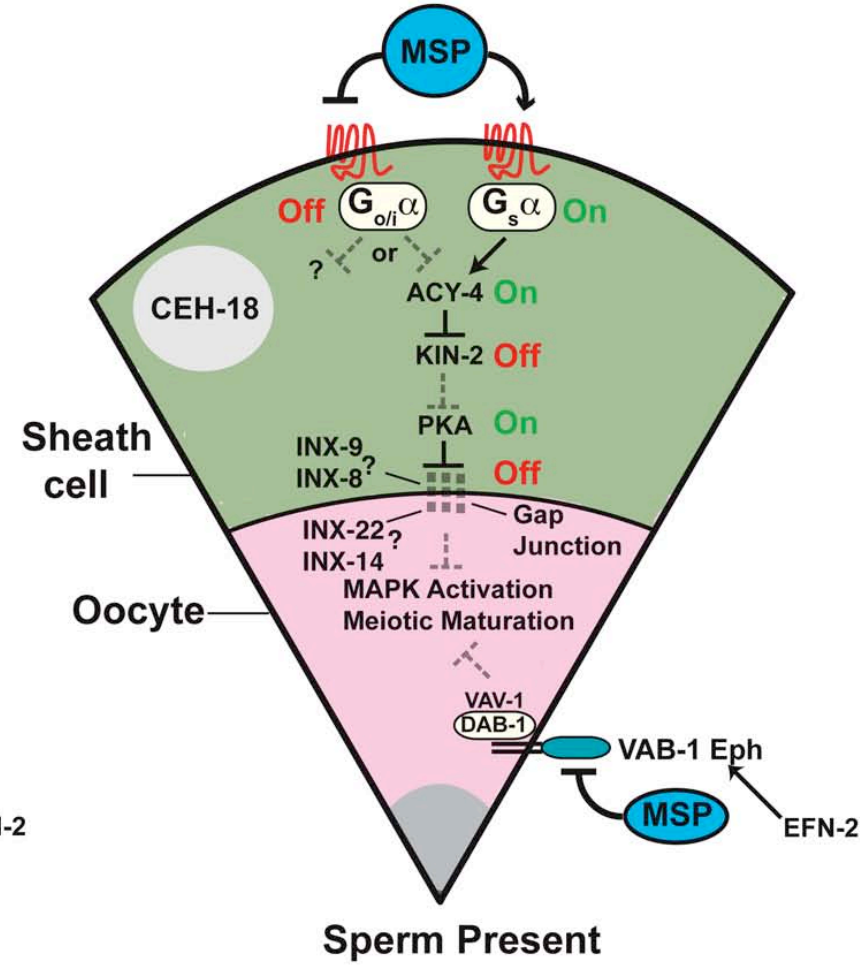
MSP
Off
$G_{o/i}\alpha$
$G_s\alpha$
On
?
or
CEH-18
ACY-4 On
KIN-2 Off
PKA On
Sheath cell
INX-9
INX-8?
Off
INX-22?
INX-14
Gap Junction
Oocyte
MAPK Activation
Meiotic Maturation
VAV-1
DAB-1
VAB-1 Eph
MSP
EFN-2
Sperm Present

In addition, I discuss some future studies needed to test my model. Further, I present some alternative models that need to be considered.

A sperm-sensing mechanism regulates oocyte meiotic maturation in *C. elegans*

In the presence of sperm, the most proximal (–1) oocyte undergoes meiotic maturation and ovulation (Miller et al., 2001). In contrast, when sperm is absent, the oocytes arrest at prophase of meiosis I (McCarter et al., 1999). The oocytes resume meiosis and undergo maturation when sperm is supplied by mating. Previously, it was shown that two parallel pathways defined by the VAB-1/Eph receptor and a somatic gonadal pathway, defined by the POU-protein CEH-18 inhibit meiotic maturation in the absence of sperm. MSP promotes meiotic maturation by inhibiting these parallel pathways (Miller et al., 2003). Together, VAB-1 and CEH-18 pathways define a sperm-sensing mechanism that regulates oocyte meiotic maturation depending on sperm availability.

To address how VAB-1 and CEH-18 pathways regulate meiotic maturation, I conducted a genome-wide RNAi screen in a female background. I screened for and identified 16 genes, which resulted in MSP-independent meiotic maturation. Further, I showed that six of these genes are required to inhibit MAPK activation in the absence of sperm. In addition, I showed that some of these genes functions within the germline while others are sufficient in the soma to inhibit meiotic maturation. I showed that DAB-1/disabled is necessary within the germline to inhibit meiotic maturation (Fig. 37). DAB-1 functions likely in the VAB-1 pathway to inhibit oocyte meiotic maturation. DAB-

1 is related to the mammalian disabled proteins DAB-1 and DAB-2. Both the disabled proteins function as adapter proteins and are involved in several intracellular signaling pathways (Holmes et al., 2007). *C. elegans* DAB-1 is closely related to mammalian DAB2 by sequence similarity. In *C. elegans*, during vulval development, DAB-1 binds to and activates LRP-1 and LRP-2/lipoprotein receptor-mediated secretion of EGL-17/FGF (Kamikura and Cooper, 2003). In this pathway, DAB-1 is thought to function as a clathrin adaptor for vesicles containing LRPs and EGL-17 (Kamikura and Cooper, 2003; Kamikura and Cooper, 2006). Recently, DAB-1 was shown to be required for receptor-mediated endocytosis of yolk in oocytes (Holmes et al., 2007). All these findings suggest that DAB-1 has a general role in the clathrin-mediated endocytic pathway. DAB-1 may regulate either clathrin-dependent or independent endocytosis of VAB-1 receptor during meiotic maturation. Interestingly, DAB-1 localization is changed in the presence and absence of sperm. In the presence of sperm, DAB-1 is localized to the oocyte cortex. By contrast, in the absence of sperm, DAB-1 is localized to the oocyte cytoplasm. *In vitro* binding studies show that DAB-1 binds directly to the intracellular domain of VAB-1 (Cheng, H. and Greenstein, D. unpublished results). These results suggest a model in which MSP binding to VAB-1 may modulate the endocytosis or trafficking of VAB-1. Recent data suggest that DAB-1 is involved in regulating VAB-1 localization/trafficking in the absence of sperm (Cheng, H. and Greenstein, D. unpublished results). However, analysis of VAB-1

localization using antibodies and/or GFP fusions is required to address the role of endocytic pathways in meiotic maturation.

In the absence of sperm, the *ceh-18* sheath cell pathway is necessary to inhibit oocyte meiotic maturation and MAPK activation (Miller et al., 2003). CEH-18 is required for specification, differentiation or function of gonadal sheath cells (Greenstein et al., 1994; Rose et al., 1997). In a female background, *ceh-18(null)* mutants derepress oocyte meiotic maturation, suggesting that the sheath cells have an inhibitory role in meiotic maturation. However, the mechanism(s) by which the somatic gonad can "sense" the availability of sperm was not known. I have presented evidence that the mechanism by which the somatic gonad "senses" sperm availability is via a conserved G-protein signaling pathway (Fig. 37). Interestingly, the somatic gonad-dependent sperm sensing mechanism is not a linear inhibitory pathway. Rather, it consists of both a maturation-promoting and a maturation-inhibiting signaling pathway. The somatic GOA-1/ $G\alpha_{i/o}$ is necessary and sufficient to inhibit meiotic maturation in the absence of sperm (Fig. 37). By contrast, the somatic GSA-1/$G\alpha_s$ is necessary and sufficient to promote maturation in presence of sperm (Fig. 37). Together, my findings allow the conclusion that $G\alpha_s$ and $G\alpha_{i/o}$ pathways promote or inhibit oocyte meiotic maturation depending on the presence or absence of sperm.

In the absence of sperm, GOA-1 is necessary in the somatic sheath cells to inhibit meiotic maturation (Fig. 37). When sperm is present, MSP inhibits GOA-1 to promote meiotic maturation. MSP binds to both oocyte and sheath

cell membrane in wildtype hermaphrodites. MSP binding to the sheath cell and oocyte membrane is reduced but not eliminated in *vab-1(null)* mutant suggesting the existence of additional MSP receptors (Miller et al., 2003). Therefore, it is likely that MSP binds to $G\alpha_{i/o}$-coupled receptor GPCR at the sheath membrane to downregulate GOA-1 activity. However, in the genome-wide RNAi screen for negative regulators I did not find any GPCRs. It is possible that the reason could be due to ineffective RNAi. Alternatively, multiple GPCRs could be involved and depletion of any single GPCR may not exhibit the phenotype. In *C. elegans*, there are more than 1000 GPCR encoded in the genome (Bargmann, 1998). Despite several forward and reverse genetic screens conducted in *C. elegans* over the past twenty years, very few (less than ten) GPCRs have been discovered whose inactivation produces an apparent phenotype. Knockdown of many of the GPCRs have no obvious phenotypic consequence, suggesting that there may be a large degree of redundancy (Keating et al., 2003).

In the absence of sperm, GOA-1 is necessary and sufficient to inhibit oocyte maturation and MAPK activation (Fig. 37). This suggests that GOA-1 is active when sperm are absent. One hypothesis is that in the absence of sperm, an endogenous activating ligand binds to the $G\alpha_{i/o}$-coupled GPCRs and promotes GOA-1 activity. Biogenic amines such as tyramine and octopamine are synthesized by the gonadal sheath cells (Alkema et al., 2005). It is possible that these amines could act as autocrine signals to activate $G\alpha_{i/o}$-coupled receptor in the absence of MSP. MSP could act as an antagonist by binding

and inactivating the $G\alpha_{i/o}$-coupled GPCR. To test this hypothesis, one could examine *tdc-1*/tyrosine decarboxylase and *tbh-1*/ tyramine beta hydroxylase mutants in the presence and absence of sperm. TDC-1 and TBH-1 are required for the biosynthesis of tyramine and octopamine respectively by the gonadal sheath cells (Alkema et al., 2005). An alternative possibility is that the Go-coupled receptor could be a constitutively active receptor that is agonist-independent. MSP could act as an antagonist and thereby "turn off" the signaling.

In the presence of sperm, GSA-1 functions in the somatic sheath-spermathecal cell lineages to promote oocyte meiotic maturation. When sperm is present, MSP likely activates GSA-1 via a $G\alpha_s$-coupled GPCR to promote meiotic maturation (Fig. 37). Therefore, I predicted that elimination of such a GPCR by RNAi should result in low maturation rates in a hermaphrodite background despite the presence of sperm. To identify the $G\alpha_s$-coupled GPCR, I performed RNAi screen against most of the GPCRs in hermaphrodite background (J.A.G. and D.G., unpublished results). In this screen, I was unable to identify any GPCR that display *gsa-1(RNAi)* maturation defect.

In canonical $G\alpha_s$ signaling, activated $G\alpha_s$ stimulates adenylate cyclase resulting in production of cAMP, which binds the regulatory subunit of cAMP-dependent PKA, thereby releasing the active catalytic subunit. *acy-4*, which encodes a homologue of vertebrate adenylate cyclases, is likely to be a downstream effector of $G\alpha_s$ signaling because homozygous *acy-4(ok1806)* and *acy-4(tm2510)* mutants exhibit a phenotype similar to that of *gsa-1(RNAi)*. But

unlike the *gsa-1(null)* mutant, *acy-4(ok1806)* is homozygous viable suggesting that ACY-4 is an effector of $G\alpha_s$ for oocyte maturation but not for other phenotypes. GSA-1 functions in the canonical G-protein signaling pathway to promote meiotic maturation because I identified *kin-2* in the genome-wide RNAi screen. *kin-2*, which encodes the regulatory subunit of cAMP-dependent PKA, is a strong negative regulator of meiotic maturation (Fig. 38). In addition, I showed that KIN-2 functions in the soma to inhibit oocyte maturation in the absence of sperm. Furthermore, KIN-2 functions downstream of GSA-1 because the reduction-of-function mutant in *kin-2* can suppress the *gsa-1(RNAi)* maturation defect. These data suggest that the catalytic subunit of cAMP-dependent PKA should be a positive regulator of meiotic maturation. In *C. elegans*, *kin-1* and F47F2.1 encode proteins that are homologous to the catalytic subunit of cAMP-dependent PKA. However, I do not know whether these proteins are involved, because the RNAi experiments were uninformative and *kin-1(null)* mutants are inviable.

How does GSA-1 signaling in the sheath cell promote meiotic maturation? One interesting model is that GSA-1 promotes meiotic maturation by antagonizing inhibitory sheath/oocyte gap-junctional communication (Fig. 38). This hypothesis originates from the observation that *ceh-18(null)* and *inx-22(null)* mutants can suppress the *gsa-1(RNAi)* maturation defect. *ceh-18* encodes a POU-homeoprotein expressed in gonadal sheath cells which is required for the proper formation and differentiation of sheath cells (Greenstein et al., 1994; Rose et al., 1997).

Figure 38. Speculative models of how GSA-1 may promote oocyte meiotic maturation

In this model, GSA-1 may promote meiotic maturation in part by destabilizing inhibitory gap junctions. Alternatively, GSA-1 may promote maturation by inhibiting either generation or gap junctional transfer of a “maturation inhibiting substance”. In the absence of sperm, GOA-1 generates this “maturation inhibiting substance”.

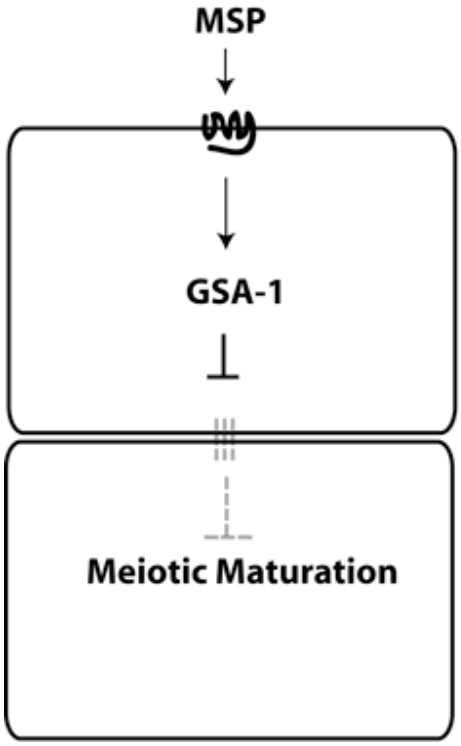
MSP
GSA-1
Meiotic Maturation

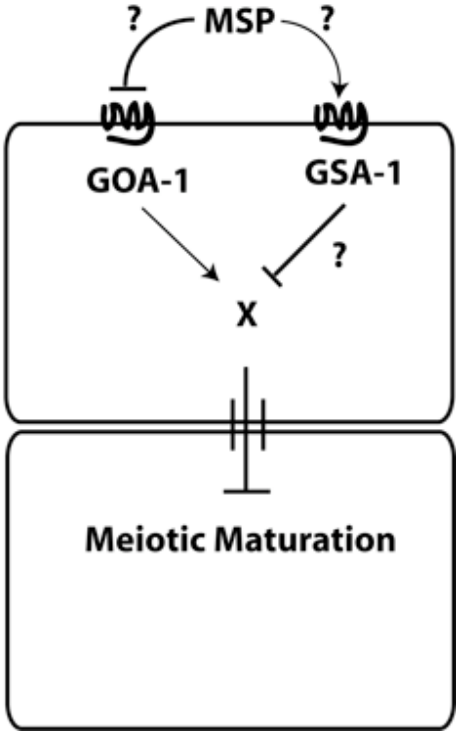
?
MSP
?
GOA-1
GSA-1
?
X
Meiotic Maturation

Ultrastructural studies show the existence of sheath cell-oocyte gap junctions in *C. elegans* (Hall et al., 1999). Interestingly, in *ceh-18(null)* mutants, sheath cells and oocytes are not in close apposition and sheath/oocyte gap junctions are rare or absent (Rose et al., 1997). In the genome-wide RNAi screen, I identified *inx-14* and *inx-22*, which encode for "invertebrate connexin" proteins (Phelan et al., 1998; Phelan and Starich, 2001; Starich et al., 2001). I predict that *inx-14* and *inx-22* are likely oocyte components of the sheath/oocyte gap junctions. Since sheath/oocyte gap junctions must be lost during ovulation, I considered the simplest hypothesis that $G\alpha_s$ signaling may promote meiotic maturation in part by destabilizing inhibitory sheath/oocyte gap junctions (Fig. 38). Studies in some mammalian systems have shown that G protein signaling promotes phosphorylation and disassembly of gap junctions by cAMP-dependent protein kinase A (Dekel, 2005; Lampe et al., 2001; Sela-Abramovich et al., 2006; Somekawa et al., 2005). It is interesting that during meiotic maturation in mice, lutenizing hormone signaling induces phosphorylation of connexin 43 by MAPK resulting in the destabilization of gap junctions (Edry et al., 2006; Sela-Abramovich et al., 2006). Therefore it is possible that MAPK may phosphorylate and target gap junctions for degradation during maturation. Alternatively, $G\alpha_s$ could promote meiotic maturation by inhibiting gap junctional transfer of a "maturation inhibiting substance" (Fig. 38). When sperm is absent, the GOA-1 pathway could generate a "maturation inhibiting substance", which is transferred via gap junctions to the oocytes.

Figure 39. Similarities and Differences in Meiotic Maturation Signaling in *C. elegans* and Mammals

In mammals, both the somatic cells and the oocyte play roles in oocyte meiotic maturation. LH binds to a $G\alpha_s$-coupled GPCR in the somatic cells of the follicle to promote meiotic maturation in part through triggering the release of EGF-like ligands. In addition, gap junctional transfer of cAMP from the cumulus cells to the oocyte is also thought to maintain meiotic arrest. This may involve a second $G\alpha_s$ signaling from the cumulus cells. LH signaling is thought to abrogate this signaling by destabilizing cumulus cell-oocyte gap junctional communication. Another $G\alpha_s$-coupled GPR3 orphan GPCR functions within the oocyte to maintain meiotic arrest. In *C. elegans*, $G\alpha_s$ signaling in somatic cells promotes oocyte meiotic maturation. When sperm is absent, $G\alpha_{o/i}$ pathway inhibits $G\alpha_s$ signaling to maintain meiotic arrest. In the presence of sperm, $G\alpha_s$ may promote meiotic maturation in part by destabilization of the sheath cell-oocyte gap junctions.

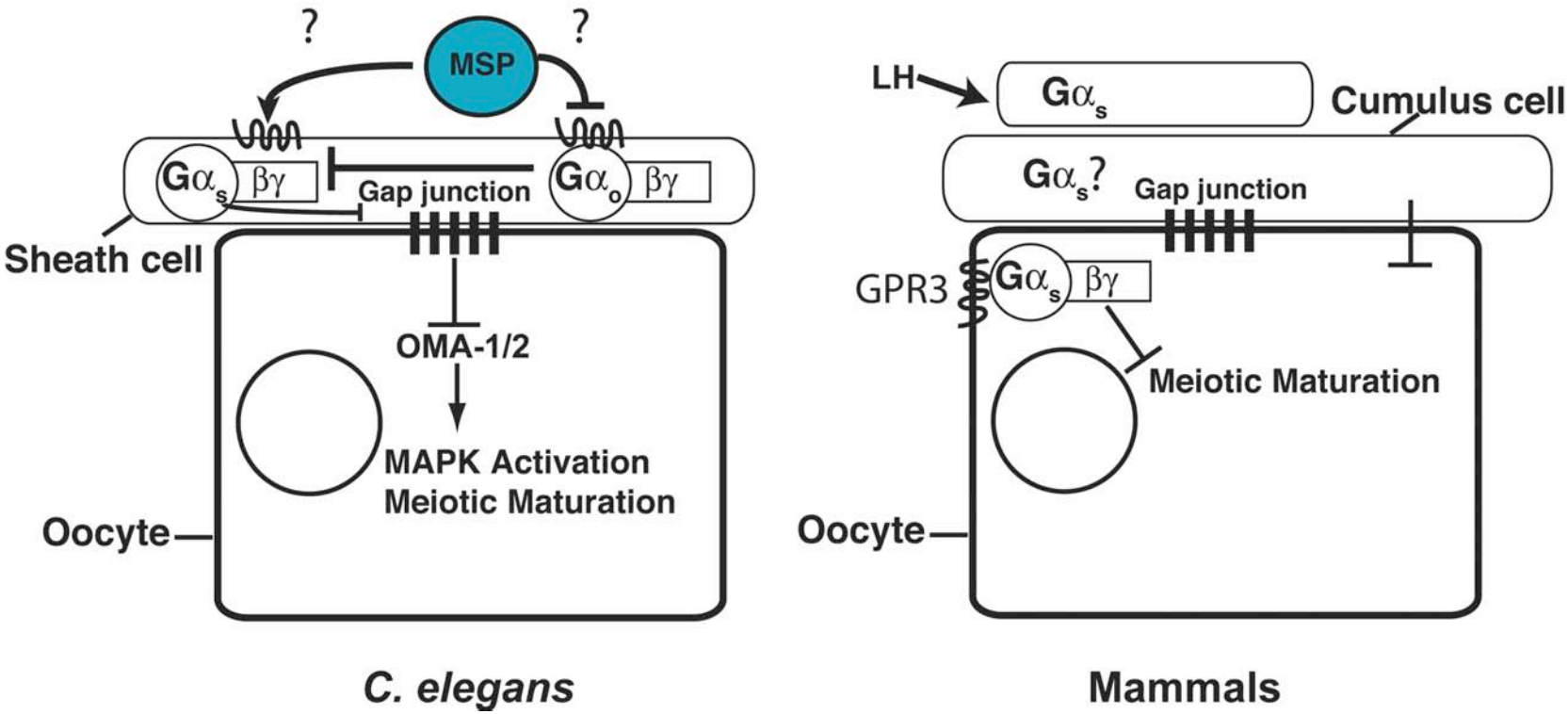
?
MSP
?
Gαs
βγ
Gap junction
Gαo
βγ
Sheath cell
OMA-1/2
MAPK Activation
Meiotic Maturation
Oocyte
C. elegans
LH
Gαs
Cumulus cell
Gαs?
Gap junction
GPR3
Gαs
βγ
Meiotic Maturation
Oocyte
Mammals

In the presence of sperm, activation of the $G\alpha_s$ pathway could inhibit either generation of this substance or its gap junctional transfer (Fig. 38). Additional cell biological as well as ultrastructural studies are necessary to examine this model. In addition, studies of the gap junctional dynamics during meiotic maturation is needed to address the temporal sequence of gap junctional disassembly in *C. elegans*.

My findings highlight interesting parallels and underscore fundamental differences between the control of meiotic maturation in *C. elegans* and mammals (Fig. 39). In both cases, the somatic gonad may function to promote or inhibit meiotic progression depending on the hormonal status of the organism (Fig. 39). For example, removal of oocytes from large antral follicles causes meiotic resumption in most mammals (Edwards, 1965; Pincus and Enzmann, 1935). At the same time, LH receptor signaling in the mural granulosa cell compartment of the follicle promotes meiotic maturation in part through the triggered release of EGF-like ligands that induce meiotic resumption (Park et al., 2004). The LH receptor is a $G\alpha_s$-coupled GPCR, and thus in mammals and *C. elegans*, $G\alpha_s$ signaling in somatic cells has a meiotic maturation-promoting function (Fig. 39). In contrast, $G\alpha_s$ signaling within oocytes involving the GPR3 orphan GPCR plays a critical role in promoting meiotic arrest in mice and rat (Hinckley et al., 2005; Mehlmann, 2005a; Mehlmann, 2005b; Mehlmann et al., 2004). In mammals, these multiple levels of control, involving the somatic gonad and the germ line (Fig. 39), may serve to maintain oocyte homeostasis during prolonged meiotic arrest, while at the same time integrating the

behaviors of the somatic gonad and the germ line so as to coordinate nuclear and cytoplasmic meiotic maturation events with ovulation. In humans, defects in female meiosis I represent the leading cause of congenital birth defects and miscarriage and frequency of these meiotic errors increases with maternal age (Hassold and Hunt, 2001). In the aging ovarian environment, defective hormonal signaling responses may be a factor underlying the high rate of aneuploidy. The conserved regulatory genes described here are therefore expected to give insights on understanding of how perturbations in hormonal signaling might contribute to aneuploidy.

Further outstanding questions

How does somatic G-protein signaling regulate oocyte meiotic maturation and microtubule reorganization?

My study provides an initial characterization of the complex molecular pathways involved in *C. elegans* oocyte meiotic maturation. In addition, this study has raised several interesting questions that need to be examined in the future. Of all the questions, the most interesting one is how the G-protein signaling in the somatic gonad regulates oocyte meiotic maturation and microtubule reorganization. In many species including mammals, the somatic gonad plays an important role in meiotic maturation (Mehlmann, 2005b). Furthermore, the soma-germline interaction involves G-protein signaling in most of the species examined suggesting that somatic G-protein signaling may be an ancient and evolutionarily conserved mechanism. Depending on the species, somatic G-protein signaling either promotes or inhibits meiotic maturation

(Voronina and Wessel, 2003). In addition, recent studies in mice have demonstrated a requirement for G-protein signaling within the oocyte for meiotic maturation (Mehlmann, 2005b; Mehlmann et al., 2004). Therefore, it is important to address how G-protein signaling in the soma controls oocyte meiotic maturation. In *C. elegans*, two antagonistic G-protein signaling pathways function in the somatic gonadal sheath cells to regulate meiotic maturation depending on the presence or absence of sperm. As I mentioned in the Chapter IV, I have begun to address this question using a genetic approach. Since *gsa-1(null)* mutant is larval-lethal (Korswagen et al., 1997), I screened for viable EMS-induced mutations that suppress the *gsa-1 (RNAi)* meiotic maturation defect. We isolated thirty-five mutations that fell into sixteen complementation groups. A genetic screen for temperature-sensitive mutations in essential genes that can suppress the *gsa-1 (RNAi)* meiotic maturation defect is in progress (Borewicz, K., J.A.G., and D.G., unpublished results). Phenotypic and genotypic analysis of these mutants will provide significant insights on the mechanism by which the G-protein signaling regulates meiotic maturation.

How does GOA-1 inhibit oocyte meiotic maturation in the absence of MSP?

Our genetic mosaic analysis suggests that *gsa-1* is epistatic to *goa-1* suggesting that $G\alpha_{o/i}$ signaling might inhibit the $G\alpha_s$ pathway at some level. Three models can be envisioned on the mechanism by which *goa-1* may antagonize $G\alpha_s$ signaling. First, $G\alpha_{o/i}$ signaling could modulate $G\alpha_s$ activity via RGS proteins. In *C. elegans*, GOA-1 inhibits the EGL-30/ $G\alpha_q$ pathway to

regulate egg laying and locomotion (Hajdu-Cronin et al., 1999; van der Linden et al., 2001). In this pathway, GOA-1 is thought to activate the EAT-16/regulator of G-protein signaling (RGS), which inhibit the EGL-30/ $G\alpha_q$ pathway. It is possible that GOA-1 activates a RGS, which in turn inhibits GSA-1. To test this hypothesis, one could examine whether the RGS genes have a role in meiotic maturation. Several of the RGS genes have knock outs and/RNAi clones already available. These mutants could be examined in the presence or absence of sperm for maturation defects. Second, it is possible that $G\alpha_s$ and $G\alpha_{o/i}$ antagonize each other by positively and negatively regulating a common target, such as adenylate cyclase. Third, $G\alpha$s and $G\alpha$o/i may converge at some point far downstream, in effect defining parallel regulatory inputs.

Does the EGL-30/$G\alpha_q$ pathway have a role in meiotic maturation?

In *C. elegans*, the $G\alpha_s$, $G\alpha_q$ and $G\alpha_{o/l}$ pathways function together to control acetylcholine release by the ventral cord motor neurons during egg-laying and locomotion (Reynolds et al., 2005; Schade et al., 2005).
In this pathway, the $G\alpha_q$ and $G\alpha_{o/l}$ function antagonistically to each other to regulate acetylcholine release whereas $G\alpha_s$ positively modifies the signaling output via an unknown mechanism. Therefore, it is possible that the $G\alpha_q$ pathway has a similar role in meiotic maturation. To test this one could examine loss-of-function and gain-of-function alleles of $G\alpha_q$ in the hermaphrodite and female backgrounds.

What are the GPCRs involved in oocyte meiotic maturation?

This study has provided evidence that G-protein signaling pathways in the somatic gonad regulate oocyte meiotic maturation in *C. elegans*. This raises an interesting question of which GPCRs are involved in oocyte meiotic maturation. More than 1000 GPCRs are present in *C. elegans*. It is possible that multiple GPCRs are involved in the process. Previous DNA microarray and in-situ expression data can be used to generate a list of candidate GPCRs that are enriched in the gonadal sheath cells. Combinatorial RNAi and/or null mutants can be performed to examine oocyte meiotic maturation in presence and absence of sperm. In addition, one can express the GPCRs in heterologous cell culture to determine whether MSP can bind to any of these candidate receptors. Genetic epistasis analysis can be performed with the genes in $G\alpha_s$ and $G\alpha_{o/i}$ pathways to elucidate the role of the candidate GPCRs in meiotic maturation.

How is oocyte meiotic maturation so strictly spatially regulated?

In the presence of sperm, the most proximal oocyte undergoes meiotic maturation every ~ 20 minutes. Meiotic maturation is spatially restricted to the most proximal (–1) oocyte; suggesting that there must be mechanism(s) to prevent distal (–2, –3 and so on) oocytes from maturing. How this spatial restriction is maintained is unknown. So far, no mutants have been described in which the spatial order of maturation is disrupted. It will be interesting to see whether the somatic G-protein pathways have a role in this process. GOA-1 and KIN-2 are strong negative regulators of meiotic maturation; however, the

spatial order of maturation is still maintained in the mutant hermaphrodites or females. This suggests that there must be additional mechanism(s) by which the meiotic maturation is blocked in the more distal oocytes.

How does VAB-1 regulate oocyte meiotic maturation?

In the absence of sperm, the VAB-1/Eph receptor pathway is necessary within the germline to inhibit oocyte meiotic maturation (Miller et al., 2003). MSP promotes meiotic maturation by binding directly to VAB-1 and antagonizing its function (Govindan et al., 2006; Miller et al., 2003) . VAB-1 is the only known MSP receptor involved in oocyte meiotic maturation. However, the mechanism by which VAB-1 inhibits meiotic maturation and how MSP signaling antagonizes VAB-1 signaling to promote meiotic maturation are not known. The identification of DAB-1, VAV-1, PQN-19, and PKC-1 as potential candidates for genes in the VAB-1 pathway raises several interesting questions that need to be investigated in the future. First, how DAB-1, VAV-1, PQN-19, and PKC-1 regulate oocyte meiotic maturation needs to be examined. Second, how these proteins regulate VAB-1 function needs to be addressed. Third, since DAB-1, VAV-1, PQN-19, and PKC-1 have several conserved domains; it will be interesting to analyze the necessity and sufficiency of these domains for the protein function which likely provide significant insights. Fourth, whether these proteins interact directly with VAB-1 can be tested. Finally, the functional interaction between these genes can be examined to address how they coordinately regulate meiotic maturation.

How do gap junctions regulate germline development?

Ultrastructural studies have demonstrated the existence of sheath cell-oocyte gap junctions and we have hypothesized that these play a role in regulating oocyte meiotic maturation (Hall et al., 1999; Rose et al., 1997). My studies identified two innexins (INX-22 and INX-14), which encode invertebrate connexins, as negative regulators of oocyte meiotic maturation. How gap junctions regulate meiotic maturation is not known. Since oocytes constantly undergo maturation and ovulation in hermaphrodites, gap junctions must be constantly assembled and disassembled as the next-to-be matured oocyte moves proximally in the gonad arm. In the females, oocytes are arrested and the dynamics of gap junction assembly/disassembly may be altered in such a way that the gap junctions are more stable. My studies suggest that the gap junctions are targets of G-protein signaling. It is possible that during meiotic maturation, $G\alpha_s$ signaling destabilizes the gap junctions between the sheath cell and the -1 oocyte while the gap junctions in between the sheath cell and the distal oocytes are stable. However, the localization pattern of gap junctions with respect to the position of the oocyte needs to be examined.

To address these issues, we can examine gap junctions using ultrastructural and or cell biological tools in the presence and absence of sperm. Also, we can examine gap junctions in *gsa-1(RNAi)* hermaphrodites and *goa-1(null)* females. Recently, two putative null mutations in *inx-14* became available to us. A preliminary examination of these mutants has revealed that homozygous *inx-14(null)* mutants are sterile because their germlines do not proliferate. At

present, the reason for the proliferation defect is not known. In contrast, *inx-22(null)* mutants are viable and do not display any early germline proliferation defects suggesting that *inx-14* may function with a different innexin to regulate germline proliferation. The *inx-14(null)* germline proliferation defect is intriguing because previous ultrastructural studies did not reveal any gap junctions in the distal germline. Therefore, cell biological and extensive ultrastructural studies at various stages of development are required to investigate the role of gap junctions during early germline development.

Summary

In humans, defects in female meiosis I represent the leading cause of congenital birth defects and miscarriage, and the frequency of these meiotic errors increases with maternal age. In the aging ovarian environment, defective hormonal signaling responses may be a factor underlying the high rate of aneuploidy. In this dissertation research, I focused on understanding the signaling mechanisms that control meiotic progression using *C. elegans* as a model organism. My studies show that conserved signaling genes negatively regulate oocyte meiotic maturation in *C. elegans*. However, in the absence of negative regulators, meiotic maturation proceeds normally with no appreciable defects in meiotic spindle assembly. My hypothesis is that additional layers of control, such as those provided by the spindle checkpoint mechanism, may ensure a high fidelity of timely chromosome segregation. Thus, perturbations in hormonal signaling combined with defective spindle checkpoint may contribute

to aneuploidy in *C. elegans*. As we peel back the layers of control, it will be interesting to determine whether similar mechanisms might operate in the ageing human ovarian environment.

REFERENCES

Abrieu, A., Doree, M. and Fisher, D. (2001). The interplay between cyclin-B-Cdc2 kinase (MPF) and MAP kinase during maturation of oocytes. *J Cell Sci* **114**, 257-67.

Adams, P. D. and Parker, P. J. (1992). Activation of mitogen-activated protein (MAP) kinase by a MAP kinase- kinase. *J. Biol. Chem.* **267**, 13135-13137.

Adams, R. R., Carmena, M. and Earnshaw, W. C. (2001). Chromosomal passengers and the (aurora) ABCs of mitosis. *Trends Cell Biol* **11**, 49-54.

Afshar, K., Willard, F. S., Colombo, K., Johnston, C. A., McCudden, C. R., Siderovski, D. P. and Gonczy, P. (2004). RIC-8 is required for GPR-1/2-dependent Galpha function during asymmetric division of C. elegans embryos. *Cell* **119**, 219-30.

Albertson, D. G. and Thomson, J. N. (1993). Segregation of holocentric chromosomes at meiosis in the nematode, Caenorhabditis elegans. *Chromosome Res* **1**, 15-26.

Alkema, M. J., Hunter-Ensor, M., Ringstad, N. and Horvitz, H. R. (2005). Tyramine Functions independently of octopamine in the Caenorhabditis elegans nervous system. *Neuron* **46**, 247-60.

Anderson, N. G., Maller, J. L., Tonks, N. K. and Sturgill, T. W. (1990). Requirement for integration of signals from two distinct phosphorylation pathways for activation of MAP kinase. *Nature* **343**, 651.

Arantes-Oliveira, N., Apfeld, J., Dillin, A., and Kenyon, C. (2002). Regulation of life-span by germ-line stem cells in Caenorhabditis elegans. Science 295, 502–505.

Audhya, A., Hyndman, F., McLeod, I. X., Maddox, A. S., Yates, J. R., 3rd, Desai, A. and Oegema, K. (2005). A complex containing the Sm protein CAR-1 and the RNA helicase CGH-1 is required for embryonic cytokinesis in Caenorhabditis elegans. *J Cell Biol* **171**, 267-79.

Austin, J., and Kimble. J. (1987) *glp-1* is required in the germ line for regulation of the decision between mitosis and meiosis in *C. elegans*. *Cell* **51**, 589-599.

Bargmann, C. I. (1998). Neurobiology of the Caenorhabditis elegans genome. *Science* **282**, 2028-33.

Bastiani, C. and Mendel, J. (2006). Heterotrimeric G proteins in *C. elegans* WormBook, ed. The C. elegans Research Community, WormBook, http://www.wormbook.org.

Batchelder, C., Dunn, M. A., Choy, B., Suh, Y., Cassie, C., Shim, E. Y., Shin, T. H., Mello, C., Seydoux, G. and Blackwell, T. K. (1999). Transcriptional repression by the Caenorhabditis elegans germ-line protein PIE-1. *Genes Dev* **13**, 202-12.

Bembenek, J. N., Richie, C. T., Squirrell, J. M., Campbell, J. M., Eliceiri, K. W., Poteryaev, D., Spang, A., Golden, A. and White, J. G. (2007). Cortical granule exocytosis in C. elegans is regulated by cell cycle components including separase. *Development*.

Benian, G., L'Hernault, S. & Morris, M. (1993). Additional sequence complexity in the muscle gene, *unc-22*, and its encoded protein, twitchin, of *Caenorhabiditis elegans*. *Genetics* **134**, 1097–1104.

Berger, A. J., Hart, A. C. and Kaplan, J. M. (1998). Galpha s-Induced Neurodegeneration in Caenorhabditis elegans. *J. Neurosci.* **18**, 2871-2880.

Berry, L. W., Westlund, B., and Schedl, T. (1997). Germ-line tumor formation caused by activation of *glp-1*, a Caenorhabditis elegans member of the Notch family of receptors. *Development* **124,** 925–936.

Bhalla, N. and Dernburg, A. F. (2005). A conserved checkpoint monitors meiotic chromosome synapsis in Caenorhabditis elegans. *Science* **310**, 1683-6.

Bottino, D., Mogilner, A., Roberts, T., Stewart, M. and Oster, G. (2002). How nematode sperm crawl. *J Cell Sci* **115**, 367-84.

Boxem, M., Srinivasan, D. G. and van den Heuvel, S. (1999). The Caenorhabditis elegans gene ncc-1 encodes a cdc2-related kinase required for M phase in meiotic and mitotic cell divisions, but not for S phase. *Development* **126**, 2227-39.

Boyle, J. A. and Ernst, S. G. (1989). Sea urchin oocytes possess elaborate cortical arrays of microfilaments, microtubules, and intermediate filaments. *Dev Biol* **134**, 72-84.

Brenner, S. (1974). The genetics of Caenorhabditis elegans. *Genetics* **77**, 71-94.

Brundage, L., Avery, L., Katz, A., Kim, U. J., Mendel, J. E., Sternberg, P. W. and Simon, M. I. (1996). Mutations in a C. elegans Gqalpha gene disrupt movement, egg laying, and viability. *Neuron* **16**, 999-1009.

Bui, Y. K. and Sternberg, P. W. (2002). Caenorhabditis elegans inositol 5-phosphatase homolog negatively regulates inositol 1,4,5-triphosphate signaling in ovulation. *Mol Biol Cell* **13**, 1641-51.

Burrows, A. E., Sceurman, B. K., Kosinski, M. E., Richie, C. T., Sadler, P. L., Schumacher, J. M. and Golden, A. (2006). The C. elegans Myt1 ortholog is required for the proper timing of oocyte maturation. *Development* **133**, 697-709.

Cabrera-Vera, T. M., Vanhauwe, J., Thomas, T. O., Medkova, M., Preininger, A., Mazzoni, M. R. and Hamm, H. E. (2003). Insights into G protein structure, function, and regulation. *Endocr Rev* **24**, 765-81.

Carabatsos, M. J., Sellitto, C., Goodenough, D. A. and Albertini, D. F. (2000). Oocyte-granulosa cell heterologous gap junctions are required for the coordination of nuclear and cytoplasmic meiotic competence. *Dev Biol* **226**, 167-79.

Carazo-Salas, R. E., Guarguaglini, G., Gruss, O. J., Segref, A., Karsenti, E. and Mattaj, I. W. (1999). Generation of GTP-bound Ran by RCC1 is required for chromatin-induced mitotic spindle formation. *Nature* **400**, 178-81.

Champion, M. D., & Hawley, R. S. (2002). Playing for half the deck: the molecular biology of meiosis. *Nat Cell Biol, 4 Suppl,* s50-56.

Chase, D., Serafinas, C., Ashcroft, N., Kosinski, M., Longo, D., Ferris, D. K. and Golden, A. (2000). The polo-like kinase PLK-1 is required for nuclear envelope breakdown and the completion of meiosis in Caenorhabditis elegans. *Genesis* **26**, 26-41.

Chiba, K., Kontani, K., Tadenuma, H., Katada, T. and Hoshi, M. (1993). Induction of starfish oocyte maturation by the beta gamma subunit of starfish G protein and possible existence of the subsequent effector in cytoplasm. *Mol. Biol. Cell* **4**, 1027-1034.

Chiba, K., Tadenuma, H., Matsumoto, M., Takahashi, K., Katada, T. and Hoshi, M. (1992). The primary structure of the alpha subunit of a starfish guanosine-nucleotide-binding regulatory protein involved in 1-methyladenine-induced oocyte maturation. *Eur J Biochem* **207**, 833-8.

Chin-Sang, I. D., George, S. E., Ding, M., Moseley, S. L., Lynch, A. S. and Chisholm, A. D. (1999). The ephrin VAB-2/EFN-1 functions in neuronal signaling to regulate epidermal morphogenesis in C. elegans. *Cell* **99**, 781-90.

Chin-Sang, I. D., Moseley, S. L., Ding, M., Harrington, R. J., George, S. E. and Chisholm, A. D. (2002). The divergent C. elegans ephrin EFN-4 functions inembryonic morphogenesis in a pathway independent of the VAB-1 Eph receptor. *Development* **129**, 5499-510.

Church, D. L., Guan, K. L. and Lambie, E. J. (1995). Three genes of the MAP kinase cascade, mek-2, mpk-1/sur-1 and let-60 ras, are required for meiotic cell cycle progression in Caenorhabditis elegans. *Development* **121**, 2525-35.

Clandinin, T. R., DeModena, J. A. and Sternberg, P. W. (1998). Inositol trisphosphate mediates a RAS-independent response to LET-23 receptor tyrosine kinase activation in C. elegans. *Cell* **92**, 523-33.

Clandinin, T. R. and Mains, P. E. (1993). Genetic studies of mei-1 gene activity during the transition from meiosis to mitosis in Caenorhabditis elegans. *Genetics* **134**, 199-210.

Clark-Maguire, S. and Mains, P. E. (1994a). Localization of the mei-1 gene product of Caenorhaditis elegans, a meiotic-specific spindle component. *J Cell Biol* **126**, 199-209.

Clark-Maguire, S. and Mains, P. E. (1994b). mei-1, a gene required for meiotic spindle formation in Caenorhabditis elegans, is a member of a family of ATPases. *Genetics* **136**, 533-46.

Colaiácovo, M. P. (2006) The many facets of SC function during *C. elegans* meiosis. *Chromosoma* **115,** 195-211.

Coleman, T. R. and Dunphy, W. G. (1994). Cdc2 regulatory factors. *Curr Opin Cell Biol* **6**, 877-82.

Colledge, W.H., Carlton, M.B.L., Udy, G.B., Evans, M.J. (1994) Disruption of c-mos causes parthenogenetic development of unfertilized mouse eggs. *Nature* **370**, 65-68.

Colombo, K., Grill, S. W., Kimple, R. J., Willard, F. S., Siderovski, D. P. and Gonczy, P. (2003). Translation of Polarity Cues into Asymmetric Spindle Positioning in Caenorhabditis elegans Embryos. *Science* **300**, 1957-1961.

Conti, M., Andersen, C. B., Richard, F., Mehats, C., Chun, S. Y., Horner, K., Jin, C. and Tsafriri, A. (2002). Role of cyclic nucleotide signaling in oocyte maturation. *Mol Cell Endocrinol* **187**, 153-9.

Corrigan, C., Subramanian, R. and Miller, M. A. (2005). Eph and NMDA receptors control Ca2+/calmodulin-dependent protein kinase II activation during C. elegans oocyte meiotic maturation. *Development* **132**, 5225-37.

Cowan, C. R. and Hyman, A. A. (2004). Centrosomes direct cell polarity independently of microtubule assembly in C. elegans embryos. *Nature* **431**, 92-6.

Cowan, C. W., Shao, Y. R., Sahin, M., Shamah, S. M., Lin, M. Z., Greer, P. L., Gao, S., Griffith, E. C., Brugge, J. S. and Greenberg, M. E. (2005). Vav family GEFs link activated Ephs to endocytosis and axon guidance. *Neuron* **46**, 205-17.

Crews, C. M., Alessandrini, A. and Erikson, R. L. (1992). The primary structure of MEK, a protein kinase that phosphorylates the ERK gene product. *Science* **258**, 478-480.

Davis, M. W., Hammarlund, M., Harrach, T., Hullett, P., Olsen, S. and Jorgensen, E. M. (2005). Rapid single nucleotide polymorphism mapping in C. elegans. *BMC Genomics* **6**, 118.

De Vries, L., Zheng, B., Fischer, T., Elenko, E. and Farquhar, M. G. (2000). The Regulator of G Protein Signaling Family. *Annual Review of Pharmacology and Toxicology* **40**, 235-271.

Dekel, N. (2005). Cellular, biochemical and molecular mechanisms regulating oocyte maturation. *Mol Cell Endocrinol* **234**, 19-25.

Detwiler, M. R., Reuben, M., Li, X., Rogers, E. and Lin, R. (2001). Two zinc finger proteins, OMA-1 and OMA-2, are redundantly required for oocyte maturation in C. elegans. *Dev Cell* **1**, 187-99.

DeWire, S. M., Ahn, S., Lefkowitz, R. J. and Shenoy, S. K. (2007). β-Arrestins and Cell Signaling. *Annual Review of Physiology* **69**, 483-510.

Dong, M. Q., Chase, D., Patikoglou, G. A. and Koelle, M. R. (2000). Multiple RGS proteins alter neural G protein signaling to allow C. elegans to rapidly change behavior when fed. *Genes Dev* **14**, 2003-14.

Doree, M. and Hunt, T. (2002). From Cdc2 to Cdk1: when did the cell cycle kinase join its cyclin partner? *J Cell Sci* **115**, 2461-4.

Duffy, H.S., Iacobas, I., Hotchkiss, K., Hirst-Jensen, B.J., Bosco, A., Dandachi, N., Dermietzel, R., Sorgen, P.L., Spray, D.C. (2007). The gap

junction protein connexin32 interacts with the Src homology 3/hook domain of discs large homolog 1. *J. Biol. Chem* **282,** 9789-9796.

Edry, I., Sela-Abramovich, S. and Dekel, N. (2006). Meiotic arrest of oocytes depends on cell-to-cell communication in the ovarian follicle. *Mol Cell Endocrinol* **252**, 102-6.

Edwards, R. G. (1965). Maturation in vitro of mouse, sheep, cow, pig, rhesus monkey and human ovarian oocytes. *Nature* **208**, 349-51.

Eggan, K., Jurga, S., Gosden, R., Min, I. M. and Wagers, A. J. (2006). Ovulated oocytes in adult mice derive from non-circulating germ cells. *Nature* **441**, 1109-14.

Eppig, J. J. (1991). Intercommunication between mammalian oocytes and companion somatic cells. *Bioessays* **13**, 569-74.

Eyers, P. A., Liu, J., Hayashi, N. R., Lewellyn, A. L., Gautier, J. and Maller, J. L. (2005). Regulation of the G2/M Transition in Xenopus Oocytes by the cAMP-dependent Protein Kinase. *J. Biol. Chem.* **280**, 24339-24346.

Fan, H. Y. and Sun, Q. Y. (2004). Involvement of mitogen-activated protein kinase cascade during oocyte maturation and fertilization in mammals. *Biol Reprod* **70**, 535-47.

Farfel, Z., Bourne, H. R. and Iiri, T. (1999). The Expanding Spectrum of G Protein Diseases. *N Engl J Med* **340**, 1012-1020.

Ferguson, S. S. (2001). Evolving concepts in G protein-coupled receptor endocytosis: the role in receptor desensitization and signaling. *Pharmacol Rev* **53**, 1-24.

Ferrell, J. E., Jr. (1999a). Building a cellular switch: more lessons from a good egg. *Bioessays* **21**, 866-70.

Ferrell, J. E., Jr. (1999b). Xenopus oocyte maturation: new lessons from a good egg. *Bioessays* **21**, 833-42.

Fire, A. (1986). Integrative transformation of C. elegans. *EMBO Journal* **5**, 2673-2680.

Flower, D. R. (1999). Modelling G-protein-coupled receptors for drug design. *Biochimica et Biophysica Acta (BBA) - Reviews on Biomembranes* **1422**, 207.

Fraser, A. G., Kamath, R. S., Zipperlen, P., Martinez-Campos, M., Sohrmann, M. and Ahringer, J. (2000). Functional genomic analysis of C. elegans chromosome I by systematic RNA interference. *Nature* **408**, 325.

Fukuto, H. S., Ferkey, D. M., Apicella, A. J., Lans, H., Sharmeen, T., Chen, W., Lefkowitz, R. J., Jansen, G., Schafer, W. R. and Hart, A. C. (2004). G protein-coupled receptor kinase function is essential for chemosensation in C. elegans. *Neuron* **42**, 581-93.

Furukawa, M., He, Y. J., Borchers, C. and Xiong, Y. (2003). Targeting of protein ubiquitination by BTB-Cullin 3-Roc1 ubiquitin ligases. *Nat Cell Biol* **5**, 1001-7.

Gallo, C. J., Hand, A. R., Jones, T. L. and Jaffe, L. A. (1995). Stimulation of Xenopus oocyte maturation by inhibition of the G-protein alpha S subunit, a component of the plasma membrane and yolk platelet membranes. *J. Cell Biol.* **130**, 275-284.

Gautier, J., Minshull, J., Lohka, M., Glotzer, M., Hunt, T. and Maller, J. L. (1990). Cyclin is a component of maturation-promoting factor from Xenopus. *Cell* **60**, 487-94.

Gautier, J., Norbury, C., Lohka, M., Nurse, P. and Maller, J. (1988). Purified maturation-promoting factor contains the product of a Xenopus homolog of the fission yeast cell cycle control gene cdc2+. *Cell* **54**, 433-9.

George, S. E., Simokat, K., Hardin, J. and Chisholm, A. D. (1998). The VAB-1 Eph receptor tyrosine kinase functions in neural and epithelial morphogenesis in C. elegans. *Cell* **92**, 633-43.

Gibert, M. A., Starck, J. and Beguet, B. (1984). Role of the gonad cytoplasmic core during oogenesis of the nematode Caenorhabditis elegans. *Biol Cell* **50**, 77-85.

Gilchrist, R. B., Ritter, L. J. and Armstrong, D. T. (2004). Oocyte-somatic cell interactions during follicle development in mammals. *Anim Reprod Sci* **82-83**, 431-46.

Gilliland, W. D. and Hawley, R. S. (2005). Cohesin and the maternal age effect. *Cell* **123**, 371-3.

Gilman, A. G. (1987). G Proteins: Transducers of Receptor-Generated Signals. *Annual Review of Biochemistry* **56**, 615-649.

Goldstein, B. and Hird, S. N. (1996). Specification of the anteroposterior axis in Caenorhabditis elegans. *Development* **122**, 1467-74.

Gosden, R. G., Laing, S. C., Felicio, L. S., Nelson, J. F. and Finch, C. E. (1983). Imminent oocyte exhaustion and reduced follicular recruitment mark the transition to acyclicity in aging C57BL/6J mice. *Biol Reprod* **28**, 255-60.

Gotta, M. and Ahringer, J. (2001). Distinct roles for Galpha and Gbetagamma in regulating spindle position and orientation in Caenorhabditis elegans embryos. *Nat Cell Biol* **3**, 297-300.

Govindan, J., Cheng, H., Harris, J. and Greenstein, D. (2006). Galpha(oVi) and Galpha(s) Signaling Function in Parallel with the MSP\/Eph Receptor to Control Meiotic Diapause in C. elegans. *Curr Biol* **16**, 1257-1268.

Greenstein, D. (2005). Control of oocyte meiotic maturation and fertilization. *WormBook, ed. The C. elegans Research Community, WormBook.* http://www.wormbook.org.

Greenstein, D., Hird, S., Plasterk, R. H., Andachi, Y., Kohara, Y., Wang, B., Finney, M. and Ruvkun, G. (1994). Targeted mutations in the Caenorhabditis elegans POU homeo box gene ceh- 18 cause defects in oocyte cell cycle arrest, gonad migration, and epidermal differentiation. *Genes Dev* **8**, 1935-48.

Greenstein, D. and Lee, L. A. (2006). Oocyte-to-embryo transition: kinase cabal plots regime change. *Curr Biol* **16**, R93-5.

Gumienny, T. L., Lambie, E., Hartwieg, E., Horvitz, H. R. and Hengartner, M. O. (1999). Genetic control of programmed cell death in the Caenorhabditis elegans hermaphrodite germline. *Development* **126**, 1011-22.

Hajdu-Cronin, Y. M., Chen, W. J., Patikoglou, G., Koelle, M. R. and Sternberg, P. W. (1999). Antagonism between Goalpha and Gqalpha in Caenorhabditis elegans: the RGS protein EAT-16 is necessary for Goalpha signaling and regulates Gqalpha activity. *Genes Dev.* **13**, 1780-1793.

Hall, D. H., Winfrey, V. P., Blaeuer, G., Hoffman, L. H., Furuta, T., Rose, K. L., Hobert, O. and Greenstein, D. (1999). Ultrastructural features of the adult hermaphrodite gonad of Caenorhabditis elegans: relations between the germ line and soma. *Dev Biol* **212**, 101-23.

Hamm, H. E. (1998). The Many Faces of G Protein Signaling. *J. Biol. Chem.* **273**, 669-672.

Harris, J. E., Govindan, J. A., Yamamoto, I., Schwartz, J., Kaverina, I., & Greenstein, D. (2006). The major sperm protein signals the reorganization of oocyte microtubles prior to fertilization in Caenorhabditis elegans. *Dev Biol* **299**, 105-121.

Hart, M. J., Jiang, X., Kozasa, T., Roscoe, W., Singer, W. D., Gilman, A. G., Sternweis, P. C. and Bollag, G. (1998). Direct Stimulation of the Guanine Nucleotide Exchange Activity of p115 RhoGEF by G{alpha}13. *Science* **280**, 2112-2114.

Hartman, J. J. and Vale, R. D. (1999). Microtubule disassembly by ATP-dependent oligomerization of the AAA enzyme katanin. *Science* **286**, 782-5.

Hashimoto, N., Watanabe, N., Furuta, Y., Tamemoto, H., Sagata, N., Yokoyama, M., Okazaki, K., Nagayoshi, M., Takeda, N., Ikawa, Y., Aizawa, S. (1994). Parthenogenetic activation of oocytes in *c-mos-deficient* mice. *Nature* **370**, 68-71.

Hassold, T. and Hunt, P. (2001). To err (meiotically) is human: the genesis of human aneuploidy. *Nat Rev Genet* **2**, 280-91.

Hassold, T., Hunt, P. A. and Sherman, S. (1993). Trisomy in humans: incidence, origin and etiology. *Curr Opin Genet Dev* **3**, 398-403.

Hassold, T. and Sherman, S. (2000). Down syndrome: genetic recombination and the origin of the extra chromosome 21. *Clin Genet* **57**, 95-100.

Hassold, T., Sherman, S. and Hunt, P. A. (1995). The origin of trisomy in humans. *Prog Clin Biol Res* **393**, 1-12.

Heald, R., Tournebize, R., Blank, T., Sandaltzopoulos, R., Becker, P., Hyman, A. and Karsenti, E. (1996). Self-organization of microtubules into bipolar spindles around artificial chromosomes in Xenopus egg extracts. *Nature* **382**, 420-5.

Hildebrandt, J. D. (1997). Role of subunit diversity in signaling by heterotrimeric G proteins. *Biochemical Pharmacology* **54**, 325.

Hinckley, M., Vaccari, S., Horner, K., Chen, R. and Conti, M. (2005). The G-protein-coupled receptors GPR3 and GPR12 are involved in cAMP signaling and maintenance of meiotic arrest in rodent oocytes. *Dev Biol* **287**, 249-61.

Hirsh, D., Oppenheim, D. and Klass, M. (1976). Development of the reproductive system of Caenorhabditis elegans. *Dev Biol* **49**, 200-19.

Hodges, C. A., Ilagan, A., Jennings, D., Keri, R., Nilson, J. and Hunt, P. A. (2002). Experimental evidence that changes in oocyte growth influence meiotic chromosome segregation. *Hum Reprod* **17**, 1171-80.

Hodges, C. A., Revenkova, E., Jessberger, R., Hassold, T. J. and Hunt, P. A. (2005). SMC1beta-deficient female mice provide evidence that cohesins are a missing link in age-related nondisjunction. *Nat Genet* **37**, 1351-5.

Holmberg, J. and Frisen, J. (2002). Ephrins are not only unattractive. *Trends Neurosci* **25**, 239-43.

Holmes, A., Flett, A., Coudreuse, D., Korswagen, H. C. and Pettitt, J. (2007). C. elegans Disabled is required for cell-type specific endocytosis and is essential in animals lacking the AP-3 adaptor complex. *J Cell Sci* **120**, 2741-51.

Hoskins, R., Hajnal, A. F., Harp, S. A. and Kim, S. K. (1996). The *C. elegans* vulval induction gene *lin-2* encodes a member of the MAGUK family of cell junction proteins. *Development* **122**, 97-111.

Hsin, H., and Kenyon, C. (1999). Signals from the reproductive system regulate the lifespan of *C. elegans*. Nature 399, 362–366.

Hsu, J. Y., Sun, Z. W., Li, X., Reuben, M., Tatchell, K., Bishop, D. K., Grushcow, J. M., Brame, C. J., Caldwell, J. A., Hunt, D. F. et al. (2000). Mitotic phosphorylation of histone H3 is governed by Ipl1/aurora kinase and Glc7/PP1 phosphatase in budding yeast and nematodes. *Cell* **102**, 279-91.

Hubbard, E. J. and Greenstein, D. (2000). The Caenorhabditis elegans gonad: a test tube for cell and developmental biology. *Dev Dyn* **218**, 2-22.
Hunt, P. A. and Hassold, T. J. (2002). Sex matters in meiosis. *Science* **296**, 2181-3.

Hunt, P. A., Koehler, K. E., Susiarjo, M., Hodges, C. A., Ilagan, A., Voigt, R. C., Thomas, S., Thomas, B. F. and Hassold, T. J. (2003). Bisphenol a exposure causes meiotic aneuploidy in the female mouse. *Curr Biol* **13**, 546-53.

Hunt, P. A. and LeMaire-Adkins, R. (1998). Genetic control of mammalian female meiosis. *Curr Top Dev Biol* **37**, 359-81.

Hurowitz, E. H., Melnyk, J. M., Chen, Y.-J., Kouros-Mehr, H., Simon, M. I. and Shizuya, H. (2000). Genomic Characterization of the Human Heterotrimeric G Protein {alpha}, {beta}, and {gamma} Subunit Genes. *DNA Res* **7**, 111-120.

Italiano, J. E., Jr., Roberts, T. M., Stewart, M. and Fontana, C. A. (1996). Reconstitution in vitro of the motile apparatus from the amoeboid sperm of Ascaris shows that filament assembly and bundling move membranes. *Cell* **84**, 105-14.

Italiano, J. E., Jr., Stewart, M. and Roberts, T. M. (2001). How the assembly dynamics of the nematode major sperm protein generate amoeboid cell motility. *Int Rev Cytol* **202**, 1-34.

Ivanovska, I., Lee, E., Kwan, K. M., Fenger, D. D. and Orr-Weaver, T. L. (2004). The Drosophila MOS ortholog is not essential for meiosis. *Curr Biol* **14**, 75-80.

Iwasaki, K., McCarter, J., Francis, R. and Schedl, T. (1996). emo-1, a Caenorhabditis elegans Sec61p gamma homologue, is required for oocyte development and ovulation. *J Cell Biol* **134**, 699-714.

Jaffe, L. A., Gallo, C. J., Lee, R. H., Ho, Y. K. and Jones, T. L. (1993). Oocyte maturation in starfish is mediated by the beta gamma-subunit complex of a G-protein. *J. Cell Biol.* **121**, 775-783.

Jansen, G., Thijssen, K. L., Werner, P., van derHorst, M., Hazendonk, E. and Plasterk, R. H. A. (1999). The complete family of genes encoding G proteins of Caenorhabditis elegans. *Nat Genet* **21**, 414.

Jaramillo-Lambert, A., Ellefson, M., Villeneuve, A. M. and Engebrecht, J. (2007). Differential timing of S phases, X chromosome replication, and meiotic prophase in the C. elegans germ line. *Dev Biol* **308**, 206-21.

Johnson, J., Bagley, J., Skaznik-Wikiel, M., Lee, H. J., Adams, G. B., Niikura, Y., Tschudy, K. S., Tilly, J. C., Cortes, M. L., Forkert, R. et al. (2005). Oocyte generation in adult mammalian ovaries by putative germ cells in bone marrow and peripheral blood. *Cell* **122**, 303-15.

Johnson, J., Canning, J., Kaneko, T., Pru, J. K. and Tilly, J. L. (2004). Germline stem cells and follicular renewal in the postnatal mammalian ovary. *Nature* **428**, 145-50.

Kaitna, S., Mendoza, M., Jantsch-Plunger, V. and Glotzer, M. (2000). Incenp and an aurora-like kinase form a complex essential for chromosome segregation and efficient completion of cytokinesis. *Curr Biol* **10**, 1172-81.

Kaitna, S., Pasierbek, P., Jantsch, M., Loidl, J. and Glotzer, M. (2002). The aurora B kinase AIR-2 regulates kinetochores during mitosis and is required for separation of homologous Chromosomes during meiosis. *Curr Biol* **12**, 798-812.

Kalab, P., Pu, R. T. and Dasso, M. (1999). The ran GTPase regulates mitotic spindle assembly. *Curr Biol* **9**, 481-4.

Kalinowski, R. R., Jaffe, L. A., Foltz, K. R. and Giusti, A. F. (2003). A receptor linked to a Gi-family G-protein functions in initiating oocyte maturation in starfish but not frogs. *Dev Biol* **253**, 139-49.

Kamath, R. S. and Ahringer, J. (2003). Genome-wide RNAi screening in Caenorhabditis elegans. *Methods* **30**, 313-21.

Kamath, R. S., Fraser, A. G., Dong, Y., Poulin, G., Durbin, R., Gotta, M., Kanapin, A., Le Bot, N., Moreno, S., Sohrmann, M. et al. (2003). Systematic functional analysis of the Caenorhabditis elegans genome using RNAi. *Nature* **421**, 231-7.

Kamikura, D. M. and Cooper, J. A. (2003). Lipoprotein receptors and a disabled family cytoplasmic adaptor protein regulate EGL-17/FGF export in C. elegans. *Genes Dev* **17**, 2798-811.

Kamikura, D. M. and Cooper, J. A. (2006). Clathrin interaction and subcellular localization of Ce-DAB-1, an adaptor for protein secretion in Caenorhabditis elegans. *Traffic* **7**, 324-36.

Kanatani, H., Shirai, H., Nakanishi, K. and Kurokawa, T. (1969). Isolation and Identification of Meiosis Inducing Substance in Starfish Asterias amurensis. *Nature* **221**, 273.

Kariya, K., Kim Bui, Y., Gao, X., Sternberg, P. W. and Kataoka, T. (2004). Phospholipase Cepsilon regulates ovulation in Caenorhabditis elegans. *Dev Biol* **274**, 201-10.

Keating, C. D., Kriek, N., Daniels, M., Ashcroft, N. R., Hopper, N. A., Siney, E. J., Holden-Dye, L. and Burke, J. F. (2003). Whole-genome analysis of 60 G protein-coupled receptors in Caenorhabditis elegans by gene knockout with RNAi. *Curr Biol* **13**, 1715-20.

Kelly, W. G., Xu, S., Montgomery, M. K. and Fire, A. (1997). Distinct requirements for somatic and germline expression of a generally expressed Caernorhabditis elegans gene. *Genetics* **146**, 227-38.

Khodjakov, A., Cole, R. W., Oakley, B. R. and Rieder, C. L. (2000). Centrosome-independent mitotic spindle formation in vertebrates. *Curr Biol* **10**, 59-67.

Kilmartin, J. V., Wright, B. and Milstein, C. (1982). Rat monoclonal antitubulin antibodies derived by using a new nonsecreting rat cell line. *J Cell Biol* **93**, 576-82.

Kimble, J. and Hirsh, D. (1979). The postembryonic cell lineages of the hermaphrodite and male gonads in Caenorhabditis elegans. *Developmental Biology* **70**, 396.

Kimble, J. E. and White, J. G. (1981). On the control of germ cell development in Caenorhabditis elegans. *Dev Biol* **81**, 208-19.

Klass, M. R., Kinsley, S. and Lopez, L. C. (1984). Isolation and characterization of a sperm-specific gene family in the nematode Caenorhabditis elegans. *Mol Cell Biol* **4**, 529-37.

Korswagen, H. C., Park, J. H., Ohshima, Y. and Plasterk, R. H. (1997). An activating mutation in a Caenorhabditis elegans Gs protein induces neural degeneration. *Genes Dev.* **11**, 1493-1503.

Korswagen, H. C., van der Linden, A. M. and Plasterk, R. H. (1998). G protein hyperactivation of the Caenorhabditis elegans adenylyl cyclase SGS-1 induces neuronal degeneration. *Embo J* **17**, 5059-65.

Kosinski, M., McDonald, K., Schwartz, J., Yamamoto, I. and Greenstein, D. (2005). C. elegans sperm bud vesicles to deliver a meiotic maturation signal to distant oocytes. *Development* **132**, 3357-69.

Kozasa, T., Jiang, X., Hart, M. J., Sternweis, P. M., Singer, W. D., Gilman, A. G., Bollag, G. and Sternweis, P. C. (1998). p115 RhoGEF, a GTPase Activating Protein for G{alpha}12 and G13. *Science* **280**, 2109-2111.

Kullander, K. and Klein, R. (2002). Mechanisms and functions of Eph and ephrin signalling. *Nat Rev Mol Cell Biol* **3**, 475-86.

Laing, J. G., Chou, B. C., Steinberg, T. H. (2005). ZO-1 alters the plasma membrane localization and function of Cx43 in osteoblastic cells. *J Cell Sci* **118,** 2167–2176.

Lampe, P. D., Qiu, Q., Meyer, R. A., TenBroek, E. M., Walseth, T. F., Starich, T. A., Grunenwald, H. L. and Johnson, R. G. (2001). Gap junction assembly: PTX-sensitive G proteins regulate the distribution of connexin43 within cells. *Am J Physiol Cell Physiol* **281**, C1211-22.

Lee, J., Jongeward, G. D. and Sternberg, P. W. (1994). unc-101, a gene required for many aspects of Caenorhabditis elegans development and behavior, encodes a clathrin-associated protein. *Genes Dev* **8**, 60-73.

Lee JY, Orr-Weaver TL (2001) The molecular basis of sister-chromatid cohesion. Annu Rev Cell Dev Biol 17: 753–777

Lee, M-H., Ohmachi, M., Arur, S., Nayak, S., Francis, R., Church, D., Lambie., E and Schedl, T. (2007) Multiple functions and dynamic activation of MPK-1 ERK signaling in *Caenorhabditis elegans* germline development. *Genetics* 177: 2039–2062

Liang, C. G., Su, Y. Q., Fan, H. Y., Schatten, H. and Sun, Q. Y. (2007). Mechanisms regulating oocyte meiotic resumption: roles of mitogen-activated protein kinase. *Mol Endocrinol* **21**, 2037-55.

Lindsay, L. L., Hertzler, P. L. and Clark, W. H. (1992) Extracellular Mg^{2+} induces an intracellular Ca^{2+} wave during oocyte activation in the marine shrimp *Sicyonia ingentis*. *Dev. Biol* **152,** 94–102.

Liu, Y., Wu, C., Lyu, Q., Yang, D., Albertini, D. F., Keefe, D. L. and Liu, L. (2007). Germline stem cells and neo-oogenesis in the adult human ovary. *Dev Biol* **306**, 112-20.

Lohka, M. J., Hayes, M. K. and Maller, J. L. (1988). Purification of maturation-promoting factor, an intracellular regulator of early mitotic events. *Proc Natl Acad Sci U S A* **85**, 3009-13.

Mains, P. E., Kemphues, K. J., Sprunger, S. A., Sulston, I. A. and Wood, W. B. (1990). Mutations affecting the meiotic and mitotic divisions of the early Caenorhabditis elegans embryo. *Genetics* **126**, 593-605.

Maller, J. L., Krebs, E. G. (1977). Progesterone-stimulated meiotic cell division in Xenopus oocytes. Induction by regulatory subunit and inhibition by catalytic subunit of adenosine 3':5'-monophosphate-dependent protein kinase. *J Biol Chem* **252**,1712–1718.

Maller, J., Gautier, J., Langan, T. A., Lohka, M. J., Shenoy, S., Shalloway, D. and Nurse, P. (1989). Maturation-promoting factor and the regulation of the cell cycle. *J Cell Sci Suppl* **12**, 53-63.

Marshall, C. J. (1994). MAP kinase kinase kinase, MAP kinase kinase and MAP kinase. *Curr Opin Genet Dev* **4**, 82-9.

Masui, Y. (1996). A quest for cytoplasmic factors that control the cell cycle. *Prog Cell Cycle Res* **2**, 1-13.

Masui, Y. (2001). From oocyte maturation to the in vitro cell cycle: the history of discoveries of Maturation-Promoting Factor (MPF) and Cytostatic Factor (CSF). *Differentiation* **69**, 1-17.

Masui, Y. and Clarke, H. J. (1979). Oocyte maturation. *Int Rev Cytol* **57**, 185-282.

Masui, Y. and Markert, C. L. (1971). Cytoplasmic control of nuclear behavior during meiotic maturation of frog oocytes. *J Exp Zool* **177**, 129-45.

Matten, W. T., Copeland, T. D., Ahn, N. G. and Vande Woude, G. F. (1996). Positive Feedback between MAP Kinase and Mos during Xenopus Oocyte Maturation. *Developmental Biology* **179**, 485.

Matthies, H. J., McDonald, H. B., Goldstein, L. S. and Theurkauf, W. E. (1996). Anastral meiotic spindle morphogenesis: role of the non-claret disjunctional kinesin-like protein. *J Cell Biol* **134**, 455-64.

McCarter, J., Bartlett, B., Dang, T. and Schedl, T. (1997). Soma-Germ Cell Interactions inCaenorhabditis elegans:Multiple Events of Hermaphrodite Germline Development Require the Somatic Sheath and Spermathecal Lineages. *Developmental Biology* **181**, 121.

McCarter, J., Bartlett, B., Dang, T. and Schedl, T. (1999). On the control of oocyte meiotic maturation and ovulation in Caenorhabditis elegans. *Dev Biol* **205**, 111-28.

McNally, F. J. and Vale, R. D. (1993). Identification of katanin, an ATPase that severs and disassembles stable microtubules. *Cell* **75**, 419-29.

McNally, K. L. and McNally, F. J. (2005). Fertilization initiates the transition from anaphase I to metaphase II during female meiosis in C. elegans. *Dev Biol* **282**, 218-30.

McNally, K. P., Buster, D. and McNally, F. J. (2002). Katanin-mediated microtubule severing can be regulated by multiple mechanisms. *Cell Motil Cytoskeleton* **53**, 337-49.

Mehlmann, L. M. (2005a). Oocyte-specific expression of Gpr3 is required for the maintenance of meiotic arrest in mouse oocytes. *Dev Biol* **288**, 397-404.

Mehlmann, L. M. (2005b). Stops and starts in mammalian oocytes: recent advances in understanding the regulation of meiotic arrest and oocyte maturation. *Reproduction* **130**, 791-9.

Mehlmann, L. M., Saeki, Y., Tanaka, S., Brennan, T. J., Evsikov, A. V., Pendola, F. L., Knowles, B. B., Eppig, J. J. and Jaffe, L. A. (2004). The Gs-linked receptor GPR3 maintains meiotic arrest in mammalian oocytes. *Science* **306**, 1947-50.

Meijer, L., Dostmann, W., Genieser, H. G., Butt, E. and Jastorff, B. (1989). Starfish oocyte maturation: evidence for a cyclic AMP-dependent inhibitory pathway. *Dev Biol* **133**, 58-66.

Mello, C. C., Kramer, J. M., Stinchcomb, D. T. and Ambros, V. R. (1991). Efficient gene transfer in C. elegans: Extrachromosomal maintenance and integration of transforming sequences. *EMBO Journal* **10**, 3959-3970.

Mendel, J. E., Korswagen, H. C., Liu, K. S., Hajdu-Cronin, Y. M., Simon, M. I., Plasterk, R. H. and Sternberg, P. W. (1995). Participation of the protein Go in multiple aspects of behavior in C. elegans. *Science* **267**, 1652-5.

Miller, K. G. and Rand, J. B. (2000). A role for RIC-8 (Synembryn) and GOA-1 (G(o)alpha) in regulating a subset of centrosome movements during early embryogenesis in Caenorhabditis elegans. *Genetics* **156**, 1649-60.

Miller, M. A., Cutter, A. D., Yamamoto, I., Ward, S. and Greenstein, D. (2004). Clustered organization of reproductive genes in the C. elegans genome. *Curr Biol* **14**, 1284-90.

Miller, M. A., Nguyen, V. Q., Lee, M. H., Kosinski, M., Schedl, T., Caprioli, R. M. and Greenstein, D. (2001). A sperm cytoskeletal protein that signals oocyte meiotic maturation and ovulation. *Science* **291**, 2144-7.

Miller, M. A., Ruest, P. J., Kosinski, M., Hanks, S. K. and Greenstein, D. (2003). An Eph receptor sperm-sensing control mechanism for oocyte meiotic maturation in Caenorhabditis elegans. *Genes Dev* **17**, 187-200.

Moghal, N. and Sternberg, P. W. (2003). The epidermal growth factor system in Caenorhabditis elegans. *Exp Cell Res* **284**, 150-9.

Moore, C. A., Milano, S. K. and Benovic, J. L. (2007). Regulation of receptor trafficking by GRKs and arrestins. *Annu Rev Physiol* **69**, 451-82.

Murai, K. K. and Pasquale, E. B. (2003). 'Eph'ective signaling: forward, reverse and crosstalk. *J Cell Sci* **116**, 2823-32.

Murchison, E. P., Stein, P., Xuan, Z., Pan, H., Zhang, M. Q., Schultz, R. M. and Hannon, G. J. (2007). Critical roles for Dicer in the female germline. *Genes Dev* **21**, 682-93.

Musch, A. (2004). Microtubule organization and function in epithelial cells. *Traffic* **5**, 1-9.

Nakano, T., Kontani, K., Kurosu, H., Katada, T., Hoshi, M. and Chiba, K. (1999). G-protein betagamma subunit-dependent phosphorylation of 62-kDa

protein in the early signaling pathway of starfish oocyte maturation induced by 1-methyladenine. *Dev Biol* **209**, 200-9.

Nebreda, A. R. and Ferby, I. (2000). Regulation of the meiotic cell cycle in oocytes. *Current Opinion in Cell Biology* **12**, 666.

Neves, S. R., Ram, P. T. and Iyengar, R. (2002). G Protein Pathways. *Science* **296**, 1636-1639.

Nishimura, A. L., Al-Chalabi, A. and Zatz, M. (2005). A common founder for amyotrophic lateral sclerosis type 8 (ALS8) in the Brazilian population. *Hum Genet* **118**, 499-500.

Norman, K. R., Fazzio, R. T., Mellem, J. E., Espelt, M. V., Strange, K., Beckerle, M. C. and Maricq, A. V. (2005). The Rho/Rac-family guanine nucleotide exchange factor VAV-1 regulates rhythmic behaviors in C. elegans. *Cell* **123**, 119-32.

Nurse, P. (1990). Universal control mechanism regulating onset of M-phase. *Nature* **344**, 503-8.

Ohba, T., Nakamura, M., Nishitani, H. and Nishimoto, T. (1999). Self-organization of microtubule asters induced in Xenopus egg extracts by GTP-bound Ran. *Science* **284**, 1356-8.

Okumura, E., Fukuhara, T., Yoshida, H., Hanada, S.-i., Kozutsumi, R., Mori, M., Tachibana, K. and Kishimoto, T. (2002). Akt inhibits Myt1 in the signalling pathway that leads to meiotic G2/M-phase transition. *Nat Cell Biol* **4**, 111.

Page, A. W. and Orr-Weaver, T. L. (1997). Activation of the meiotic divisions in Drosophila oocytes. *Dev Biol* **183**, 195-207.

Page, B. D., Guedes, S., Waring, D. and Priess, J. R. (2001). The C. elegans E2F- and DP-related proteins are required for embryonic asymmetry and negatively regulate Ras/MAPK signaling. *Mol Cell* **7**, 451-60.

Page, S. L. and Hawley, R. S. (2004). The genetics and molecular biology of the synaptonemal complex. *Annu Rev Cell Dev Biol* **20**, 525-58.

Pall, G. S., Wallis, J., Axton, R., Brownstein, D. G., Gautier, P., Buerger, K., Mulford, C., Mullins, J. J. and Forrester, L. M. (2004). A novel transmembrane MSP-containing protein that plays a role in right ventricle development. *Genomics* **84**, 1051-9.

Palmer, A. and Klein, R. (2003). Multiple roles of ephrins in morphogenesis, neuronal networking, and brain function. *Genes Dev.* **17,** 1429-1450.

Pang, K. M., Ishidate, T., Nakamura, K., Shirayama, M., Trzepacz, C., Schubert, C. M., Priess, J. R. and Mello, C. C. (2004). The minibrain kinase homolog, mbk-2, is required for spindle positioning and asymmetric cell division in early C. elegans embryos. *Dev Biol* **265**, 127-39.

Park, J. H., Ohshima, S., Tani, T. and Ohshima, Y. (1997). Structure and expression of the gsa-1 gene encoding a G protein alpha(s) subunit in C. elegans. *Gene* **194**, 183-90.

Park, J. Y., Su, Y. Q., Ariga, M., Law, E., Jin, S. L. and Conti, M. (2004). EGF-like growth factors as mediators of LH action in the ovulatory follicle. *Science* **303**, 682-4.

Patel, S. and Latterich, M. (1998). The AAA team: related ATPases with diverse functions. *Trends Cell Biol* **8**, 65-71.

Pellettieri, J., Reinke, V., Kim, S. K. and Seydoux, G. (2003). Coordinate activation of maternal protein degradation during the egg-to-embryo transition in C. elegans. *Dev Cell* **5**, 451-62.

Pellettieri, J. and Seydoux, G. (2002). Anterior-posterior polarity in C. elegans and Drosophila--PARallels and differences. *Science* **298**, 1946-50.

Pennetta, G., Hiesinger, P. R., Fabian-Fine, R., Meinertzhagen, I. A. and Bellen, H. J. (2002). Drosophila VAP-33A directs bouton formation at neuromuscular junctions in a dosage-dependent manner. *Neuron* **35**, 291-306.

Pepper, A. S., Lo, T. W., Killian, D. J., Hall, D. H., Hubbard, E. J. (2003). The establishment of Caenorhabditis elegans germline pattern is controlled by overlapping proximal and distal somatic gonad signals. *Dev. Biol.* **259,** 336–350.

Phelan, P., Bacon, J. P., Davies, J. A., Stebbings, L. A., Todman, M. G., Avery, L., Baines, R. A., Barnes, T. M., Ford, C., Hekimi, S. et al. (1998). Innexins: a family of invertebrate gap-junction proteins. *Trends Genet* **14**, 348-9.

Phelan, P. and Starich, T. A. (2001). Innexins get into the gap. *Bioessays* **23**, 388-96.

Pierce, K. L., Premont, R. T. and Lefkowitz, R. J. (2002). SEVEN-TRANSMEMBRANE RECEPTORS. *Nature Reviews Molecular Cell Biology* **3**, 639.

Pincus, G. and Enzmann, E. V. (1935). THE COMPARATIVE BEHAVIOR OF MAMMALIAN EGGS IN VIVO AND IN VITRO: I. THE ACTIVATION OF OVARIAN EGGS. *J. Exp. Med.* **62**, 665-675.

Pintard, L., Willis, J. H., Willems, A., Johnson, J. L., Srayko, M., Kurz, T., Glaser, S., Mains, P. E., Tyers, M., Bowerman, B. et al. (2003). The BTB protein MEL-26 is a substrate-specific adaptor of the CUL-3 ubiquitin-ligase. *Nature* **425**, 311-6.

Pitcher, J. A., Freedman, N. J. and Lefkowitz, R. J. (1998). G protein-coupled receptor kinases. *Annu Rev Biochem* **67**, 653-92.

Posada, J. and Cooper, J. A. (1992). Requirements for phosphorylation of MAP kinase during meiosis in Xenopus oocytes. *Science* **255**, 212-215.

Praitis, V., Casey, E., Collar, D. and Austin, J. (2001). Creation of low-copy integrated transgenic lines in Caenorhabditis elegans. *Genetics* **157**, 1217-26.

Premont, R. T. and Gainetdinov, R. R. (2007). Physiological Roles of G Protein Coupled Receptor Kinases and Arrestins. *Annual Review of Physiology* **69**, 511-534.

Quintin, S., Mains, P. E., Zinke, A. and Hyman, A. A. (2003). The mbk-2 kinase is required for inactivation of MEI-1/katanin in the one-cell Caenorhabditis elegans embryo. *EMBO Rep* **4**, 1175-81.

Radhika, V. and Dhanasekaran, N. (2001). Transforming G proteins. *Oncogene* **20**, 1607.

Resing, K. A., Mansour, S. J., Hermann, A. S., Johnson, R. S., Candia, J. M., Fukasawa, K., Vande Woude, G. F. and Ahn, N. G. (1995). Determination of v-Mos-catalyzed phosphorylation sites and autophosphorylation sites on MAP kinase kinase by ESI/MS. *Biochemistry* **34**, 2610-20.

Reynolds, N. K., Schade, M. A. and Miller, K. G. (2005). Convergent, RIC-8-dependent Galpha signaling pathways in the Caenorhabditis elegans synaptic signaling network. *Genetics* **169**, 651-70.

Robas, N., O'Reilly, M., Katugampola, S. and Fidock, M. (2003). Maximizing serendipity: strategies for identifying ligands for orphan G-protein-coupled receptors. *Current Opinion in Pharmacology* **3**, 121.

Roberts, T. M. and Stewart, M. (2000). Acting like actin. The dynamics of the nematode major sperm protein (msp) cytoskeleton indicate a push-pull mechanism for amoeboid cell motility. *J Cell Biol* **149**, 7-12.

Rogers, E., Bishop, J. D., Waddle, J. A., Schumacher, J. M. and Lin, R. (2002). The aurora kinase AIR-2 functions in the release of chromosome cohesion in Caenorhabditis elegans meiosis. *J Cell Biol* **157**, 219-29.

Romano, A., Guse, A., Krascenicova, I., Schnabel, H., Schnabel, R. and Glotzer, M. (2003). CSC-1: a subunit of the Aurora B kinase complex that binds to the survivin-like protein BIR-1 and the incenp-like protein ICP-1. *J Cell Biol* **161**, 229-36.

Romo, X., Hinrichs, M. V., Guzman, L. and Olate, J. (2002). G(alpha)s levels regulate *Xenopus laevis* oocyte maturation. *Mol Reprod Dev* **63**, 104-9.

Rongo, C., Whitfield, C. W., Rodal, A., Kim, S. K., and Kaplan, J. M. (1998). LIN-10 is a shared component of the polarized protein localization pathways in neurons and epithelia. *Cell* **94**, 751-759.

Rose, K. L., Winfrey, V. P., Hoffman, L. H., Hall, D. H., Furuta, T. and Greenstein, D. (1997). The POU gene *ceh-18* promotes gonadal sheath cell differentiation and function required for meiotic maturation and ovulation in Caenorhabditis elegans. *Dev Biol* **192**, 59-77.

Ross, E. M. and Wilkie, T. M. (2000). GTPASE-ACTIVATING PROTEINS FOR HETEROTRIMERIC G PROTEINS: Regulators of G Protein Signaling (RGS) and RGS-Like Proteins. *Annual Review of Biochemistry* **69**, 795-827.

Runft, L. L., Jaffe, L. A. and Mehlmann, L. M. (2002). Egg activation at fertilization: where it all begins. *Dev Biol* **245**, 237-54.

Sadler, K. C. and Ruderman, J. V. (1998). Components of the signaling pathway linking the 1-methyladenine receptor to MPF activation and maturation in starfish oocytes. *Dev Biol* **197**, 25-38.

Sagata, N. (1998). Introduction: meiotic maturation and arrest in animal oocytes. *Semin Cell Dev Biol* **9**, 535-7.

Sagata, N., Daar, I., Oskarsson, M., Showalter, S. D. and Vande Woude, G. F. (1989). The product of the mos proto-oncogene as a candidate "initiator" for oocyte maturation. *Science* **245**, 643-6.

Sagata, N., Oskarsson, M., Copeland, T., Brumbaugh, J. and Vande Woude, G. F. (1988). Function of c-mos proto-oncogene product in meiotic maturation in Xenopus oocytes. *Nature* **335**, 519-25.

Sampath, S. C., Ohi, R., Leismann, O., Salic, A., Pozniakovski, A. and Funabiki, H. (2004). The chromosomal passenger complex is required for

chromatin-induced microtubule stabilization and spindle assembly. *Cell* **118**, 187-202.

Sato, K., Sato, M., Audhya, A., Oegema, K., Schweinsberg, P. and Grant, B. D. (2006). Dynamic regulation of caveolin-1 trafficking in the germ line and embryo of Caenorhabditis elegans. *Mol Biol Cell* **17**, 3085-94.

Schade, M. A., Reynolds, N. K., Dollins, C. M. and Miller, K. G. (2005). Mutations that rescue the paralysis of Caenorhabditis elegans ric-8 (synembryn) mutants activate the G alpha(s) pathway and define a third major branch of the synaptic signaling network. *Genetics* **169**, 631-49.

Schatten, G. (1994). The centrosome and its mode of inheritance: the reduction of the centrosome during gametogenesis and its restoration during fertilization. *Dev Biol* **165**, 299-335.

Schisa, J. A., Pitt, J. N. and Priess, J. R. (2001). Analysis of RNA associated with P granules in germ cells of C. elegans adults. *Development* **128**, 1287-98.

Schmitt, A. and Nebreda, A. R. (2002). Signalling pathways in oocyte meiotic maturation. *J Cell Sci* **115**, 2457-9.

Schumacher, J. M., Golden, A. and Donovan, P. J. (1998). AIR-2: An Aurora/Ipl1-related protein kinase associated with chromosomes and midbody microtubules is required for polar body extrusion and cytokinesis in Caenorhabditis elegans embryos. *J Cell Biol* **143**, 1635-46.

Segalat, L., Elkes, D. A. and Kaplan, J. M. (1995). Modulation of serotonin-controlled behaviors by Go in Caenorhabditis elegans. *Science* **267**, 1648-1651.

Segbert, C., Barkus, R., Powers, J., Strome, S., Saxton, W. M. and Bossinger, O. (2003). KLP-18, a Klp2 kinesin, is required for assembly of acentrosomal meiotic spindles in Caenorhabditis elegans. *Mol Biol Cell* **14**, 4458-69.

Sela-Abramovich, S., Edry, I., Galiani, D., Nevo, N. and Dekel, N. (2006). Disruption of gap junctional communication within the ovarian follicle induces oocyte maturation. *Endocrinology* **147**, 2280-6.

Severson, A. F., Hamill, D. R., Carter, J. C., Schumacher, J. and Bowerman, B. (2000). The aurora-related kinase AIR-2 recruits ZEN-4/CeMKLP1 to the mitotic spindle at metaphase and is required for cytokinesis. *Curr Biol* **10**, 1162-71.

Seydoux, G. and Dunn, M. A. (1997). Transcriptionally repressed germ cells lack a subpopulation of phosphorylated RNA polymerase II in early embryos of Caenorhabditis elegans and Drosophila melanogaster. *Development* **124**, 2191-201.

Seydoux, G., Mello, C. C., Pettitt, J., Wood, W. B., Priess, J. R. and Fire, A. (1996). Repression of gene expression in the embryonic germ lineage of C. elegans. *Nature* **382**, 713-6.

Shilling, F., Mandel, G. and Jaffe, L. A. (1990). Activation by serotonin of starfish eggs expressing the rat serotonin 1c receptor. *Cell Regul* **1**, 465-9.

Shirayama, M., Soto, M. C., Ishidate, T., Kim, S., Nakamura, K., Bei, Y., van den Heuvel, S. and Mello, C. C. (2006). The Conserved Kinases CDK-1, GSK-3, KIN-19, and MBK-2 Promote OMA-1 Destruction to Regulate the Oocyte-to-Embryo Transition in C. elegans. *Curr Biol* **16**, 47-55.

Sijen, T., Fleenor, J., Simmer, F., Thijssen, K. L., Parrish, S., Timmons, L., Plasterk, R. H. and Fire, A. (2001). On the role of RNA amplification in dsRNA-triggered gene silencing. *Cell* **107**, 465-76.

Simmer, F., Moorman, C., van der Linden, A. M., Kuijk, E., van den Berghe, P. V. E., Kamath, R. S., Fraser, A. G., Ahringer, J. and Plasterk, R. H. A. (2003). Genome-Wide RNAi of C. elegans Using the Hypersensitive rrf-3 Strain Reveals Novel Gene Functions. *PLoS Biology* **1**, e12.

Simon, A. M., Goodenough, D. A., Li, E. and Paul, D. L. (1997). Female infertility in mice lacking connexin 37. *Nature* **385**, 525-9.

Simske, J. S., Kaech, S. M., Harp, S. A. and Kim, S. K. (1996). LET-23 receptor localization by the cell junction protein LIN-7 during C. elegans vulval induction. *Cell* **85**, 195-204.

Singson, A. (2001). Every sperm is sacred: fertilization in Caenorhabditis elegans. *Dev Biol* **230**, 101-9.

Singson, A., Hill, K. L. and L'Hernault, S. W. (1999). Sperm competition in the absence of fertilization in Caenorhabditis elegans. *Genetics* **152**, 201-8.

Singson, A., Mercer, K. B. and L'Hernault, S. W. (1998). The C. elegans spe-9 gene encodes a sperm transmembrane protein that contains EGF-like repeats and is required for fertilization. *Cell* **93**, 71-9.

Skold, H. N., Komma, D. J. and Endow, S. A. (2005). Assembly pathway of the anastral Drosophila oocyte meiosis I spindle. *J Cell Sci* **118**, 1745-55.

Smardon, A., Spoerke, J. M., Stacey, S. C., Klein, M. E., Mackin, N. and Maine, E. M. (2000). EGO-1 is related to RNA-directed RNA polymerase and functions in germ-line development and RNA interference in C. elegans. *Curr Biol* **10**, 169-78.

Somekawa, S., Fukuhara, S., Nakaoka, Y., Fujita, H., Saito, Y. and Mochizuki, N. (2005). Enhanced functional gap junction neoformation by protein kinase A-dependent and Epac-dependent signals downstream of cAMP in cardiac myocytes. *Circ Res* **97**, 655-62.

Speliotes, E. K., Uren, A., Vaux, D. and Horvitz, H. R. (2000). The survivin-like C. elegans BIR-1 protein acts with the Aurora-like kinase AIR-2 to affect chromosomes and the spindle midzone. *Mol Cell* **6**, 211-23.

Spiegel, A. M. (1996). Defects in G Protein-Coupled Signal Transduction in Human Disease. *Annual Review of Physiology* **58**, 143-170.

Srayko, M., Buster, D. W., Bazirgan, O. A., McNally, F. J. and Mains, P. E. (2000). MEI-1/MEI-2 katanin-like microtubule severing activity is required for Caenorhabditis elegans meiosis. *Genes Dev* **14**, 1072-84.

Srayko, M., Kaya, A., Stamford, J. and Hyman, A. A. (2005). Identification and characterization of factors required for microtubule growth and nucleation in the early C. elegans embryo. *Dev Cell* **9**, 223-36.

Srinivasan, D. G., Fisk, R. M., Xu, H. and van den Heuvel, S. (2003). A complex of LIN-5 and GPR proteins regulates G protein signaling and spindle function in C. elegans. *Genes Dev.* **17**, 1225-1239.

Starich, T., Sheehan, M., Jadrich, J. and Shaw, J. (2001). Innexins in C. elegans. *Cell Commun Adhes* **8**, 311-4.

Stitzel, M. L., Pellettieri, J. and Seydoux, G. (2006). The C. elegans DYRK Kinase MBK-2 Marks Oocyte Proteins for Degradation in Response to Meiotic Maturation. *Curr Biol* **16**, 56-62.

Strader, C. D., Fong, T. M., Tota, M. R., Underwood, D. and Dixon, R. A. F. (1994). Structure and Function of G Protein-Coupled Receptors. *Annual Review of Biochemistry* **63**, 101-132.

Strathmann, M., Wilkie, T. M. and Simon, M. I. (1989). Diversity of the G-Protein Family: Sequences from Five Additional alpha Subunits in the Mouse. *PNAS* **86**, 7407-7409.

Strathmann, M. P. and Simon, M. I. (1991). G{alpha}12 and G{alpha}13 Subunits Define a Fourth Class of G Protein {alpha} Subunits. *PNAS* **88**, 5582-5586.

Strome, S. (1986). Fluorescence visualization of the distribution of microfilaments in gonads and early embryos of the nematode Caenorhabditis elegans. *J Cell Biol* **103**, 2241-52.

Sulston, J. E. and Horvitz, H. R. (1977). Post-embryonic cell lineages of the nematode, Caenorhabditis elegans. *Developmental Biology* **56**, 110.

Sulston, J. E., Schierenberg, E., White, J. G. and Thomson, J. N. (1983). The embryonic cell lineage of the nematode Caenorhabditis elegans. *Developmental Biology* **100**, 64.

Sun, Q. Y., Breitbart, H. and Schatten, H. (1999). Role of the MAPK cascade in mammalian germ cells. *Reprod Fertil Dev* **11**, 443-50.

Sundaram, M. V. (2006). RTK/Ras/MAPK signaling. *WormBook, ed. The C. elegans Research Community, WormBook, http://www.wormbook.org.*

Susiarjo, M., Hassold, T. J., Freeman, E. and Hunt, P. A. (2007). Bisphenol A exposure in utero disrupts early oogenesis in the mouse. *PLoS Genet* **3**, e5.

Sutton, M. L., Gilchrist, R. B. and Thompson, J. G. (2003). Effects of in-vivo and in-vitro environments on the metabolism of the cumulus-oocyte complex and its influence on oocyte developmental capacity. *Hum Reprod Update* **9**, 35-48.

Szollosi, D., Calarco, P. and Donahue, R. P. (1972). Absence of centrioles in the first and second meiotic spindles of mouse oocytes. *J Cell Sci* **11**, 521-41.

Tachibana, K., Tanaka, D., Isobe, T. and Kishimoto, T. (2000). c-Mos forces the mitotic cell cycle to undergo meiosis II to produce haploid gametes. *PNAS* **97**, 14301-14306.

Tadenuma, H., Takahashi, K., Chiba, K., Hoshi, M. and Katada, T. (1992). Properties of 1-methyladenine receptors in starfish oocyte membranes: involvement of pertussis toxin-sensitive GTP-binding protein in the receptor-mediated signal transduction. *Biochem Biophys Res Commun* **186**, 114-21.

Tenenhaus, C., Schubert, C. and Seydoux, G. (1998). Genetic requirements for PIE-1 localization and inhibition of gene expression in the embryonic germ lineage of Caenorhabditis elegans. *Dev Biol* **200**, 212-24.

Tenenhaus, C., Subramaniam, K., Dunn, M. A. and Seydoux, G. (2001). PIE-1 is a bifunctional protein that regulates maternal and zygotic gene expression in the embryonic germ line of Caenorhabditis elegans. *Genes Dev* **15**, 1031-40.

Thomas, P. , Zhu, Y. & Pace, M. (2002). Progestin membrane receptors involved in the meiotic maturation of teleost oocytes: a review with some new findings. *Steroids* **67**, 511-517

Thomas, F. H. and Vanderhyden, B. C. (2006). Oocyte-granulosa cell interactions during mouse follicular development: regulation of kit ligand expression and its role in oocyte growth. *Reprod Biol Endocrinol* **4**, 19.

Tilly, J. L. and Johnson, J. (2007). Recent arguments against germ cell renewal in the adult human ovary: is an absence of marker gene expression really acceptable evidence of an absence of oogenesis? *Cell Cycle* **6**, 879-83.

Treisman, R. (1996). Regulation of transcription by MAP kinase cascades. *Curr Opin Cell Biol* **8**, 205-15.

Tsou, M.-F. B., Hayashi, A. and Rose, L. S. (2003). LET-99 opposes G{alpha}/GPR signaling to generate asymmetry for spindle positioning in response to PAR and MES-1/SRC-1 signaling. *Development* **130**, 5717-5730.

Tunquist, B. J. and Maller, J. L. (2003). Under arrest: cytostatic factor (CSF)-mediated metaphase arrest in vertebrate eggs. *Genes Dev* **17**, 683-710.

Van der Linden, A. M., Simmer, F., Cuppen, E. and Plasterk, R. H. A. (2001). The G-Protein {beta}-Subunit GPB-2 in Caenorhabditis elegans Regulates the Go{{alpha}}-Gq{{alpha}} Signaling Network Through Interactions With the Regulator of G-Protein Signaling Proteins EGL-10 and EAT-16. *Genetics* **158**, 221-235.

Varmark, H. (2004). Functional role of centrosomes in spindle assembly and organization. *J Cell Biochem* **91**, 904-14.

Vassilatis, D. K., Hohmann, J. G., Zeng, H., Li, F., Ranchalis, J. E., Mortrud, M. T., Brown, A., Rodriguez, S. S., Weller, J. R., Wright, A. C. et al. (2003). The G protein-coupled receptor repertoires of human and mouse. *PNAS* **100**, 4903-4908.

Veitia, R. A., Gluckman, E., Fellous, M. and Soulier, J. (2007). Recovery of female fertility after chemotherapy, irradiation, and bone marrow allograft: further evidence against massive oocyte regeneration by bone marrow-derived germline stem cells. *Stem Cells* **25**, 1334-5.

Verlhac, M. H., de Pennart, H., Maro, B., Cobb, M. H. and Clarke, H. J. (1993). MAP kinase becomes stably activated at metaphase and is associated with microtubule-organizing centers during meiotic maturation of mouse oocytes. *Dev Biol* **158**, 330-40.

Verlhac, M. H., Kubiak, J. Z., Weber, M., Geraud, G., Colledge, W. H., Evans, M. J. and Maro, B. (1996). Mos is required for MAP kinase activation and is involved in microtubule organization during meiotic maturation in the mouse. *Development* **122**, 815-822.

Verlhac, M. H., Lefebvre, C., Kubiak, J. Z., Umbhauer, M., Rassinier, P., Colledge, W. and Maro, B. (2000). Mos activates MAP kinase in mouse oocytes through two opposite pathways. *Embo J* **19**, 6065-74.

Voronina, E. and Wessel, G. M. (2003). The regulation of oocyte maturation. *Curr Top Dev Biol* **58**, 53-110.

Walczak, C. E., Vernos, I., Mitchison, T. J., Karsenti, E. and Heald, R. (1998). A model for the proposed roles of different microtubule-based motor proteins in establishing spindle bipolarity. *Curr Biol* **8**, 903-13.

Wang, X., Roy, P. J., Holland, S. J., Zhang, L. W., Culotti, J. G. and Pawson, T. (1999). Multiple ephrins control cell organization in C. elegans using kinase-dependent and -independent functions of the VAB-1 Eph receptor. *Mol Cell* **4**, 903-13.

Ward, S., Burke, D. J., Sulston, J. E., Coulson, A. R., Albertson, D. G., Ammons, D., Klass, M. and Hogan, E. (1988). Genomic organization of major sperm protein genes and pseudogenes in the nematode Caenorhabditis elegans. *J Mol Biol* **199**, 1-13.

Ward, S. and Carrel, J. S. (1979). Fertilization and sperm competition in the nematode Caenorhabditis elegans. *Dev Biol* **73**, 304-21.

Ward, S., Roberts, T. M., Strome, S., Pavalko, F. M. and Hogan, E. (1986). Monoclonal antibodies that recognize a polypeptide antigenic determinant shared by multiple Caenorhabditis elegans sperm-specific proteins. *J Cell Biol* **102**, 1778-86.

Warren, W. D. and Gorringe, K. L. (2006). A molecular model for sporadic human aneuploidy. *Trends Genet* **22**, 218-24.

Wessel, G. M., Brooks, J. M., Green, E., Haley, S., Voronina, E., Wong, J., Zaydfudim, V. and Conner, S. (2001). The biology of cortical granules. *Int Rev Cytol* **209**, 117-206.

Westermann, S. and Weber, K. (2003). Post-translational modifications regulate microtubule function. *Nat Rev Mol Cell Biol* **4**, 938-47.

Wettschureck, N. and Offermanns, S. (2005). Mammalian G Proteins and Their Cell Type Specific Functions. *Physiol. Rev.* **85**, 1159-1204.

Wilde, A. and Zheng, Y. (1999). Stimulation of microtubule aster formation and spindle assembly by the small GTPase Ran. *Science* **284**, 1359-62.

Wise, A., Jupe, S. C. and Rees, S. (2004). THE IDENTIFICATION OF LIGANDS AT ORPHAN G-PROTEIN COUPLED RECEPTORS. *Annual Review of Pharmacology and Toxicology* **44**, 43-66.

Wolke, U., Jezuit, E. A. and Priess, J. R. (2007). Actin-dependent cytoplasmic streaming in C. elegans oogenesis. *Development* **134**, 2227-36.

Yamamoto, I., Kosinski, M. E. and Greenstein, D. (2006). Start me up: cell signaling and the journey from oocyte to embryo in C. elegans. *Dev Dyn* **235**, 571-85.

Yang, H. Y., Mains, P. E. and McNally, F. J. (2005). Kinesin-1 mediates translocation of the meiotic spindle to the oocyte cortex through KCA-1, a novel cargo adapter. *J Cell Biol* **169**, 447-57.

Yang, H. Y., McNally, K. and McNally, F. J. (2003). MEI-1/katanin is required for translocation of the meiosis I spindle to the oocyte cortex in C elegans. *Dev Biol* **260**, 245-59.

Yochem, J., Gu, T. and Han, M. (1998). A New Marker for Mosaic Analysis in Caenorhabditis elegans Indicates a Fusion Between hyp6 and hyp7, Two Major Components of the Hypodermis. *Genetics* **149**, 1323-1334.

Yochem, J. (2006). Nomarski images for learning the anatomy, with tips for mosaic analysis *WormBook*, ed. The *C. elegans* Research Community, WormBook, http://www.wormbook.org.

Zhu, Y., Bond, J. and Thomas, P. (2003a). Identification, classification, and partial characterization of genes in humans and other vertebrates homologous to a fish membrane progestin receptor. *Proc Natl Acad Sci U S A* **100**, 2237-42.

Zhu, Y., Rice, C. D., Pang, Y., Pace, M. and Thomas, P. (2003b). Cloning, expression, and characterization of a membrane progestin receptor and evidence it is an intermediary in meiotic maturation of fish oocytes. *Proc Natl Acad Sci U S A* **100**, 2231-6.

Zuckerman S. (1951). The number of oocytes in the mature ovary. *Recent Prog Horm Res*. **6,** 63-109.